

**Deriving an in vitro source of canine
corneal stromal cells for future studies of
corneal disease and therapeutic
applications**

**A thesis submitted for the degree of Doctor of Philosophy
(PhD)**

University College London (UCL) 2021

Christiane Kafarnik

Supervised by

**Professor Julie T. Daniels, PhD FRSB
Professor Alison Hardcastle, PhD, BSc Hons
Rescue, Repair & Regeneration Theme
UCL Institute of Ophthalmology, 11-43 Bath Street, London, EC1V 9EL**

**Dr. Deborah J. Guest, PhD, BSc
Stem Cell Department, Centre for Preventive Medicine
Animal Health Trust, Lanwades Park, Newmarket, CB8 7UU**

Declaration

I, Christiane Kafarnik, confirm that the work presented in this thesis is my own. Where information has been derived from other sources, I confirm that this has been referenced in the thesis.

Name: Christiane KAFARNIK

Signature:

Date: 16/12/2021

Abstract

The cornea is the transparent tissue located at the front of the eye, that transmits and refracts light onto the retina. Despite great advances in corneal stem cell biology in human and laboratory animal research, no information is available in dogs.

Corneal pathology, as corneal crystalline dystrophy has a prevalence of up to 15% and has been described in eight different canine breeds. Cholesterol and phospholipids are deposited in the stroma, similar to Schnyder's dystrophy (SCD) in humans. Chronic corneal fibrosis is one of the leading causes of visual impairment in veterinary ophthalmology. Similar to the situation in human ophthalmology, there is a shortage of corneal donor tissue. Therefore, the overall aim was first to investigate whether corneal stromal stem cells exist in the canine cornea., The second aim was to determine the potential of deriving an *in vitro* source of corneal stroma cells from corneal stromal stem cells, adipose derived mesenchymal stromal cells (adMSC) and canine induced pluripotent stem cells (ciPSC), to provide a resource for studies investigating the pathogenesis of inherited stromal dystrophies, and for the development of novel cell-based therapies for dogs. First, a canine corneal stromal cell (CSC) population was characterised that demonstrated mesenchymal stromal cell properties, they differentiated into keratocyte-like cells (KDCs) *in vitro* and appeared to be immune privileged. Second, canine adMSC were differentiated into KDCs, but expressed high levels of a myofibroblastic marker, similar to those found in fibrotic tissue. Third, a modified protocol was established whereby ciPSCs were induced

into neural crest (stem) cell lineages and then into KDCs. This led to the successful expression of some keratocyte associated markers in absence of a myofibroblastic expression. Taken together, a novel cell population was characterised in the canine corneal stroma. The differentiation protocols of adMSC and ciPSC led to preliminary results and built a basic foundation for future studies.

Impact statement

In this thesis a novel approach was developed to establish sources of corneal stromal cells to support the investigation of the genetics and cell biology of canine corneal crystalline dystrophy and other corneal pathologies (e.g. corneal scarring, inflammation), so that veterinary medicine can take advantage of the significant advances being made with cell therapies in humans.

The overall aim was first to investigate whether corneal stromal stem cells exist in dogs, and further to investigate the potential of deriving a source of corneal stromal cells from corneal stromal stem cells (CSC), adipose derived mesenchymal stromal cells (adMSC) and canine induced pluripotent stem cells (ciPSC). With this study a baseline for the methodology in this species and a basic foundation to establish a laboratory tool for the research community and future research funding was provided (including scholarships).

For the first time a cell population in the dog cornea was characterised that demonstrated mesenchymal stromal cell properties such as multipotency and self-renewal and appeared to be immune privileged. Overall, this finding will contribute to the research community of stem cell researchers and in the field of veterinary ophthalmology and is published in Stem Cells and Development Journal (see attached publication). However, CSCs are present in very small numbers in the cornea, and they have limited self-renewal in contrast to human corneal stromal stem cells (CSSC). This would make it difficult to

utilise them clinically as a large source of donor corneas would still be required.

To overcome the limited availability of canine CSCs, MSCs were used which can be isolated in large numbers from a variety of canine tissues including fat tissue. It was demonstrated that canine MSCs can differentiate directly into keratocytes under similar conditions to CSCs. However, undifferentiated canine adMSCs express a high level of alpha-smooth muscle actin (α -SMA) and this is maintained following their differentiation to keratocytes. The clinical relevance of this is not fully understood, but it may have a negative impact as it is a myofibroblastic marker and commonly associated with a scarring response *in vitro* and *in vivo*. To overcome the limitations of using CSCs and adMSCs and to enable disease models of corneal stromal dystrophy in the future, it was determined whether canine iPSCs could be differentiated into keratocyte-like cells. A modified two-step protocol was established whereby the ciPSCs were first induced into neural crest (stem) cell lineages and then into keratocytes. This led to the expression of some keratocyte associated markers in absence of any α -SMA expression. However, the expression levels of keratocyte related genes were significantly lower in ciPSC-keratocytes than in CSC- or adMSC- derived keratocytes. Further optimisation of the differentiation protocol is therefore required in future studies.

Acknowledgement

I would like to thank my supervisors, Prof. Julie T. Daniels and Dr. Deborah Guest (Animal Health Trust) for the support and inspirational guidance, patience and continuous encouragement they have provided throughout my PhD. I would like to thank my secondary supervisor, Prof. A. Hardcastle for her regular advice and expertise.

I would like to acknowledge my colleagues from the Cells for Sight team (UCL) and the team of the stem cell department (Animal Health Trust) for their expertise especially Dr. Marc Dziasko, Dr. Alevna Kureshi and Dr. Arabella Baird.

Finally, a big thank you goes to my partner Stuart Robson, my friends and my family for their continuous support and presence.

The Petplan Charitable Trust (S16-204-397), Bertie's Mission and the European College of Veterinary Ophthalmologists funded this research.

List of abbreviations

- adMSC Adipose derived Mesenchymal Stromal Cell
- adMSC-CSC Adipose derived Mesenchymal Stromal Cell derived Corneal Stromal Cells
- adMSC-CSC-KDC Adipose derived Mesenchymal Stromal Cell derived Corneal Stromal Cells differentiated into keratocyte-like cells
- adMSC-KDC Adipose derived Mesenchymal Stromal Cell derived differentiated keratocyte-like cells
- AHT Animal Health Trust
- bFGF Basic fibroblast growth factor
- bp base pair
- ciPSC Canine induced pluripotent stem cell
- ciPSC-NCC Canine induced pluripotent stem cell derived neural crest-like cell
- ciPSC-NCC-KDC Canine induced pluripotent stem cell derived neural crest-like cell differentiated into keratocyte-like cells
- CSC Corneal stromal cell
- CSC-KDC Corneal stromal cell derived keratocyte-like differentiated cell
- CSSC Corneal stromal stem cell
- DAPI 4',6-diamidino-2-phenylindole
- FBS Fetal bovine serum
- FCS Fetal Calf Serum
- GFP Green fluorescent protein
- GMP Good manufacturing practise
- H&E Haematoxylin and Eosin
- hiPSC Human induced pluripotent stem cell
- HPF High Power Field
- HRP Horseradish Peroxidase
- ICC Immunocytochemistry

- IF Immunofluorescence
- IHC Immunohistochemistry
- kDa kilo Dalton
- KD keratocyte differentiation
- KDM Keratocyte differentiation media
- MSC Mesenchymal Stromal Cell
- PAS Periodic acid-Schiff
- PDT Population doubling time
- PBS Phosphate Buffered Solution
- PBMC Peripheral blood mononuclear cell
- PFA Paraformaldehyde
- P/S Penicillin/Streptomycin
- PVDF Polyvinylidene difluoride
- Rpm Revolutions per minute
- RCF Relative centrifugal force
- RT Room temperature
- SE Standard error
- WB Western Blot
- qPCR Quantitative reverse transcriptase polymerase chain reaction

Table of contents

Declaration	2
Abstract	3
Impact statement	5
Acknowledgement	7
List of abbreviations	8
Table of contents	10
List of figures	19
List of tables	28
Chapter 1: General introduction	30
1.1. The cornea: embryology, ultrastructure and function	30
A) Embryology	32
B) Corneal epithelium	37
C) Corneal stroma	38
D) Corneal endothelium	46
E) Corneal innervation	47
1.2 Canine corneal stromal disease	48
1.2.1 Canine corneal stromal dystrophy	48

1.2.2 Corneal fibrosis	55
1.2.3 Surgical treatment of Schnyder's dystrophy and other corneal stromal dystrophies.....	59
1.3 General introduction to stem cells	62
1.3.1 Waddington's landscape and reprogramming.....	64
1.4 Stem cells in the corneal limbus and stroma	66
1.4.1 Anatomical aspects of the limbus	66
1.4.2 Limbal epithelial stem cells and corneal epithelial homeostasis ..	69
1.4.3 Molecular aspects of the limbal epithelial stem cell niche	72
1.4.4 Corneal stromal stem cells.....	75
A) Cellular and molecular aspects of CSSC	75
B) Immunomodulatory aspects of CSSC	78
C) Positive and negative mesenchymal stromal cell markers	80
D) Differentiation of hCSSC in keratocytes <i>in vitro</i>	85
1.5 Canine mesenchymal stromal cells	87
1.6 Immune privilege and immunomodulatory properties in mammalian MSC.....	89
1.7 Induced pluripotent stem cells	93
1.7.1 Canine iPSC	95

1.7.2 IPSC differentiation into keratocyte-like cells via neural crest lineage differentiation.....	102
A) The neural crest lineage differentiation	102
B) hiPSC and hESC differentiation into keratocyte-like cells <i>in vitro</i> ...	106
1.8 Introduction to the concept of cell-based therapies in corneal regenerative medicine	109
1.8.1 Stem cell therapy in corneal regenerative medicine	111
A) Limbal epithelial stem cells.....	111
B) Corneal stromal stem cells	112
C) Mesenchymal stromal cells	113
D) Mesenchymal stromal cells in veterinary ophthalmology	116
1.9 Conclusion and aims	117
Chapter 2: General materials and methods	121
2.1 Canine tissue and ethics statement	122
2.2 Cell culture	125
2.2.1 Cell counting	125
2.2.2 Cryopreservation and thawing	125
2.2.3 Cell observation, fixation and imaging of cell morphology	126
2.2.4 Cell culture and differentiation media.....	127

2.3 Protein analysis	128
2.3.1 Immunofluorescence staining protocol and imaging	128
2.3.2 Protein extraction from cells.....	133
2.3.3 Acetone protein precipitation	134
2.3.4 Protein extraction from corneal tissue.....	134
2.3.5 Western Blot analysis	136
2.4 Gene expression analysis	142
2.4.1 RNA extraction and isolation from cells and tissues	142
2.4.2 Reverse transcription and quantitative polymerase chain reaction	144
2.4.3 Primer design and efficiency test on positive control cells/tissue	145
2.4.4 Gel electrophoresis	152
2.4.5 Canine reference gene analysis	155
2.5 Statistical analysis.....	158
Chapter 3: Localisation, isolation and characterisation of canine corneal stromal cells in the limbal and central cornea of healthy dogs	159
3.1 Introduction	160
3.2 Materials and methods	160
3.2.1 Corneal harvesting and corneal storage medium	160

3.2.2 Histology: Cryosectioning, OCT embedding and histological analysis.....	161
3.2.3 Immunohistochemistry and immunocytochemistry	164
3.2.4 Tissue dissection, cell isolation and cell culture.....	164
A) Tissue dissection and cell isolation	164
B) Cell culture in corneal stem cell media	166
C) Cell culture assay at Passage 0.....	166
3.2.5 Cell culture kinetics of CSC	167
A) Cell expansion.....	167
B) Population doubling time and population doublings	168
3.2.6 Cell culture of adipose-derived mesenchymal stromal cells.....	168
3.2.7 Flow cytometry.....	169
3.2.8 Assays for trilineage differentiation	172
A) Adipogenesis.....	173
B) Osteogenesis	173
C) Chondrogenesis.....	174
3.2.9 Peripheral blood mononuclear cell isolation from lymph nodes .	174
3.2.10 Cytospin of PBMCs on slides.....	175

3.2.11 PBMC co-cultures	175
3.3 Results	179
3.3.1 Macroscopic and histological features of the canine limbal niche and central cornea	179
3.3.2 Western Blot results of the antibodies tested for cross- reactivity and specificity to dog proteins.....	184
3.3.3 A distinct population of mesenchymal stromal stem cells are present in the limbal and central corneal stroma	186
3.3.4 Short-term culturing of isolated corneal cells contains small population of mesenchymal stromal cells	191
3.3.5 The CSC cell morphology changes with cell density	193
3.3.6 Cell culture kinetics of limbal and central derived CSC are similar, and both have limited self-renewal potential	194
3.3.7 Limbal and central derived CSCs have mesenchymal stromal cell characteristics.....	202
3.3.8 Evaluation of corneal stromal cells in PBMC co-culture assay ..	213
3.3.9 CSCs are immune privileged <i>in vitro</i>	215
3.3.10 CSC differentiate into keratocyte-like cells in vitro during which bFGF plays an essential role in downregulation of α -SMA	216
3.4 Discussion	223

Chapter 4: Differentiation of adipose derived mesenchymal stromal cells into keratocyte-like cells	237
4.1. Introduction	238
4.2. Materials and methods	238
4.2.1 Cell culture of adipose-derived mesenchymal stromal cells.....	239
4.2.2 Corneal stromal stem cell media.....	239
4.2.3 Keratocyte differentiation of adMSC: culture condition	239
4.3 Results.....	241
4.3.1 AdMSC-KDC show keratocyte-like morphology and form a cell syncytium. The cell expansion of adMSC-KDC is influenced by the seeding density and bFGF.....	241
4.3.2 Pre-culturing adMSC in CSSC media up regulates <i>Keratocan</i> and <i>Lumican</i> expression. AdMSC respond similar to the keratocyte differentiation than corneal stromal cells but retain myofibroblastic expression.	245
4.4 Discussion.....	254
Chapter 5: Establishing a differentiation protocol for canine induced pluripotent stem cells into keratocyte-like cells	262
5.1. Introduction	263
5.2. Materials and methods	264

5.2.1 Primary mouse embryonic fibroblast (MEF) cell culture and inactivation (feeder cells)	264
5.2.2 Canine iPSC	265
Details of the iPSC media are in the Supplementary table S6. A) Cell culture of ciPSC on a feeder system.....	266
B) CiPSC colony dissociation and a feeder-free coating system	267
5.2.3 Neural crest induction and keratocyte differentiation: culture condition and protocol.....	269
A) Seeding density.....	269
B) Neural crest and keratocyte differentiation	270
5.2.4 RNA extraction, qPCR and primers	272
5.2.5 Immunofluorescence staining	273
5.3 Results	274
5.3.1 Establishing a ciPSC-NCC differentiation protocol	274
A) Culture conditions	274
B) Higher concentration of Activin/Nodal/TGF β inhibitor (SB) and Wnt/ β -catenin activator (CHIR) changed the ciPSC-NCC cell morphology and marker expression of Sox10	276
5.3.2 CiPSC-NCC-KDCs exposed to corneal stromal stem cell media expressed keratocyte markers but not Keratocan.....	282

5.4. Discussion	292
Chapter 6: General discussion and future work	302
6.1 General discussion	303
6.2 Future work.....	313
Supplementary material	316
Supplementary tables	316
Supplementary figures	322
References	326
Publications	358

List of figures

Chapter 1

Figure 1.1 Layers of the canine and human cornea.....	31
Figure 1.2 Overview of the developing canine eye and cornea.....	34
Figure 1.3 Organisation of keratocytes and corneal collagen lamellae.....	40
Figure 1.4 Corneal proteoglycans.....	45
Figure 1.5 Canine corneal (crystalline) stromal dystrophy.....	49
Figure 1.6 Histopathology of canine stromal dystrophy.....	50
Figure 1.7 Clinical appearance of Schnyders corneal dystrophy human patients with confirmed UBIAD1 gene mutation.....	55
Figure 1.8 Clinical presentation of corneal fibrosis after corneal graft surgery.....	57
Figure 1.9 The epigenetic landscape of Conrad Waddington.....	66
Figure 1.10 Overview of the human limbal niche.....	69
Figure 1.11 X, Y, Z hypothesis of corneal epithelial maintenance.....	72
Figure 1.12 Mechanism of action and interaction of MSCs with immune cells.....	92
Figure 1.13 GSK3 inhibition via small chemical molecule CHIR activates conical WNT signalling.....	105

Figure 1.14 Smad 2/3 inhibition via small chemical molecule SB.....	106
Figure 1.15 Tissue engineering for corneal replacement.....	110
Chapter 2	
Figure 2.1 Preparation and homogenisation of corneal protein.....	135
Figure 2.2 Example of primer efficiency evaluation on corneal RNA for ALDH1A3.....	149
Figure 2.3. Gel electrophoresis assay of PCR products (I).....	153
Figure 2.4 Gel electrophoresis assay of PCR products (II).....	154
Figure 2.5 Gel electrophoresis assay of PCR products (III).....	154
Figure 2.6 Amplification cycles (CT) and melt curves in duplicates of reference genes 18S, 19 ribosomal protein S (RPS) and 5 RPS.....	157
Chapter 3	
Figure 3.1 Macroscopic investigation of the limbus and orientation for the dissection of the canine cornea.....	163
Figure 3.2 Tissue dissection for the cell isolation of limbal and central derived CSCs.....	165
Figure 3.3 Set-up of peripheral blood mononuclear cell co-culture.....	178
Figure 3.4 Comparative human and canine macroscopic images of the limbus	179

Figure 3.5 Comparative histological images of the canine and human limbus.....	181
Figure 3.6 Histology of the canine limbus and central cornea with focus on the anterior stroma and basement membrane.....	183
Figure 3.7 Western Blot results of the antibodies tested for cross-reactivity and specificity to dog proteins.....	185
Figure 3.8 Immunohistological staining results with CD90 of the limbal and central cornea.....	187
Figure 3.9 Hair follicle served as positive control for CD90.....	188
Figure 3.10 Internal positive control for alpha smooth muscle actin (α -SMA).....	189
Figure 3.11 Immunohistology of the corneal stroma with keratocyte markers Lumican, Keratocan and ALDH1A3 (positive control)	190
Figure 3.12 Phase contrast image of limbal epithelial cells and outgrowing corneal stromal cells (CSC) and immunocytological staining of short term cultured corneal stromal cells (P0)	192
Figure 3.13 Morphological changes of corneal stromal cells (CSC) during cell culture expansion and confluency.....	194
Figure 3.14 Comparison of the mean maximal culture time and passage frequency in four limbal and five central derived corneal stromal cells (CSC)	195

Figure 3.15 Comparison of the cell numbers of limbal and central corneal stromal cells (CSC) over six passages.....	197
Figure 3.16 Comparison of the population doubling time and cumulative cell doublings of limbal and central corneal stromal cells (CSC)	198
Figure 3.17 Morphological classification of corneal cells cultured isolated from fresh corneal tissue.....	199
Figure 3.18 Comparison of the relative classification of the cell culture composition between limbal and central CSCs.....	201
Figure 3.19.A (I) Immunocytological staining results of limbal corneal stromal cells (CSC).....	203
Figure 3.19.A (II) Immunocytological staining results of limbal corneal stromal cells (CSC).....	204
Figure 3.19.B (I) Immunocytological staining results of central corneal stromal cells (CSC).....	205
Figure 3.19.B (II) Immunocytological staining results of central corneal stromal cells (CSC).....	206
Figure 3.19.C (I) Immunocytological staining results of adipose derived MSCs.....	207
Figure 3.19.C (II) Immunocytological staining results of adipose derived MSCs.....	208

Figure 3.20 CD34 positive control on peripheral blood mononuclear cells.....	209
Figure 3.21 Flow cytometry results of MSC markers and Pax6 in limbal CSC.....	210
Figure 3.22 Results of trilineage differentiation of limbal and central corneal stromal cells in comparison to adipose derived MSCs.....	212
Figure 3.23 Mytomycin C (MMC) growth arrest assay of limbal corneal stromal cells (CSC)	214
Figure 3.24 Evaluation of limbal corneal stromal cell density for peripheral blood mononuclear (PBMC) co-culture assay.....	215
Figure 3.25 Co-culture results of allogeneic limbal CSC with peripheral blood mononuclear cells (PBMCs).....	216
Figure 3.26 Results of the cell culture conditions of corneal stromal cells (CSC) undergo keratocyte differentiation.....	218
Figure 3.27 Morphological change of corneal stromal cells (CSC) in keratocyte differentiated cells (KDC) in keratocyte differentiation media.....	219
Figure 3.28 Immunocytochemical staining results of limbal corneal stroma cell derived keratocyte differentiated cells (CSC-KDC).....	221
Figure 3.29 Fold change of gene expression (qPCR) of corneal stroma cell derived keratocyte differentiated cells (CSC-KDC).....	222

Figure 3.30 Relative gene expression data of α -SMA in corneal stromal cell derived keratocyte differentiated cells (CSC-KDC) cultured without and without basic fibroblastic growth factor (bFGF).....	222
--	-----

Chapter 4

Figure 4.1 Change of cell morphology and cell orientation of adipose derived mesenchymal stromal cells (adMSC) cultured in corneal stem cell media (CSSC) followed by keratocyte differentiation media (KDM).....	242
---	-----

Figure 4.2 Influence of the seeding density and basic fibroblastic growth factor on cell expansion of adipose derived mesenchymal stromal cell differentiated keratocytes (adMSC-KDC).....	243
--	-----

Figure 4.3 The cell morphology of adipose derived MSC differentiated keratocytes (asMSC-KDC) cultured in keratocyte differentiation media (KDM) in comparison to limbal CSC-KDC.....	244
--	-----

Figure 4.4 Adipose derived MSC cultured in corneal stromal stem cell media (CSSC).....	246
--	-----

Figure 4.5. A Adipose derived MSC cultured in corneal stromal stem cell (CSSC) followed by keratocyte differentiation media.....	247
--	-----

Figure 4.5. B Adipose derived MSC cultured in corneal stromal stem cell (CSSC) followed by keratocyte differentiation media (KDM).....	248
--	-----

Figure 4.6 Relative gene expression level of adipose derived MSCs with and without pre-culturing in CSSC media followed by keratocyte differentiation.....250

Figure 4.7 Comparison of the relative gene expression level of keratocyte, stem cell genes and α -SMA of corneal and adMSC derived cells and their keratocyte-differentiated cells.....252

Chapter 5

Figure 5.1 Manual passaging of canine induced pluripotent stem cells (ciPSC) on feeder cell.....267

Figure 5.2 Differentiation protocol of canine induced pluripotent stem cells (ciPSC), neural crest induction (Media2), CSSC media culture and keratocyte differentiation.....271

Figure 5.3 Comparison of different seeding densities for the neural crest induction.....275

Figure 5.4 Change of cell morphology with increased concentration of SB431542 and CHIR99021.....277

Figure 5.5.A Immunocytochemical staining results of ciPSCs induced neural crest cells (ciPSC-NCC) cultured in Media 1 (10 μ M SB431542, 1 μ M CHIR99021).....278

Figure 5.5.B Immunocytochemical staining results of ciPSCs induced neural crest cells (ciPSC-NCC) cultured in Media 1 (10 μ M SB431542, 1 μ M CHIR99021).....279

Figure 5.6.A Immunocytochemical staining results of ciPSCs induced neural crest cells (ciPSC-NCC) cultured in Media 2 (20μM SB431542, 2μM CHIR99021).....	280
Figure 5.6.B Immunocytochemical staining results of ciPSCs induced neural crest cells (ciPSC-NCC) cultured in Media 2 (20μM SB431542, 2μM CHIR99021).....	281
Figure 5.7 Change of cell morphology of canine iPSC neural crest differentiated cells (ciPSC-NCC) in corneal stromal stem cell (CSSC) and keratocyte differentiation media (KDM).....	283
Figure 5.8.A Immunocytochemical staining results of canine iPSC neural crest differentiated cells (ciPSCs-NCC) cultured in CSSC media.....	284
Figure 5.8.B Immunocytochemical staining results of canine iPSC neural crest differentiated cells (ciPSCs-NCC) cultured in CSSC media media....	285
Figure 5.9.A Immunocytochemical staining results of ciPSCs-NCCs cultured in corneal stromal stem cell (CSSC) and keratocyte differentiation media (KDM).....	286
Figure 5.9.B Immunocytochemical staining results of ciPSCs-NCCs cultured in corneal stromal stem cell (CSSC) media and keratocyte differentiation media (KDM).....	287
Figure 5.10 The relative gene expression level of keratocyte-, neural crest-, stem cell genes and α-SMA of ciPSCs, ciPSC-NCCs derived cells cultured in CSSC media and their keratocyte differentiated cells.....	289

Figure 5.11 Comparison of fold change of gene expression level to the keratocyte differentiation (KD) in corneal stromal cells, adipose derived MSC and canine iPSCs.....291

List of tables

Chapter 1

Table 1.1 Description of different stages of activated keratocytes and the phenotype (adapted from Hassell and Birk 2010).....	41
Table 1.2 Summary of clinical, histological aspects and mode of inheritance in canine corneal stromal dystrophy.....	52
Table 1.3 Dog breeds of the AHT ophthalmology population diagnosed with corneal stromal dystrophy between 2007-2015.....	53
Table 1.4 Overview of mesenchymal stromal cells of the human, bovine, and porcine corneal stroma.....	82

Chapter 2

Table 2.1 Donor details of dogs.....	124
Table 2.2 Overview of protein markers.....	130
Table 2.3 Components of the SDS-polyacrylamide gel with different densities.....	137
Table 2.4 Overview of protein markers and secondary antibodies used in western blot assay.....	142
Table 2.5 Primer design settings.....	146
Table 2.6 Overview of primers details.....	147

Table 2.7 Summarises the efficiency test of canine specific designed primers on positive control RNA and the associated standard curves.....150

Chapter 3

Table 3.1 Overview of primary antibody, secondary and IgG isotype controls used in flow cytometry.....172

Table 3.2 Overview of flow cytometry results of three donors.....210

Chapter 1: General introduction

The introduction will provide a basic understanding of the ultrastructure of the cornea, followed by an introduction to the corneal pathology that initiated this research. The general concepts of stem cells are explained followed by a literature review of the limbal stem cell niche and human corneal stromal stem cells. The current research of canine MSCs and the status of canine iPSCs are described followed by the status of cell-based therapies in human corneal regenerative medicine.

The introduction aimed to provide an overview into a research field that is mainly based on human and laboratory animal studies; however, the literature was compared to studies in dogs when available.

1.1. The cornea: embryology, ultrastructure and function

The cornea is a highly organised nearly transparent tissue forming the anterior part of the fibrous tunic of the eye. The cornea is an essential part of the biodefense and refractive system of the eye.

The basic anatomic structure of the cornea is similar between mammals and is composed of an anterior epithelium and its basement membrane, a broad stroma, and the Descemet's membrane, which is the basement membrane formed by a single layered-posterior endothelium. However, a distinct layer comparable to the acellular anterior limiting lamina composed of thin, less organised fibrils (Bowman's layer) that is present in the human cornea does

not exist in dogs (Figure 1.1) (Wilson 2020). The central cornea thickness (CCT) in adult dogs based on ultrasonic pachymetric measurements is $603.7 \pm 43.4\mu\text{m}$ (Guresh, Horvath et al. 2021), with the superior perilimbal corneal thickness being significantly greater than inferior, nasal and temporal perilimbal thickness (Hoehn, Thomasy et al. 2018). The CCT increases with age and weight (Hoehn, Thomasy et al. 2018) and female dogs have significantly thinner corneas (Gilger, Whitley et al. 1991). A recent publication measured a higher CCT of $629.73 \pm 64.57 \mu\text{m}$, by spectral-domain optical coherence tomography (Wolfel, Pederson et al. 2018) but Hoehn and colleagues measured a significantly lower CCT when using Fourier domain optical coherence tomography than ultrasound pachymetry (Hoehn, Thomasy et al. 2018).

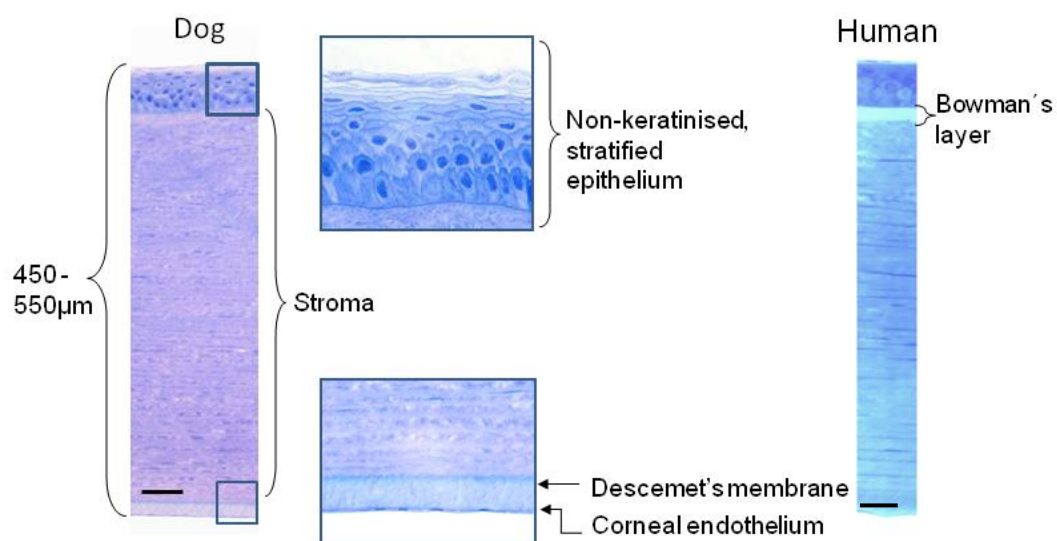


Figure 1.1 Layers of the canine and human cornea.

Histological section of the canine cornea demonstrating the three cellular layers composed of a non-keratinised stratified epithelium (magnified in the grey box), stroma and endothelium (magnified in the grey box). The Bowman's layer which is an acellular layer below the basement membrane of the anterior epithelium (human), is absent in the dog. The Descemet's membrane is the basement membrane of the corneal endothelial cells. The endothelial cells form a single layer. (Dog: H&E stain, human: Toluidine blue; epoxy resin embedded, scale bar: 50 µm)

A) Embryology

The cornea develops from the cranial ectoderm. The stratified epithelium covering the outermost surface of the cornea is of ectodermal origin, whereas the corneal stroma and the endothelial cell layer are both derived from neural crest cells. Stromal cells continue to proliferate and synthesize extracellular matrix (ECM). They become embedded in the ECM and change their morphology from mesenchymal cells towards flattened keratocytes. The expression of collagen and its interaction with proteoglycans (keratan, chondroitin/dermatan sulphate, lumican, mimecan) are essential for fibrillogenesis and the development of a clear cornea. Most studies are based on chickens, humans and mice (Lwigale 2015).

Keratocytes become entrapped in the developing stroma, become quiescent at E14 in chicks and after eyelid opening in mice and are believed to stay in a “dormant” state until normal corneal homeostasis is disturbed by an insult (Lwigale 2015).

In the dog at day 25 of gestation, the lens vesicle is detached from the surface ectoderm and the surface ectoderm is intact. The mesenchyme, mostly of neural crest origin surrounds the optic cup. The surface ectoderm, which will develop into the corneal epithelium, secretes a thick acellular matrix, the primary stroma, which is composed of collagen fibrils and glycosaminoglycans. Mesenchymal neural crest cells migrate between the „corneal stroma“ and the vesicle of the lens. The proteolysis of collagen IX triggers hydration of hyaluronic acid which forms the first anterior chamber (Figure 1.2 A).

Developing keratocytes secrete collagen I fibrils and fibronectin and form the secondary stroma. Subsequent dehydration occurs resulting in less fibronectin production and the stroma is reduced in thickness and contains less fluid. The developing endothelial cell layer contributes to the dehydration of the cornea. At day 30-35 of canine gestation, patches of endothelial cells become confluent and zonula occludens are developing as well as the first Descemet's membrane. The corneal endothelium forms when periocular neural crest cells migrate between the corneal epithelium and vesicle of the lens. The neural crest cells form a monolayer that covers the posterior surface of the cornea and will transition from mesenchyme-to-epithelial cells (Cook 2013). In reptiles, birds, and humans, the corneal endothelium forms because of neural crest cell migration into the region of the developing cornea. In rodents, cats, dogs, rabbits, and cattle, the cells closest to the lens vesicle transition from mesenchyme to epithelium and merge to form a single endothelial layer (Lwigale 2015) (Figure 1.2 C). In the dog, the cornea achieves relative transparency at the end of gestation (58 to 68 days).

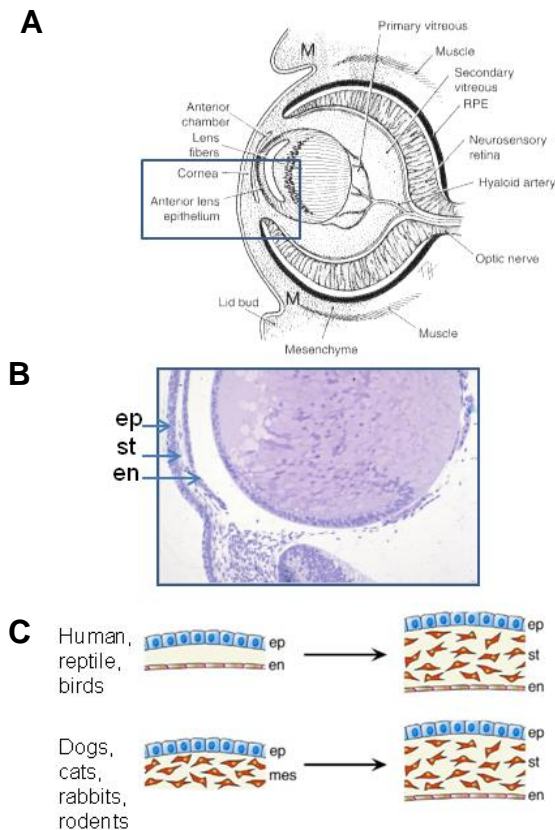


Figure 1.2 Overview of the developing canine eye and cornea

A) The developing canine eye (day 29 of gestation) is surrounded by mesenchyme (M) of neural crest origin. The first primitive cornea is formed during the developing anterior chamber. The lid buds start to form, and primary lens fibres are visible. The hyaloid artery enters the optic cup and anastomoses with the capillaries of the tunica vasculosa lentis. B) The axial migration of mesenchyme forms the corneal stroma (st) and endothelium (en). The epithelium is of ectodermal origin (ep) (H&E stain, adapted from Cook 2013). C) The schematic demonstrates species-specific differences in neural crest cell migration between the corneal epithelium (ep) and lens during the formation of the corneal endothelium (en) and stroma (st). mes, neural crest mesenchyme. In humans, reptiles and birds, the endothelium (en) is formed because of neural crest cell migration into the developing cornea. In dogs, cats, rabbits, and rodents the periorcular neural crest cells migrate as mesenchyme. The cells closest to the lens vesicle (see A) will transition from mesenchyme to epithelium and form a single endothelial layer. (Adapted from Lwigale 2015).

The developmental processes of the cornea are under the control of multiple signaling pathways during the ocular development, but the exact mechanisms of how these neural crest genes interact are not completely

understood. Morphogens (retinoic acid), signaling molecules (bone morphogenetic protein (BMP4), transforming growth factor (TGF- β , Wingless Int-1 (Wnt) and fibroblastic growth factor (FGF), and transcription factors (Pax6, Sox2, Sox 3, Pitx2, and Fox genes) are involved in the corneal development (Lwigale 2015).

Pax6 is a critical factor during the formation of the anterior eye. The activity of the *Pax6* gene is controlled by the MicroRNA miR450b5p and is responsible for maintaining the multipotent state of the surface ectoderm (Shalom-Feuerstein, Serror et al. 2012). *Pax6* is one of the first ocular transcription factors expressed in the neural plate, then in the primitive eye cup and later, in corneal tissue progenitors. Lens vesicle detachment is a critical stage in the eye development and requires a diploid level of *Pax6* expression (Tidu, Schanne-Klein et al. 2020). The lens fails to detach from the overlying cornea resulting in an opaque cornea in aniridia and in the mouse heterozygous small eye (*Sey*) model. A precise level of expression of *Pax6* is necessary for a complete and normal corneal development (Shaham, Menuchin et al. 2012).

Pax6 is expressed in all cells of the anterior eye development, but at different time points and intensities. In a limited number of ocular cells and tissues, other genes such as *PITX2*, *PITX3*, *FOXE3*, *FOXC1* and *c-MAF* co-regulate the same and similar processes as *PAX6* (Cvekl and Tamm 2004).

A high expression of *Pax6* in surface ectoderm cells and the lens, corneal epithelium, iris, and ciliary epithelial cells are required for the expression of transcription factors *Six3*, *c-Maf*, *MafA/L-Maf* and *Prox1* for the migration of

neural crest cells into the eye. Whereas a low expression of Pax6 plays a role in the formation of corneal endothelium and keratocytes and differentiation of trabecular meshwork (Chow and Lang 2001, Cvekl and Tamm 2004). In most differentiated cells, Pax6 is downregulated but remains present in mature cell such as the corneal epithelial, lens epithelial, retinal amacrine cells (Macdonald and Wilson 1997).

Wnt/ β -catenin signaling pathway is of major importance in the corneal development and has a paracrine effect on the corneal stroma. Expression of Frizzled receptors (Fzd) correlated with an activation of Wnt signaling in the stromal mesenchyme and corneal endothelium (Liu, Mohamed et al. 2003). Fzd3 is involved in neural crest cell induction and migration. A reduced expression of Fzd3 and Fzd4 coupled with upregulation of Fzd10 is required for corneal cell differentiation and avascularity (Tidu, Schanne-Klein et al. 2020).

TGF β 2 and TGF β 3 is essential for neural crest cell migration, differentiation, and proliferation, and is expressed by the lens epithelium. TGF β -induced upregulation of several regulators of ECM remodeling and collagen synthesis leading to the transition from proliferative to differentiating neural crest cells (Ma and Lwigale 2019).

Retinoid acid is synthesised in the neuroepithelium and optic cup and induces expression of the transcription factors Foxc1 (forkhead box C1) and the homeodomain transcription factor Pitx2 in the periocular mesenchyme. Foxc2 and Foxc1 together are essential for the morphogenesis of the ocular surface via the Wnt signaling. In corneas of Foxc1 $^{-/-}$ mice, the epithelium is

thickened, the stroma is disorganised and the endothelial cells are undifferentiated (Tidu, Schanne-Klein et al. 2020).

Canine specific reports are not available. However, transcription factors and cell-signalling factors such as Wnt are highly evolutionarily conserved in animals and are expected to be similar across animal species. A report of canine Pax6 deficiency as a large animal model for aniridia similar in people, showed that the gene organisation and map location were highly homologous with that of the human gene (Hunter, Sidjanin et al. 2007).

B) Corneal epithelium

The canine epithelium is a non-keratinised, stratified squamous epithelium of 25-40 μm thickness, composed of a basement membrane formed by mitotically active columnar basal cells, which generate new suprabasal cells as well as secrete matrix molecules to maintain the basement membrane and stroma. The basal cells are attached to the basement membrane via hemidesmosomes. The wing cell layer is composed of 2-3 layers of polyhedral cells that rarely undergo division and migrate to the 2-3 layers of superficial squamous cells. They have extensive desmosomes and lateral zonula occludens at their lateral junctions to protect against pathogens and prevent the draining of the precorneal tear film into the tissue. On the ocular cell surface are extensive microvilli and microplicae that associate with the mucin layer of the precorneal tear film (Samuelson 2013). The cornea is avascular; hence the corneal metabolism relies on the oxygen from the tear film and aqueous humour. The corneal epithelial metabolism utilises glucose,

amino acids, and vitamins from the aqueous humour via diffusion. However, the corneal epithelial cells can store glycogen (Thoft & Friend, 1977).

C) Corneal stroma

The substantia propria, which occupies approximately 90% of the entire thickness of the cornea, is composed of keratocytes, a small proportion of immune-competent cells, extracellular matrix (collagen, crystalline aldehydes, proteoglycans) and water.

There are approximately 2.4 million keratocytes in the human adult cornea. Keratocytes are “quiescent cells” that form a syncytium and communicate via gap junctions at the end of their long dendritic processes (Moller-Pedersen, Ledet et al. 1994, Watsky 1995). Keratocytes have a compact cell body (15-20µm) with numerous cytoplasmic lamellipodia, that gives them a dendritic-like or stellate morphology and form interconnections between cells in a three-dimensional network (Muller, Pels et al. 1995, Hahnel, Somodi et al. 2000). The compact cell body minimises the surface area of the keratocytes that are exposed to light, and this probably serves to reduce light scattering while their processes provide cell-cell communications. In all levels of the cornea, keratocytes are highly spatially organised in a clock-wise direction similar to a cork screw (Forrester, Dick et al. 2016) (Figure 1.3 B).

The anterior third of the human cornea has more stromal keratocytes with 2-3 times more mitochondria, which correlates with the higher oxygen tension of the anterior cornea (Muller, Pels et al. 1995, Hahnel, Somodi et al. 2000). An *in vivo* confocal microscopy study in dogs has also shown a higher cell

density in the anterior stroma, and that the shape of the cell bodies changes from a more bean-shaped to an elongated shape morphology in the posterior stroma (Kafarnik, Fritsche et al. 2007) (Figure 1.3 E-F). In healthy Beagles the anterior stroma contains 993 ± 134 cells/mm² and 789 ± 87 cells/mm² in the posterior stroma (Strom, Cortés et al. 2016).

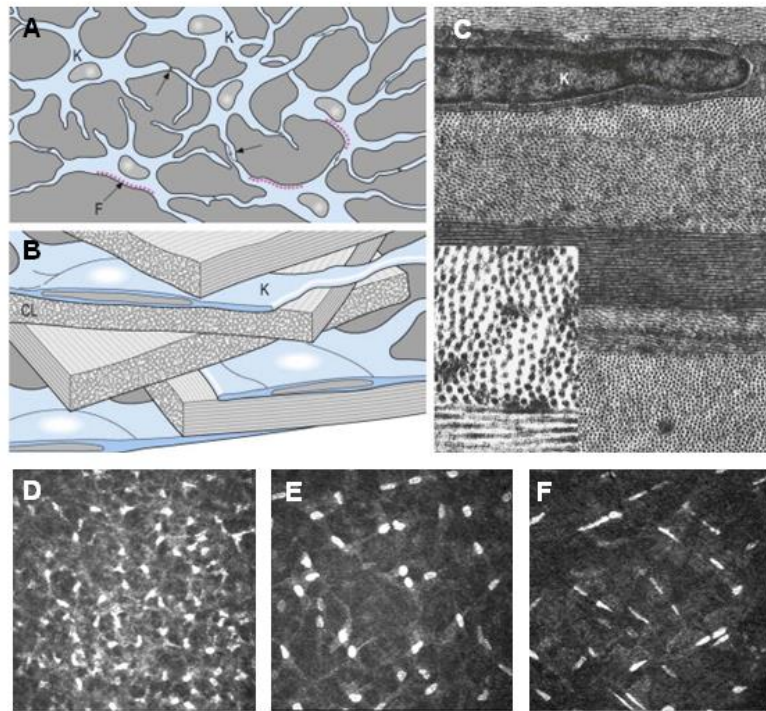


Figure 1.3 Organisation of keratocytes and corneal collagen lamellae

A) The schematic diagram shows, that the dendritic keratocytes (K) communicating via gap junctions (black arrows) and fenestrations (F). B) The collagenous lamellae (CL) are strictly arranged in a cork screw like pattern and interposed are the flattened keratocytes (K); C) The electron micrograph is illustrating a keratocyte nucleus (K) in between the regularly spaced collagen lamellae, the inset is demonstrating the collagen fibrils (longitudinal and cross- section), collagen I has diameter of 25nm (original magnification: $\times 20\,000$) (A-C) is adapted from (Forrester, Dick et al. 2016) D) In vivo confocal microscopy images of the canine cornea with higher cell density in the anterior stroma, E) bean-shaped cell bodies in the mid stroma and F) reduced cell density and elongated cell bodies in the posterior stroma (384x384 μm image size) (adapted from (Kafarnik, Fritsche et al. 2007).

Keratocytes can be activated to differentiate into fibroblasts and myofibroblasts in response to injury. Corneal wound healing is very complex and not all mechanisms involved are fully understood. For example, keratocyte mitosis and migration and myofibroblast transformation of keratocytes is regulated by a wide range of factors including transforming

growth factor (TGF β 1-3), fibroblast growth factor (FGF), epidermal growth factor (EGF), platelet-derived growth factor (PDGF), Tenascin, connective tissue growth factor (CTGF), insulin-like growth factor (IGF) and Substance P (Maycock and Marshall 2014).

The following table provides a summary of different terms used in the human literature of cell types, origin and phenotypical description of keratocytes and their different forms (Hassell and Birk 2010) (Table 1.1).

Cell Type	Cell Derivation	Phenotype
Keratocytes	Keratoblasts	Replace the hyaluronan-rich ECM with an ECM consistent with transparency containing densely packed collagen fibrils and proteoglycans during late embryonic and post-natal development
Quiescent Keratocytes	Keratocytes	Contain a low level of biosynthetic activity to maintain the ECM produced by keratocytes
Hypercellular Myofibroblasts	Keratocytes/Quiescent Keratocytes	Contain α smooth muscle actin and produce <u>low levels</u> of ECM which results in densely packed cells in a sparse ECM
Myofibroblasts	Hypercellular Myofibroblasts	Contain α smooth muscle actin and produce a <u>high level</u> of ECM, but containing components like hyaluronan that are normally not present and which results in an ECM inconsistent with transparency
Wound Fibroblasts	Hypercellular Myofibroblasts	Are possibly myofibroblasts and produce an ECM of densely packed fibrils and proteoglycans that restores transparency
Corneal Fibroblasts	Keratocytes/Quiescent Keratocytes	Result from cell culture in media containing fetal bovine serum. A varying proportion contain α smooth muscle actin

Table 1.1 Description of different stages of activated keratocytes and the phenotype (adapted from Hassell and Birk 2010).

In addition to keratocytes, can a small population (10-15%) of bone marrow-derived immune cells found in the peripheral and central cornea of human and mice. The innate immunity is controlled by dendritic cells, mast cells (MCs), macrophages, natural killer cells, innate lymphoid cells (ILC) and $\gamma\delta$ T cells. The main cells are comprising tissue-resident macrophages (histiocytes), dendritic cells (Langerhans cells, LCs), MCs, lymphocytes, and ILCs. The corneal limbus contains lymphatic and capillarie vessels that serve as exit and entry routes for the immune cells (Liu and Li 2021). In dogs, LCs were found in the stroma of the corneal limbus, conjunctival epithelium and very small numbers in the central cornea (Williams 2005).

Keratocytes secrete collagen, glycosaminoglycans (GAGs) and crystalline proteins (such as ALDH1A1), which all contribute to corneal transparency (Jester 2008).

The ECM of the stroma is composed of collagen fibrils of mainly collagen I which is combined with collagen V in most species, to a lesser degree type III, VI and XII. Collagen fibrils are uniformly arranged into lamellae with a strict periodicity of 620-640Å which allows 99% of light entering the cornea to pass without scattering. There are approximately 300 corneal lamellae in the human central cornea; most lamellae are mainly composed of bundles of collagen I and V fibrils of 25nm with 20nm space around them (Dawson, Ubels et al. 2011). In the dog, collagen lamellae in the central portion (253 lamellae, 796 nm/lamellae thickness) were nearly the same in number but were thinner than in the peripheral cornea (236 lamellae, 1113 nm/lamellae) (Nagayasu, Hirayanagi et al. 2009). The degree of fibre branching in the

canine stroma is similar to other mammals and was higher anterior than the more lamellar and non-branching posterior stroma. This correlated positive to corneal stiffness (Leonard, Cosert et al. 2020).

The collagen fibrils are associated with proteoglycans that form 15-25% of stroma, whereas the majority of the stroma (75-85%) is composed of water (Meekins, Rankin et al. 2021).

The molecular basis of corneal transparency is not only based on the lattice-like structure of collagen fibrils which will produce minimal light scattering. It is known that the interaction of collagens, proteoglycans and crystalline proteins are equally essential factors.

Proteoglycans (PG) are complex extracellular macromolecules. They consist of a multidomain core protein with one or more glycosaminoglycan (GAG) chains attached (PG= GAGs + core protein) (Figure 1.4). There are nine members of small leucine-rich proteoglycans (SLRPs), of which the following are most relevant for the cornea: decorin, mimecan, lumican and keratocan. Their function is to provide tissue volume and spatial order of collagen fibrils as well as resisting compressive forces and provide viscoelastic properties. The GAGs side chains extend into the interfibrillar spaces. SLRPs are composed of 10-15 nm diameter globular core protein with attached GAGs, 7 nm wide x 45-70 nm in length. They reach into the stroma perpendicular to the collagen fibril (Figure 1.4 B). GAGs are charged negatively, and are stiff polymers that extend into the space, where they form duplexes with adjacent GAG- side chains (Hassell and Birk 2010, Dawson, Ubels et al. 2011).

The genes that produce four types of corneal stromal proteoglycans: *Decorin*, contains a single dermatan sulphate GAG side chain, *Keratocan* contains three, whereas *Lumican* and *Mimecan* have a single keratan sulphate GAG side chain (Hassell and Birk 2010). The human cornea consists mainly of 60% keratan sulphate GAGs (70nm) and 40% dermatan sulphate GAGs (45nm). Briefly, GAGs are repeated disaccharides of galactose and N-acetylglucosamine or iduronic acid and N-acetylgalactosamine (Scott 1995). Dermatan sulphate can bind more water and is found at higher concentrations in the more oxygen-rich anterior portion of the cornea, whereas keratan sulphate is found in the posterior stroma with lower oxygen levels and less water binding capacities (Scott and Bosworth 1990). These studies are based on bovine, mice and human corneas; there is one report available in dogs comparing different SLRPs in various tissues. In the cornea, the relative expression of *Lumican* and *Decorin* was highest but *Fibromodulin*, *Biglycan*, *Versican*, *Osteoglycin* and *Prolagin* were also expressed (Yang, Culshaw et al. 2012).

Defective proteoglycan synthesis has been shown to result in blindness with disrupting the organisation of the collagen fibrils resulting in corneal dystrophies. Knockout of *keratocan* in the cornea of mice lead to thin corneas and increased collagen fibril diameter, but the cornea stayed transparent (Liu, Birk et al. 2003). Whereas *Mimecan* and *lumican* knockout mice have also increased diameter of corneal collagen fibrils but only the *lumican* deficient mice have opaque corneas (Chakravarti, Petroll et al. 2000, Tasheva, Koester et al. 2002) (Figure 1.4 E).

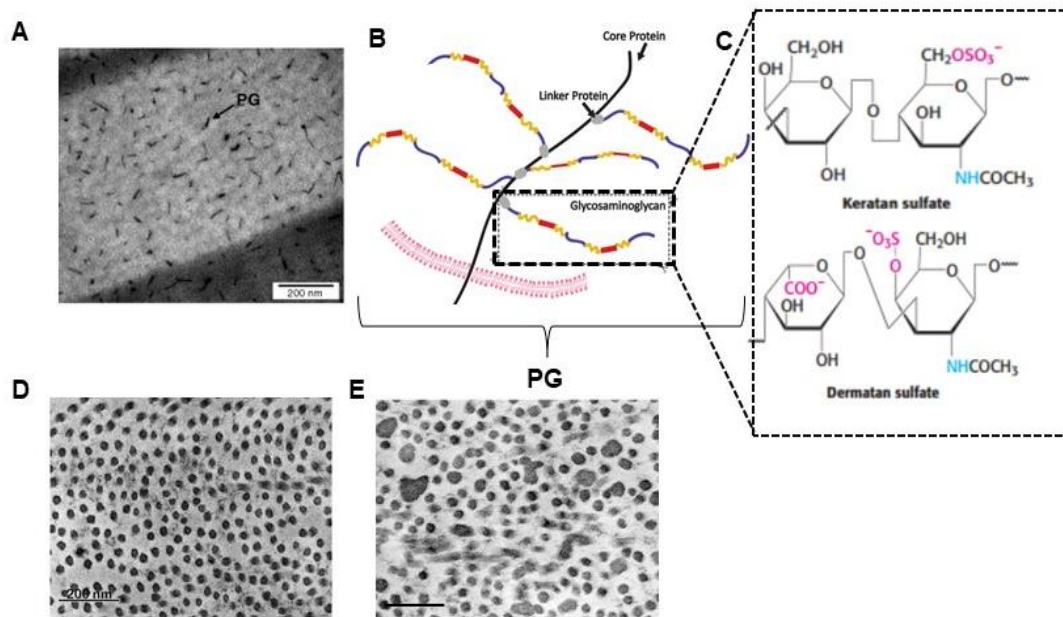


Figure 1.4 Corneal proteoglycans

A) Transmission electron microscopy image (TEM) of proteoglycans (PG) (black arrow) extending in the interfibrillar space and showing a distribution of $110 \pm 96 \text{ nm}^2$ in the human cornea (adapted from Akhtar et al. 2008). B) Schematic illustration of a PG which is composed of a core protein, a linker protein to which single or multiple glycosaminoglycan chains are attached (modified from ambio.com). C) Chemical structure of single units of GAGs such as chondroitin sulphate and keratan sulphate which are most relevant in the corneal stroma (modified from (Berg, Tymoczko et al. 2011)). D) TEM imaged of the regular fibril arrangement in a wildtype mouse in comparison to (E) a Lumican null mouse which alters regulation of fibril assembly primarily in the posterior stroma (adapted from Hassell and Birk 2010).

In a wide range of species, corneas express corneal crystallins, which are water-soluble proteins/enzyme. They contribute to the maintenance of corneal transparency and have a role in UV light absorption (Jester et al., 2007; Pei et al., 2006; Stagos et al., 2010). Many of these corneal crystallins are identical to lens crystallins (i.e. aldehyde dehydrogenase 1A1 (ALDH1A1)/ η -crystallin, α -enolase/ τ -crystallin, glutathione-S-transferase/ Ω -crystallin, lactic dehydrogenase/ ϵ -crystallin, glyceraldehyde-3-phosphate

dehydrogenase (G3PDH)/ π -crystallin, and arginino-succinate lyase/ δ -crystallin). The most common corneal crystalline in most mammals is ALDH3A1, which is protective against UV and oxidative stress-induced apoptosis. Like in the lens, it has been proposed that corneal crystallin proteins in corneal epithelial cells and keratocytes accumulating to a high proportion to limit light scattering. A study in mice has shown that there are different ALDHs in the cornea such as ALDH3A1, which was present in higher quantities than ALDH1B1 followed by ALDH2 > ALDH1A1 > ALDH7A1 >ALDH1A3> ALDH3A2 > ALDH1A2 > ALDH4A1 (Stagos, Chen et al. 2010, Kumar, Dolle et al. 2017). Canine-specific reports are not available.

D) Corneal endothelium

Descemet's membrane (DM), is the basement membrane of the corneal endothelium and is composed of collagen (I, III, IV, V, VI, VIII) and non-collagenous components (fibronectin, laminin, heparan sulphate) (Murphy 1993, Levy, McCartney et al. 1995, Samuelson 2013). DM has a thickness of approximately 10-15 μm in adult dogs and increasing DM thickness with increasing age is presumed but has not been reported in dogs (Murphy 1993). The DM is approximately two times thicker in the dog than in humans (Engerman and Colquhoun 1982). The corneal posterior endothelium is a single layer of hexagonal cells, that are described as quiescent in humans (G0/1 phase) whereas in young dogs in response to an injury, increases of the mitotic rate and cell hypertrophy of 14% and 86% respectively, have been reported (Gwin, Warren et al. 1983). The endothelial cell density is >3600 cells/mm² in dogs <1 year (Kafarnik, Fritsche et al. 2007). The number will

decrease with age. The corneal endothelial cells contain a Na-K-ATPase active pump mechanism to maintain hydration of the cornea, which will decompensate with a cell number of 800-500 cell/mm² and lower (Gwin, Lerner et al. 1982, Kafarnik, Fritsche et al. 2007).

E) Corneal innervation

The cornea is a highly innervated and corneal nerves arising from the short ciliary nerves of the ophthalmic branch of the trigeminal nerve (Murphy 1993). Several stromal nerves enter the cornea in the anterior-mid stroma to form an arborising, dichotomous network of sensitive and sympathetic, unmyelinated nerves ending as free nerve endings in the corneal epithelium. Histochemical and in vivo confocal microscopy studies on canine corneal innervation found an anterior stromal plexus and a rich epithelial innervation, of horizontally oriented “basal epithelial leashes” similar described in humans (Marfurt, Murphy et al. 2001, Kafarnik, Fritsche et al. 2008). “Leash” axons in all areas of the corneal epithelium oriented mainly towards a common locus from the perilimbal cornea towards the centre (Marfurt, Murphy et al. 2001).

The corneal innervation is not only essential for the protection of the eye but has also plays a key role in maintaining the cornea through the production of neuropeptides (Substance P, Neurokinin A) and neurotransmitters (Acetylcholine) (Sloniecka, Le Roux et al. 2015). For example, a synergistic effect of Substance P, EGF and insulin-like growth factor (IGF1), increase epithelial migration and mitosis (Nakamura, Nishida et al. 1997, Marfurt, Murphy et al. 2001).

1.2 Canine corneal stromal disease

1.2.1 Canine corneal stromal dystrophy

Corneal dystrophy in dogs is defined as a primary, bilateral, not necessarily symmetrical, inherited disorder of the cornea that is primarily not accompanied by corneal inflammation or systemic disease (Ledbetter 2013).

Corneal dystrophy can affect different layers of the cornea and in the majority of dog breeds the stromal layer is affected. In crystalline stromal dystrophy, opacities are in the stromal layer caused by deposits of phospholipids and cholesterol and shows similarities to Schnyder's corneal dystrophy in humans (SCD). This type of corneal dystrophy is a condition described only in humans and dogs. The term crystalline stromal dystrophy is used for the disease described in Cavalier King Charles Spaniel and Rough Collies (Crispin 2016). Historically, there are different terms used in different breeds (Table 1.2), therefore the following introduction uses the wider term of corneal stromal dystrophy.

Clinically grey-white, crystalline opacities in the central or paracentral cornea often with round, circular, and well-demarcated edges are seen, commonly in young adult dogs, with a varying degree of progression (Figure 1.5). The overlying corneal epithelium is commonly intact and of normal thickness. Extracellular crystals of lipids predominate; however, chronicity of lipid accumulation may lead to cell death, with secondary inflammation and corneal vascularisation, which is then commonly named corneal

degeneration (Ledbetter 2013). The pathogenesis remains unknown, but a fundamental metabolic/enzyme defect in keratocytes in the coolest part in the cornea (central) is presumed, the role of the temperature remains also unknown (Crispin 2002).

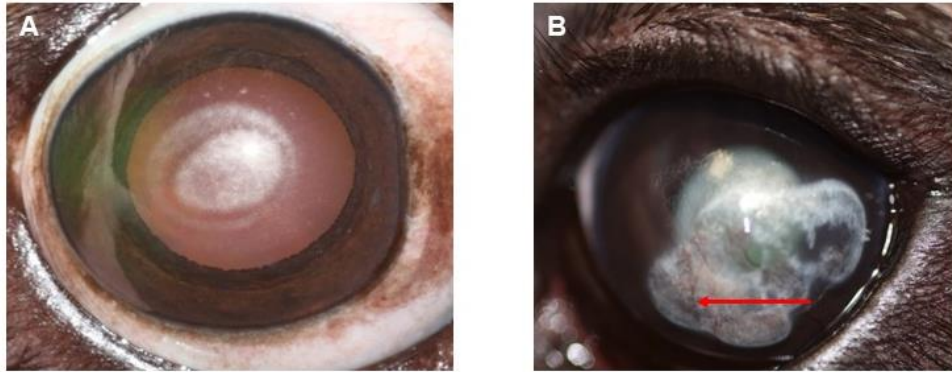


Figure 1.5 Canine corneal (crystalline) stromal dystrophy

A) Photography of the corneal crystalline dystrophy in the axial cornea in 2.8-year-old, male-neutered Cavalier King Charles Spaniel. B) Marked corneal stromal dystrophy and secondary neovascularisation (red file) in a 1.2-year-old female German shepherd. The blood results in both patients showed an absence of hyperlipoproteinaemia and normal thyroid function.

Histopathological investigations found predominantly free and esterified cholesterol, but also free fatty acids whereas triglycerides were absent. The phospholipid production is upregulated. Phosphorylation of lipids allows forming an emulsion up to a critical point and then crystallization occurs (Figure 1.6). Electron microscopy has demonstrated intra- and extracellular laminated vacuoles in abnormal fibroblasts (= keratocytes). The epithelium, basal lamina, Descemet's membrane and endothelial cells were intact (Crispin 1988).

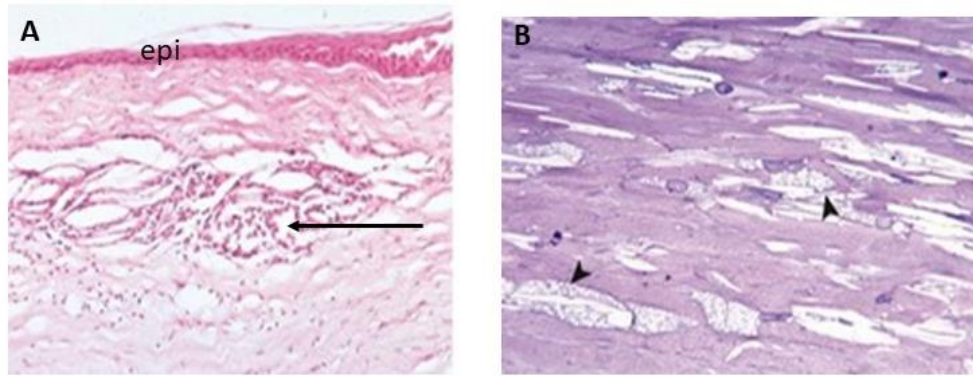


Figure 1.6 Histopathology of canine stromal dystrophy

A) Histopathology of a cholesterol deposits and a secondary granuloma (black arrow in the midsuperficial stroma; epi, epithelium (stain: H&E). B) The image shows keratocytes with vacuolated cytoplasm with accumulated lipid contents (black arrows heads) (Toluidine blue stain). Images are modified from (Dubielzig, Ketring et al. 2010).

To diagnose corneal stromal dystrophy, systemic disease influencing the lipid metabolism, serum chemistry, high-density/low-density lipoprotein, cholesterol, triglycerides, blood glucose, phosphorus and calcium levels need to be tested to rule out thyroid and adrenal disease (Crispin 2016).

There is no current treatment for corneal dystrophy; a low-fat diet may prevent the progression of the disease, whereas topical anti-inflammatories can lead to the progression of the disease. The opacity can progress to corneal blindness. Surgical removal (keratectomy) will lead to a initial clinical improvement but complete recurrence is seen as very likely (Whitley and Hamor 2021). Clinical follow-up studies in dogs are missing.

Corneal stromal dystrophy occurs in many dog breeds. A prevalence of as high as 15% were demonstrated in Beagle dogs in which hyperlipidaemia was excluded (Roth, Ekins et al. 1981). The incidence remains unknown. The mode of disease inheritance is not clear and appears to vary between

breeds. (Roth, Ekins et al. 1981, Waring 1986, Crispin 1988). Pedigree analyses for Cavalier King Charles Spaniels, Rough Collies and Siberian Huskies were performed. In Rough Collies with stromal dystrophy an autosomal dominant mode or multifocal mode of inheritance were considered. Test matings in Siberian Huskies suggested possible recessive mode with variable expression (Waring 1986). Many breeds seem to be predisposed and a hereditary component is assumed in the Afghan hound, German Shepherd, Samoyed, Bichon Frise (Cooley and Dice 1990). Whether the different forms of corneal stromal dystrophy in various dog breeds are of the same (genetic) disease entity is unknown. There is no gender predisposition described, however, in females a hormonal component might influence the onset and progression as seen in bitches in oestrus, lactation and pregnancy (Crispin 2002).

The following table (Table 1.2) summarises clinical appearance, age of onset, pathology, and mode of inheritance of canine corneal stromal dystrophy (epithelial and endothelial corneal dystrophies are not included).

Stromal dystrophy	Breed	Age	Clinical appearance	Pathology	Inheritance
Central “oval”crystalline dystrophy (*1-4)	Beagle (84/497= 16% ,8-15y) ^{1,2}	Young adult	3-5mm nebular type (superficial 1/3 stroma), race-track type (full-thickness); white arc (full thickness)	Neutral fats (intra- and extracellular), cholesterol (intracellular), phospholipids (intracellular) ^{3,4}	-
Central “oval”crystalline dystrophy (*5)	Siberian Husky	5-27 month	Round, oval central, clinical 5 forms described with the first involving the posterior stroma developing through 5 th form affecting entire stroma		Recessive trait with variable penetrance
Crystalline corneal dystrophy (*6)	Cavalier King Charles Spaniel	2-4 years	Subepithelial, paracentral “bull eye” shaped. Sometimes lesions occur after the first estrus	Cholesterol and phospholipids	Polygenic mode of inheritance
Stromal corneal dystrophy (*7)	Airedale Terrier	9-11 month	Eosinophilic reflective bodies, subepithelial and deep stromal	Lipid	Possible x-linked, recessive pattern
Subepithelial corneal dystrophy (*8)	Rough Collie		Central and paracentral, subepithelial; can start after the estrus	Cholesterol, phospholipids, free fatty acid	-

Table 1.2 Summary of clinical, histological aspects and mode of inheritance in canine corneal stromal dystrophy

*The table provides an overview of the clinical age of onset, clinical appearance, pathology and mode of inheritance of canine corneal stromal dystrophy in different breeds. **

references: 1. (Waring, Muggli et al. 1977), 2. (Waring, Ekins et al. 1979), 3. (Roth, Ekins et al. 1981), 4. (Ekins, Waring et al. 1980). 5. (Waring 1986), 6. (Crispin 1987), 7. (Dice 1974), 8. (Crispin 1988).

A retrospective survey of the ophthalmology referral population at the Animal Health Trust revealed that the total number of dogs diagnosed with corneal

stromal dystrophy between 2007-2015 included 123 patients of 23 different breeds, of which 15% were presented with concurrent corneal ulcerations (19/123) and 7% (9/123) underwent a corneal surgery. Breeds with two or fewer representatives were not included in Table 1.3.

Dog breeds	Number of dogs diagnosed with corneal stromal dystrophy /total number presented to the ophthalmology department (2007-2015)	= %
Cavalier King Charles Spaniel *	38/248	15.3
Siberian Husky*	3/23	13.0
Bichon Frise	11/98	11.2
Boxer	17/165	10.3
Labrador Retriever	27/1006	2.6
Yorkshire Terrier	3/127	2.4
English Springer Spaniel	3/162	1.8
Border Collie	3/317	0.9
Golden Retriever	3/397	0.7

Table 1.3 Dog breeds of the AHT ophthalmology population diagnosed with corneal stromal dystrophy between 2007-2015.

*The table summarises the results of a retrospective survey of the AHT ophthalmology referral population of dogs diagnosed with corneal stromal dystrophy. Breeds with <2 representatives are not listed. *, described in the literature. Most commonly presented was the Cavalier King Charles Spaniel, followed by the Labrador Retriever (represented only 2.6% of the referral population of this breed) and the Boxer. All dog breeds listed apart from the CKSP (*) and Siberian Husky (*) are not described in the literature.*

Schnyder's corneal dystrophy in humans is known to be a rare corneal autosomal dominant disease that starts in the first or -second decade of life. The central, but also the peripheral cornea can be affected. The affected

peripheral cornea forms an arcus lipoides (Seitz and Lisch 2011, Moshirfar, Bennett et al. 2021).

An arcus lipoides formation is not described in any form of corneal stromal dystrophy in dogs (compare Figure 1.5 A, B and Figure 1.7 A, B). Bilateral corneal arcus lipoides in dogs, in contrast to humans, is associated with systemic hyperlipoproteinaemia, most commonly secondary to metabolic diseases such as hypothyroidism (Crispin 2002).

In human SCD, dermal fibroblasts can be involved in the disease progression, but this has been not reported in dogs. An Ubi A prenyltransferase domain containing 1 (*UBIAD1*) mitochondrial alteration has been postulated as a presumed causative mutation that affects cholesterol metabolism. *UBIAD1* encodes a prenyltransferase and interacts physically with apolipoproteins (Orr, Dube et al. 2007, Nickerson, Kostihä et al. 2010). In ten families with SCD novel mutations in the *UBIAD1* gene have been described and immunohistochemistry revealed that wild type and one of the mutant proteins (N102S) were localised subcellularly to mitochondria using antibodies specific for *UBIAD1* protein in keratocytes (Nickerson, Kostihä et al. 2010).

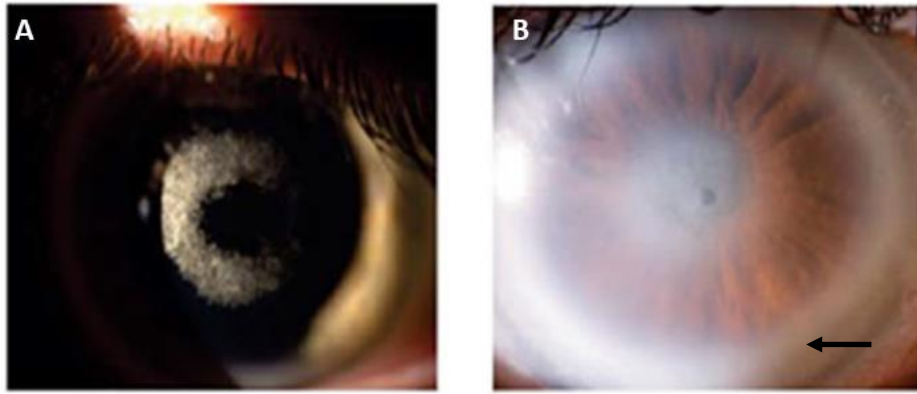


Figure 1.7 Clinical appearance of Schnyders corneal dystrophy in human patients with confirmed *UBIAD1* gene mutation.

The photographs are modified from (Nickerson, Kostihina et al. 2010). A) Photograph of the cornea demonstrating paracentral crystalline deposition (25-year-old male). B) Central crystalline deposit, peripheral haze, and an arcus lipoides (black arrow) are present in a 61-year-old male.

Genetic analysis in Cavalier King Charles Spaniels is currently under investigation and has so far excluded an *UBIAD 1* mutation (Maini, Ricketts et al. 2018)

1.2.2 Corneal fibrosis

Human and veterinary patients are frequently subjected to corneal injury (Gray and West 2014, Labelle, Psutka et al. 2014), the cause of which may be pathological or surgical after a transplant procedure (Guell, Verdaguer et al. 2015) or conjunctival grafting (Pumphrey, Pizzirani et al. 2011). Regardless of the aetiology, fibrosis can result in loss of corneal transparency due to dysregulated healing (Fini and Stramer 2005). Corneal fibrosis is one of the main causes of blindness in people worldwide (Pascolini and Mariotti 2012, Robaei and Watson 2014).

Demographic and molecular biological studies in dogs with chronic corneal fibrosis are lacking in the veterinary literature. The long-term outcome of corneal surgeries in dogs after corneal suturing or graft surgery/keratoplasties are believed to be poor due to chronic corneal fibrosis and loss of transparency (Figure 1.8).

Veterinary patients presenting with ocular injuries that result in corneal fibrosis are clinically common (Kern 1990). Impaired visual field and depth perception may result in reduced quality of life also in dogs, decreased performance and work. Visually impaired service dogs and guide dogs for blind people, are unable to safely perform, execute search and rescue operations. An *in vitro* and *in vivo* canine fibrotic model for human research was established given the similar the corneal dimensions to humans. An anti-fibrotic agent would help physician but also veterinary ophthalmologists (Gronkiewicz, Giuliano et al. 2016, Berkowski, Gibson et al. 2018).

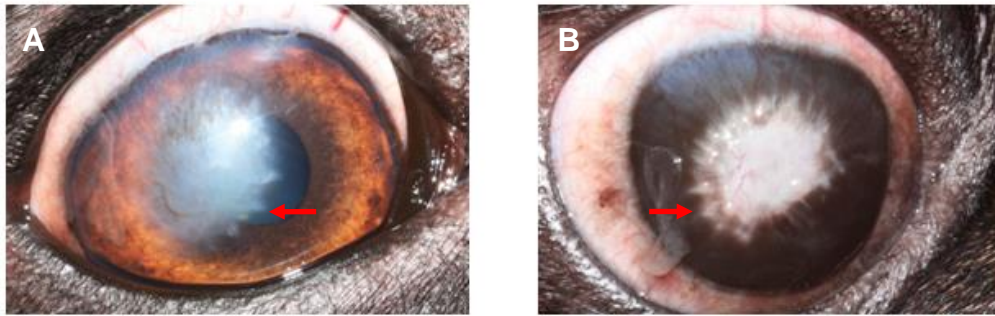


Figure 1.8 Clinical presentation of corneal fibrosis after corneal graft surgery

The clinical photographs demonstrate the clinical outcome after an amnion graft surgery for a deep stromal ulcer (i.e., Descemetocoele, not perforated) A) axial and para-axial corneal fibrosis, 3-month post-surgery in a 2.5-year-old male Labrador Retriever. B) Axial, dense fibrosis with complete peripheral pigmentation and vascularisation of the cornea 2.5-month post-surgery in a 5-year-old female Pug; (the red arrows indicate the fibrotic extension where sutures have been placed).

Corneal wound healing is a complex process, of numerous cytokines, activation of keratocytes, formation of both fibroblasts and myofibroblasts, increase of ECM and matrix metalloproteinases (MMP) up-regulation (Medeiros, Marino et al. 2018).

One of the key cytokines is TGF- β 1, which has been shown to be a major player in corneal fibrosis via modulation of Smad proteins, keratocytes get converted into myofibroblasts, matrix metalloproteinases (MMP) are upregulated, and deacetylation of histones (Sharma, Sinha et al. 2015). TGF- β 1 can also activate other mitogen-activated protein kinases (MAPKs) such as extracellular sigma regulated kinases (ERK), c-Jun N-terminal kinase (JNK) and p38 MAPK (Tandon, Tovey et al. 2010).

The molecular mechanism has been also studied in canine corneal fibroblasts *in vitro*. TGF- β 1 treatment caused increase in phosphor-Smad2/3

and phosphor-p38 MAPK signaling (but not ERK) and *MMP1/MMP9* mRNA expression but not *MMP2* expression (Gronkiewicz, Giuliano et al. 2016).

The development and persistence of mature myofibroblasts is a critical in the development of fibrosis of the stroma. TGF- β and PDGF will transform (rabbit) keratocyte-derived and fibrocyte-derived precursors into vimentin +, α -SMA desmin + mature myofibroblasts (Chaurasia, Kaur et al. 2009).

Myofibroblasts are contractile cells with decreased intracellular crystallin expression and production of disorganised ECM. The increased deposition of type I collagen and fibronectin lack the fibrillary organisation and volume fraction necessary for appropriate light transmission. Corneal fibroblasts are also generated by trauma or infections, but tend to be transient and produce only small amounts of disarranged ECM (Hassell and Birk 2010).

Stromal cells themselves produce TGF- β , but the amount is insufficient to drive myofibroblast differentiation, however the epithelium and/or the aqueous humour do provide sufficient levels. The integrity of epithelial basement membranes (EBM), anterior and posterior (=Descemet's membrane), play a critical role because they form a barrier to reduce the amount of ("profibrotic") TGF- β 1, TGF- β 2 (both heparin binding), the non-heparin-binding TGF- β 3 and PDGF into the stroma (Kim, Mohan et al. 1999, Rider 2006). TGF- β 1 and TGF- β 2 are described as pro-fibrotic whereas TGF- β 3 is a fibro-modulatory partner to the other two isoforms to control the response to injury (Wilson 2021). TGF- β and PDGF continue to reach into the stroma if the EBM of the epithelium is delayed in healing or the

regeneration is defective. Hence activating the development of myofibroblasts (Medeiros, Marino et al. 2018).

Whether all myofibroblasts undergo apoptosis or some myofibroblasts could revert to a fibroblast with a keratocyte phenotype remains not fully known. An *in vitro* study in rabbit corneal keratocytes has shown that heparin, FGF-1 or FGF-2 reversed the myofibroblast and had impact on the fibroblast phenotype and it was concluded that these are not final differentiated cells (Maltseva, Folger et al. 2001).

Suberanilohydroxamic acid (SAHA) is a histone deacetylase inhibitor (HDAC), which can block TGF- β signal transduction. Pirfenidone (5-methyl-1-phenyl-2[1H]-pyridone) is a nonpeptide pharmacologic agent, which has demonstrated significant efficacy as an inhibitor of TGF- β and may have an inhibitory effect on platelet-derived growth factor (PDGF) and connective tissue growth factor (CTGF). Both have shown promising first results in an ex vivo canine corneal wound model to reduce corneal fibrosis (Berkowski, Gibson et al. 2018).

1.2.3 Surgical treatment of Schnyder's dystrophy and other corneal stromal dystrophies

In human ophthalmology, surgical treatment options includes the use of an excimer laser for phototherapeutic keratectomy (PTK) as the method of choice (Fagerholm 2003, Köksal, Kargi et al. 2004). PTK can be repeated and therefore postpone a corneal transplantation (lamellar or penetrating)

(Seitz and Lisch 2011). Steger and co-workers (2016) used femto-laser-assisted lamellar keratectomy (in eight patients) and additional deep anterior lamellar keratoplasty (if required) and described a recurrence rate of one to 15 years (Steger, Romano et al. 2016).

Laser-based surgical treatments are highly precise but expensive tools that are not available in the field of veterinary ophthalmology. Surgical removal of the dystrophic corneal stroma in dogs is performed via a manual superficial lamellar keratectomy with or without an additional graft (amnion, cornea, conjunctival graft). The surgery will only lead to a short interval of clinical improvement and complete recurrence is likely (Whitley and Hamor 2021).

Corneal transplantation in dogs is rare due to a shortage of donors, expensive storage costs, and the lack of a canine corneal tissue bank (Gelatt 2011). An understanding of corneal immunology and corneal allografting in domestic animals is very limited. In the last decade, there has been a clinical attempt to develop and improve corneal surgery, i.e. lamellar, penetrating keratoplasty surgery in dogs using frozen or fresh corneas (Whitley and Hamor 2021). A recent study in dogs used corneal autografts harvested from healthy peripheral cornea of the ipsilateral eye with a limited set depth of 0.3 mm (Jaksz, Fischer et al. 2021). In human ophthalmology penetrating keratoplasties have a survival rate of 86% after one year but decline over ten years to 62% in low-risk corneal transplants (Aboshiha, Jones et al. 2018). Corneal transplants classified as “high risk” are vascularised corneas with previous episodes of inflammation. In “high-risk” corneal transplants, rejections occurred in 30%–60% of grafts. Despite local or systemic

immunosuppressive therapy, up to 70% failed within 10 years (Armitage, Goodchild et al. 2019, Mahabadi, Czyz et al. 2021). Evidenced-based studies in veterinary ophthalmology are limited to one study where a clinical allograft rejection rate of 56% has been reported. This can be explained by the fact that the majority of patients belong to a “high risk” host group with pre-existing neovascularisation and chronic keratitis. However, the success in restoring the corneal anatomy was 85% with some subjective improvement of sight over 200- day follow-up (Lacerda, Pena Gimenez et al. 2016).

1.3 General introduction to stem cells

Stem cells are present during the embryonic, fetal, juvenile, and adult life. Stem cells are undifferentiated cells found in multicellular organisms and have the ability to self-renew, and to differentiate into several specialised cell types. Stem cells are classified upon their potential of differentiation or their tissue origin. Stem cells classified according to the ability to differentiate into different lineages are totipotent, pluripotent, multipotent oligopotent and unipotent stem cells (Burgess 2016).

a) The most undifferentiated cells are totipotent stem cells. These are found in the fertilized oocyte or zygote and resulting from the two first cell divisions. These cells will differentiate into all the extraembryonic and embryonic tissues (Burgess 2016).

b) Embryonic stem cells (ESCs) are pluripotent stem cells and forming the inner cell mass. The blastocyst is composed of the inner cell mass and the trophoblast. The inner cell mass will form three primary germ layers (ectoderm, mesoderm, endoderm) and the trophoblast will form the placenta. These undifferentiated cells express several transcription factors: NANOG (Tir nan Òg, “the mythical Celtic land of youth”), sex determining region Y HMG-box 2 (Sox2), octamer-binding transcription factor (OCT4) and reduced expression-1 (Rex-1) (Burgess 2016).

c) Multipotent stem/stromal cells are found in adult tissues and can differentiate into multiple lineages. Mesenchymal stromal cells (MSCs) are multipotent stem cells, originally identified in the bone marrow stroma, and

are also found in the adipose tissue, heart muscle, uterus or the corneal stroma (Burgess 2016). There is a controversy whether tissue-specific mesenchymal stem cells are true stem cells and it is postulated to use the term multipotent mesenchymal stromal cell, which was taken into account in the present study (Horwitz, Le Blanc et al. 2005). MSCs have the following features: they are fibroblast-like plastic-adherent, express multiple stromal cell markers such as CD105, CD90, CD73 and they have the ability to generate colonies in culture (colony-forming units (CFU)) and differentiate into osteogenic, chondrogenic and adipogenic lineages driven by by specific culture conditions (Dominici, Le Blanc et al. 2006). Hematopoietic stem cells give rise to lymphoid and myeloid lineages and present also MSCs located in the bone marrow (Burgess 2016).

d) Oligopotent stem cells have limited capacities to differentiate into lineages within a specific tissue but still exhibit self-renewal. An oligopotent progenitor are found in as conjunctival keratinocytes and goblet cells in the human ocular surface (Pellegrini, Golisano et al. 1999). Whereas in pigs and mice, oligopotent stem cells with the capacity to generate individual colonies of conjunctival and corneal cells (Majo, Rochat et al. 2008).

e) Limbal epithelial stem cells (LESC) in the human cornea are unipotent stem cells have self-renewal capacities and differentiate into one specific cell type (i.e. one single lineage) (Burgess 2016).

1.3.1 Waddington's landscape and reprogramming

Waddington's epigenetic landscape is a model to illustrate the stem cell potency which has long been thought of a "one-way path". The downhill progression from an undifferentiated stem cell to a physiologically mature cell (Waddington, 1957). Cells "roll down" this landscape into deeper, inescapable developmental valleys (i.e. cell lineages representing cell fate determination) until they reach a stable state at the bottom (i.e. representing their final cell fate) (Figure 1.9).

The pathways reflect the ability of pluripotent and multipotent stem cells to differentiate into a different lineage, depending on where the "ball" descends. The "basin" where the ball potentially stops, corresponds to a state of potency. The "ridges" represent the prevention to develop from one cell fate into another "valley" (i.e. determined cell fate) (Wiley, Burnight et al. 2015).

However, since 1957 stem cell research discovered that cell fate appears to be more interchanagable and not that rigid, 'transdifferentiation', 'dedifferentiation', 'transdetermination' and 'reprogramming' describe the conversion of cell fates (Takahashi 2012).

Using still the illustration of Waddington's landscape, describes dedifferentiation to the process where cells roll "back up" of their differentiation path and become more immature, to finally convert into the pluripotent stem cell state. Transdifferentiation, transdetermination and reprogramming is the process of cells to progress from one cell fate to another without "going up", i.e. reaching pluripotency before differentiating

into a nother cell fate. This refers to crossing “a ridge” in the epigenetic landscape of Waddington. However, the precise meaning and use of these terms are differently used (Takahashi 2012).

The dedifferentiation was discovered by the use of ‘reprogramming factors’. This is the combination of four transcription factors OCT3/4 (also known as POU5F1), SOX2, Krüppel-like factor 4 (KLF4) and cellular “Myelocytomatosis” (MYC) factor, to revert differentiated somatic cells to an embryonic cell fate similar to embryonic stem cells. The term “reprogramming” is commonly used when describing the return to a differentiated cell back to a pluripotent state (Takahashi and Yamanaka 2006).

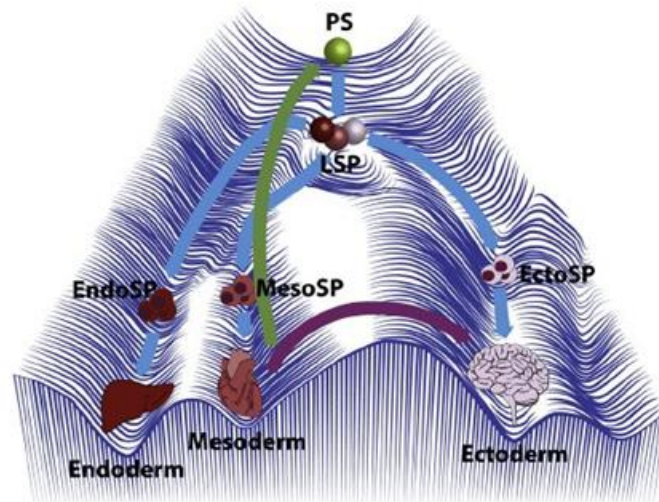


Figure 1.9 The epigenetic landscape of Conrad Waddington

Waddington (1957) proposed that pluripotent stem cells (PS) undergo differentiation into lineage specific progenitor cells (LSP) and then stepwise differentiation (blue arrows), into lineage-specific progenitor cells (EndoSP, MesoSP and EctoSP) followed by germ layer-specific progenitor cells. These layer-specific progenitor cells produce cells of germ layer-specific organs for example the endoderm (liver), mesoderm (heart) and ectoderm (brain). Gurdon and Yamanaka demonstrated that somatic cells from any germ layer could be reprogrammed into pluripotent stem cells, “dedifferentiation” (green arrow) and directly converted from one somatic cell type into another somatic cell type (purple arrow) via direct reprogramming or “transdifferentiation”. The illustration is modified from (Wiley, Burnight et al. 2015).

1.4 Stem cells in the corneal limbus and stroma

1.4.1 Anatomical aspects of the limbus

The limbus is the transition zone localised at the interface between the cornea and the conjunctiva and sclera. In humans, the limbus is a ring of tissue (approximately 1mm) that is demarcated by the corneal Bowman’s layer. The human limbal epithelium is composed of a nonkeratinised multi-layered stratified epithelium. Within the limbal epithelium, in contrast to

epithelium of the central cornea, melanocytes and mature MHC-II + cells (i.e. Langerhan's cells) are present. Within the limbal zone, basal cells are small and less columnar than basal cells of the corneal epithelium (Dziasko and Daniels 2016).

Morphological features of the limbal basal cells such as small cell size and a high nuclear/cytoplasmic (N/C) ratio have been suggested as phenotypes to correspond to limbal epithelial stem cells (LESCs) (Romano, Espana et al. 2003, Chen, de Paiva et al. 2004). This has been similarly described in the canine limbus (see 1.4.2) (Morita, Fujita et al. 2015, Patruno, Perazzi et al. 2017).

The limbal stromal connective tissue of the human cornea is irregularly arranged than in the central cornea and contains capillaries, small arterioles, venules and lymphatic vessels, nerves. The limbal stroma hosts a mixed population of cells: limbal stromal cells (with mesenchymal stromal cell characteristics, also referred to corneal stromal stem cells (CSSCs) (Hertsenberg and Funderburgh 2015), mast cells, Langerhan's cells, melanocytes, T-lymphocytes (Baum 1970, Vantrappen, Geboes et al. 1985), fibroblast-like cells and keratocytes (Dziasko and Daniels 2016, Yazdanpanah, Haq et al. 2019).

In the canine corneoscleral junction, the anterior corneal epithelium is continuous with the bulbar conjunctiva. The corneoscleral junction is oblique and often pigmented, where the deep stromal part is more posterior than the anterior. The stromal collagen fibres are less organised in the junction to the

sclera (Murphy 1993). There are no detailed anatomical/histological reports of the limbus (epithelium/stroma) available in dogs.

Within the limbus region, the palisades of Vogt and limbal crypts interact with the underlying stroma to form a “niche” that hosts a subpopulation of small, putative stem cell limbal epithelial stem cells (LECS) (Figure 1.10). The palisades of Vogt correspond to undulations of the epithelium and the stroma and can be seen as radiating lines on slit lamp biomicroscopy. Here, the epithelium is marked by the intervening stromal areas. Histologically, the limbal epithelial crypts are the “interpalisades” that appear as thick ridges filled by epithelial cells (Yazdanpanah, Haq et al. 2019). Direct cellular interaction between limbal epithelial stem cells and stromal cells and interruption of the basement membrane is described in humans (Dziasko, Armer et al. 2014).

The major anatomical difference comparing dogs to humans is the absence of limbal crypts and palisades of Vogt, instead a slight invagination of the epithelium in the stroma is described (Patrino, Perazzi et al. 2017). Well-defined palisades of Vogt are present in the pig but not in the rabbit and rodent eyes (Gipson 1989, Notara, Schrader et al. 2011). In rabbits, epithelial rete ridges that project into the subjacent stroma, exhibits discontinuities with the basal lamina which is interrupted with evidence of direct interaction between stromal and limbal epithelial cells (Goldberg and Bron 1982, Gipson 1989, Goes, Barbosa et al. 2008). Detailed histological and molecular investigations of the limbus in dogs are lacking.

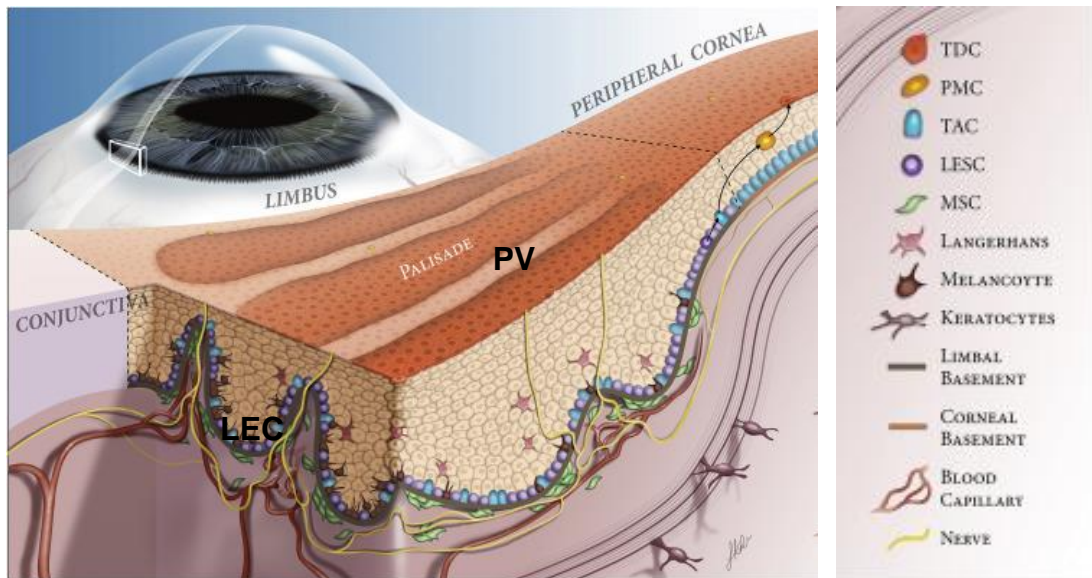


Figure 1.10 Overview of the human limbal niche

Schematic drawing adapted from Yazdanpanah et al. 2019 illustrating the human limbal niche, containing the Palisades of Vogt (PV) and limbal epithelial crypts (LECs), which are highly innervated and vascularised. The limbal epithelial stem cells (LESCs) are in close contact with melanocytes and mesenchymal stromal cells (MSCs). For maintaining homeostasis, the limbal basement membrane is focally interrupted and therefore different to the peripheral cornea. In the basal epithelial layer of the LEC, the LESCs can divide in two identical cells (symmetrically) or asymmetrically, which then give rise to LESCs and further transient amplifying cell (TAC). The TACs or basal epithelial cells divide into cells, that are postmitotic (PMCs) when they migrate centripetally. The PMCs are further differentiated into terminally differentiated cells (TDCs) towards the surface.

1.4.2 Limbal epithelial stem cells and corneal epithelial homeostasis

Limbal epithelial progenitors are unipotent stem cells and are small in size in the basal cell layer. During normal corneal homeostasis LESC are in a quiescent state. *In vitro*, epithelial can generate colonies of tight, packed epithelial cells (Arpitha, Prajna et al. 2005). *In vitro* LESCs generate

holoclones with a high proliferative potential cultured on growth-arrested irradiated mouse fibroblasts (3T3) (Pellegrini, Golisano et al. 1999).

The following panel of putative stem cell markers used in combination to define LESC (Secker and Daniels 2008): cytokeratins such as CK15, CK14 and CK19 (Yoshida, Shimmura et al. 2006, Schlotzer-Schrehardt, Dietrich et al. 2007), transporters proteins such as ABCG2 and ABCB5 (Watanabe, Nishida et al. 2004, Ksander, Kolovou et al. 2014) transcription factors such as Pax6, p63 α and its Δ Np63 α isoform (Di Iorio, Barbaro et al. 2005, Kawakita, Shimmura et al. 2009), cell adhesion molecules and receptors including N-cadherin, Frizzled 7 (Mei, Nakatsu et al. 2014), Notch-1 (Thomas, Liu et al. 2007) and in mice integrin β 1 and α 9 were found (Pajoohesh-Ganji, Pal-Ghosh et al. 2006). A recent study using single cell transcriptomic profiling of human cornea identified novel markers such as probable serine carboxypeptidase (CPLV), caveolin-1 (CAV1), homer scaffolding protein 3 (HOMER3) in the corneal epithelial limbal stem cell niche. Highly proliferative transit amplifying cells expressed cyclin-dependent kinases regulatory subunit 2 (CKS2), stathmin 1 (STMN1) and ubiquitin conjugating enzyme E2 C (UBE2C), whereas C-X-C motif chemokine ligand 14 (CXCL14) was expressed only in the suprabasal limbus. Exclusively stromal keratocytes expressed N-methyltransferase (NNMT) (Català, Groen et al. 2021).

A recent study in our lab investigated the canine limbus. In most dogs the limbus was densely pigmented, limbal epithelial basal cells were expressing the stem cell marker Δ Np63, and Pax6. A colony efficiency test was positive at an early stage of passages of cells arising from the limbus (Dziasko,

Sanchez, Daniels 2021 in submission). Another group concluded that ABCG2 expression was localised in the basal layer of the limbal epithelium and was significantly higher than Δ Np63, whereas Δ Np63 was widely detected in the entire corneal epithelia (Morita, Fujita et al. 2015).

The corneal epithelium is constantly renewed throughout life, it has been proposed, based on rabbit models, that the epithelial half-life is approximately 9 weeks whereas every 9-12 months, the entire corneal epithelium is renewed (Sharma and Coles 1989). In dogs, this information is limited, but in most species once the entire corneal epithelium is removed, the surface can be re-epithelialised within 48 to-72hours (Whitley and Gilger 1999).

The X, Y and Z hypothesis of Thoft and Friend 1983 postulated that vertically corneal epithelial cells grow from the basal cell layer to the surface (X) and cells migrate centripetal (Y). This had to be equal to the cell loss from the corneal surface (Z) (Thoft and Friend 1983). LESC self-renew and generate daughter cells; these are transient amplifying cells (TACs) that have great mitotic potential. Transient amplifying cells (i.e. basal cells of the corneal epithelium) migrate towards the central corneal epithelium and proliferate in the suprabasal layers. Then TACs differentiate into post-mitotic cells, move further vertically and finally terminally differentiated cells and desquamate from the ocular surface (Figure 1.11).

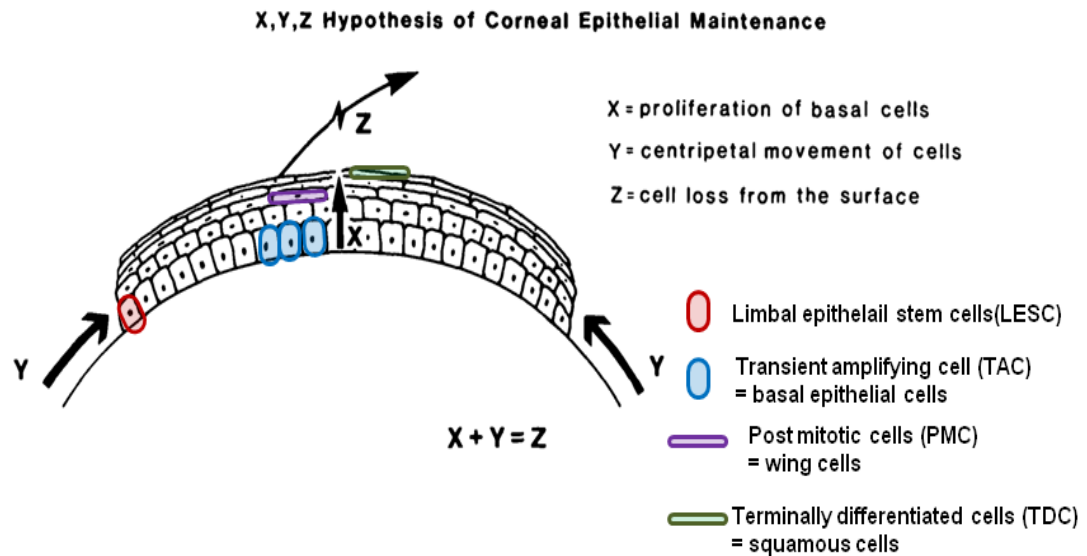


Figure 1.11 X, Y, Z hypothesis of corneal epithelial maintenance

The schematic was modified from Thoft and Friend 1983 and illustrates that transient amplifying cells (TAC) are moving centripetally and proliferating vertically to become postmitotic cells (PMC) to balance the loss of terminally differentiated cells (TDC) desquamating for the corneal surface.

1.4.3 Molecular aspects of the limbal epithelial stem cell niche

The “stem cell niche” is the specific location where adult stem cells reside. Epithelial stem cell niches have been identified in different locations not only in the limbus of the human cornea (Cotsarelis, Cheng et al. 1989) but also in the terminal bronchioles of the epithelial airway (Giangreco, Reynolds et al. 2002), the bulge of the hair follicle (Cotsarelis, Sun et al. 1990), the base of the crypt in the small intestine (Booth and Potten 2000). In dogs, a hair bulge stem cell niche (de Castro, Tavares et al. 2018) has been reported as well as the intestinal stem cells niche (Mochel, Jergens et al. 2017). The hematopoietic niche of humans, dogs and mice showed similar morphology, frequency, and distribution of bone marrow mesenchymal stromal cell within trabecular bone marrow (Meza-León, Gratzinger et al. 2021).

The niche is unique and specialised microenvironment (Dziasko and Daniels 2016). Multiple maintaining factors are involved: 1) direct cell-to-cell interactions, 2) soluble factors, 3) mechanical forces, 4) local extracellular matrix (ECM), and 5) physicochemical factors (pH, O₂).

Briefly, there is evidence of direct limbal epithelial-stromal and melanocyte-epithelial cell interaction (Dziasko and Daniels 2016) and was demonstrated by high-resolution imaging techniques of the human limbal niche (Dziasko, Armer et al. 2014). N-cadherin expressing epithelial cells, a subpopulation of limbal basal epithelial cells and limbal melanocytes, had the greatest secondary colony-forming potential and significantly higher expression of stem cell-related markers (Hayashi, Yamato et al. 2007). Chen and co-workers (2011) found that epithelial cells associated with stromal cells had the highest secondary clonogenic potential and were expressing pluripotent factors such as OCT4, Sox2, NANOG, Rex1, SSEA4 but also vimentin, Nestin, N-cadherin and CD34 (Chen, Hayashida et al. 2011).

A subpopulation of stromal cells expressing vimentin and aquaporin 1 were penetrating the epithelial basal membrane. These were close to K15 and p63 expressing epithelial cell clusters (Higa, Kato et al. 2013). Within the limbal crypts could volume electron microscopy and 3D reconstruction demonstrate focal basement membrane interruptions and direct contact between small basal epithelial cells and stromal cell extensions (Dziasko, Armer et al. 2014).

Cytokines and growth factors influence multiple signaling pathways in the LESC niche. Wingless-related integration sites (Wnts) are secreted signalling glycoproteins. A major player is the conical Wnt/b-catenin signalling pathway

has been demonstrated to regulate the stem cell proliferation and differentiation (Clevers, Loh et al. 2014). Wnt2, Wnt6, Wnt11, Wnt16b are found in the human limbus (Nakatsu, Ding et al. 2011). Wnts bind to the N-terminal extra cellular domain of the Fz receptor family, which then leads to the release of β -catenins from its inhibitory complex, they accumulate and translocate into the nucleus where they activate and suppresses specific target genes (Clevers, Loh et al. 2014).

LEC and underlying stromal fibroblasts expressed interleukin 6 (IL6) and could potentially be involved in epithelial-stromal cell interaction. IL6-induced signal transducer and transcription 3 (STAT3) activation was effective to maintain an undifferentiated state of mouse embryonic stem cells. Notara and colleagues (2010) further described that IL6 expressing cells induced Stat3 time-dependent phosphorylation and when both inhibited (IL6 or STAT3) significant reduction of secondary LEC colonies were observed (Notara, Shortt et al. 2010).

External forces influence the stem cell fate. This refers to the pure compression of neighbouring cells and the surrounding ECM. The extracellular matrix and stem cell interactions can be mediated by integrins (laminins, tenascin, fibronectin, collagen). These are transmembrane receptors connecting the extracellular matrix to the intracellular cytoskeleton. The basement membrane of the limbal epithelium exhibit α 1/ α 2 collagen IV and α 2/ β 2 laminin chains. The central corneal epithelium contains type IV collagen α 3 and α 5 chains (Ljubimov, Burgeson et al. 1995). Ahmed and co-workers (2007) described that limbal epithelial-like cells were derived from

either ESC or corneal central epithelial cells in the presence of various factors and collagen IV (Ahmad, Stewart et al. 2007).

Chondroitin sulphate/dermatan sulphate and certain sulphation motifs are present in stem cell niches in different tissues. Ashworth and co-workers (2020) demonstrated evidence that chondroitin sulphation motifs identified stem cell populations and their activated progenitor cells via protein marker of the chondroitin sulfate (CS) glycosaminoglycan side chains of the 4C3, 7D4 and 3B3, and postulated they play a vital roles in cell to cell signalling, tissue homeostasis and wound healing (Ashworth, Harrington et al. 2020).

In addition, physicochemical factors such as oxygen levels are reported to promote self-renewal or differentiation. Murine ESC lines cultured under 5% O₂ compared to the 20% O₂ conditions were more likely to express pluripotent stem cell markers such as NANOG and OCT4. It was concluded that culturing conditions oxidant cell stress in physiological oxygen (and glucose) and increased the success of establishing new ESC lines (Wang, Thirumangalathu et al. 2006).

1.4.4 Corneal stromal stem cells

A) Cellular and molecular aspects of CSSC

Funderburgh et al. in 2005 first described a small population of Pax6 expressing cells (<4%) in the bovine corneal stroma and identified them as progenitor cells. The Pax6 gene encodes the paired box protein Pax6 (i.e. aniridia type II protein (AN2) or oculorhombin), which is one of the major

transcription factors for ocular embryogenesis and lack protein expression in differentiated keratocytes (Funderburgh, Du et al. 2005).

Stromal cells expressing mesenchymal stem cell markers in the anterior stroma close to the limbus were later also identified in humans. These cells represent less than 1% of the total cell population, however single cells also expressed ATP-binding cassette superfamily G member 2(ABCG2), which is an unspecific stem cell marker for in the anterior stroma of the central cornea (Funderburgh, Du et al. 2005). Cell sorting to enrich for ABCG2 positive cells (named as “side population” cells) showed clonal growth up to 18 passages and expressed stem cell markers such as Polycomb complex protein 1 (Bmi1), translocation-associated receptor Notch1, receptor tyrosine kinase (cKit), sine oculis homeobox (Six2) and Pax6.

The cells were differentiated into keratocytes under serum-free conditions and expressed keratocyte specific genes and proteins such as Keratocan and ALDH (Du, Funderburgh et al. 2005). These putative stem cells were also differentiated into chondrogenic and neurogenic cells as indicators of multipotency.

Following this report multiple publications have now described similar properties of corneal stromal cells in humans and mice using different synonyms, such as limbal stromal niche cells, mesenchymal cells in the limbal stroma and limbal fibroblast-like cells (Branch, Hashmani et al. 2012, Tomasello, Musso et al. 2016). A recent publication relating to human cells has also described a mesenchymal stromal stem cell population that originates from the central corneal stroma. RNA sequencing of these cells

found an expression profile closer to bone marrow-derived MSCs (BM-MSCs) and not to LESC (Vereb, Poliska et al. 2016).

However, for a cell to be characterised as a multipotent mesenchymal stromal cell, the international society for cellular therapy (ISCT) has defined multiple criteria that must be established: expression of CD90, CD105, CD73 (>95%) in absence (<2%) of CD45, CD34, CD14 or CD11b, CD79a or CD19 and HLA-DR expression as well as tri-lineage differentiation into chondrocytes, adipocytes, osteoblasts. Cells must show clonal growth (colony forming units (CFU)) and adherence to plastic culture dishes (Dominici, Le Blanc et al. 2006). Human corneal stromal stem cells fulfill these criteria and are recognised as mesenchymal stromal cells (see 1.4.4 C).

To date the function of CSSC are not fully determined but thought to have support function for LESC (Table 1.4). This theory is supported by the fact that basal epithelial cells in the limbal niche are in direct contact with stromal cells and both cells produce N-cadherin (see 1.4.3). LESC co-cultured with limbal CSSC have higher expansion and clonogenicity rates. This was less intense with central corneal stromal cells (Higa, Kato et al. 2013, Dziasko, Armer et al. 2014). In addition, a role in corneal tissue homeostasis and wound healing is discussed (Vereb, Poliska et al. 2016).

The current literature is based mainly on mouse and human corneal stromal cells; however, a recent porcine study has shown putative limbal CSSC that expressed CD29 and showed cross-reactivity with (anti-human) CD45, CD90, CD105, CD146, and MHC-class I antigens A,B,C (HLA-ABC), but

differentiated into the adipogenic and osteogenic but only the chondrogenic trilineage differentiation (Fernandez-Perez, Binner et al. 2017). At time of writing, studies in canine corneas are not available. Proteomic studies of CSSC are not available in the current literature.

B) Immunomodulatory aspects of CSSC

Like many other mesenchymal stromal cells, CSSC can be immunomodulatory and immune-privileged, which is of great interest for tissue engineering to prevent graft rejection, (details in 1.6).

An *in vivo* study in mice revealed that CSSC injected into a corneal fibrotic model prevented fibrosis and there was no T-cell mediated tissue rejection (Basu, Hertsenberg et al. 2014). An *in vivo* mouse model has shown that TGF β 3 is one of the major components in hCSSC inducing a scar-free corneal response (Weng, Funderburgh et al. 2020). Furthermore, an *ex vivo* model culturing sheep corneas with seeded CSSC after a LASIK procedure (laser in situ keratomileusis) showed significantly increased adherence of LASIK-like flaps and corneal transparency was maintained by the lack of myofibroblasts (Morgan, Dooley et al. 2016).

Importantly, Hertsenberg et al. 2017 demonstrated the secretion of tumor necrosis factor-inducible gene 6 protein (TSG-6) was up-regulated in CSSC in response to tumour necrosis factor α (TNF), and in CSSC during their differentiation process into keratocytes. TSG6 is inhibiting neutrophil migration into the cornea by CSSC was reversed when TSG-6 expression was knocked down (Hertsenberg, Shojaati et al. 2017).

Furthermore, a recent *in vitro* (human) and *in vivo* study in mice has demonstrated that CSSCs induced apoptosis of macrophages. The same study showed in an *in vitro* angiogenesis assay that CSSCs promoted a distinct CD14-CD16-CD163-CD206 immunophenotype in macrophages that reduced the angiogenic effect. An *in vivo* corneal injury study in mice showed when CSSCs were applied to murine corneas, the macrophage infiltration was reduced and CD206 expression in macrophages was increased. Also CSSC-“educated” (i.e. =co-cultured) macrophages demonstrated high expression of CD163, CD206, CD14, and CD16. This was consistent with a profile M2 macrophages, i.e. macrophages phagocytizing apoptotic cells including neutrophils (Eslani, Putra et al. 2018).

Immunosuppressive properties of central derived CSSC were shown to inhibit the proliferation of activated immune cells also in low cell numbers. This was demonstrated by a mixed lymphocyte reaction (MLR). Furthermore, when central derived CSSC were treated with proinflammatory cytokines (TNF α , IFN γ , IL-1 β) and toll-like receptor ligands (LPS, Poly:IC), secretion levels of IL-6, interleukin-8 (IL-8) and C-X-C motif chemokine 10 (CXCL-10) were increased. IL-6 is needed for prostaglandin E2 (PGE2) production and secretion. PGE2 plays a key role in the inhibition of T-cell proliferation and dendritic cell maturation. The authors concluded that CXCL10 which has anti-angiogenic properties, act as a chemokine for MSC, such as CSSCs. CXCL10 basic secretion was also measured in not stimulated central derived CSSC but not in BM-MSCs (Vereb, Poliska et al. 2016).

Recent research is also focused on exosomes and their function in intercellular signalling. Corneal epithelial wound healing was promoted by exosomes from human –CSSC (CSSC-Exo) in an *in vivo* epithelial scratch model using a monolayer of corneal epithelial cells, which showed significantly smaller wound area in the treated compared to the control group (Samaeekia, Rabiee et al. 2018). Human CSSC derived extracellular vesicle (EV) produced EVs with a 130-150 nm in diameter and CD63, CD81, and CD9 surface proteins and are delivery vehicles for miRNAs. Treatment in a *in vivo* wound model in mice with CSSC-EV decreased gene expression of fibrotic genes *Col3a1* and *Acta2* (α -SMA), blocked neutrophil infiltration, and promoted normal tissue morphology (Shojaati, Khandaker et al. 2019).

C) Positive and negative mesenchymal stromal cell markers

There are publications on CSSC from different research groups. These cells were named and characterised differently in various publications. An overview is summarised in Table 1.4. (See ISCT criteria in 1.4.4. A).

Author	Name	Markers (+)	Markers (-)	Colony Forming Potential	Multipotency	Function
Du et al. 2005	Corneal stromal stem cells (CSSC) - human-	Pax6; ABCG2; Bmi1; CD90; CD73	NP	NP	yes	Transparency
Branch et al. 2012	Peripheral and limbal corneal stromal cells (PLCSC) -human-	CD73, CD90, CD105, CD29, CD44, HLA-ABC CD34 (up to P3)	CD11b, CD19, CD34, CD45	yes	yes	Trans-differentiation
Polisetty et al. 2008	Limbal mesenchymal cells - human-	CD90; CD105; vimentin; CD29	CD34	yes	yes	-
Vereb et al. 2016	Corneal Stroma-derived MSC-like cells (CSMSC of the central cornea) -human-	CD73, CD90, CD105, CD140b	CD34, CD45, CD11a, CD31, CD69, CD133, HLA-DR, VEGFR2	NP	yes	Corneal tissue homeostasis, immunomodulatory
Nakatsu et al. 2014	Limbal Mesenchymal cells -human-	CD105; CD34+; N-cadherin; vimentin	NP	NP	NP	Support for LESC
Chen et al. 2011	Limbal niche cells -human-	CD34; Nanog; SSEA4; Sox2; Nestin; N-cadherin	NP	Np	NP	Support for LESC
Li et al. 2012	Limbal nice cells -human-	D73, CD90, and CD105	CD34, CD31, and CD45	yes	yes	Stromal wound healing, anti angiogenesis
Tomaseilo et al. 2016	Limbal fibroblast-like stem cells (fLSC) -human-	ABCG2, OCT3/4, NANOG	CD34, CD45, HLA-DR	-	yes	-

Funderburgh et al. 2005	Progenitor cells for keratocytes - bovine-	CD90, CD73, Pax6, Six3, Six2, Cd166, Bmi 1, ABCG2 (based on Gene expression)	NP	NP	NP	Stromal wound healing
Fernandez Perez et al. 2018	Porcine limbal stromal cells (PLSC)	CD29,CD45, CD90, CD105, CD146, HLA-ABC ALDH3A1, Keratocan, and alpha smooth muscle actin	CD73, CD45	NP	NP	Antiangiogenesis, support LESC

Table 1.4 Overview of mesenchymal stromal cells of the human, bovine, and porcine corneal stroma

The table summarises publications on limbal stromal cells with mesenchymal stromal cell properties that have been described in several publications using various names, their protein marker profile, colony forming potential, multipotency and function. Central-derived stromal cells have been only described by (Vereb, Poliska et al. 2016). Corneal stromal cells have been proposed to be involved in the maintenance of the corneal transparency, corneal homeostasis, wound healing and maintenance and support of the epithelial progenitors in the limbal niche. Abbreviations: LESC, limbal epithelial stem cell; NP, not performed

The mesenchymal stem cell and cytoskeleton markers used in the present study are described in more detail as they have been found to have a wide range of biological functions.

CD34: CD34 is a transmembrane glycoprotein expressed in progenitor cells, endothelial cells and lymphohematopoietic stem cells. The expression of CD34 in CSSC and keratocytes is controversial. CD34 is a hematopoietic stem cell marker, which is defined to be absent (<2%) in MSC (Dominici, Le Blanc et al. 2006). This was also confirmed for human limbal and central CSSC (Polisetty, Fatima et al. 2008, Vereb, Poliska et al. 2016). Joseph et al 2003 described CD34 as a characteristic marker of quiescent keratocytes in the human cornea (Joseph, Hossain et al. 2003). Another study

characterising limbal mesenchymal stromal cells showed a drop of CD34 marker expression with increasing cell proliferation and a shift to a more progenitor cell type expressing CD34, Pax6, ABCG2, SSEA-4. This seems to be influenced significantly by the composition of culture media (Branch, Hashmani et al. 2012, Hashmani, Branch et al. 2013, Sidney, Branch et al. 2015).

CD73: CD73 is an ectoenzyme with a 5'-nucleotidase activity, it has a role participating in cell-cell and cell-matrix interactions. CD73 is expressed in stromal cells, follicular dendritic cells, and endothelial cells but also in B cells and some T-cell subsets (Monteiro, Vigano et al. 2018). The secreted antibodies from hybridoma cell lines (SH) SH3 and SH-4 recognised epitopes on the surface of human MSCs. The protein of a molecular weight of 67 kDa was identified as CD73 (ecto-5-nucleotidase) (Barry, Boynton et al. 2001).

CD90: Thy-1 (CD90) is a glycoposphatidylinositol (GPI)-linked outer membrane leaflet glycoprotein that is expressed predominantly on subsets of fibroblasts and lymphocytes. However, CD90 is a well-accepted human and canine mesenchymal stromal cell marker (Dominici, Le Blanc et al. 2006, Takemitsu, Zhao et al. 2012).

CD105: Endoglin (CD105) epitopes were found to bind SH2 and SH3; these are accepted surface antigen markers that seem to identify MSCs (Barry, Boynton et al. 1999). CD105 is expressed on cellular lineages within the vascular system and proliferating endothelial cells, is involved in blood vessels development (Fonsatti, Sigalotti et al. 2003). Endoglin is a co-receptor for the TGF- β 1 and TGF- β 3 receptor complex (Guerrero-Esteo,

Sanchez-Elsner et al. 2002) that are linked to the capacity of trilineage differentiation (Yamamoto, Nakata et al. 2014).

PAX6: Paired Box 6 is a transcription factor that plays a critical role in ocular development synchronizing the critical events during the formation of the anterior eye. Pax6 is expressed in all cell of the anterior eye development, however with different time points and intensity (Chow and Lang 2001).

N-cadherin: is a transmembrane protein expressed in multiple tissues (cardiac muscle, intercalated discs, neural adhesion protein). N-cadherin was described as a putative marker for LESC (Hayashi, Yamato et al. 2007, Higa, Kato et al. 2013) and was included in the present study as potential (additional) stem cell marker.

Alpha-SMA: Alpha-SMA (ACTA2) is a protein expressed in the differentiation of the smooth muscle cells during development and is transiently expressed by a variety of mesodermal cells during development and tissue repair (Liu, Deng et al. 2013). Tissue repair and tumor microenvironment can convert MSCs into contractile myofibroblasts (MF) that form α -SMA-containing stress fibres (Hinz, Celetta et al. 2001, Hinz, Phan et al. 2012). Persistent MFs contribute to fibrosis by producing and contracting collagenous ECM to provide stiff scar tissue (Hinz, Phan et al. 2012). Peled et al 1991 found that the expression of α -SMA in murine, bone -marrow MSC is reversible and inversely related to hematopoietic activity (Peled, Zipori et al. 1991). In corneal fibrosis, it is described that TGF- β and PDGF will differentiate (rabbit) keratocyte-derived and fibrocyte derived precursors into vimentin +, α -SMA+, desmin + mature myofibroblasts (Chaurasia, Kaur et al. 2009).

D) Differentiation of hCSSC in keratocytes *in vitro*

In vitro, human CSSC were differentiated into keratocytes using a low glucose, serum-free media containing ascorbic acid and fibroblastic growth factor. The resulting keratocytes expressed *Lumican*, *Keratocan*, and *ALDH1A1* and lost expression of *Pax6* and *ABCG2*. Serum supplementation (10% v/v) led to keratocyte differentiation into fibroblasts with loss of keratocan expression (Du, Funderburgh et al. 2005, Foster, Gouveia et al. 2015, Kureshi, Dziasko et al. 2015). A stable keratocyte phenotype has been described in relation to the differentiation process; however, the degree of a subpopulation of fibroblast/myofibroblast differentiated cells increased with increasing passage number of CSSC. A-SMA was not expressed by cultured keratocytes up to the 5th passage, and fibroblastic morphology was not noted until the fourth passage in CSSC (Funderburgh, Du et al. 2005, Garcia, Garcia-Suarez et al. 2016).

A specific keratocyte marker does not exist, but a combination of keratocyte associates markers (and genes) are described.

The keratocyte markers used in this study are following described in more detail:

Keratocan: There are nine members of small leucine-rich proteoglycans (SLRPs), of which the following are most relevant for the cornea: decorin, mimecan, lumican and keratocan. Their function is to resist compressive forces and provide tissue volume, maintain spatial order of collagen fibrils, and provide viscoelastic properties. Lumican and Mimecan have a single

keratan sulphate glycosaminoglycans (GAG) side chain and Keratocan has three keratan sulphate GAG side chains (Hassell and Birk 2010) (see 1.1. C) Even though keratocan is described as a cornea-specific keratan sulphate proteoglycan it is also expressed by osteoblasts and is regulated by lumican (Carlson, Liu et al. 2005). Keratocan $-/-$ mouse had impaired bone formation, lower expression of bone specific markers and impaired mineralization (Igwe, Gao et al. 2011).

Lumican: is an SLRP present in the cornea and more weakly expressed in cartilage and bone. Lumican and Fibromodulin-deficient mice develop severe tendinopathy demonstrating the importance of this SLRP in the development of correctly aligned and sized collagen fibres in tendons (Mienaltowski and Birk 2014). Recently reports have shown that Lumican is also expressed in several types of malignant tumours including oesophageal, lung, gastrointestinal, breast, colorectal, and pancreatic cancers in humans (Xu, Tang et al. 2019).

ALDH1A3: is an aldehyde dehydrogenase and is part of a larger range of corneal crystallins. A study in mice has shown that $ALDH3A1 > ALDH1B1 > ALDH2 > ALDH1A1 > ALDH7A1 > ALDH1A3 > ALDH3A2 > ALDH1A2 > ALDH4A1$ are present in decreasing quantities in the cornea (Stagos, Chen et al. 2010, Kumar, Dolle et al. 2017).

1.5 Canine mesenchymal stromal cells

Canine MSCs are well characterised in the veterinary field, including adipose derived, amniotic-derived and bone marrow derived MSCs (Park, Kim et al. 2012, Takemitsu, Zhao et al. 2012, Baird, Barsby et al. 2015, (Russell, Chow et al. 2016, Kriston-Pal, Czibula et al. 2017, Uder, Bruckner et al. 2018). MSCs, especially adMSCs seem an ideal source for cell-based therapies: they are an abundant cell population of adult stem cells in adipose tissue, which are minimally invasive to retrieve. The isolation and culturing method is well established, they can be differentiated into multiple lineages, have immunomodulatory, anti-angiogenesis and anti-inflammation capacities, which seem ideal for corneal reconstruction (Yi and Song 2012, Mansoor and Ong 2019).

The International Society for Cellular Therapy (ISCT) has defined a set of criteria that must be established to be characterised as a multipotent mesenchymal stromal cell (Dominici, Le Blanc et al. 2006). Canine MSCs studies fulfilled these criteria, however positive and negative MSC marker profiles differ in various studies, some studies also demonstrated cells were positive for the pluripotency-associated genes NANOG, OCT4, and SOX2 (Guercio, Di Bella et al. 2013, Bearden, Huggins et al. 2017). Canine MSCs are not a homogenous cell population. Hence, proliferation time and capacity are described to be lower in bone marrow (BM)-MSCs in contrast to adMSCs and synovial MSCs (Russell, Chow et al. 2016, Bearden, Huggins et al. 2017). Stemness has also been shown to decrease with increasing cell culture passages (Volk, Wang et al. 2012, Guercio, Di Bella et al. 2013).

Breed related differences are described, i.e. BM-MSCs of Howavart's had significantly fewer colony forming units (CFU) than German Shepherd, Flat-coated Retriever or Golden Retriever in one study (Bertolo, Steffen et al. 2015).

Donor age can negatively influence human and canine MSC cell expansion and differentiation (Volk, Wang et al. 2012, Choudhery, Badowski et al. 2014). Effects of age in skeletally immature (mean age: 4.9 ± 1.9 months) and mature (mean age: 89.5 ± 20.9 months) dogs on canine BM-MSCs were studied by Volk and colleagues 2012. BM-MSCs were isolated from long bones (humerus, femurs, and tibias), cultured in high glucose DMEM substituted with 10% FBS, showed a significant negative effect of age on colony-forming units fibroblasts (CFU-f) analysis and the ability to differentiate along the osteogenic lineage (Volk, Wang et al. 2012). Guericio et al (2013) compared the age (young dogs: 1–4 years; adult dogs: 8–14 years) and the harvest site (subcutaneous versus visceral) of adMSCs cultured in low glucose DMEM and 20% FBS. Population doubling values were significantly higher for MSCs derived from subcutaneous fat and in younger dogs. High standard deviations within the age groups in their studies are presented which correlates to a high degree of heterogeneity but was not further discussed by the authors. CFU-f assay in low glucose DMEM and 5% FBS did not differ to age and harvest location site, but declined after passage > 2 (Guericio, Di Bella et al. 2013).

Canine MSCs have been shown to undergo trilineage differentiation, but protocols had to be adjusted from human studies to canines. Canine

chondrogenesis from MSCs has not been robustly demonstrated in the literature and difficulties in establishing a protocol are described (Kisiel, McDuffee et al. 2012, Russell, Chow et al. 2016). Studies in canine, human MSCs and other mammals have been shown that bone morphogenic protein (BMP)-2 or IGF-1 is required to successfully induce an osteogenic differentiation (Volk, Diefenderfer et al. 2005, Levi, Nelson et al. 2011, Bearden, Huggins et al. 2017), which is in contrast to equine adMSCs (Guest, Ousey et al. 2008).

A study in canine adMSCs has shown that multilineage potential was declined after passage 4 and the gene expression of NANOG, OCT4 and Sox2 was discussed to potentially correlate to the reduced differentiation potential of MSCs at higher passages (Guercio, Di Bella et al. 2013).

1.6 Immune privilege and immunomodulatory properties in mammalian MSC

MSCs are capable of evading immune allorecognition and can inhibit naïve, memory and activated T-cells, making them ideal candidates for aiding the regeneration of damaged tissue, application in host-versus-graft and immune-mediated disease. Surprisingly, upon implantation of allogeneic MHC-mismatched MSCs into a host, it was found that MSCs are well tolerated. This was initially demonstrated by Bartholomew and colleagues (2002), who found that baboon MSCs were not proliferating when cultured with allogeneic peripheral blood mononuclear cells (PBMCs) *in vitro*, instead

causing a > 50% reduction in proliferative action (Bartholomew, Sturgeon et al. 2002).

Alloreactivity can also be measured by the secretion of interferon γ (IFN γ) of activated lymphocytes in the mixed lymphocyte reaction (MLR) assay. This is an *ex vivo* cellular immune response assay between two allogeneic lymphocyte populations. When only one lymphocyte population respond/proliferate is used, this is a one-way MLR. MSC can suppress a lymphocytic response using both, allogeneic and autologous T - cells or dendritic cells (Barry and Murphy 2004). This also initiates alloreactive T - cells activation without inducing T - cell proliferation (Klyushnenkova, Mosca et al. 2005). Allogeneic human BM-MSC have shown to express MHC molecules activated T - cells only in the presence of CD80 and CD86 as co - stimulatory factors (Tse, Pendleton et al. 2003). Furthermore, allogeneic MSC stimulate T - cells via antigen - presenting cells (APC). Human and rat MSC could not induce any increase of IFN γ by peripheral blood mononuclear cells (PBMC) which confirmed the lack of immunogenicity of MSC (Le Blanc and Ringdén 2007). In summary, MSC can modulate the immune response directly or indirectly by communicating with other cells of the innate and the adaptive immune system (Uder, Bruckner et al. 2018).

Dias and colleagues 2019 reviewed the interaction of MSCs with the immune system (innate and adaptive) and introduced clinical trials in dogs and cats with autoimmune-disease (Dias, Pinto et al. 2019). Briefly, paracrine effects influence the immunomodulation via nitric oxide (NO), indoleamine 2,3-dioxygenase (IDO), transforming growth factor- β (TGF- β), hepatocyte growth

factor (HGF), hemeoxygenase (HO), IL6 and prostaglandin E2 (PGE2) and also through cell to cell contact (Figure 1.12). MSCs act on the innate immunity system via activation of proinflammatory monocytes and macrophages (via IL-6, PGE2, TGF- β and HGF). Classic macrophages (M1) are possessing proinflammatory functions. They then become M2 macrophages with high levels of IL-10 secretion and low capacity to stimulate the proliferation of allogeneic T cells *in vitro*. MSCs inhibit NK cell proliferation and cytotoxicity which is mediated via PGE2, IDO and TGF- β but also direct cell to cell contact (Dias, Pinto et al. 2019).

MSCs also regulate adaptive immune responses such as altering antibody production by B-lymphocytes and shifting T-lymphocyte subtypes (T helper 1-Th2 cell). MSCs induce immune tolerance to allogeneic transplants because of their lack of MHC-II expression (Dias, Pinto et al. 2019). However, the immunomodulatory capacity of MCSs is not fully understood and there are variable results concerning immunomodulatory therapies with MSCs (Gao, Chiu et al. 2016).

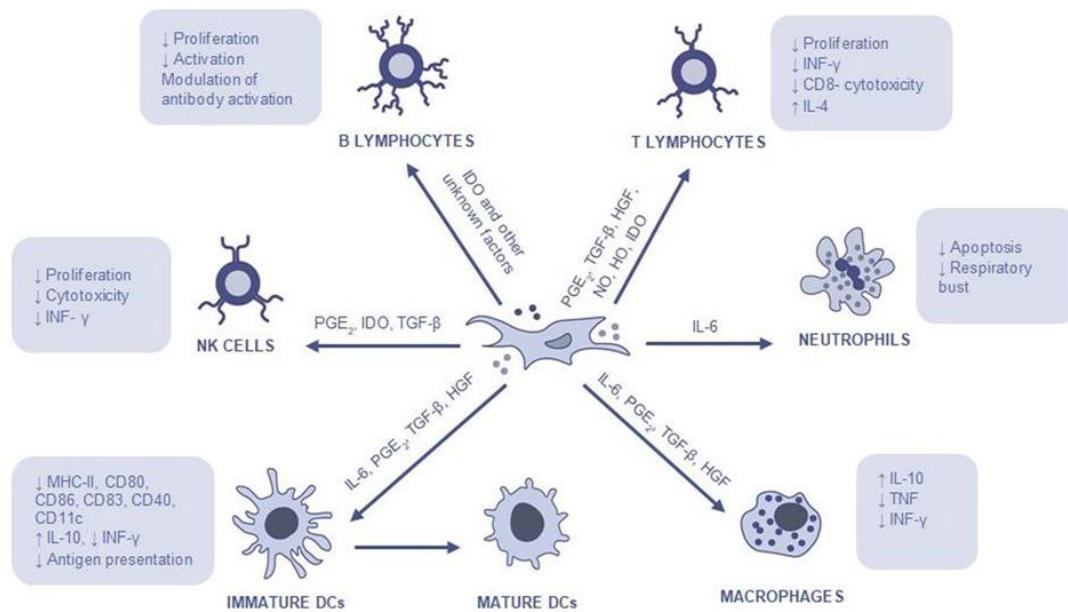


Figure 1.12 Mechanism of action and interaction of MSCs with immune cells

The illustration (modified from Dias et al. 2019) provides an overview of how paracrine factors of MSCs influences the innate immune system (macrophages, immature dendritic cells (DC), neutrophilic granulocytes, natural killer cells (NK)) and adaptive immune system (B and T-lymphocytes). Abbreviations: indoleamine 2,3-dioxygenase (IDO), transforming growth factor- β (TGF- β), hepatocyte growth factor (HGF), hemoxygenase (HO), interleukin (IL)-6 and prostaglandin E2 (PGE2).

Clinical application of MSCs in dogs of natural occurring disease included orthopaedic (Meyer-Lindenberg and Kilchling 2018) semitendinosus myopathy, supraspinatus tendinopathy, cruciate ligament rupture, bone defects, and osteoarthritis (Dias, Cardoso et al. 2021), intervertebral disc disease (Steffen, Smolders et al. 2017), and inflammatory bowel disease (Perez-Merino, Uson-Casaus et al. 2015) and atopic dermatitis (Hall, Rosenkrantz et al. 2010).

1.7 Induced pluripotent stem cells

IPS cells can be directly derived from patient somatic cells and therefore they can be used to generate cells for disease models, tissue-specific cell therapies and in pharmacology for drug development and screening. iPSCs also overcame the ethical issue of the destruction of embryos. In canine research, the ethical issue is that surgery is required for the derivation of canine ESCs (i.e., isolation of blastocyst stage embryos requires ovariectomy or surgical laparotomy followed by flushing of the uterine horns) Therefore, iPSCs opened a new research field not only in human medicine but also in the veterinary field.

Yamanaka and co-workers (2006) demonstrated that reprogramming somatic cells of mice (Takahashi and Yamanaka 2006), followed in humans one year later (Takahashi, Tanabe et al. 2007), into a pluripotent state was possible by the overexpression of four transcription factors, OCT4, Sox2, Klf4, C-MYC (OKSM). These iPSCs exhibited significant features of ESCs such as unlimited self-renewal, expressed ESC specific genes, formed embryoid bodies (EB), teratomas and contributed to chimeric embryos in mice (Takahashi and Yamanaka 2006).

All these methods are based on viral vectors and require integrating into the host genome with the potential risk of gene mutations or even tumor formation. Therefore, integration-free induced pluripotent stem cells (iPSCs) have been developed such as Sendai RNAvirus system, the piggyBac transposon system, a minicircle vector, synthetic mRNA, recombinant proteins, and episomal vectors (Fusaki et al.2009; Kim et al.2009; Woltjen et

al.2009; Yu et al.2009; Jia et al.2010; Okita et al.2011). Among integration-free methods, the episomal method is a technically not demanding but the episomal vectors showed low reprogramming efficiency in contrast to viral vectors (Okita et al.2010; Zhou and Zeng 2013). This was then optimized by Bang and colleagues (2018) using higher concentrations of episomal vectors (OCT4/p53, SOX2/KLF4, L-MYC/LIN28A) and optimized plating cell densities (Bang, Choi et al. 2018).

Since 2007, human iPSC technology has evolved fast to generate human disease models and drug screening (i.e. efficacy and toxicity tests) (Doss and Sachinidis 2019).

There is a large scale of disease model research for hiPSC-derivatives, which have traditionally been utilised in two-dimensional monocultures, recent advances in generating more complex hiPSC-based systems using three-dimensional organoids, tissue engineering, microfluidic organ-chips, and humanized animal systems (Sharma, Sances et al. 2020).

Advances in gene editing, such as the development of CRISPR technology, can generate iPSCs where predicted causal variant is introduced into wild type cells, or corrected in diseased cells, this technique is used for example in inherited retinal disease such as retinitis pigmentosa and Leber's congenital amaurosis, age-related macular degeneration (AMD) (Benati, Patrizi et al. 2020). Shi et al 2020 recently reviewed clinical and preclinical studies that have tested PSC-derived retinal pigment epithelial cells as a potential treatment for AMD, which seem at an early regulatory approval

stage safe and preliminary signs of efficacy were observed in a few patients (Sharma, Bose et al. 2020).

Further information about characterisation, differentiation and culture methods can be found in 1.7.1.

1.7.1 Canine iPSC

Dogs are of interest as large animal models in human research, given that the biology of some canine cancers is similar to human cancers as they share food, environment and carcinogenic load (Glickman, Raghavan et al. 2004, Cadieu and Ostrander 2007). Likewise, there is also growing interest in veterinary regenerative medicine within the last years (Ezashi, Yuan et al. 2016, Paterson, Kafarnik et al. 2017, Figueiredo Pessôa 2019).

Shimada et al. 2009 first reported canine iPSCs derived from canine embryonic fibroblasts using lentiviral transfection with canine OSKM factors (Shimada, Nakada et al. 2010), several other groups followed (Whitworth, Ovchinnikov et al. 2012, Koh, Thomas et al. 2013, Nishimura, Hatoya et al. 2013, Baird, Barsby et al. 2015, Goncalves, Bressan et al. 2017).

Predominantly viral expression vectors (lentivirus and retrovirus) have been used for the integration of human or mouse OKSM reprogramming factors in ciPSC generation except for one report which used six- factor reprogramming (Whitworth, Ovchinnikov et al. 2012) (OCT4, Sox2, Klf4, C-MYC, NANOG and LIN28) and one report used canine Oct4, Sox2, Klf4 and C-MYC (Shimada, Nakada et al. 2010). The continued expression of the viral transgenes has been variable in reports on canine iPSCs, in which a

significant reduction but detectable expression was noted (Luo, Suhr et al. 2011, Whitworth, Ovchinnikov et al. 2012, Koh, Thomas et al. 2013, Nishimura, Hatoya et al. 2013). It is worth pointing out that the viral transgenes were upregulated in teratomas in one study, compared to the undifferentiated iPSCs from which they were derived (Koh, Thomas et al. 2013). This highlights that there is still a potential risk of continued transgene expression. However, another study demonstrated that transgene expression was essential for the maintenance of the pluripotent state of ciPSCs (Nishimura, Hatoya et al. 2017). In addition, the “foot-print free” reprogramming Sendai-virus system has been used successfully in a recent study. Sendai virus is a genome integration-free and completely exogenous gene-silenced RNA virus, which is believed to be safer to use *in vivo* (Chow, Johnson et al. 2017).

CiPSCs have generally been derived from fibroblasts from either adult (Luo, Suhr et al. 2011, Whitworth, Ovchinnikov et al. 2012, Koh, Thomas et al. 2013) or fetal animals (Goncalves, Bressan et al. 2017, Nishimura, Hatoya et al. 2017) and the reprogramming of MSCs has also been reported (Baird, Barsby et al. 2015). It has been generally shown that adult stem cells generally being easier to reprogram than fully differentiated cell types (Gonzalez, Boue et al. 2011).

CiPSCs have been derived from both mixed and pure breed dogs (Whitworth, Ovchinnikov et al. 2012, Nishimura, Hatoya et al. 2013) such as beagles (Nishimura, Hatoya et al. 2017), poodles (Chow, Johnson et al. 2017), Weimaraner (Baird, Barsby et al. 2015) and German shorthair

pointers (Luo, Suhr et al. 2011). Whether or not there is genetic diversity in different breeds, affecting the reprogramming is unknown (Baird, Barsby et al. 2015). It is also not clear whether differences in reprogramming factors of a different species (human) have any effect on the efficiency of canine iPSC derivation (Paterson, Kafarnik et al. 2017, Scarfone, Pena et al. 2020).

Culture conditions for ciPSC largely rely on combinations of feeder cells, leukaemia inhibitory factor (LIF) and basic fibroblast growth factor (bFGF). The requirement of each factor and the role are largely unknown in companion animal stem cells and as can be seen in the media used varies between publications. However, a transcriptome study demonstrated the requirement for both bFGF and LIF by ciPSCs and began to dissect their signalling pathways (Luo and Cibelli 2016).

Tobias and co-workers (2016) have shown that 2i media (containing inhibitors of glycogen synthase kinase 3b and mitogen-activated protein kinase 1/2) plus LIF moves canine ESCs towards a more naïve pluripotent state (Tobias, Brooks et al. 2016). These are advances in understanding the culture requirements of pluripotent stem cells from companion animals however, both studies still required the addition of a feeder cell layer (mouse embryonic fibroblasts). If companion animal pluripotent stem cells are to be used in a clinical setting or for large scale drug testing, then the growth conditions warrant better definition and standardisation. The use of feeder cells from other species carries the risk of disease transmission and immune rejection. Working towards a feeder-free system would improve safety in

clinical applications. Nishimura et al. 2017 reported a feeder-free culture of ciPSCs in a doxycycline- inducible system (Nishimura, Hatoya et al. 2017).

Most current studies have used mechanical passaging to maintain small colonies of cells, although enzymatic methods have been used on horse, dog ESCs and iPSCs (Nishimura, Hatoya et al. 2017). A major hurdle in pluripotent stem cell culture is that the survival of the cells following thawing, and passaging is poor. The use of Rho-kinase (ROCK) inhibitors to promote human ESC survival during passaging was first reported in 2007 (Watanabe, Ueno et al. 2007) and was also used in ciPSC culture (Baird, Barsby et al. 2015).

Correct assessment and characterisation of pluripotency is critical with the development of iPSC technology to assess the state of reprogramming and to minimise the production of inaccurate data, or cell lines which have increased tumorigenicity and spontaneous differentiation potential (Paterson, Kafarnik et al. 2017).

To determine the differentiation potential, putative stem cells can be injected into immunodeficient mice to assess whether teratomas can be formed, which then can be histologically examined to determine the presence of three embryonic germ layers. In companion animals ESCs and iPSCs teratoma studies have had limited success. There are reports in ciPSC showing teratoma formation (Lee, Xu et al. 2011, Goncalves, Bressan et al. 2017) and others were tested negative (Luo, Suhr et al. 2011, Whitworth, Ovchinnikov et al. 2012, Nishimura, Hatoya et al. 2017).

However, it is difficult to interpret if a negative result is due to experimental variations (e.g., insufficient starting number of cells) or due to an inability of the cells to form a teratoma. When interpreting teratoma formation by iPSCs generated using integrating vectors (as a lentivirus), it is important to note that continued expression of the transgenes may enhance teratoma formation due to an increased ability of the cells to proliferate (Nagy, Sung et al. 2011, Koh, Thomas et al. 2013).

An alternative *in vitro* assay is the generation of embryoid bodies (EB) which occur when pluripotent cells are allowed to spontaneously differentiate, producing derivatives of the three germ layers. This assay does not need to use experimental animals and to date EBs are formed by almost all species of ESC and iPSC including those from cats, dogs and horses (Paterson, Kafarnik et al. 2017).

A third differentiation assay is the directed differentiation *in vitro*. Here pluripotent cells can be directed towards different lineages by the addition of growth factors and stimulating agents into the culture media. Directed differentiation of ciPSCs towards hematopoietic (Schneider, Adler et al. 2007, Vaags, Rosic-Kablar et al. 2009, Nishimura, Hatoya et al. 2013), endothelial (Vaags, Rosic-Kablar et al. 2009, Lee, Xu et al. 2011), mesodermal, endodermal, ectodermal (Baird, Barsby et al. 2015) and chondrogenic (Hayes, Fagerlie et al. 2008, Whitworth, Frith et al. 2014) lineages were performed.

Furthermore, pluripotency can also be confirmed using various cell surface markers, telomerase and alkaline phosphatase activity assays. Stage

Specific Embryonic Antigens (SSEAs (SSEA-1, SSEA-3 and SSEA-4)), and Tumour Rejection Antigens (TRA) such as TRA-1-60 and TRA-1-81, are cell surface markers involved in the regulation of early embryogenesis. There is variability across companion animal species, within species, with conflicting data on the exact SSEA and TRA markers. SSEA4 in canine iPSC were tested to be positive in most studies whereas SSEA1 was not expressed as reported in two studies (Whitworth, Ovchinnikov et al. 2012, Baird, Barsby et al. 2015).

The transcription factors that play key roles in maintaining self-renewal, include NANOG, OCT4 and Sox2, which are demonstrated in all pluripotent stages from naïve to primed (Nichols, Zevnik et al. 1998, Chambers, Colby et al. 2003, Mitsui, Tokuzawa et al. 2003, Kuroda, Tada et al. 2005). Other factors such as Rex1, KLF4, KLF2 and estrogen-related receptor beta (ESRRB) are found to be naïve markers and are also often used (Guo, Yang et al. 2009, Silva, Nichols et al. 2009, Kalkan and Smith 2014) which are determined via immunocytochemistry and reverse transcription polymerase chain reaction (RT-PCR). Transcription factors associated with pluripotency can also be used to help establish more homogenous cell populations. Here cells are labelled by tagging the desired transcription factor with a fluorescent marker, for example OCT4-GFP or NANOG-GFP, allowing sorting (via fluorescence activated cell sorting (FACS)) of the different subpopulations of high and low expressing cells with the aim to produce a purer population (Karwacki-Neisius, Goke et al. 2013). To date, OCT4 is the most well characterised marker across all species with its expression being consistently demonstrated in companion animal pluripotent stem cells. However, when

detecting OCT4 with quantitative RT-PCR a high number of retroseudogenes can lead to false positive results (Lengner, Welstead et al. 2008).

Like humans, dogs suffer from inherited conditions (Mellersh 2012). To study the disease *in vitro* is often limited by the availability of relevant, expandable cell types from affected and control animals, whereas iPSCs can provide lineage-specific cells and be successfully utilised in human disease modelling (Sharma, Bose et al. 2020).

Disease modelling using companion animal iPSCs may result in new treatments for inherited diseases in the future (Paterson, Kafarnik et al. 2017, Scarfone, Pena et al. 2020). There are currently no updates on clinical trials in dogs, but a cardiac infarction model showed that ciPSC-endothelial cells engrafted onto the heart muscle of mice and improved the cardiac contractility but donor cells were lost over time (Lee, Xu et al. 2011).

The safety and immune regulatory aspects of ciPSC generated MSCs have been pre-clinically evaluated. Chow et al. 2017 showed that canine MSCs derived from iPSCs, had a high expansion rate and immune-modulatory characteristics, similar to that of canine ad-MSCs and BM-MSCs. The safety of canine MSCs was evaluated by systemic injection to immune-deficient mice and to adult dogs. Dogs were without teratoma formation of up to 15 months and also in mice there was no evidence of teratomas in 6 months of follow-up (Chow, Johnson et al. 2017).

1.7.2 IPSC differentiation into keratocyte-like cells via neural crest lineage differentiation

A) The neural crest lineage differentiation

The anterior neural crest is the embryological origin of the corneal stroma (i.e. keratocytes) and corneal endothelial cells (Lwigale 2015). Therefore, all reports on the differentiation of human pluripotent stem cells into these types first induce a neural crest cell (NCC) lineage.

Different NCC induction protocols based on chemically defined media influence the following signaling pathways: SMAD, which standing for Activin/Nodal/TGF β branches inhibition, blocking BMP signalling and activation of WNT signalling (Figure 1.13, Figure 1.14). Dual SMAD inhibition via chemical factor SB431542 blocks Activin/Nodal/TGF β , BMP signalling via the chemical factor Noggin and glycogen synthase kinases 3 β (GSK-3 β) inhibitor (BIO or CHIR) induce the early WNT signalling activation.

Chambers and colleagues concluded that this protocol leads to naive anterior NCCs (Chambers, Mica et al. 2016). Generally, these cell-signalling pathways maintain the undifferentiated state of a cell. It was found in hESCs the TGF-beta/activin/nodal pathway is activated via the signal transducer SMAD2/3. The BMP/GDF pathway (SMAD1/5) is only active in mitotic cells. James and colleagues (2005) further reported that in the early differentiation, the SMAD2/3 signalling is decreased while SMAD1/5 signalling is activated (James, Levine et al. 2005). It is also described that mesoderm induction is

promoted via WNT signalling when differentiating hESCs/hiPSCs (Leung, Murdoch et al. 2016).

Fukuta et al. (2014) developed an induction protocol using chemically defined medium containing inhibitors for TGF- β signalling (SB431542) and inhibitors of GSK3 β (CHIR99021) to activate the canonical WNT-signaling pathway but not blocked the BMP pathway using Noggin and/or LDN 19389. HESCs or hiPSCs were differentiated into NCC with a high efficiency (70%–80%), they could be expanded and were then free of viral-integration or plasmids. Cells were cultured feeder-free and xeno-free systems. Generated hNCCs, among other cell types, were further differentiated into corneal endothelial cells (Fukuta, Nakai et al. 2014).

Menendez et al 2011 found out that higher concentration of BIO/CHIR was leading to an increase of the WNT signalling activation (Figure 1.13). That was related to a dose-dependent manner, which consequently increased the number of Hnk1/p75NRT cells in a more native stage with downregulation of neurogenic progenitors *Pax6*, *Sox2* and upregulation of neural crest factors *P75*, *Ap2* and *Slug* transcription factor. That was established on human ESC and iPSCs and the author concluded that an elevated WNT signalling and low SMAD activity directs cells away from Pax6 positive NCCs (=neural progenitor cells) to more neural crest cell fate. The authors could also show that omission of Noggin (= to block BMP signalling) had no major impact on this effect. They concluded that the higher cell NCC yield would remove the need for FACS-assisted purification (Menendez, Yatskievych et al. 2011).

Leung and co-researchers (2016) found that the activation of WNT signalling (via CHIR) is the major component in the NCC induction of hESC/iPSC and found that activin/TGF β antagonism using the type I Activin/TGF β receptor inhibitor SB 431542 (Chambers et al., 2013; Menendez et al., 2011) alone were not promoting effect on NC differentiation (Figure 1.14). Whereas only blocking the BMP signaling with the BMP inhibitor Noggin led to a dramatic inhibition of human NC induction. It was concluded that NC induction requires an early and balanced BMP activity. An important role was also seen in endogenous FGF signalling which was found to required for NC induction, and that exogenous FGF triggers mesoderm formation (Leung, Murdoch et al. 2016). A recent NCC differentiation protocol for hiPSC were further modified in a combination of glycogen synthase kinase 3 (GSK-3) inhibitor CHIR99021, TGF- β inhibitor SB431542 with added BMP4 and DMH1, a BMP receptor inhibitor for ALK2, which let to a stable NCC population (Gong, Duan et al. 2021).

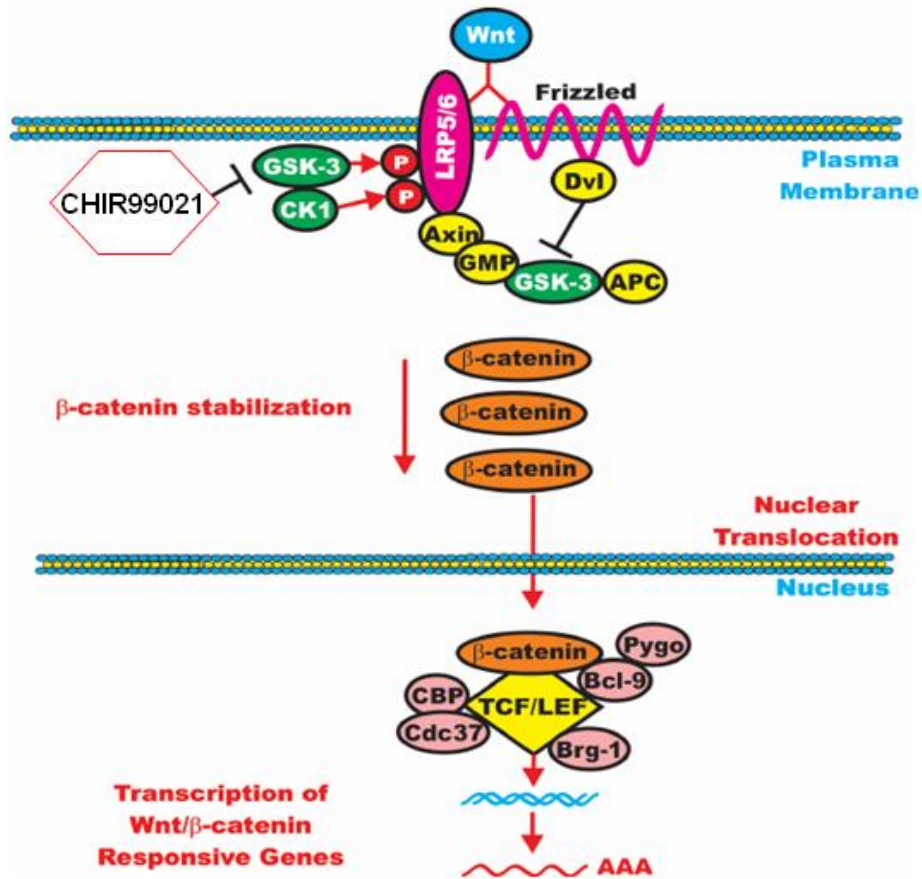


Figure 1.13 GSK3 inhibition via small chemical molecule CHIR activates conical WNT signalling

CHIR99021 (synthetic small chemical molecule) inhibits GSK3 and activates WNT-signalling via the binding of WNT-protein to its receptor, dishevelled Dvl, a cytoplasmic phosphoprotein, is recruited and inhibits the GSK3 (in the beta-catenin destruction complex). This leads to accumulation of free non-phosphorylated β-catenin in the cytosol. From there it is translocated to the nucleus and activates WNT-target genes together with the T-cell factor (TCF)/lymphoid-enhancing factor (LEF). Hence, pharmacological inhibition of the GSK3 leads to the activation of the conical WNT-signalling pathway. (Illustration is modified from AG scientific.com).

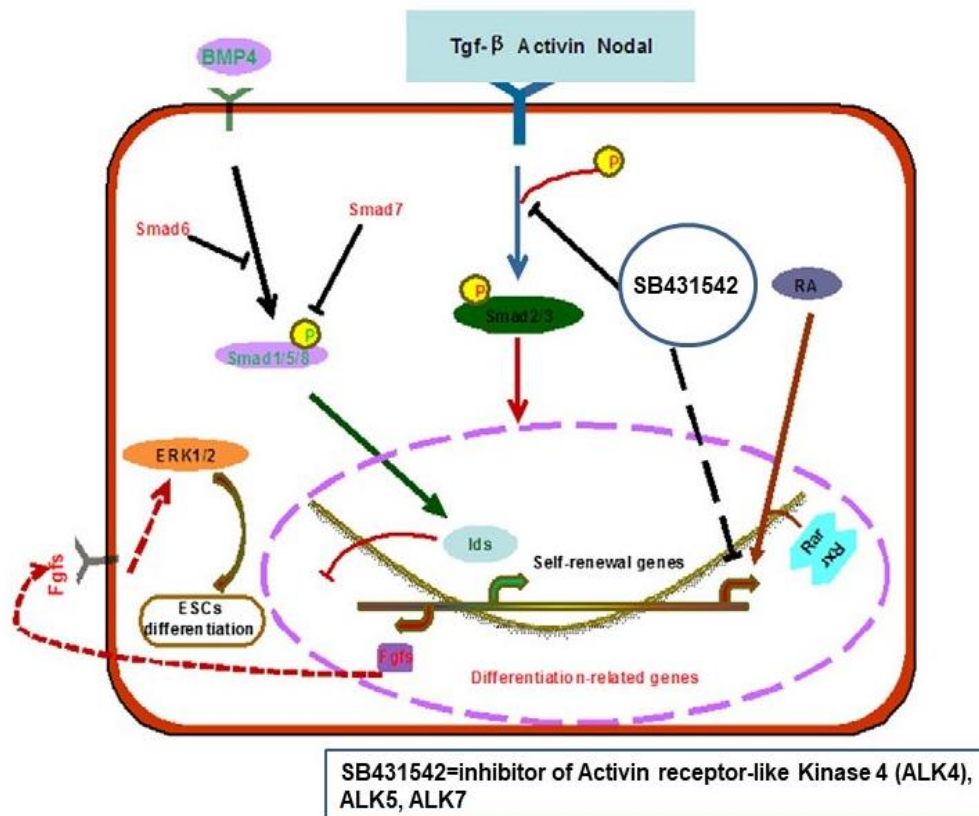


Figure 1.14 SMAD 2/3 inhibition via small chemical molecule SB

The schematic diagram was modified from Du et al. (2014) and illustrates the function of SB431542. This is an ATP-binding site inhibitor of activin receptor-like kinase 4 (ALK4), ALK5, and ALK7, which are TGF-β type 1 receptors that blocks Smad2/3 mediated-signalling transduction. SB mainly functions by inhibiting differentiation. Intrinsic differentiation-related transcripts including fibroblast growth factor family members (Fgfs) were significantly downregulated by SB. SB could partially inhibit the retinoic acid response (RA) to neuronal differentiation (Du, Wu et al. 2014).

B) hiPSC and hESC differentiation into keratocyte-like cells *in vitro*

In human corneal research, 2D and 3D *in vitro* studies have generated limbal epithelial stem cells-like cells (Sareen, Saghizadeh et al. 2014), epithelial-like cells (Mikhailova, Ilmarinen et al. 2014, Hayashi, Ishikawa et al. 2016, Mikhailova, Ilmarinen et al. 2016), keratocytes-like cells (Naylor, McGhee et

al. 2016) and endothelial-like cells (Fukuta, Nakai et al. 2014, Zhao and Afshari 2016) from hiPSC. Furthermore, human corneal organoids were generated from human iPSCs (Foster, Wahlin et al. 2017, Isla-Magrané, Veiga et al. 2021).

Cells with features of keratocytes were generated from human embryonic stem cells (ESCs) in Funderburgh's group (2013) using a co-culturing system of hES cell line WA01(H1) with mouse PA6 fibroblasts, which upregulated neural crest genes nerve growth factor receptor (*NGFR*, also known as *CD271* or *p75NRT*), *SNAI1*, *NTRK3*, *SOX9*, and *MSX1*. Cells were then isolated by immunoaffinity adsorption, 60% of these cells were NGFR+. These cell-sorted NCC-like cells were expanded and underwent 2-week keratocyte differentiation in a 3D pellet using the same culture media as described in this thesis. The cells upregulated keratocyte genes *AQP1*, *B3GNT7*, *PTDGS*, *ALDH3A1* and *Keratocan* was highly upregulated (Chan, Hertszenberg et al. 2013, Hertszenberg and Funderburgh 2016).

Naylor and colleagues (2016) established a chemically defined culture method to differentiate human iPSC into neural crest cells (NCC), and further into keratocyte-like cells. In this work, a dual SMAD inhibition/WNT activation method was used which Chambers and colleagues (2016) established (Chambers, Mica et al. 2016).

The generated NCCs expressed Sox2 protein (pluripotent marker), had dendritic cell morphology and a cell yield of > 80% AP2a and p75 NTR positive cells (NCC) along with an upregulation of neural crest genes *Pax3*, *Sox9*, *Sox10*, *ZIC1* and *TFAP2A*. After the NCC step, Naylor et al (2016)

cultured pelleted NC cells (non-scaffold 3D) in the same keratocyte differentiation media as in the present study for three weeks. This induced a conversion towards a keratocyte-like fate and led to upregulation of keratocyte genes, in particular *BMP3*, *CDH5*, *B3GnT7*, *PtDGS*, *AQP1* and *KLF4* were >10-fold more highly expressed, but also *ALDH1A1*, *ALDH3A1*, *Keratocan* and *CHST6* were increased (Naylor, McGhee et al. 2016). Gong and co-workers (2021) differentiated keratocyte-like cells from hiPSC-derived NCCs but cultured and characterised the cells in 2D (Gong, Duan et al. 2021).

Whereas Naylor et al (2016) further seeded hiPSC-derived NCCs on a decellularised/protein epitope free human corneal limbal rim model (*ex vivo* model) where the system was cultured in KDM for 3 weeks. The seeded cells migrated over the sclera part into the corneal region of the rim. They then were followed to migrate around the free dissected lateral corneal edges into the exposed stromal collagen fibrils. Intrastromal hiPSC-NCC cells acquired a keratocyte-like morphology, and corneal keratocyte protein markers were expressed (Vimentin, Keratocan, ABCB5), but the cells also maintained NCC-specific protein marker labelling (HNK1 and AP2a). The mRNA expression analysis revealed that *PAX3*, *ZIC1*, *SOX10*, *SNAIL*, *TWIST*, *ZIC5*, *FOXD3*, *MSX1* and *MSX2* (all NCC markers) were similar to expression levels found in undifferentiated human corneal keratocytes; however, *TFAP2A*, *CX32*, *P75NTR* and *ID2* had levels of expression that were higher in the rim-cultured NCCs-KDCs relative to undifferentiated human corneal keratocytes. Keratocyte markers such as *ALDH1A1*, *BMP3*, *B3GnT7*, *CHST6*, *PtDGS*, *AQP1* and *KLF4* were similar between NCCs-KDCs (seeded

on limbal rims) and human corneal keratocytes, whereas ALDH3A1 and Keratocan showed lower expression levels whereas CDH5 was higher expressed than in corneal keratocytes. Overall the similarity of mRNA gene expression profile of rim-cultured NCCs differentiated keratocyte-like cells was higher than pelleted 3D-cultured NCCs to endogenous (undifferentiated) corneal keratocytes (Naylor, McGhee et al. 2016). Currently, there are no reports in dogs.

In spring 2019, permission was given for to the first four human *in vivo* corneal transplantation of iPSC derived cells in Japan (Kohji Nishida, Osaka University) but peer reviewed published results are pending (2nd September 2019 online news, Nature).

1.8 Introduction to the concept of cell-based therapies in corneal regenerative medicine

The concept of regenerative medicine is the process of “repair, replacement or regeneration of cells, tissues, or organs to restore or establish normal function” and is a branch of translational research of tissue engineering generating and using stem cells (Mason and Dunnill 2008).

In the 1970’s pioneering work by W.T. Green and his research team to grow cells (chondrocytes) on a 3D scaffold system (bone spicules) instead of a 2D system led to the speculation that “smart scaffolds” are an advancement to the 2D system. Their observations were maybe the platform of “tissue

engineering". Tissue engineering defined by Y.C. Fung 1985 involves the isolation, culture, expansion, and manipulation of cells with or without scaffolds to develop therapeutic tissues (Burgess 2016) (Figure 1.15).

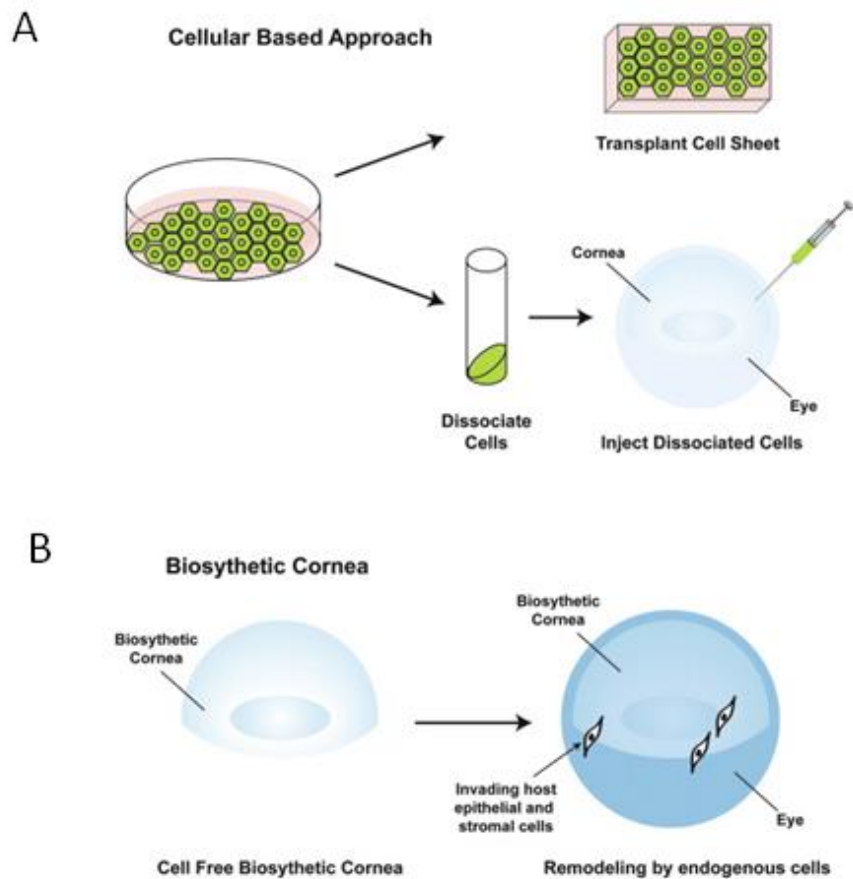


Figure 1.15 Tissue engineering for corneal replacement

A): The schematic illustrates the cell-based approach, which can either be transplanted as a cell sheet or seeded on/within a scaffold material or then be transplanted. Dissociated cells either can be injected into the cornea (or topically applied, not included in the illustration) B): The biosynthetic cornea is remodeled by endogenous cells from the host. The illustration was modified from (McCabe and Lanza 2014).

1.8.1 Stem cell therapy in corneal regenerative medicine

The following chapter will provide an overview of *in vivo and ex vivo* models and *in vitro* studies in human and laboratory animal corneal research. In humans there are clinical applications of LESC transplantations, to date, there are no studies in canines.

A) Limbal epithelial stem cells

Limbal epithelial stem cell deficiency (LSCD) disorders caused by trauma (chemical burn), immune-mediated disease (Steven Johnson syndrome), aniridia (Pax6 deficiency) or contact lens-induced keratopathy will lead to a failure of renewal of corneal epithelial cells, pain, neovascularisation of the cornea, fibrosis and reduced vision or blindness. Limbal epithelial stem cells (LESC) are isolated either from a donor tissue or autologous, from the healthy remaining eye of the recipient. LESCs are expanded and can be seeded on a scaffold, like an amniotic membrane, and successfully surgically transplanted (O'Callaghan and Daniels 2011). Treatment of other or severe corneal disease require corneal transplantation, that is still the only clinically relevant approach. However, the procedure is limited by donor shortage, and by risk of immune rejection (Aharony, Michowiz et al. 2017). For example, the yearly UK NHS statistic (2016-2017) showed that 2791 corneas were donated, whereas 3613 corneal transplants were needed. This sequela led to intensive research in the field of tissue engineering and to find an alternative stem cell source. Kumar and colleagues (2021) provided an overview of 19 international registered clinical trials (@clinicaltrials.gov) for LSCD (Kumar, Yun et al. 2021).

B) Corneal stromal stem cells

Cell-based therapy using CSSCs, embedded in various materials to prepare an artificial stroma, is the focus of several corneal research groups. CSSCs have been shown to produce extracellular matrix (ECM) producing fibrils of equal diameters and collagen spacing similar to the human stroma. Also proteoglycans (keratan sulphate and keratocan) were secreted, which are cornea-specific member of the small leucine-rich proteoglycan family. These bind to collagen fibres with highly charged glycosaminoglycan chains extending into the interfibrillar space that mediate the distance between adjacent collagen fibres. This is essential for corneal transparency (Wu, Du et al. 2012). Furthermore, CSSCs cultured on 3D scaffolds of aligned polymeric nanofibers produced an ECM similar to the corneal stroma (Wu, Du et al. 2012, Wu, Du et al. 2014). A study using scaffold-free substrate with aligned microgrooves produced strongly emulated stromal lamellae of native corneal tissue (Syed-Picard, Du et al. 2016). In addition, silk protein in the form of films has been used as a substrate to engineer the corneal epithelium and stroma layers. Seeded human CSSC showed upregulation of keratocyte-gene expression and maintained transparency of the silk films for 9 weeks. Furthermore, silk films are a suitable material for corneal stroma reconstruction in a rabbit model (Wang, Ma et al. 2015). RAFT (Real Architecture For 3D Tissue) tissue equivalents of rat tail/bovine plastic compressed collagen were developed and used to co-culture limbal epithelial and CSSC to mimic the limbal niche (Kureshi, Dziasko et al. 2015, Levis, Kureshi et al. 2015). Mukhey and co-workers (2018) observed that human CSSC showed the phenomenon of cellular self-alignment in tethered gels

and co-alignment of collagen fibrils in RAFT, that coincided with a loss of PAX6 expression in CSSCs, indicating maturation into keratocytes (Mukhey, Phillips et al. 2018).

Unpublished data from our laboratory revealed that human CSSC derived keratocytes were successfully cultured in RAFT tissue equivalents, transplanted in rabbit corneas, and resulted in no inflammatory response within a three-week study period (Morgan L., Daniels submitted manuscript).

In vivo studies in human are lacking to date, however, *in vivo* animal experiments include that injected CSSC into a murine cornea of lumican deficient mice (lum^{-/-}) revealed promising clearing of the fibrosed cornea, while a T-cell response was absent (Du, Carlson et al. 2009). Basu and co-workers (2014) isolated CSSC from the limbal stroma, embedded these cells in fibrinogen carrier medium and could show the successful reduction of fibrosis in an *in vivo* mouse model (Basu, Hertsenberg et al. 2014).

C) Mesenchymal stromal cells

In vivo studies in mammals transplanting MSCs into the cornea used either undifferentiated MSCs, or MSCs derived keratocyte-like cells.

Undifferentiated MSCs were studied using different application pathways such as topically on the cornea (Mittal, Omoto et al. 2016), injected subconjunctivally (Sanchez-Abarca, Hernandez-Galilea et al. 2015), intrastromally in to the cornea (Liu, Zhang et al. 2012) or intravenously (Lohan, Murphy et al. 2018). Research is also focused on the paracrine action of MSCs to use MSC retrieved exosomes intracorneally as an

alternative approach to cell-based therapy (Blazquez, Sanchez-Margallo et al. 2014, Zieske, Hutcheon et al. 2019).

Topically applied BM-MSC secreted a high amount of hepatocyte growth factor (HGF) in a mouse fibrosis model. HGF indirectly contributes to the clearance of corneal fibrosis via suppression of TGF-beta stimulation, the major contributor to myofibroblast differentiation. However, topically applied HGF alone had a similar effect and may have therapeutic potential (Mittal, Omoto et al. 2016).

BM-MSC when injected into corneas of chimeric mice deficient in keratocan and lumican (keratocan $-/-$, lumican $-/-$), differentiated into keratocyte-like cells expressing keratocan and lumican after 1 week without any immune response. The donor cells remained detectable for the 6-week follow up study period without an immune response observed. In contrast when naive BM-MSCs were intrastromally intransplanted via injection, the cells had a limited survival time of 4 weeks and there was a significant increase in the number of pan-T cells and macrophages at multiple time points after transplantation (Liu, Zhang et al. 2012).

In an ocular graft versus host disease (oGVHD) model in mice, GFP labelled human BM-MSCs that were subconjunctivally injected underwent migration into all three cell layers of the cornea after 10 days until day 40 at the end of the study period (Sanchez-Abarca, Hernandez-Galilea et al. 2015) In the host, a therapeutic effect was observed with the regeneration of damaged tissues and a reduction of corneal inflammation (absence of CD3⁺ cells) (Martinez-Carrasco, Sanchez-Abarca et al. 2019). Intravenously injected allogeneic

MSCs prevented rejection in a high-risk corneal transplant model for oGVHD in mice through the promotion, by allo-MSCs, of alternatively-activated macrophages in the lung followed by enhanced regulatory T-cell numbers (Lohan, Murphy et al. 2018).

Extracellular vesicles or “exosomes” are produced in the endosomal compartment of eukaryotic cells and serve as a paracrine signal to other cells. The content of luminal exosomes are nucleic acids such as DNA, mRNA, miRNAs, long noncoding RNAs, proteins and lipids. It has been shown that human adMSC-derived exosomes can downregulate the proliferation of natural killer cells, macrophages, dendritic cells and IFN release from effector T-cells (Blazquez, Sanchez-Margallo et al. 2014).

MSCs have also been differentiated into keratocyte-like cells and then either investigated *in vivo* in 2D or in 3D settings or *in vitro* transplanted in animal models. Human MSCs can be differentiated using serum-free and serum reduced media supplemented with bFGF and ascorbate. These cells expressed keratocyte associated genes and protein markers such as Keratocan, keratan sulphate and ALDH3A1 at similar levels to CSSC derived keratocytes (Du, Roh et al. 2010). Under these conditions, the MSC-keratocytes can also express ALDH1A1 and Lumican, whilst alpha smooth muscle actin expression was lost (Park, Kim et al. 2012). Alpha smooth muscle actin (α -SMA) is a marker of a myofibroblast. They are dramatically increased during wound repair contributing to corneal fibrosis and wound contraction (Jester, Petroll et al. 1995, Werner and Grose 2003).

However, studies to determine the organisation of ECM, secreted by keratocyte-like cells derived from adMSC, have not been performed (Du, Roh et al. 2010). Whether MSC derived keratocytes contributes to tissue repair *in vivo* (i.e. clinical trials) remains unknown.

Alio and colleagues (2019) found in a human *in vivo* study of intrastromal implantation of undifferentiated autologous adMSCs remained without complications and were considered moderately effective for the treatment of advanced keratoconus (Alió, Alió Del Barrio et al. 2019).

D) Mesenchymal stromal cells in veterinary ophthalmology

Veterinary ophthalmology related studies are limited to two non-controlled studies treating immune mediated keratoconjunctivitis sicca (KCS) *in vivo* by injecting allogeneic adMSCs inside the lacrimal glandular tissue. This resulted in increased tear production in a follow-up period of 9 month (Villatoro, Fernandez et al. 2015) and 12month (Bittencourt, Barros et al. 2016). In a case series of 20 dogs with immune-mediated KCS showed increased expression of CD4, IL-6, IL-1 and TNF α , with significant reductions in the expression levels of all the markers 6 months post MSC subconjunctival injections. The authors concluded that topical MSC treatment as adjuvant therapy of KCS in dogs (Sgrignoli, Silva et al. 2019). A small case series of horses with immune-mediated keratitis were treated using autologous BM-MSCs via subconjunctival injections with variable outcome (Davis, Schnabel et al. 2019). Both studies reported no complications and concluded the method to be safe.

1.9 Conclusion and aims

The dog cornea has many anatomic similarities to the human cornea. However, as pointed out in the comparative introduction, there is lack of basic research in the canine cornea and a lot of information is abstracted from human research. Canines are affected by inherited ocular disease and serve as a large animal model for a variety of different human eye disease (Bunel, Chaudieu et al. 2019). The application of stem cells to treat pathological conditions in the dog would benefit the dogs as companion animals but will also promote the progress of human regenerative medicine.

Corneal pathology, like corneal crystalline dystrophy in dogs share phenotypical features with Schnyder's dystrophy (SCD) in humans (Crispin 2016). Chronic corneal fibrosis is one of the leading causes of visual impairment in veterinary ophthalmology and is considered as major problem in human ophthalmology. Discovering a successful antifibrotic agent in dogs would help both, physicians, and veterinary ophthalmologists (Gronkiewicz, Giuliano et al. 2016). Like the situation in human ophthalmology, there is a shortage of corneal donor tissue in dogs.

Human CSSCs have been shown to reduce corneal scarring *in vivo* (Basu, Hertsenbergh et al. 2014) and have been described in the human, (Du, Funderburgh et al. 2005, Poliseti, Agarwal et al. 2010, Branch, Hashmani et al. 2012, Vereb, Poliska et al. 2016), bovine (Funderburgh, Du et al. 2005),

rabbit, mouse (Li, Dai et al. 2015) and porcine cornea (Fernandez-Perez, Binner et al. 2017) but reports in canines are missing.

Given the corneal donor shortage and the immunomodulatory features, MSCs seem an alternative cell source. Canine MSCs are well characterised in the literature *in vitro* (Levi, Nelson et al. 2011, Takemitsu, Zhao et al. 2012, Volk, Wang et al. 2012, Guercio, Di Bella et al. 2013, Park, Reilly et al. 2013, Bertolo, Steffen et al. 2015, Bearden, Huggins et al. 2017, Chow, Johnson et al. 2017) and reports of differentiated keratocyte-like cells of human MSCs show promising results (Du, Roh et al. 2010, Park, Kim et al. 2012).

To study the inherited disease *in vitro* is often limited by the availability of relevant, expandable cell types from affected and control animals. iPSCs can provide lineage specific cells and be successfully utilised in human disease modelling (Sharma, Bose et al. 2020). Canine iPSCs have been established and characterised by different research groups (Lee, Xu et al. 2011, Luo, Suhr et al. 2011, Whitworth, Frith et al. 2014, Baird, Barsby et al. 2015, Chow, Johnson et al. 2017, Nishimura, Hatoya et al. 2017, Tsukamoto, Nishimura et al. 2018). Human iPSC can be induced into neural crest cells and further differentiated into keratocyte-like cells (Naylor, McGhee et al. 2016, Gong, Duan et al. 2021) but to date there are no reports available on ciPSC.

The overall aim of this thesis was to establish sources of canine corneal stromal cells derived from the cornea, adMSCs and ciPSCs, to support the investigation of the genetics and cell biology of canine crystalline corneal dystrophy and other corneal pathologies (i.e. corneal scarring, inflammation)

and provide a basis for cell-based therapies in veterinary ophthalmology in the future.

It was hypothesised that:

1. A subpopulation of limbal and central corneal stromal cells has mesenchymal stromal cell properties in the dog cornea similar to corneal stromal stem cells as described in humans.

The specific objectives were:

1a) To describe histologically the anatomy of the limbal stem cell niche in the normal corneal limbus of dogs with specific focus of location of stromal and epithelial cells and configuration of the basement membrane

1b) To isolate and characterise corneal stromal cells of the limbus and central cornea in healthy dogs and investigate whether they have multipotent MSC properties

1c) To establish a method to differentiate limbal and central derived CSC into keratocytes

1d) To determine the immune properties of corneal stromal cells via a PBMC co-culture system

2. Canine adipose derived mesenchymal stromal cells can be differentiated into cells with keratocyte characteristics *in vitro*.

The objective was:

To study canine adMSC and their response to keratocyte differentiation based on methods established for corneal stromal cells

3. Canine induced pluripotent stem cells can be differentiated into cell with keratocyte characteristics *in vitro*.

The objective was:

To establish a differentiation protocol to induce a neural crest cell fate from canine iPSCs from healthy donors and to differentiate these cells into keratocyte like cells based on methods established for corneal stromal cells

Chapter 2:

General materials and methods

2.1 Canine tissue and ethics statement

All canine tissue and cells that were isolated in this thesis were collected post-mortem from privately owned dogs that had been euthanized for reasons unrelated to this project and were donated to this project. Research consent and all experiments were approved by the approval of the Animal Health Trust Ethical Review Committee (AHT_31_2013). The following table summarises the details of all canine tissues and cells used in this project.

Sample number	Patient number	Age (month)	Sex	Breed	Reason for euthanasia
Corneas					
1a	W48066	15	m	Staffordshire bull terrier	behaviour
1b	W48066	15	m	Staffordshire bull terrier	behaviour
2a	W48134	14	m	Staffordshire bull terrier	behaviour
2b	W48134	14	m	Staffordshire bull terrier	behaviour
3a	W48150	17	m	Staffordshire bull terrier	behaviour
3b	W48150	17	m	Staffordshire bull terrier	behaviour
4a	W48170	20	m	Staffordshire bull terrier	behaviour
4b	W48170	20	m	Staffordshire bull terrier	behaviour
5a	W58338	24	fs	Cross breed	behaviour
5b	W58338	24	fs	Cross breed	behaviour

6a	W58442	12	m	Staffordshire cross breed	behaviour
6b	W58442	12	m	Staffordshire cross breed	behaviour
7	AHT16/1036 b	1.2	m	Dalmatian	deaf
8	AHT16/1036 a	1.2	m	Dalmatian	deaf
9a	06/1044	2	f	Old English sheepdog	deaf
9b	06/1044	2	f	Old English sheepdog	deaf
10a	16/2051	96	mn	Springer Spaniel	renal failure
10b	16/2051	96	mn	Springer Spaniel	renal failure
11a	16/3278	144	mn	Lurcher	renal failure
11b	16/3278	144	mn	Lurcher	renal failure
12a	donated to AHT	144	mn	Golden Retriever	oral melanoma
12b	donated to AHT	144	mn	Golden Retriever	oral melanoma
13a	14/3107	24	fs	Border Collie	brain herniation
13b	14/3107	24	fs	Border Collie	brain herniation
14a	16/3591	96	fs	Labrador	venous embolus
14b	16/3591	96	fs	Labrador	venous embolus
15a	17/2089	144	fs	Golden Retriever	kidney failure

adMSC (AHT)					
16	AHT	132	mn	Mix	anaemia
17	AHT	96	mn	Irish Setter	epileptic
18	AHT	1.2	m	Dalmatian	deaf
iPSC (AHT)					
19	AHT	11	f	Weimaraner	N/A
PBMC					
20	06/3066	2	f	Bull Terrier	deaf
21	18/389	60	fs	Pug	BOAS
22*	(3H Bio-medical)	72	f	Crossbreed	N/A
23*	3H Bio-medical)	72	m	Labrador Retriever	N/A
Control tissue/cells					
24	12/4322	60	f	Border Collie (cerebellum)	ataxia
25	16/1036	1.2	m	Dalmatian (Skin fibroblasts)	deaf

Table 2.1 Donor details of dogs

Summarised the donor details of dogs and the reason for euthanasia; Abbreviations: a, left eye; b, right eye; m, male, mn, male neutered; f, female; fs, female spayed; adMSC, adipose derived mesenchymal stromal cells; iPSC, induced pluripotent stem cells; AHT, Animal Health Trust; N/A, not applicable; PBMC, peripheral blood mononuclear cells; BOAS, brachycephalic obstructive airway syndrome; *, commercial canine PBMC, 3H Biomedical, Uppsala, Sweden

2.2 Cell culture

2.2.1 Cell counting

Cell numbers were counted manually using a haemocytometer (Neubauer chamber). Cells were detached with TrypLE express® (Invitrogen, Thermo-Fisher Scientific, Paisley, UK) or Trypsin with EDTA 0.5% (Invitrogen) for 2-3 minutes at room temperature and 4 minutes at 37°C respectively, resuspended in three times the amount of culture media and centrifuged 5 minutes at 1000rpm. The cell pellet was resuspended in 1ml culture media, from which 10 µl of cell suspension was added to 10 µl of Trypan blue (0.4% Gibco, Life Technologies, Paisley, UK). All cells not stained with Trypan blue (i.e. live cells) were counted in four squares and then averaged. Trypan blue itself dilutes a cell suspension by the factor two, the final cell concentration (cells/ml) was calculated: Concentration (cell/ml) = number of living cells (large square) x 10000 x 2.

2.2.2 Cryopreservation and thawing

Expanded cells (CSC, adMSC, iPSC) were cryopreserved in liquid nitrogen at different passages using the same protocol. CSCs were cryopreserved between passage 2-4, adMSCs and iPSCs were cryopreserved in higher passage number. The cells were trypsinised, resuspended in 1 ml culture media, counted and frozen in 1 ml aliquots of 5×10^5 - 2×10^6 cells in freezing media. The iPSCs were mechanically passaged as small colonies and a cell count before freezing was therefore not performed (find details in Materials and Methods, Chapter 5).

The freezing media for CSCs was made from of CSSC medium (containing 2% fetal bovine serum (FBS), (Gibco) with the addition of 20% (v/v) FBS and 10% (v/v) dimethylsulfoxide (DMSO) (Sigma-Aldrich, Gillingham, Dorset, UK). For adMSCs and iPSCs 10% (v/v) DMSO was added to the standard cell culture medium containing 10% (adMSCs) or 15% (iPSCs) FBS. The vials were transferred into a -70 °C freezer within less than 10 minutes, to minimise the cell death in DMSO at room temperature. For optimal cryopreservation (-1°C per minute cooling rate), cryovials (Fisher Scientific, Loughborough Leicestershire, UK) were placed into a freezing container (Mr Frosty, Nalgene, Thermo Fisher, Life Technologies, Paisley, UK) at -70°C and stored in liquid nitrogen (-196°C) long-term.

A fast-thawing procedure over 3-5 minutes was used. Cryovials were placed in a 37°C water bath until a fluid phase was reached and drop-wise, over approximately 1-2 minutes, added to 10ml cell culture medium followed by immediate centrifugation (1000 rpm, 5 minutes) to remove the DMSO containing freezing media. The cell pellet was suspended in culture media and plated in tissue culture flasks (CSC – T75), tissue culture plates (adMSC – 10cm) or on prepared feeder cells on culture plates (iPSC -6 well plate). A detailed description of iPSC cell culture can be found in Materials and Methods, Chapter 5.

2.2.3 Cell observation, fixation and imaging of cell morphology

Cell culture images were taken and stored every 3-4 days using a phase-contrast microscope (EVOS XL Core, Life Technologies).

Single cells were then counted (see 2.2.1) and plated onto fibronectin (FNC Coating Mix, Athena Enzyme Systems™, Baltimore, USA) coated soda glass slides (Nunc® Lab-Tek® II Chamber Slide™ system, Sigma-Aldrich) at a density of 40,000 cells per slide. Then they were cultured for further 2-3 days in culture media, fixed with 3% paraformaldehyde for 20 minutes, followed by 3 x 5 minute washes in phosphate-buffered saline (PBS) and stored at 4°C in PBS until further immunofluorescence staining was carried out. Detailed information on iPSCs single cells/colony fixation on chamber slides can be found in Materials and Methods Chapter 5.

An inverted phase-contrast microscope (Nikon Eclipse TS100 inverted phase-contrast microscope, Nikon Instruments Europe B. V., Surrey, UK at the Institute of Ophthalmology, UCL or EVOS® XL Core Imaging System, Life Technologies, Fisher Scientific at the AHT were used to image the morphology of cells.

2.2.4 Cell culture and differentiation media

All details of cell culture media are in the supplementary materials (see Table S2-S11). The cell culture media was changed every 2-3 days and the iPSC media was changed daily.

2.3 Protein analysis

2.3.1 Immunofluorescence staining protocol and imaging

Immunofluorescence staining was performed on corneal sections, cultured and fixed CSC and adMSC in a biological triplicate (i.e., tissue and cells from three biological different donors). CiPSC derived NCC/CSC and their differentiated keratocytes were stained in a technical triplicate (i.e. three independent set of cells from the same donor #19) and investigated using immunohistochemistry/-cytochemistry with the same protocol. However, before the staining procedure, the 7 μ m frozen (-20°C) sections were defrosted at room temperature (RT) and immediately fixed in 3% paraformaldehyde. (Find details on tissue preparation and cryosectioning in Material and Methods Chapter 3). Sections and fixed cells were then washed in PBS (3x5 minutes) and permeabilized in 0.1% Triton-X100 in PBS (Sigma-Aldrich) for 20min (except CD90), and again washed in PBS (3x5 minutes). For fixed cells that were used for the identification of keratocyte markers, PBS-Tween 20 (0.1%) was used for washing procedures. Depending on the primary antibody 10% goat or donkey serum (Sigma-Aldrich) was applied as a blocking agent at RT (room temperature) for 60 minutes. The primary antibody incubation was performed with added 5% of blocking serum either for 120 minutes at RT or at 4°C overnight. Details of the primary and secondary antibodies and dilutions are summarised in Table 2.2.

Slides were washed in PBS, incubated with the appropriate secondary antibody and FITC-labelled phalloidin (1:1000 concentration; Sigma-Aldrich), that binds to the actin of the cytoskeleton, for 60 minutes at RT. Secondary

antibodies/phalloidin were diluted in 5% blocking serum in PBS. FITC – labelled phalloidin was not added in all iPSC staining protocols given that these cells still expressed green fluorescent protein (GFP) which has a similar excitement/emission spectrum (488/510nm) to FITC phalloidin (496/516nm).

Slides were mounted in Vectashield with DAPI nuclear stain (Vector laboratories Inc., Peterborough, UK) cover slipped and stored light protected at 4°C.

AB IHC/ICC	Company (cat. number), Clone	Raised in	Clonality	Reactivity	Dilution	Localisation
Stem cell marker						
CD73	Bioss (bs-4834R) Clone: 4907	rabbit	polyclonal/ IgG	human, Mouse, Rat, Dog, Chicken	1:300	CM/IC
CD90	R&D systems (AF 2067) Clone: 5E10	sheep	polyclonal	human, porcine, canine	1:100	CM (N-terminal)
Anti-Pax 6	Biologend (901301) Clone: Poly 19013	rabbit	polyclonal	human, mouse, mammalian	1:500	N
CD105 (Hensley, Tang et al. 2017)	Abcam (ab156756) Clone: 8A1	mouse	monoclonal/ gG2	mouse, rat, dog, human, monkey	1:200	CM
N-cadherin	Abcam (ab18203)	rabbit	polyclonal	mouse, rat, human, pig, xenopus laevis	1:100	CM (N-terminal)
CD34	Abcam (ab81289) Clone: EP373Y	rabbit	monoclonal	human, dog, mouse, rat	1:100	CM
Cytoskeleton marker						
Alpha-SMA (Mai, Hu et al. 2015)	Abcam (ab5694)	rabbit	polyclonal	human, equine, bovine, avian, canine, mouse, rat	1:200	IC/CS
Keratocyte marker						
Lumican	Abcam (ab168348) Clone: EPR8898 (2)	rabbit	monoclonal	human, mice, rat	1:200	CM (secreted)
ALDH1A3	Abcam (ab129815)	rabbit	polyclonal	mouse, rat, dog, human, African green monkey, Syrian master	1:500	IC
Keratocan	Biorbyt (orb2975)	rabbit	polyclonal	mouse, human, rat	1:100	CM (secreted)

Neuron/Neural crest marker						
Anti β tubulin III (Baird, Barsby et al. 2015)	Sigma-Aldrich (T8660) Clone: SDL.3D10	mouse	monoclonal	pig, rat human, bovine	1:100	IC
Sox 10 (Kishimoto and Uchida 2018)	Sigma-Aldrich (SAB1402361) Clone: 1E6	mouse	monoclonal	human	1:100	IC
P 75 (=NGF R/TNFRSF16)	R&D systems (MAB367) Clone: 74902	mouse	monoclonal	human, dog	1:100	CM
Negative control						
Rabbit IgG	Abcam (ab27478)	rabbit	polyclonal/Ig G	rabbit	1:500	NA
Mouse IgG2	BioLegend (401501) Clone: MG2a-83	mouse	monoclonal	mouse	1:500	NA
Sheep IgG	R&D systems 5-001-A	sheep	polyclonal	sheep	1:500	NA
Secondary antibody						
Alexa Fluor-594 conjugated	Invitrogen A11032	goat	polyclonal	mouse	1:500	NA
Alexa Fluor-594 conjugated	Invitrogen A11037	goat	polyclonal	rabbit	1:500	NA
NorthernLights-557 conjugated	R&D systems NL010	donkey	polyclonal	sheep	1:200	NA

Table 2.2 Overview of protein markers

Information of the company, host, clonality, specific reactivity, dilution, and cell marker localisation of all primary, control and secondary antibodies used; Abbreviations: AB, antibody; IHC, immunohistochemistry; ICC, immunocytochemistry; CM, cell membrane; IC, intracytoplasmic; N, nuclear; CS, cytoskeleton; *, share the same reference

Primary antibodies were chosen according to existing references in canine tissue/cells (Table 2.2). Antibodies without a reference were first evaluated

whether a positive binding in immunofluorescence staining was present, which was then confirmed by western blot analysis (see 3.3.2). Negative controls consisted of substitution of the primary antibody with an isotype relevant IgG. (Find details of positive controls Fig.3.9, Fig. 3.10, Fig. 3.11, Fig. 3.19. (C(I)), Fig. 3.20, Fig. 3.25).

Stained slides were evaluated within 7 days after the staining procedure to avoid fading of the fluorescence. The slides were warmed up to RT 15 minutes before imaging. Images were taken either with a Zeiss 700 or 710 confocal microscope using the ZEN software (Zeiss, Cambridge, UK). Image files were imported in a TIFF file format and stored. Please find in the Supplementary material table S1 a list of primary antibodies tested which tested negative or exhibited unspecific binding in IF which could not be confirmed in the WB assay.

2.3.2 Protein extraction from cells

Preparation of whole-cell extract (WCE) from adMSC and CSC (limbal and central) was performed to perform western blot analysis. One 10 cm tissue culture dish of 90% confluent adMSC and one T75 tissue flask of 60-70% confluent CSC (approximately 1×10^6 cells) were extracted to harvest approximately 150 μg protein.

WCE buffer was composed of 20 mM HEPES pH7.9, 450 mM NaCl, 0.4 mM EDTA, 25% glycerol and 1 mM phenylmethylsulfonyl fluoride (PMFS), which was stored at -20°C . Given a half-life of 35 minutes at room temperature, PMFS was added immediately before use (product information Sigma-Aldrich).

The cell culture plate/flask was washed in PBS, cells were scraped (Corning® cell scrapers, Sigma-Aldrich) into PBS and centrifuged at 1000 rpm for 5 minutes. The cell pellet was suspended in 100 μl WCE buffer, followed by three freeze/thaw cycles on dry ice/ 37°C and briefly vortexed. After a second centrifugation at 12000 rpm at 4°C for 20 minutes, the spectrophotometric quantification of the protein in the supernatant was measured using a NanoDrop instrument (Thermo Fisher, Paisley, UK) (A280, set at 1Abs = 1mg/ml). The WCE was stored at -20°C until use. If less than 1mg/ml of protein was isolated, then acetone precipitation was performed as described below.

2.3.3 Acetone protein precipitation

To precipitate the protein of the WCE isolated above to reach higher relative protein concentrations, the sample was defrosted and diluted in 4 times in cooled 100% acetone at -20°C for 60 minutes. The protein/acetone suspension was centrifuged at 14000 rpm for 10 minutes at room temperature and the supernatant was discarded. The pellet was air-dried, resuspended in 50 µl WCE buffer and quantified as above. The concentrated WCEs were stored at -20°C until use.

2.3.4 Protein extraction from corneal tissue

Protein from corneal tissue was extracted to perform western blot analysis. Six snap-frozen half corneas stored at -70°C were cut into small pieces in liquid nitrogen and ground up using a pestle and mortar until a relatively homogenous tissue mass was generated. The homogenised tissue was placed in 5 ml WCE buffer in a 15 ml Falcon tube, followed by three freeze/thaw cycles in dry ice/37°C with pipetting up and down during the thaw cycle. The Falcon tube was centrifuged (2000 rpm/10 minutes). The supernatant was transferred into 10 x 1.5 ml Eppendorf tubes and again centrifuged at 12000 rpm for 20 minutes at 4 °C. The supernatant concentration ranged between 0.8-1.88 mg/ml protein and so the corneal protein was precipitated in acetone (see 2.3.3 Acetone protein precipitation) and resuspended in 500µl WCE buffer to increase the concentration to over 1 mg/ml.

Given the difficulty in homogenising the corneal samples in liquid nitrogen using a mortar and pestle and the low protein concentration, the protein extraction technique was modified. Five corneas were thawed, the sclera rim was excised, and the cornea was cut into small pieces (4x4 mm) and transferred into a Dounce homogeniser (tight pestle, Fisher Scientific) with 500 μ l WCE buffer (Figure 2.2). The tissue pieces were grinded for 5-7 minutes. The procedure was performed within several minutes because substituted PMFS has a half-life of 35 minutes at RT. Following three freeze/thaw cycles in dry ice and 37°C were performed, during the thawing phase the tissue-buffer suspension was pipetted up and down. The suspension was centrifuged at 12000 rpm for 20 minutes at 4°C. The protein concentration in the resulting supernatant using this method was 9.23mg/ml. The corneal protein extract was stored at -20°C until use.

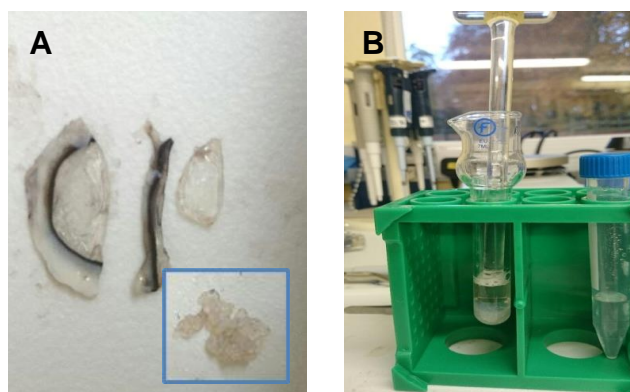


Figure 2.1 Preparation and homogenisation of corneal protein

The sclera of the thawed corneal halves was excised and cut into small 3x3mm pieces as magnified in the blue square (A) and ground in a Dounce tissue grinder in a whole-cell extraction buffer (B).

2.3.5 Western Blot analysis

In contrast to the human and laboratory animal research, several of the antibody markers used in this study were not established on canine tissue. Hence, to confirm the binding of the antibody to the specific protein, the following western blot analysis was performed (overview of antibody marker details see Table 2.4).

Deglycosylation of corneal protein

Keratan sulphate (KS) is a linear polymer that consists of a repeating disaccharide unit. Keratan sulphate is as a proteoglycan (PG) in which KS chains are attached to cell-surface or extracellular matrix proteins, these are so called core proteins. Without deglycosylation, corneal KS-PGs (i.e. lumican, mimecan and keratocan) are heterogeneous and run as a smear on SDS-PAGE gels (Carlson, Liu et al. 2005). Keratanase (= endo- β Galactosidase) digestion of KS-PGs causes partial deglycosylation, resulting in reduced smears on SDS-PAGE (Akhtar, Kerr et al. 2008). Chondroitinase will deglycosylate the corneal proteoglycan dermatan and chondroitin sulphate, this also reduces the smear and frees the epitope sites for the antibodies (Kureshi, Funderburgh et al. 2014).

Hence, to test the keratocyte markers Lumican and Keratocan, a deglycosylation step was performed using a combination of endo- β Galactosidase (Endo- β -Galactosidase from *Bacteroides fragilis*, recombinant expressed in *E.coli*, Sigma-Aldrich G6920) 0.57 Units/mg protein and Chondroitinase ABC (Chondroitinase ABC from *Proteus vulgaris*, Sigma-

Aldrich, C2905) 0.6 Units/mg protein for 4 h at 37°C, on 100 µg of corneal protein.

Gel preparation

According to the variation of molecular weights (i.e. 25-135kDa) of the proteins being detected, the western blot gel density was chosen and prepared. (Table 2.3).

% SDS-polyacrylamide gel (Total volume 30ml)	15%	10%	7.5%	5%
Linear range of protein separation (kDa)	12-43	16-68	36-94	57-212
ProtoGel® 30% (EC890, National Diagnostics)	15ml	10ml	7.5ml	5ml
Resolving buffer (EC 892, national diagnostics)	7.8ml	7.8ml	7.8ml	7.8ml
Dist. H ₂ O	6.9ml	11.9ml	14.4ml	16.9ml
10% ammonium persulphate (APS, Sigma-Aldrich)	300µl	300µl	300µl	300µl
Tetramethylethylene-diamine (TEMED, T7024SigmaAldrich)	30µl	30µl	30µl	30µl

Table 2.3 Components of the SDS-polyacrylamide gel with different densities

Components for different densities of gels (in %) and the linear range of protein separation in kDa required for various markers.

After preparing the x percentage resolving gel solution (APS and TEMED were added last to solidify the gel), the rack for gel solidification was assembled (Biorad®, Biorad Laboratories, Watford, UK). Approximately 12

ml of resolving gel was filled between the glass slide chamber (until the first line marking), covered with 2-isopropanolol, and left to set for 30 minutes. Following this, the 2-isopropanol was removed, and the stacking gel was overlaid to the upper line margin. This was immediately followed by placing a 1 mm well spacer (Biorad®) in the stacking gel phase. Ten ml 4% stacking gel was composed of: 1.3 ml Protogel, 2.5 ml stacking buffer (National Diagnostics, Nottingham, UK), 6.1 ml H₂O, 50 µl APS, 10 µl TEMED. The stacking gel was solidified within 20minutes

Sample preparation

Twenty or 40 µg of protein (see Table 2.4) containing 1x SDS loading buffer and made up to 20 µl with distilled H₂O was loaded per lane. The SDS-buffer was composed of 250 mM Tris-HCl (pH 6.5), 5% mercaptoethanol, 10% sodium dodecyl sulphate, 50% glycerol and 2-3 crystals of bromophenol blue.

A broad range biotinylated marker served as molecular weight indicator ladder (2.5 µl) (BIO-RAD 161-0319, Biorad®), 2 µl SDS-buffer and 5.5 µl distilled H₂O was added to the ladder. Additionally, 10 µl Spectra multicolour broad range protein ladder® (Thermo Fisher) was loaded between different sample lanes.

The samples and biotinylated ladder were heated on a heat block for 10 minutes at 100°C.

Electrophoresis and electrotransfer

The gels were transferred in running buffer at 150 V for 1 hour or until the dye front ran off the bottom of the gel. The running buffer was composed of Tris-Glycine SDS-Page Buffer® (National Diagnostics) and distilled H₂O (1:9).

Proteins were transferred to a polyvinylidene fluoride (PDVF) membrane that had been pre-wet in 100% methanol for 5 min, rinsed in water and soaked in transfer buffer (39 nM glycine, 48mM tris (trisaminomethane), 0.037% SDS, 20% methanol and 80% H₂O) using a Mini Trans-Blot® Electrophoretic Transfer Cell (Biorad). The wet transfer was performed at 100V for 1h. To visualize successful protein transfer, the membrane was stained in Ponceau S red 0.01% stain (Sigma-Aldrich) for 1-2 minutes, washed in methanol and rinsed in distilled H₂O.

Blocking and antibody incubation

The membrane was blocked in 5% skimmed milk in 0.1% Tween in PBS (PBS-T) for 1 hour. The primary antibody (see table 4) was added in 5% skimmed milk PBS-T for 60 minutes on a rocker at room temperature. The membrane was washed in 0.1% PBS-T for 2 x15min, followed by 3 x 5min on a rocker.

The membrane was incubated in the secondary antibody in 5% skimmed milk in PBS-T for 1 hour on the rocker at room temperature apart from the secondary antibody of the biotinylated ladder where 1:20.000 Streptavidin-Horseradish Peroxidase (HRP) (Biorad) was used in 0.1% PBS-T. The

membrane was washed in 0.1% TBST for 2x15 minutes, followed by 3x 5min on the rocker.

The membrane was incubated with chemiluminescence ECL Western blotting detection reagent (Amersham®, GE healthcare, Fisher Scientific) for 5 minutes.

In the dark room an x-ray film was placed on the membrane and exposed for 1-10min (depending on the primary antibody) and following development in the developer solution (Photsol CD18 x-ray developer 1:4 in tap water) until bands appeared (30 seconds – 5 minutes). The film was placed in fixative solution (CF42 fixer) for 1-3 minutes until the background was cleared, rinsed in tap water and air-dried.

To strip and re-probe the membrane with another antibody, the membrane was washed in PBS and stripped the same day using a stripping buffer (0.1 M mercaptoethanol, 2% SDS, 62.5 mM tris (pH 6.7) and 73% H₂O) at 60°C for 30 minutes. The membrane was washed 3 times in PBS (5 min) and re-blocked in 5% skimmed milk in 0.1% PBS-T overnight at 4C before incubating with another primary antibody.

Find in Table 2.4 the overview of antibodies tested in western blot assays.

Primary AB WB	Company (number)	Observed and predicted band size (kDa)	WB dilution	Cell lysate/tissue protein (μ g)
CD73	Bioss (bs-4834R)	Isoform 1: 63 Isoform 2: 58 predicted: 63	1:500	40 (CSSC/ adMSC)
CD90	R&D systems (AF 2067)	27 predicted: 23-30	1:500	20 (CSSC, adMSC)
Anti-Pax 6	Biolegend (901301)	50-52 predicted: 47-50	1:100	20 (CSSC, adMSC)
N-cadherin	Abcam (ab18203)	100 (unsp. band 135) predicted: 100	1:1000	20 (CSSC, adMSC)
Lumican	Abcam (ab168348)	36 (unsp. band 51) predicted: 38	1:1000	40 (corneal protein)
ALDH1A3	Abcam (ab129815)	55 (unsp. bands 30 and 15) predicted: 56	1:500	40 (corneal protein)
Keratocan	Biorbyt (orb2975)	50 (unsp. bands 141, 41, 25) predicted: 40	1:250	20 (corneal protein)
Secondary antibody				
Polyclonal swine anti-rabbit or anti mouse-HRP	Dako, Agilent, Santa Clara, USA	NA	1:1000	NA
Anti-sheep-HRP	R&D systems (HAF016)	NA	1:500	NA

Table 2.4 Overview of protein markers and secondary antibodies used in western blot assay

The table summarises the company details, observed and predicted band size, dilution and amount of cell lysate/tissue tested on, of the primary antibodies evaluated using the Western blot method.

(Supplementary material table S1 provides a list of primary antibodies tested that were not included in the study due to negative IF or unspecific binding in IF which could not be confirmed in WB assay.)

2.4 Gene expression analysis

2.4.1 RNA extraction and isolation from cells and tissues

Total RNA was extracted from corneal tissue (donor #15), 1×10^6 limbal CSC (passage 4-5) and 1×10^6 of their keratocyte-like differentiated cells (KDC) from different donors (donor # 3, 6, 11, 12, 13), adMSC (passage 4-5), after 7 days in CSSC media (adMSC-CSC) and their KDC (adMSC-KDC) and (adMSC-CSC-KDC) of three different donors (donor # 16, 17, 18), iPSC (passage 10-18) and their KDCs (donor # 19), cerebellum (donor # 24), skin fibroblasts (donor # 25) (details of donor tissue and cells see Table 2.1).

There are different techniques described to purify RNA (Tan and Yiap 2009). The general principle used in this study is of a single-step technique. The RNA is separated from DNA after extraction with an acidic solution composed of guanidinium thiocyanate, sodium acetate, phenol, and chloroform. The total RNA is then recovered by precipitation with isopropanol or ethanol (Rio, Ares et al. 2010).

The cells were trypsinised and cell count was performed. The cells were centrifuged at 1000rpm for 5 min and the pellet was resuspended in TRI-Reagent (Sigma-Aldrich). Alternatively, the culture media was aspirated from the culture dish, washed in PBS, aspirated and 1ml TRI-Reagent (Sigma-

Aldrich) per 10cm plate was added. Following, the cells were manually scrapped off using a cell lifter (Corning®, Sigma-Aldrich). The suspension was transferred in an Eppendorf pipette and stored at - 80°C.

The cornea (#15) and cerebellum (#24) tissue samples served as positive controls for keratocyte and neural crest specific primers respectively (find details in 2.4.3). Tissue pieces were cut in small pieces and ground up in 1ml TRI-Reagent (Sigma-Aldrich) using a pestle and mortar until a relatively homogenous tissue mass was generated. The fluid phase was transferred in an Eppendorf pipette and stored at -80°C. Generally, 50-100 mg of tissue was homogenised in 1ml Tri-reagent (Sigma-Aldrich).

The samples in TRI-Reagent (Sigma-Aldrich) were thawed and incubated in RT for 5 minutes, 0.3 ml chloroform was added per ml of tri-reagent and samples were vortexed, incubated for 5 minutes (RT) and then centrifuged at 12000 rpm for 15 minutes at 4°C. Centrifugation separates the mixture into 3 phases: a lower red protein organic phase, an DNA containing interphase, and a clear upper aqueous RNA phase. The RNA containing aqueous phase was transferred in a new Eppendorf pipette.

The aqueous phase was then mixed via pipetting with 1x the volume of 70% ethanol. RNA was then purified using the RNeasy mini kit (Qiagen, Manchester, UK) according to the manufacture instructions and treated with Ambion DNA-free (Life Technologies) to remove genomic DNA also according to manufactures instructions. Yields were in the range of 146–1218 ng per sample. The 260/280 nm ratios ranged between 1.7 and 1.99 (Nanodrop). The RNA was stored at -80°C until use.

2.4.2 Reverse transcription and quantitative polymerase chain reaction

Complementary DNA was made from 1 µg of RNA using the sensiFAST cDNA synthesis kit (Bioline, London, UK). Control reactions without adding reverse transcriptase (-RT) were performed to ensure the absence of genomic DNA contamination. The following thermal cycles for the reverse transcription were used: 10 minutes at 25°C, 15 minutes at 42°C, 15 minutes at 48°C, 5 minutes at 85°C, finish and hold 4°C. Finally, 30 µl of high-performance liquid chromatography (HPLC) water was added to each cDNA and -RT sample prior to storage at -20°C.

Canine gene-specific intron spanning primers were designed as described below (find details in 2.4.3 Primer design, Table 2.6). QPCR was carried out using the Bio-Rad C1000 Touch Thermal Cycler (Bio-Rad, Watford, UK). Each PCR reaction was performed in duplicate in a 20 µl reaction volume using HPLC grade water. Each reaction consisted of 10 µl 2xSYBR green containing supermix (Sensimix, Sybr-NoRoxKit, Bioline, UK), 1 µl forward primer, 1 µl reverse primer (final concentration, 0.5 µM), 6 µl HPLC water and 2 µl cDNA. In each PCR reaction a negative control of HPLC water and -RT sample was tested in duplicate. The melt curves (amplification and melt temperature) were reviewed. The PCR reaction was repeated, when contamination of -RT with genomic DNA or contamination of HPLC water occurred.

QPCR cycle parameters were 95°C for 10 min, followed by 40 cycles of 95°C for 15 s, 60°C for 15 s and 72°C for 15 s. Finally, a melt curve was produced

by taking readings every 1°C from 65°C to 95°C. The levels of canine 18S rRNA did not change between treatments and it was used to normalise gene expression using the $2^{-\Delta\Delta C_t}$ method (Livak 2001).

All qPCRs were performed in a biological triplicate (i.e. RNA of cells from three biological different donors). Canine iPSCs, ciPSC derived NCC/CSCs and their differentiated keratocytes were performed in a technical triplicate (i.e. three independent qPCR reactions of cells from the same donor).

2.4.3 Primer design and efficiency test on positive control cells/tissue

Dog-specific primer sets were developed and validated given there are not yet widely commercially available for this species. The intention was to design primers that are specific for the gene of interest and span an intron unless the gene has only one annotated exon. Thirdly, to produce amplicons which, if they form any secondary structures, have a melting temperature (T_m) <60°C.

Primers were designed from annotated canine exon sequence (<https://www.ensembl.org/index.html>) for the genes of interest using primer3 (<https://primer3.org/webinterface.html>).

The following primer settings were applied (Table 2.5):

Primer design	Parameters
Product size (base pair)	50-150bp
Number to return	8
Primer size (number of nucleotide bases)	18-22
Primer T _m (melting temperature)	57-63
Primer Guanine/Cytosine ratio in %	40-60%

Table 2.5 Primer design settings

The mfold (<http://unafold.rna.albany.edu/?q=mfold>) software was used to obtain amplicons with a melting temperature (T_m) of 58°C – 62°C, without a secondary structure at T_m 60°C and of an amplicon size between 50-150 bp.

The specificity of each primer set was confirmed by blast analysis (<https://www.ensembl.org/index.html>). When the canine gene was not annotated (as for Pax6 (primer design: 2018)), the human Pax6 gene sequence was used to find the corresponding region of the canine genome. All primers were exon spanning apart from *Lumican*. Primers were produced by Sigma-Aldrich on a synthesis scale of 0.025µM and a desalt purification and a full list can be found in Table 2.6.

The amplification efficiency of each primer was calculated using a 1:2 dilution series of cDNA.

Primer sequence (5'- 3') used for qPCR			
Gene name	Forward (Genomic location)	Reverse (Genomic location)	Product size (bp)
LUM (Lumican)	AAACATTTGCGTCTGGATGG (15:31793626-31793646)	TATCAGGTGGCAGACTGGTG (15:31793591-31793611)	55
Kera (Keratocan)	TCATCTGCAGCACCTTCATC (15:31755896-31755916)	TGATTTTCATTGCCATCCAGA (15:31751604-31751624)	146
ALDH1A3	GCCCTTTATCTGGGCTCTCT (3:40153361-40153381)	GACCCCGTGAAGGCTATCTT (3:40151638-40151658)	137
CDH2 (N-cadherin)	TGTGAACGGGCAAATAACAA (7:60911935-60911955)	AGATCTGCAGCGTTTCTGTT (7:60915415-60915435)	137
Pax6[^]	ATTACTGTCCGAGGGGGTCT (18:35838044-35838064)	CTAGCCAGGTTGCGAAGAAC (18:35838844-35838863)	81
ACTA2 (Alpha-SMA)	ACTGGGACGACATGGAAAAG (26:38709974-38709994)	CACGGAGCTCGTTGTAGAAA (26:38707202-38707222)	97
NGFR-201 (P75, NGFP75)	GTTGGATTACCCGGTCCAC (9:25616068-25616087)	TAGCTCTGGCTCCTCTGTGC (9:25616119-25616139)	71
Sox10	GGAGGCTGCTGAACGAGA (10:26686533-26686549)	GCTCAGCCTCCTCAATGAA (10:26686563-26686582)	51
POU5F1 (Human Oct4*)	CGAAAGAGAAAGCGAACCCAG (8:127416553-127416573)	ACACTCGGACCACATCCTTC (8:127416672-127416692)	142
RPS5*	TCACTGGTGAGAACCCCT (1:99559938-99560115 **)	CCTGATTCACACGGCGTAG (1:99559816-99559834)	141
RPS19*	CCTTCCTCAAAAAGTCTGGG (1:112426474-112426773**)	GTTCTCATCGTAGGGAGCAAG (1:112426399-112426419)	95
RNA18S***	CCGCAGCTAGGAATAATGGA (JH373485.1:23582-23602)	CCTCAGTTCCGAAAACCAAC (JH373485.1:23623-23643)	61

Table 2.6 Overview of primers details

Summarised the gene name (alternative name), primer sequence, genomic location (CanineFam 3.1), and product size of all designed canine primers. The human Oct4* (Baird, Barsby et al. 2015) and RPS5* and RPS19* were abstracted from (Brinkhof, Spee et al. 2006); **, N.B. primer spans an exon/exon boundary so genomic positions reflect the presence of an intron; ***the RNA 18S primers were designed using Genbank sequence AY623831.1. At the time of writing, the primers align to scaffold region JH373485.1 in Camfam3.1 which has not yet been assigned to a chromosome; [^], Pax6 genomic sequence Dog - Great Dane UMICH_Zoey_3.1, www.ensembl.org (details in Hunter et al 2007).

In a standard curve, the canine-specific designed primers were tested for the specific binding efficiency to the target gene in the cell of interest and control tissue. A dilution series of 1:2 in 5 serial dilutions (2µl – 0.0625µl) of cDNA in duplicate had to be recognised by the designed primer with an acceptable variation of 90-110%. Less than 90% is a sub-optimal binding and >100% indicate non-specific binding (Figure 2.2).

Efficiency = $10^{(-1/\text{slope})}$

$10^{(-1/-3.321928)} = 2 = \text{doubling for each cycle} = 100\% \text{ efficiency}$

The slope of the standard curve (Ct or Cq vs. concentration) is related to the efficiency. This should be close to -3.321928.

R² describes the fit of the standard curve to the data points and should be close to 1.

All primers had an efficiency between 90-110% (Table 2.7)

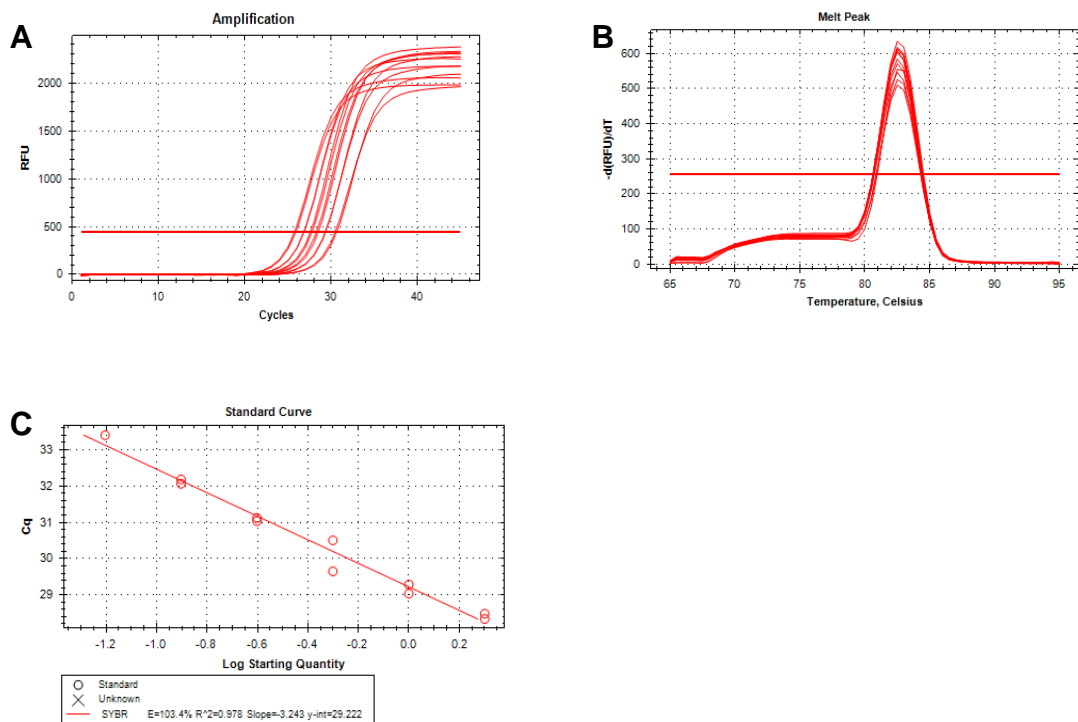
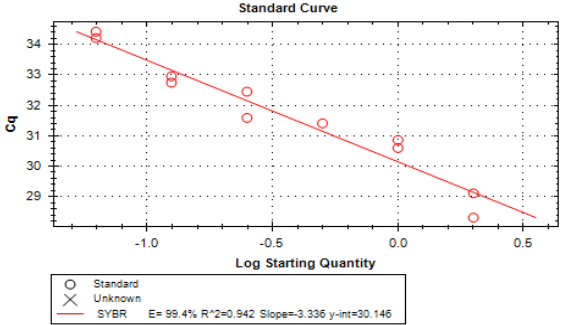
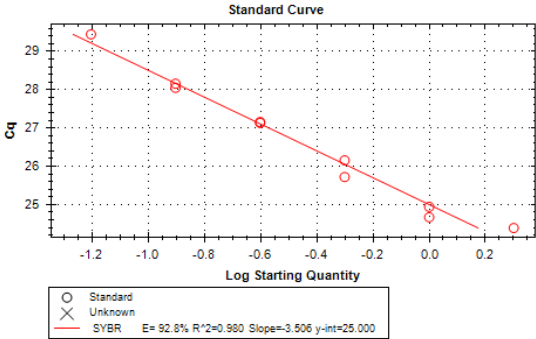
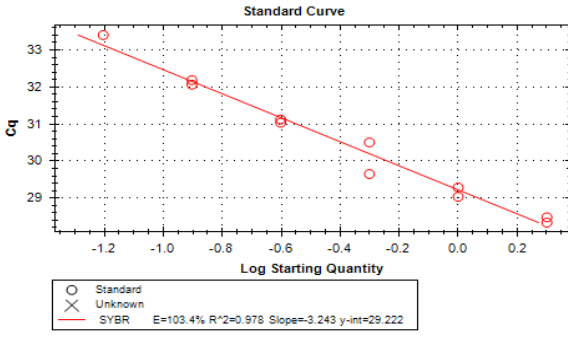
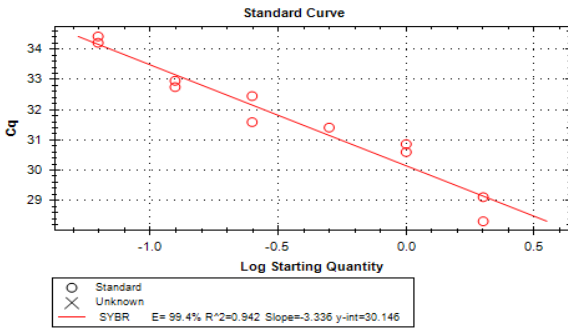
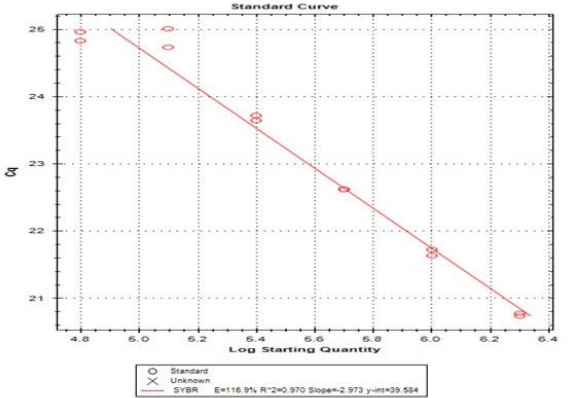
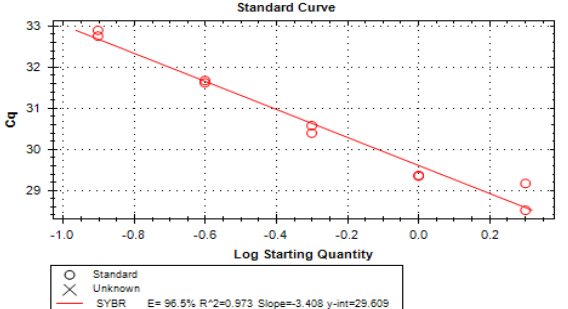
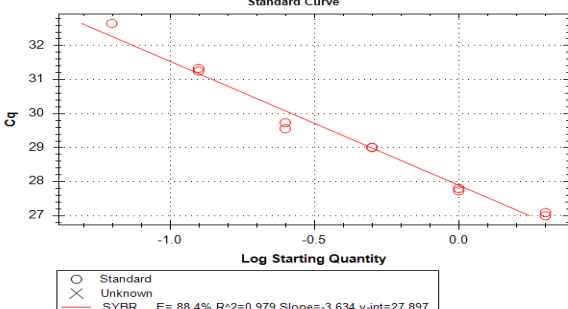
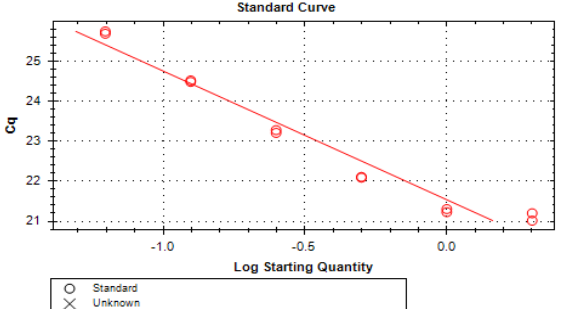


Figure 2.2 Example of primer efficiency evaluation on corneal RNA for ALDH1A3

The graphic illustrates the efficiency test, as an example, for the primer for ALDH1A3 on corneal RNA (donor #15). This was performed in one technical repeat. (A) demonstrates the amplification cycles of the dilution series (1:2) and (B) the melt curves of 82.5°C. (C) The standard curve demonstrates the Cq values to the starting quantity (log scale) with an efficiency (E) of 103% (R² of 0.978 and a slope of 3.24). Abbreviation: Cq, quantification cycles.

Primer (test tissue/cells) (E= efficiency in %)	Standard curve
Keratocan (cornea) (E = 99.4%)	
Lumican (cornea) (E = 92.8%)	
Pax6 (cultured corneal stromal cells) (E = 103.4%)	
Alpha-SMA (skin fibroblasts) (E = 99.4%)	

<p>N-cadherin (cultured corneal stromal cells)</p> <p>(E = 110%)</p>	 <p>Standard Curve</p> <p>Ct</p> <p>Log Starting Quantity</p> <p>○ Standard × Unknown — SYBR E=116.9% R²=0.970 Slope=-2.973 y-int=39.584</p>
<p>P75 (cerebellum)</p> <p>(E= 96.5%)</p>	 <p>Standard Curve</p> <p>Ct</p> <p>Log Starting Quantity</p> <p>○ Standard × Unknown — SYBR E= 96.5% R²=0.973 Slope=-3.408 y-int=29.609</p>
<p>Sox10 (cerebellum)</p> <p>(E= 98.4%)</p>	 <p>Standard Curve</p> <p>Ct</p> <p>Log Starting Quantity</p> <p>○ Standard × Unknown — SYBR E= 88.4% R²=0.979 Slope=-3.634 y-int=27.897</p>
<p>RPS5 (adipose derived MSC)</p> <p>(E = 104.5%)</p>	 <p>Standard Curve</p> <p>Ct</p> <p>Log Starting Quantity</p> <p>○ Standard × Unknown — SYBR E=104.5% R²=0.960 Slope=-3.218 y-int=21.537</p>

RPS19 (adipose derived MSC)

(E = 107.7%)

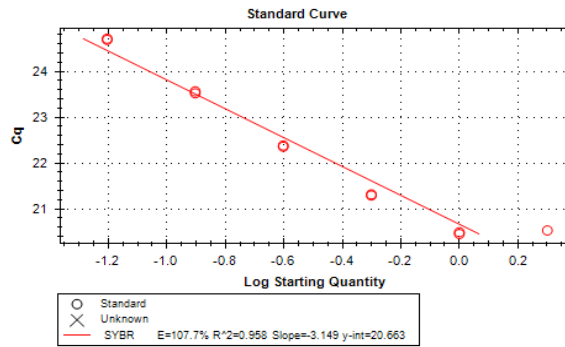


Table 2.7 Summarises the efficiency test of canine-specific designed primers on positive control RNA and the associated standard curves.

Abbreviations: E, efficiency in %; SYBR, SYBR green; R² describes the fit of the standard curve (=1); MSC, mesenchymal stromal cell; RPS, ribosomal protein s

The following positive control cells/tissues were used for the primer evaluation: cornea (Keratocan, Lumimcan, ALDH1A3), corneal stromal cells (Pax6, N-cadherin), cerebellum (Sox10, P75) and skin fibroblasts (α -SMA), adMSC (RPS 5/RPS 19). Negative controls of tissue or cells to known not expressing the gene were not performed in this study.

2.4.4 Gel electrophoresis

Gel electrophoresis (GE) was used to confirm that each primer set produced a product of the expected size. All products were run on a 2% agarose gel in TEA buffer (Tris base -acetic acid – EDTA, National Diagnostics) with Gel Red Nucleic Acid Gel Stain (Biotium, Cambridge Bioscience, Cambridge, UK). 5 μ l of PCR product was mixed with 1 μ l loading dye (6x Orange DNA loading dye, Thermo Fisher) and loaded per lane along with 5 μ l of 50 bp reference ladder (Quick Load purple 50bp Ladder, New England Biolabs, Hitchin, UK). The gels were run at 100 V for 30 to 45 minutes or until the dye front ran close off the bottom of the gel.

The bands were visualized and imaged under UV light using a gel analyser. All qPCR products showed bands of the expected size (Figure 2.3, 2.4, 2.5).

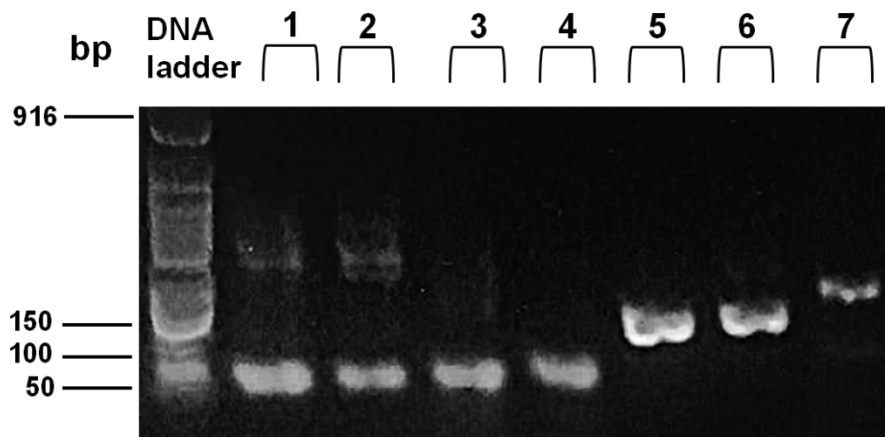


Figure 2.3. Gel electrophoresis assay of PCR products (I)

CSC and CSC-KDCs of donor #12- 15 of the following primers and their predicted product sizes: Lane 1, 2 canine18s, 61bp; lane 3,4 Lumican, 55bp; lane 5,6 Keratocan, 146 bp; lane 7, N-cadherin, 137bp. Abbreviation: bp, base pair; CSC, corneal stromal cell; CSC-KDC, Corneal stromal cell derived keratocyte-like differentiated cell

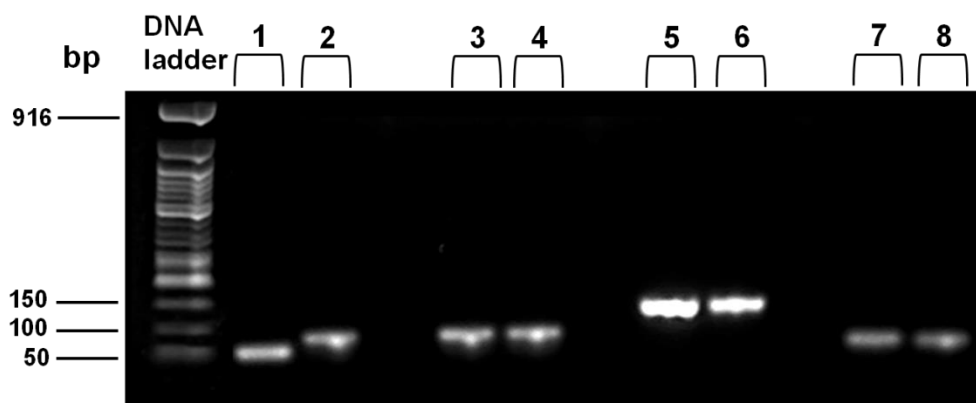


Figure 2.4 Gel electrophoresis assay of PCR products (I)

CSC donor #12-15 and CSC-KDCs of the following primers and expected band size: lane 1, canine 18s, 61bp; lane 2, 3, 4, Pax6, 81bp; lane 5, ALDH1A3, 137bp; lane 6, positive control for ALDH1A3 (corneal cDNA of donor # 15); lane 7, α -SMA, 54bp; lane 8, positive control of α -SMA using skin fibroblasts donor #25. Abbreviations: bp, base pair; CSC, corneal stromal cell; CSC-KDC, Corneal stromal cell derived keratocyte-like differentiated cell; α -SMA, alpha smooth muscle actin.

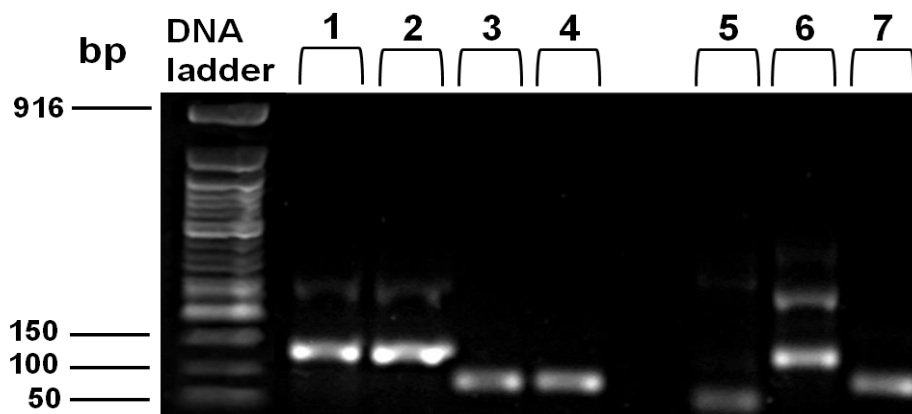


Figure 2.5 Gel electrophoresis assay of PCR products (III)

Lane 1, 2, 5RPS (CSC donor #14) 141bp; lane 3,4, 19RPS, 95bp (CSC donor #14); lane 5, canine 18s, 61bp (iPSC donor #19); lane 6, reference gene 5RPS (iPSC donor #19); lane 7, reference gene 19RPS (iPSC donor #19); Abbreviations: CSC, corneal stromal cell; RPS, ribosomal protein; iPSC, induced pluripotent stem cell.

2.4.5 Canine reference gene analysis

The stability of the “standard gene expression is essential for internal standardisation of target gene expression data, so called housekeeping genes with (assumed) stable expression can exhibit either up- or down-regulation under some experimental conditions” (Pfaffl, Tichopad et al. 2004).

Reference gene studies on canine ocular tissue are not available in the literature. Peters et al 2007 studied 11 different reference genes on eight different healthy tissues and concluded that there are no universal control genes in canine tissues and recommended the use of multiple internal control genes based from different tissue, disease groups and culture conditions (Peters, Peeters et al. 2007).

To assess the reference or housekeeping gene stability for canine 18s, 5 RPS and 19RPS in this study, the RefFinder software (<http://hongyexport.com/>, ©Dr. Zhang's lab) was used. The software compares the results of four different reference gene software programs (delta CT, Best Keeper, Normfinder and Genorm). The housekeeping gene of canine ribosomal RNA 18s was compared to 5RPS and 19RPS, which were chosen based on the findings of Brinkhof et al 2006 (Brinkhof, Spee et al. 2006). The CT values of all three housekeeping genes of CSC (donor #13), MSC (donor #17) and iPS cells (donor #19) and their keratocyte differentiated cells were compared. Overall, canine 18s had the lowest M-values which is consistent with the highest stability factor in all cell types tested. The M-value is calculated by the average pairwise variation of a single gene to all other candidate genes (Brinkhof, Spee et al. 2006). The two

biological repeats of qPCRs data per cell type and differentiated cells were therefore referenced against canine18s only. All three genes were expressed in a limbal CSC cDNA sample (donor #13) and adMSCs (donor #17). Figure 2.6 demonstrates the graphs of amplification cycles and melting temperatures. (Graphs of qPCR results normalised against all three reference genes can be found in the supplementary figures S 2 and S 3).

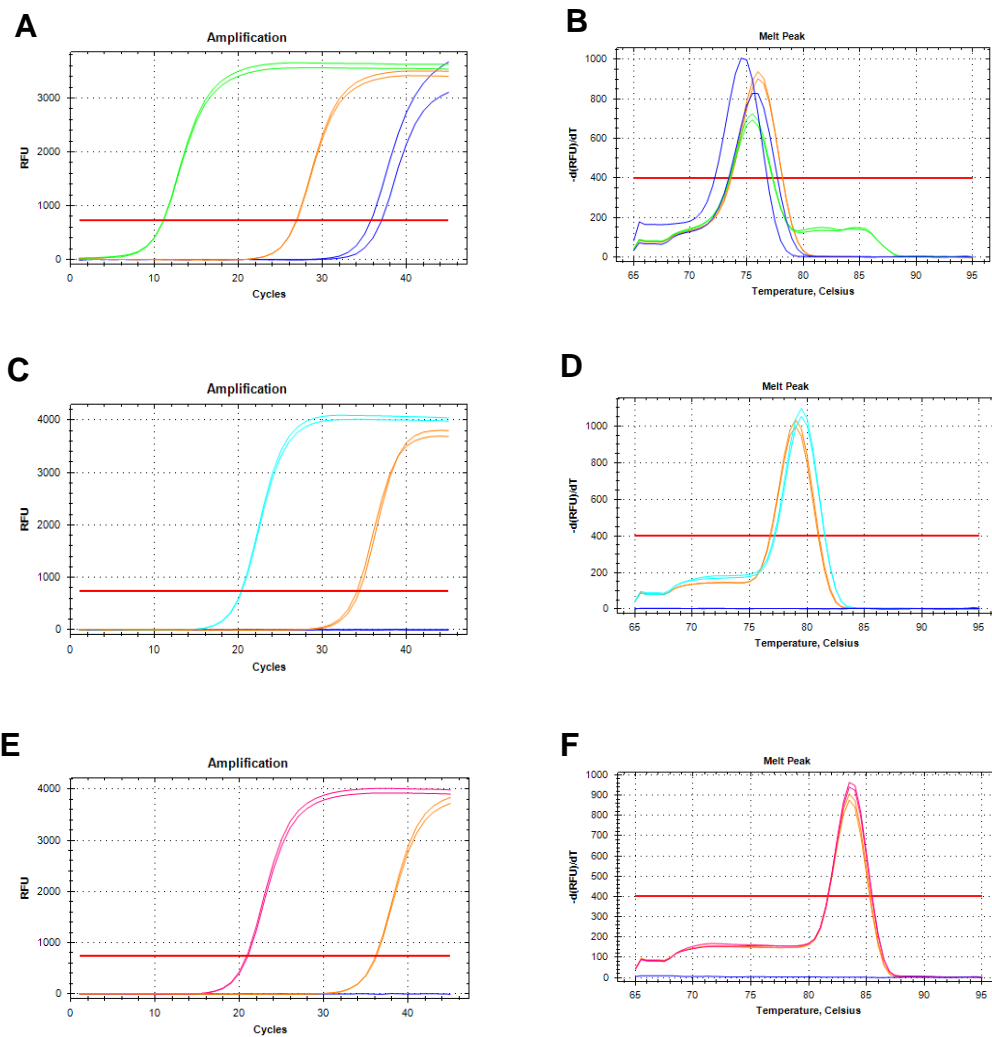


Figure 2.6 Amplification cycles (CT) and melt curves in duplicates of reference genes 18S, 19 ribosomal protein S (RPS) and 5 RPS.

The graphics illustrates the amplification cycles (CT) and melt curves in duplicates of (A/B) reference genes 18S (green) of canine CSC cDNA (donor #13), (C/D) 19 RPS (turquoise) and (E/F) 5RPS (pink). The CT values of 20 cycles in 19RSP and 5RPS were higher than in 18s with a CT value of 12. The melting temperature were consistent of 76, 79 and 83 °C for 18S (B), 19RSP (D) and 5RPS (F) respectively, which corresponds to the expected melting temperature. HPLC water (blue) and the -RT sample (orange) served as negative control.

2.5 Statistical analysis

Shapiro-Wilk normality test (XLSTAT-base, Witzhausen, Germany) for *Lumican*, *Keratocan*, *ALDH1A3*, *Pax6*, *N-cadherin* and α -SMA qPCR CT-values of CSCs, adMSCs and their KDCs of three different donors confirmed that the data were normally distributed ($P > 0.05$).

For comparisons of two groups the Student's t-test (unpaired, two-tailed) was used. $P < 0.05$ was considered to be statistically significant. If more than two means were compared, the ANOVA test was used and if significant ($P < 0.05$), secondly the Tukey's post-hoc (Tukey's honest significant difference test) test was used. These tests calculated absence of presence of significant difference of cell composition based on cell morphology (Figure 3.3.6.D, Figure 3.20) and gene expression levels of cell groups such as adMSC, ciPSC and their differentiated cells (CSC, KD) (Figure 4.3.2, Figure 4.6; Figure 5.3.2, Figure 5.10).

Chapter 3:

Localisation, isolation and characterisation of canine corneal stromal cells in the limbal and central cornea of healthy dogs

3.1 Introduction

Funderburgh et al. (2005) first described a small population of Pax6 expressing cells (<4%) in the bovine corneal stroma and identified them as progenitor cells. Stromal cells expressing mesenchymal stromal cell markers in the anterior stroma close to the limbus, were also identified in humans. (Funderburgh, Du et al. 2005). (See details in 1.1.4)

The current literature of corneal stromal stem cells is based mainly on human, murine and rabbit corneal cells (Li, Dai et al. 2015), studies in canine corneas are not available. The basic anatomic structure of the cornea between mammals is similar, a major anatomic difference of the limbus in dogs is the absence of Palisades of Vogt's and limbal epithelial crypts (Shively and Epling 1970, Morrin, Waring et al. 1982, Patruno, Perazzi et al. 2017). Given the limited information on the canine limbus, the first aim of the present chapter was to investigate the corneal limbus in healthy dogs histologically. The second aim was to isolate and characterise corneal stromal cells of the limbus and central cornea and investigate whether they have multipotent MSC properties.

3.2 Materials and methods

3.2.1 Corneal harvesting and corneal storage medium

Within 30min -12h after confirmed death, the eyes were enucleated and the cornealscleral buttons were excised under surgical conditions. A povidone-

iodine solution 1:50 in saline was used to clean the ocular surface. Once excised, the tissue was intensively flushed with 0.9% saline solution and several drops of 0.3% ofloxacin (Exocin® Allergan, Marlow, UK) containing eye drops were applied. Left and right eyes were placed in separate containers and a snip mark was cut in the sclera to identify the 12 o'clock position. The tissue was placed in a standard corneal organ culture medium containing Eagle's Minimum Essential Medium (M2279, Sigma Aldrich), 5% dextran (Sigma-Aldrich), 2% FBS (Gibco) and 1% Antibiotic-Antimycotic Mix (Sigma-Aldrich) at RT for up to 14 days.

3.2.2 Histology: Cryosectioning, OCT embedding and histological analysis

The anatomic structure of the canine limbus is not well described (Patrino, Perazzi et al. 2017); therefore corneoscleral buttons of five fresh enucleated eyes were excised (donor # 3-7) and embedded for histological investigations. For the orientation, the 12 o'clock position was marked using a tissue marker pen (Figure 3.1A) or a cut with a scalpel blade. The eyes underwent gross examination under the dissecting microscope. Photographs were taken, with special attention paid to the limbus region and the integrity of the tissue (Figure 3.1B). To discover possible anatomic regional differences, four blocks per cornea of the superior, temporal, inferior and nasal cornea were embedded in OCT tissue compound (Tissue Tek® VWR international Ltd., Lutterworth, UK). The tissue was placed in longitudinal orientation to the central cornea, snap-frozen in liquid nitrogen and cut in 7µm thick frozen sections. Sections were collected on Superfrost microscope

slides (VWR). Routine automated Haematoxylin-Eosin and Periodic Acid Schiff (PAS) staining was performed on each of the four indicated regions of three donor corneas to illustrate the histology of the limbal and central corneal stroma.

One sample of haired canine skin tissue (donor # 7) were snap-frozen, embedded in OCT media (VWR), frozen (-20°C) and cut in 7µm sections to serve as CD90 positive control.

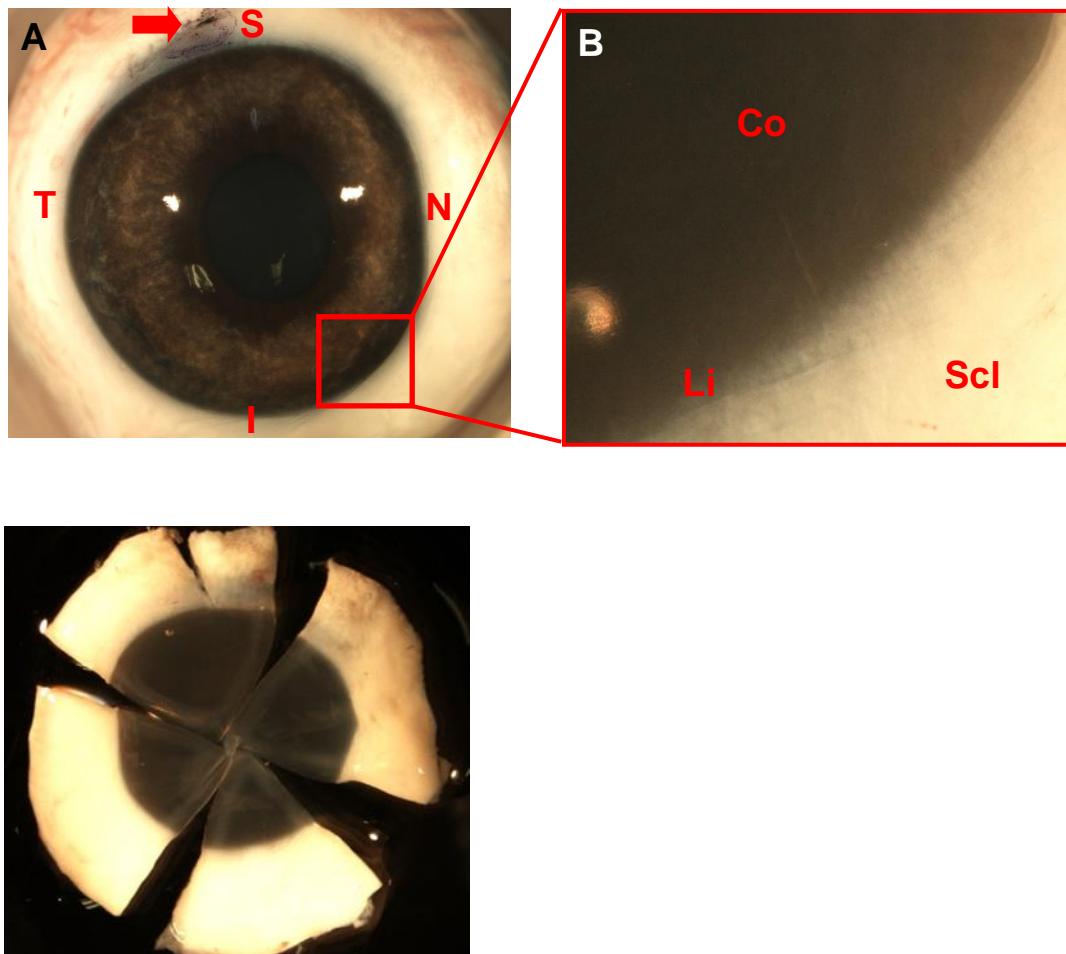


Figure 3.1 Macroscopic investigation of the limbus and orientation for the dissection of the canine cornea

A): Gross photograph of the right canine eye (donor # 7b) with a mark at 12 o'clock position (red arrow). B): The limbus was examined under higher magnification, which was not pigmented in this donor. Macroscopically visible palisades of Vogt's as in humans could not be identified; the canine limbus is smooth, and a slightly irregular junction could be noted. C): The dissected corneal scleral button with the superior (S), temporal (T), inferior (I) and nasal (N) quarter of a right eye. The superior vertical cut indicates the 12 o'clock position. The corneal sclera junction is highlighted by a dotted line. Abbreviations: Co, cornea; Li, limbus; Scl, sclera.

3.2.3 Immunohistochemistry and immunocytochemistry

Seven μm sections on Superfrost plus slides (VWR) of three donors (donor # 1, 2, 3) from each region (superior, inferior, temporal, and nasal) were used for immunohistological investigations of mesenchymal stromal cell properties. Keratocyte specific markers as internal positive control were evaluated (see Figure 3.11). Fresh isolated, cultured, and fixed (3% paraformaldehyde) CSC (donor # 1, 2, 4, 6; passage 3-5) and their differentiated keratocytes were investigated using immunocytochemistry with the same protocol. The detailed protocol is described in general methods 2.3.1 Immunofluorescence staining protocol.

3.2.4 Tissue dissection, cell isolation and cell culture

A) Tissue dissection and cell isolation

All instruments used for the dissection of the corneoscleral button to isolate CSC, were chemically sterilised for 20 minutes in ethanol. The tissue underwent three washing steps in media corneal stem cell isolation media ((DFO media), see details in Supplementary table S3)). Surrounding conjunctiva and underlying Tenon's capsule were removed. The central and limbal cornea was separately handled in all following steps of the dissection and culture process. The central cornea was trephined to approximately half of the corneal stromal depth using a 7.5 mm corneal handheld trephine (Altomed, Bolden, UK) (Figure 3.2 A, B). Following a 300 μm set depth corneal knife (BD, Beaver Visitec) was used to cut the defined central cornea in parallel epithelial-anterior stromal strips (Figure 3.2 C). The tissue strips

were excised using corneal scissors and cut into approximately 2x2 mm pieces and transferred in the digestion media. The limbus was excised using first the 300 μm set depth knife marking the sclera and corneal side. The limbus was slightly elevated in a dome-shaped fashion using Colibri forceps and the mid-stroma/epithelium was excised with corneal scissors. The long limbal tissue stripe was cut 2x2 mm pieces and transferred into the digestion media. The digestion media was composed of the collagenase from *Clostridium histolyticum* (Blend Type L, ≤ 1.0 FALGPA units/mg, Sigma-Aldrich) in DFO media in a 1:10 dilution for 14-16 hours in the incubator (37°C, 5% CO₂ in air).

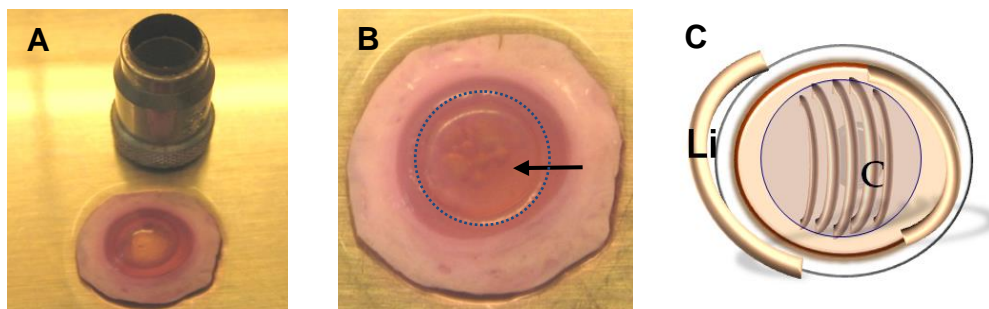


Figure 3.2 Tissue dissection for the cell isolation of limbal and central derived CSC

Photographs of the corneoscleral button and the 7.5mm corneal trephine (A), which was used to demarcate and trephine the central cornea approximately half depth (black arrow, B), followed by (C) excision of the limbus in two stripes (Li) and several stripes of central cornea (C). Corneal epithelial-anterior stromal tissue stripes were then cut in 2x2mm pieces and transferred into the digestion media.

B) Cell culture in corneal stem cell media

After the digestion process, the remaining particles were dissolved using a pipette repeatedly. After a centrifugation of 1000 rpm 5min, the cell pellet was transferred into CSSC media (Supplementary table S4) in a fibronectin-collagen coated (FNC Coating Mix, Athena Enzyme System, Baltimore, MD, USA) T25 tissue culture flask (Thermo Fisher Scientific) incubated at standard condition (37 °C, 5% CO₂ in air) for 24h. The FNC coating was initially used in all samples at each passage for the first six corneas. However, given there was no difference observed in the attachment gradient of the CSC with or without FNC coating after passage 1, FNC was only used in subsequent preparations for passages 0-1. The cells were washed in PBS and the CSSC media was replenished before incubation for 24h. Short selective trypsinization under microscope guidance was used (TrypLE (1x) express Gibco) to separate the small oval-shaped CSC from the epithelial cell islands, keratocytes and melanocytes. The selected CSCs were expanded into larger or multiple tissue culture flasks to a maximum confluency of approximately 60-70%, which is required to maintain their stem cell characteristics. The medium was changed every 48-72 hours.

C) Cell culture assay at Passage 0

To study the cell composition immediately after the cell isolation process, without selective passaging (i.e. separation of epithelial cells) and longer exposure to the CSSC media, three limbal and central corneal isolates (donor # 11, 12, 13) were investigated. The isolates were digested, resuspended in CSSC media and transferred onto FNC coated chamber

slides (4 chamber slides, Nunc LabTek, Sigma-Aldrich). The cells were incubated for 48h under standard conditions, fixed in 3% PFA and then immunocytochemically investigated.

3.2.5 Cell culture kinetics of CSC

Corneal stromal cells as a primary cell culture were isolated from the central cornea and limbus. The growth characteristic of these cells was evaluated, and a comparison was made to see whether a statistically significant difference exists between limbal and central-derived cells. A growth curve for cultured cells follows a sigmoid proliferation pattern. The growth phases of cultured cells are divided into lag phase, (the cells do not divide and adapt to the culture conditions), logarithmic (log) phase (cells proliferate with exponential cell expansion), plateau or stationary phase (cell proliferation rate decrease to 0-10%) and decline phase (cell death). Cell growth patterns of mesenchymal stromal cells differ concerning the log phase, which will exhibit an extended phase with multiple cell doubling times over an regular time interval between every 48-72h (Corradetti, Meucci et al. 2013).

A) Cell expansion

The maximal cell culture time in days and maximal passage frequency of stromal cells isolated from six corneas (limbal, central) of six different donors (# 10-15) was evaluated until the decline phase was reached. One central and two limbal cell samples were excluded due to confluency, early differentiation and early discontinuation of proliferation. Cell culture images were taken every second day using a phase-contrast microscope.

Cell counts of limbal and central derived CSC before each passage were performed in three corneas of three different donors (#7, 8, 9) over 6 passages (P1- P6).

B) Population doubling time and population doublings

The mean population doubling time (PDT) was calculated based on three randomly selected biological independent limbal and central derived CSC (donor # 10, 11, 12). The doubling time and number of cell doublings were calculated at each passage until the stationary phase was reached (P1-P6). (Roth V. 2006 Doubling Time Computing, available from: <http://www.doubling-time.com/compute.php>)

The population doubling of cells was calculated as:

The number of cell doublings (NCD) = $\log_{10}(y/x)/\log_{10}2$ (y = final density; x = initial seeding density (Polisetty, Fatima et al. 2008).

The cell number of P0-P1 was not included as CSC derived from cultured limbal and central cells had epithelial cell contamination.

3.2.6 Cell culture of adipose-derived mesenchymal stromal cells

Three lines of canine adMSC (donor # 16, 17, 18), processed and banked at the AHT (Dr. D. Guest, Newmarket, UK) served as positive control and to evaluate the comparative potential for differentiation into keratocytes (chapter 4). The derivation of the three cell lines was described by Baird et al. 2015 (Baird, Barsby et al. 2015). Briefly, subdermal adipose tissue, removed during routine surgery with owner consent, was collected into sterile cell

culture media (Dulbecco's modified Eagle's medium (DMEM) high glucose), with added FBS (10%), 1% penicillin–streptomycin, 1% L-glutamine and 1% Fungizone (all Invitrogen, Paisley, UK). The tissue was rinsed in media in several times and dissected into small pieces before incubation in media substituted with 1 mg/ml collagenase type I from *Clostridium histolyticum* (Sigma, Poole, Dorset, UK) overnight under standard culture conditions (37 °C in 5% CO₂ in air). The cell suspension was centrifuged (1500rpm, 5min) and resuspended in cell culture media lacking fungizon and transferred onto a 10-cm plate. The cells were passaged at confluency for expansion and cryopreservation of cell stocks in media containing 10% DMSO.

The cryopreserved MSCs were thawed before plating onto 10 cm tissue culture plates in MSC media (Supplementary table S5 provides details). Tissue culture conditions were maintained at 37°C in 5% CO₂ in air, with MSC media being replaced every 2-3 days. Once adherent cells reached 80% confluence, they were passaged using 0.25% trypsin/EDTA (Sigma, Poole, Dorset, UK) (every 2-3 days). MSCs were highly proliferative and were used between passages 2-5.

3.2.7 Flow cytometry

Flow cytometry was performed on three biological replicates each of limbal but not central-derived cryopreserved CSC (donor # 11, 12, 13). The CSC were thawed and expanded up to passage 6. Cells were detached and counted (see chapter 2 in general materials and methods) and fixed in 3% paraformaldehyde (Sigma-Aldrich) for 20 minutes. The fixed cells were

washed (3x 2min) by spinning (entire protocol: 1500rpm for 2minutes), removal of the supernatant by fast flicking and resuspended in PBS. The cells were distributed in 200µl PBS/1x10⁶ cells/well of a v-bottom 96 well plate (Greiner CELLSTAR, Sigma-Aldrich).

Cells should not be stored longer than 14 days at 4-8°C. The primary markers tested were suitable to be evaluated in a non-life assay. FITC was used as single fluorophore in this study. After the staining procedure, the FITC labelled cells should be used immediately, but would be suitable for flow cytometry analysis for up to 7 days as long as light protected and stored at 4°C. To identify the cell population of interest the following control samples were used: FITC labelled cells to determine unspecific binding of the fluorophore to cellular components and isotype IgG control –FITC labelled cells to determine the non-specific binding of an antibody to an FC receptor. With these controls the negative gates could be set appropriately.

The fixed cells were spun, washed in 200µl PBS, spun again and permeabilised in 0.1% Triton x-100 for 1h at RT (except for CD90). After three washing steps the cells were blocked in 10% goat or donkey serum (Sigma-Aldrich) for 30min, spun (1x) to then incubated for 45min at 4°C with primary antibody, rabbit IgG or sheep IgG, followed by incubation with the appropriate FITC labelled secondary antibody for 45min 4°C. (Details of all primary and secondary antibodies used for flow cytometry are listed in Table 3.1).

A FACS Calibur flow cytometer (BD Biosciences Immunocytometry Systems, Franklin Lakes, NJ) was used (emission filter: 530/30; laser lines: 488nm)

and the data were analysed using Novoexpress ® Software (ACEA Biosciences, San Diego, USA).

To exclude dead cells and cell debris, events were gated using forward versus side scatter height (R1). R1 events were gated to remove doublets (R2) by forward scatter height versus forward scatter area. According to Overton 1988, it was decided to gate two percent of events in the R2 isotype control and all events to the right were included in a new gate (= R3) by FITC height versus forward scatter height (Overton 1988). The overlaid events of each primary antibody gated within this new gate R3 were counted as positive. The events were expressed as means of positive cells in procent.

Primary antibody used in flow cytometry			
Antibody	Company	Raised in	Dilution
Anti-Pax 6	BioLegend (901301, San Diego, CA, USA)	rabbit	2µg/10 ⁶ cells
CD34	Abcam (ab81289, Cambridge, UK)	rabbit	2µg/10 ⁶ cells
CD73	Bioss (bs-4834R, Woburn, MA, USA)	rabbit	2µg/10 ⁶ cells
CD90	R&D systems (AF 2067, Minneapolis, MN)	sheep	2.5µg/10 ⁶
Secondary and control antibody			
Anti-Rabbit FITC	Sigma (F1262, Gillingham, UK)	goat	1:100
Anti-Sheep IgG-NL493	R&D systems (NI 012, Minneapolis, MN)	donkey	1:200
Sheep IgG (control antibody)	R&D systems (5-001-A), Minneapolis, MN, USA)	rabbit	2.5µg/10 ⁶
Rabbit IgG (control antibody)	Vectashield Laboratories (I-1000-5, Peterborough, UK)	rabbit	2µg/10 ⁶

Table 3.1 Overview of primary antibody, secondary and IgG isotype controls used in flow cytometry

Summarised the company details, host and dilution of the primary, IgG isotope controls and fluorophores used in flow cytometry.

3.2.8 Assays for trilineage differentiation

Cryopreserved and expanded central (donor # 8, 9, 12, 13) and limbal (donor # 6, 9, 11, 13) derived CSC were differentiated into adipocytes, chondrocytes and osteoblasts. AdMSC (donor # 16, 17, 18) underwent trilineage differentiation and served as a positive control (Kisiel, McDuffee et al. 2012).

The following modified protocols by Guest et al. 2008 were used (Guest, Ousey et al. 2008).

A) Adipogenesis

For adipogenic differentiation 70-80% confluent cells (CSC, adMSC) in a 10 cm tissue culture dish (seeding number: 1×10^5) were treated with antibiotic-free fat induction media for 72h, followed by antibiotic-free fat maintenance media for 72h (Supplementary table S8) for three alternating cycles before oil red O staining was carried out. For the oil red stain 0.5 g of oil red O (Sigma-Aldrich) was dissolved in 200 ml isopropanol in a 56°C water bath for 1h. Prior to use, a working solution was prepared by adding 4 parts of distilled H₂O to 6 parts of stock solution, which was then filtered through a fine filter paper (Whatman no. 42). The cells on the culture dish were gently rinsed in PBS, followed by water and 60% isopropanol. The filtered dye was applied for 30min, briefly washed in 60% isopropanol, followed several times by water. Images were immediately taken using the phase contrast microscope.

B) Osteogenesis

For osteogenic differentiation a nearly confluent monolayer of cells adMSC and 70% confluent CSC in a four-well tissue culture plate (seeding number: 1×10^4 cells/well) was cultured for 21 days in osteogenic induction media (supplementary table S9) before staining inorganic hydroxyapatite stain (OsteoImage™ Mineralization Assay, Lonza®, Walkersville, USA), van Kossa stain (Abcam®, ab150687, Cambridge, UK) and Alizarin red S (Sigma).

C) Chondrogenesis

For chondrogenic differentiation cells were treated with cartilage induction media (Supplementary table S10) for 21 days. TGF- β 1 was increased to 15ng/ml in the CSC differentiation protocol, because of failure to achieve a chondrogenic differentiation with a lower concentration used in adMSC. An Alcian blue stain (pH 1.0) (Sigma-Aldrich) was carried out overnight (Sigma-Aldrich). This was performed in 2D and 3D (biological triplicate) pellet form using a starting density of 1×10^6 cells. The pellet was embedded in Tissue Tek® OCTcompound and 10 μ m frozen sections were stained accordingly.

3.2.9 Peripheral blood mononuclear cell isolation from lymph nodes

The rapid destruction of peripheral blood mononuclear cells (PBMCs) using commercial euthanasia agents such as Eutha 77 sodium ((barbituric acid derivative, phenytoin sodium), Virbac AH Fort Worth, TX) excluded a Ficoll based method to isolate mononuclear cells from blood. Therefore, the left and right popliteii lymph nodes of two donor dogs were harvested up to 2 hours after euthanasia and transported on ice in PBMC media as described by Dutton et al. 2018 (Dutton, Dudhia et al. 2018) (see Supplementary table S11).

Briefly, lymph nodes were excised from fat and soft tissue remnants, cut in small pieces, and passaged through a 70 μ m sterile cell strainer (Sigma-Aldrich) followed by several washes. The cell suspension was centrifuged at 300 G for 15 minutes and cells were frozen at a concentration of 4×10^6 /ml in

90% PBMC media and 10% DMSO. After thawing 77-95% of PBMCs were viable.

Canine PBMCs of two dogs were commercially purchased (3H Biomedical, Uppsala, Sweden), find donor details in 2.1 Canine tissue and ethics statement.

3.2.10 Cytospin of PBMCs on slides

To perform immunocytochemistry, the PBMCs had to be placed and fixed on adhesive slides (Superfrost microscope slides (VWR)). PBMC cell suspension was resuspended in 100 μ l of PBMC media and 50 μ l FBS per 1×10^5 cells/slide. The plastic chambers were each filled with 150 μ l of cell suspension and spun down for 4 min at 800 rpm using a cytopsin centrifuge (SHANDON Cytospin 2, Marshall Scientific, Hampton, NH). Following the slides were fixed in 4°C cooled 100% Acetone for 10 minutes and stored at -20°C.

3.2.11 PBMC co-cultures

Cryopreserved limbal CSC of each donor were expanded to 1×10^6 cells (all passage 4) and growth-arrested with 15 μ g/ml (2-hour incubation) Mitomycin C (MMC) (Sigma-Aldrich). PBMC co-cultures were performed by incubating growth-arrested, allogeneic limbal CSCs on a 96 well plate (96 F-bottom, Greiner Bio-One™ CellStar™ Polystyrene 96-Well Microplates, Fisher Scientific) with effector PBMCs of two different donors in a ratio of 1:5 (CSC: PBMC) in a triplicate set-up. The experiment was performed on limbal CSC of three different donors (# 2, 3, 12).

For the negative controls, PBMCs from the same dogs were MMC treated for 30 minutes at a concentration of 50 µg/ml before being washed and cultured with autologous effector PBMCs. Growth-arrested PBMCs were cultured with allogeneic effector PBMCs for positive controls. Additionally, PBMCs were activated with 10 µg/ml of Phytohemagglutinin to serve as second positive control (PHA, Sigma-Aldrich).

In more detail, the MMC treated CSC were washed in PBS, dislocated using Triple express (Gibco) for 2min at RT, centrifuged at 1400 rpm for 5min and automated counted (T20 automated cell counter, BioRad) to ensure that further calculations were only performed live cell numbers. Further, the cells were kept in 5ml PBMC media in a Falcon tube at 37°C until used. 5x 10⁵/ml of limbal CSC were used (=5x10⁴ cells per well in 100µl media). In total 9 wells were set up with CSC (Figure 3.3).

The cryopreserved PBMCs of two different donors were thawed out in PBMC media, centrifuged at 1400rpm for 5 min, resuspended in PBMC media and automated cell count was performed. For the set-up of the negative and positive controls, the PBMCs of each donor were divided into effector cells (= active, proliferative cells) and stimulator cells (= growth arrested MMC treated cells).

First, the effector cells of each donor were calculated: 2.5x 10⁶/ml (= 2.5x10⁵cells per well in 100µl media). The cells in PBMC media were kept in a Falcon tube in the incubator until used. In total 12 wells were set up with per effector PBMC (Figure 3.3).

Secondly, the stimulator_PBMCs were treated with 50µg/ml MMC in the incubator at 37°C for 30min, while shaken 3x every 10 minutes. A cell number of 1.25x10⁶/ml (1.25x10⁵ cells per well in 100µl). In total 12 wells were set with stimulator PBMC of each donor. The MMC treated cells were washed in PBS 3x and centrifuged for 5min at 1400rpm.

Each effector PBMC (three wells per effector) were stimulated using 10 µg/ml Phytohemagglutinin (PHA, Sigma-Aldrich) (= 5µl/500µl PBMC media).

All wells were well mixed (pipette) to ensure the contact of activator and stimulator cells before the plate was incubated (37°C) for 4 days. The wells of the outer rim of the 96 well plate were filled with 200µl PBS to contribute to stable humidity.

Then the PBMCs were incubated with radioactive thymidine ([³H] thymidine) (GE Healthcare Bio-Sciences) 0.5 µCi concentration per well and incubated at 37°C, at 5% CO₂ for 16-18 hours before transferred into -20°C (3-4h). For that, 50µl of media of each well were very carefully removed, the ³H thymidine was diluted in 50µl fresh PBMC media and added to each well. Following freezing, the thawing step took place in the incubator (1.5h). The cells were harvested using a Filtermate and counted using Topcount NXT equipment. The relative fluorescence units were converted relative to the average ratio (=1) of non-activated PBMCs (= effector PBMC).

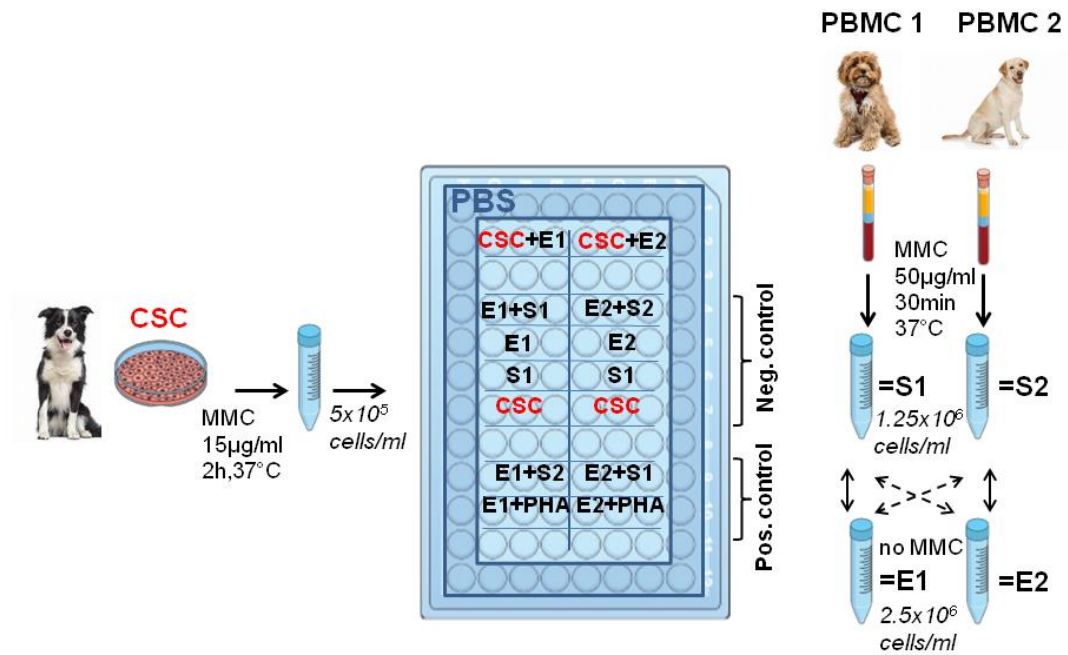


Figure 3.3 Set-up of peripheral blood mononuclear cell co-culture

The schematic illustrates the 96 well plate set-up of the peripheral blood mononuclear cell (PBMC) co-culture assay. MMC growth-arrested limbal CSC of one donor were co-cultured with PBMCs of two different donors in a ratio of 1:5 over 4 days. The stimulator PBMCs (=S) were growth-arrested but not the effector PBMCs (=E). Autologous PBMCs (E1+S1/E2+S2), stimulator and effector PBMCs as well as limbal CSC cultured alone served as a negative control. Allogeneic PBMCs (E1+S2/E2+S1) and activated effector PBMCs served as positive control. After 4 days, the cells were cultured with radioactive thymidine (16-18h) and analysed in a TopCount NXT unit.

3.3 Results

3.3.1 Macroscopic and histological features of the canine limbal niche and central cornea

Macroscopically, limbal crypts (LC) and palisades of Vogt (POV) could not be confirmed (Figure 3.4).

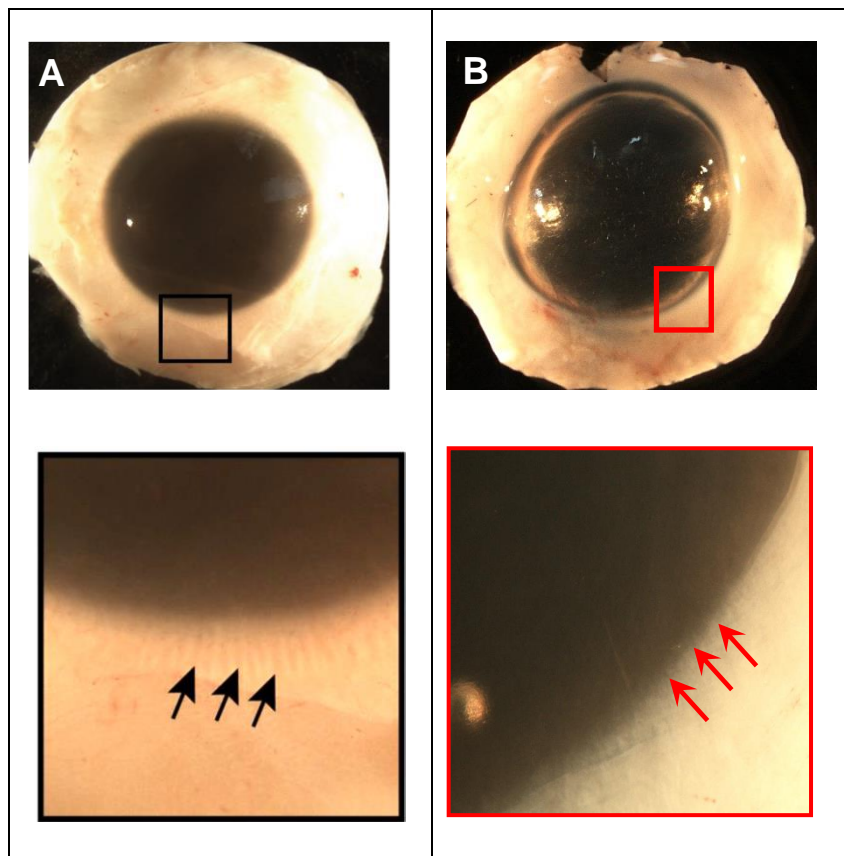


Figure 3.4 Comparative human and canine macroscopic images of the limbus

A) A non-pigmented human donor eye. Box in top panel correspond to magnified bottom panels. Black arrows indicate the limbal crypts (LC) between the palisades of Vogt. (Image A is modified from thesis M. Dziasko 2015, Localisation of corneal epithelial progenitors and characterisation of cell-cell interactions in the human limbal stem cell niche); B) A non-pigmented canine donor eye. The red arrows indicate macroscopically smooth junction between the sclera and cornea (= absence of LC). The gross examination was performed in five eyes of biological different donors (# 3-7).

LCs and POVs could also not be identified histologically (Figure 3.5). But a mild invagination of the limbal epithelium into the stroma was noted (Figure 3.5 A). In all histological sections of the corneal limbus, the basement membrane was undulated and irregularly formed (Figure 3.5 B). There was no evidence of regional differences in the superior, inferior, temporal and nasal corneal quadrant.

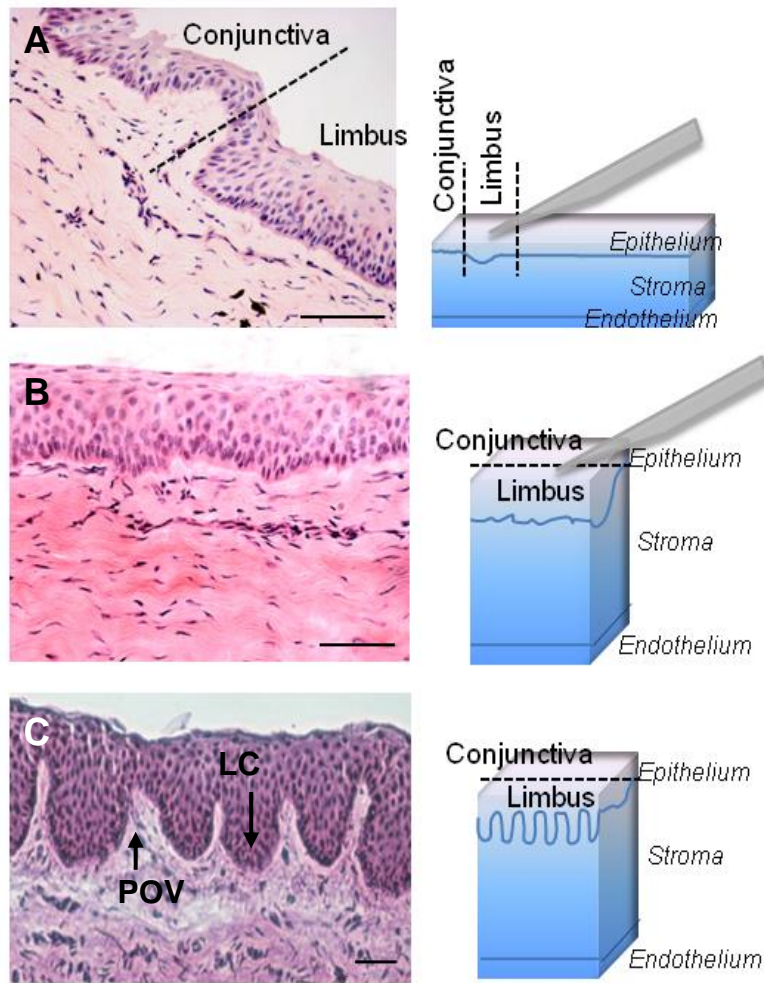


Figure 3.5 Comparative histological images of the canine and human limbus

Haematoxylin & Eosin-stained histological images of the (A) canine cornea in a longitudinal orientation (as indicated in the schematic drawing). An indentation of the epithelium in the stroma can be noted at the limbus (dotted line is indicating the junction of the limbus to the bulbar conjunctiva). (B) In the tangential orientation of the canine limbus: an irregular formed basement membrane can be noted with elongated basal cell nuclei. The histological examination was performed in biological triplicate (donor # 11-13). (C) The human limbus (tangential orientation): note the limbal crypts (LC) with its indenting extension of the epithelium and the palisades of Vogt (POV) composed of intersepted stromal tissue. (Image C is modified from thesis M. Dziasko 2015, Localisation of corneal epithelial progenitors and characterisation of cell-cell interactions in the human limbal stem cell niche). Scale barr: 50µm

In the limbal area, the basal cell layer of the epithelium was cell-rich with more elongated than cuboidal formed basal cell nuclei similar to limbal epithelial stem cells (LESC). The corneal stromal cells were in direct contact or proximity to the irregular formed basement membrane (Figure 3.6 A, C). In the central cornea, the basal cells of the epithelium were cuboidal shaped, the fine basement membrane was regularly formed, and the stromal cells were separated from the basement membrane by a layer of corneal stroma (Figure 3.6 B, D).

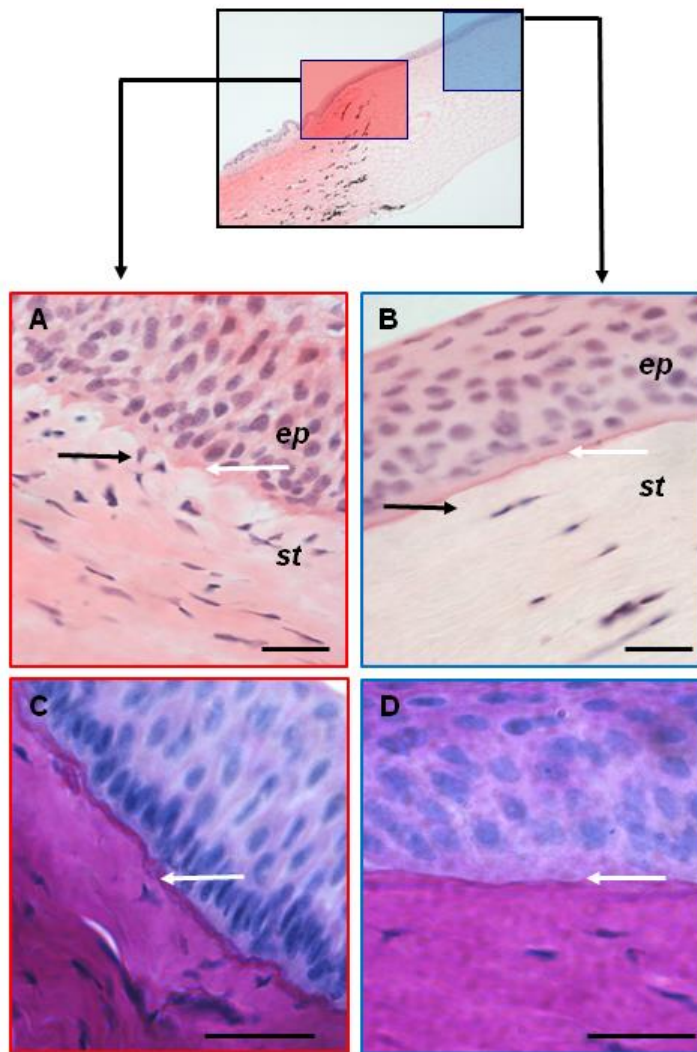


Figure 3.6 Histology of the canine limbus and central cornea with focus on the anterior stroma and basement membrane

Histological section stained with H&E (A) and Periodic acid Schiff stain (C) of the limbal area (red box) with an irregular thickened and undulated basement membrane (white arrow). Notice the proximity of stromal cells (A, black arrow). In the central cornea (B, D; blue box) a fine regular formed basement membrane (white arrows) is present. The first row of keratocyte is in distance from the basement membrane were noted (B, black arrow). The histological examination was performed in biological triplicate (donor # 11-13). Abbreviations: ep, epithelium; st, stroma; Scale bars: 20 μ m

3.3.2 Western Blot results of the antibodies tested for cross-reactivity and specificity to dog proteins

The observed band size was in proximity to the expected band size provided by the manufacturer for all markers tested, i.e. CD90 has a predicted band size of 17-20kDa in human brain and mouse adrenal cell lysate. In this study, the band size ranged between 23-30kDa on canine CSC and adMSC cell lysate. Unspecific bands were observed which were different from the expected/observed bands. For example, the manufacturer for N-cadherin described an unspecific band size of 75kDa, but on canine CSC cell lysate an additional unspecific band of 135kDa was observed (see Figure 3.7). The observation of multiple unspecific bands in ALDH1A3 on mouse, rat, human kidney tissue was also described by the manufacturer. In addition, Alexander et al. 1993, described two or three bands. This was depending on the antibody of N-cadherin (conserved cytoplasmic or cytoskeleton sequence) and the binding region (125 and 145 kDa) (Alexander, Blaschuk et al. 1993).

The following antibody markers were not tested in a western blot assay, given there were available references for dogs: CD105 (Abcam, ab156756), (Hensley, Tang et al. 2017), α -SMA (Abcam, ab5694) (Mai, Hu et al. 2015), P75 (=NGF R/TNFRSF16) (R&D systems, MAB 367, human and canine), Sox10 (Sigma-Aldrich, SAB1402361) (Kishimoto and Uchida 2018).

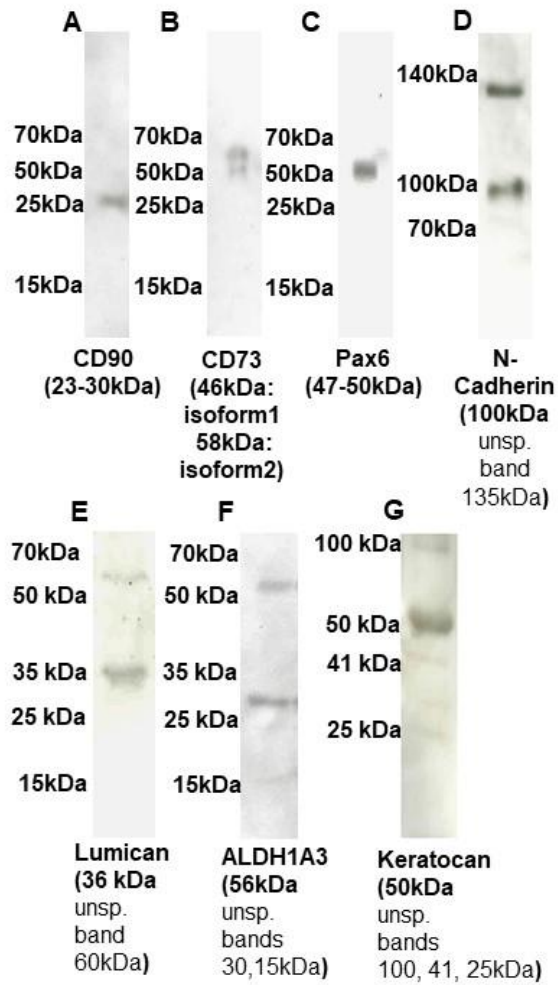


Figure 3.7 Western Blot results of the antibodies tested for cross- reactivity and specificity to dog proteins.

CD90 (A), CD73 (B), Pax6 (C), N-cadherin (D) was tested on CSC/adMSC cell lysate (20 μ g). Corneal protein (20 μ g) was extracted to test Lumican (E), ALDH1A3 (F) and Keratocan (G). This was performed in one technical experiment of cell lysate of one donor. The predicted band size (in brackets) and unspecific band sizes are listed in kDa. Abbreviations: CSC, corneal stromal cell; kDa, kilo Dalton

3.3.3 A distinct population of mesenchymal stromal stem cells are present in the limbal and central corneal stroma

A distinct, small population of CD90+ cells was present in proximity to the basement membrane of the corneal epithelium extending in the anterior to mid-stroma in the limbal region in all four quadrants (dorsal, ventral, nasal, temporal). CD90+ cells were also present in the central anterior-mid corneal stroma (Figure 3.8).

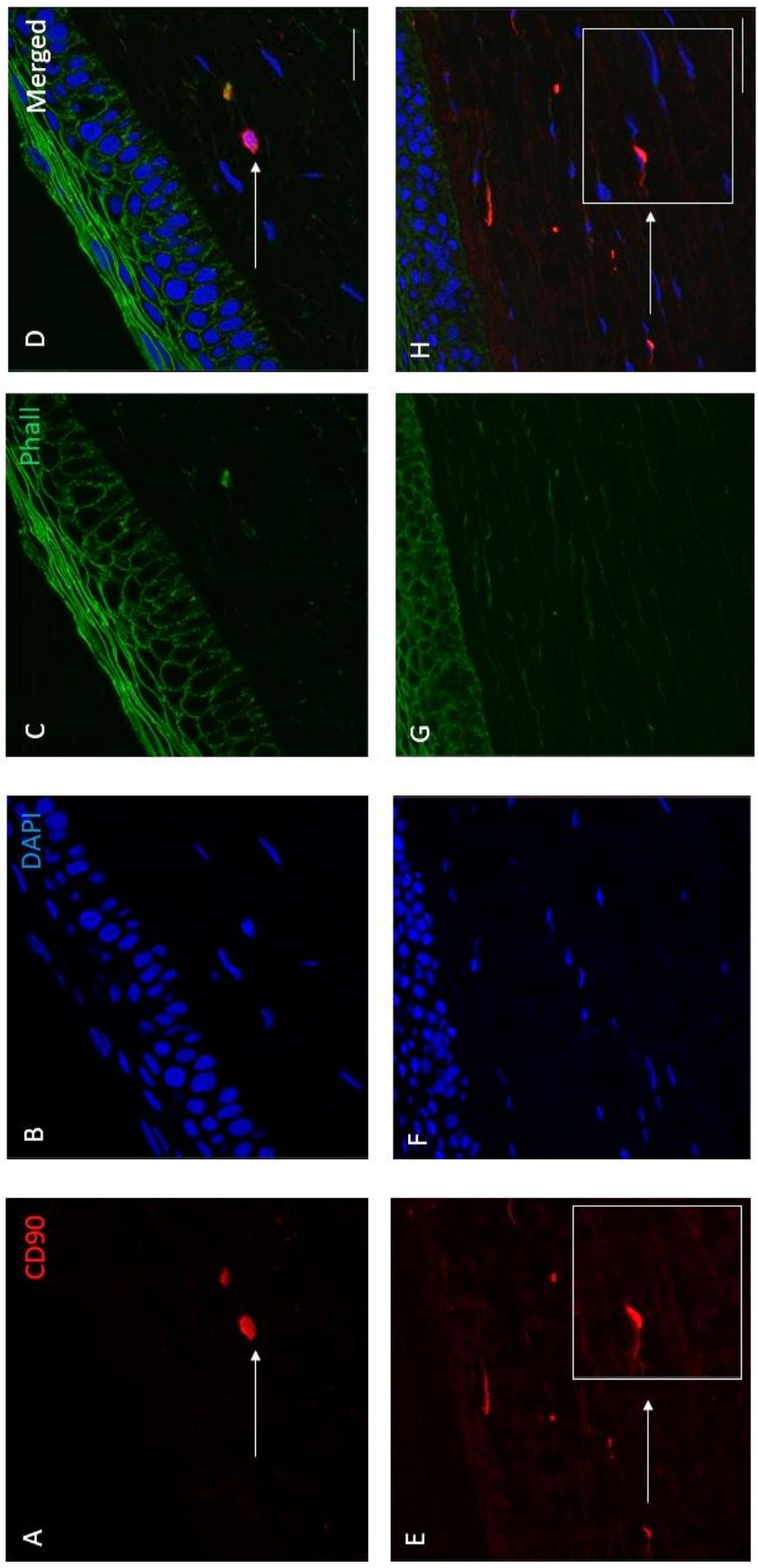


Figure 3.8 Immunohistological staining result with CD90 of the limbal and central cornea

A-D: distinct population of CD90 (red) expressing stromal cells were present in the limbal cornea (A, white arrow). E-H: central corneal stroma. A CD90 positive stromal cell cytoplasm is magnified in the white square (E, white arrow) and merged in H, white square/white arrow). This was demonstrated in a biological triplicate (donor # 11,12,13). Nuclei are shown by DAPI counter staining (B/F) and the cytoskeleton by Phalloidin (C/G). Scale bars: 20µm (D/H)

A histological section of the haired canine skin with hair follicles and hair bulb served as a positive control for the CD90 marker. CD90 expressing mesenchymal stem cells are described to surround the lower part of the anagen hair follicle (Mercati, Pascucci et al. 2009) (Figure 3.9)).

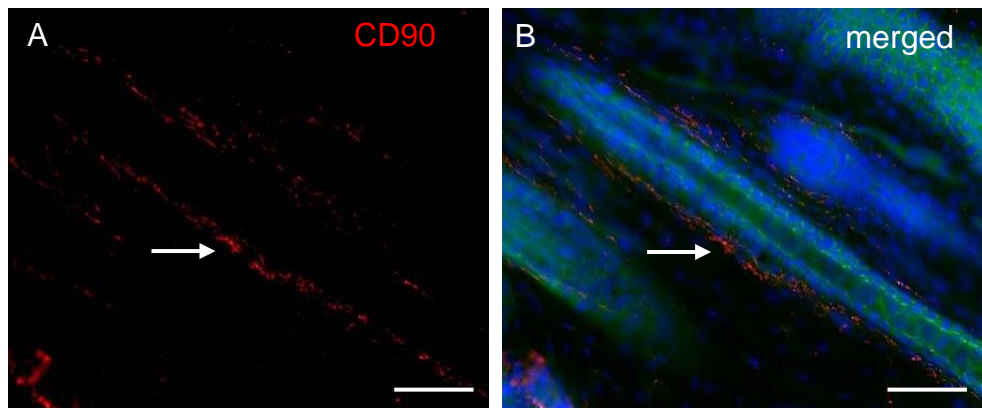


Figure 3.9 Hair follicle served as positive control for CD90

Immunohistochemistry images of demonstrates CD90 expressing mesenchymal stem cells of the hair follicle (A, white arrow). B) Merged image, cell nuclei are shown by DAPI counter stain (blue) and the cytoskeleton by Phalloidin (green). This was performed as singlicate of a skin sample of donor # 7. Scale bar: 50µm

The LESC expressed Pax6 as described by Dziasko et al. 2020 (manuscript in review) were not confirmed to express Pax6 in the corneal stroma. Alpha-SMA positive cells were only observed in the vascularisation (e.g. vascular smooth muscle cells) of the sclera/limbus junction, which served as an internal positive control (Figure 3.10).

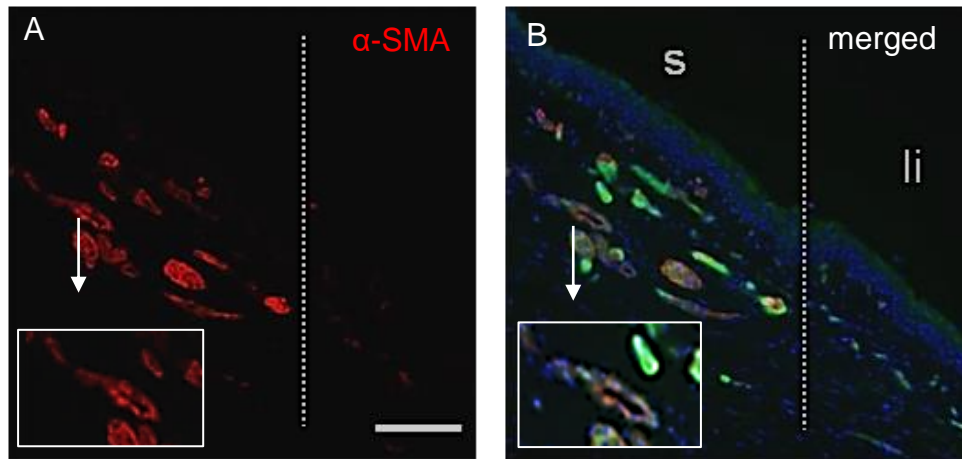


Figure 3.10 Internal positive control for alpha smooth muscle actin (α -SMA)

A) Immunohistochemistry of the corneal sclera-limbal junction demonstrating α -SMA expressing scleral blood vessels (white arrow, (magnified in white box)). B) Merged image, cell nuclei are shown by DAPI counter stain (blue) and the cytoskeleton by Phalloidin (green). This was performed in a biological triplicate (donor # 11,12,13). Scale bar: 100 μ m
Abbreviations: S, sclera; li, limbus

Keratocyte markers as Lumican, Keratocan and ALDH1A3 were expressed in keratocytes and their cytoplasmatic extension through the corneal stroma (internal positive control) (Figure 3.11). Specific binding of the three markers was confirmed via western blot analysis (see 3.3.2).

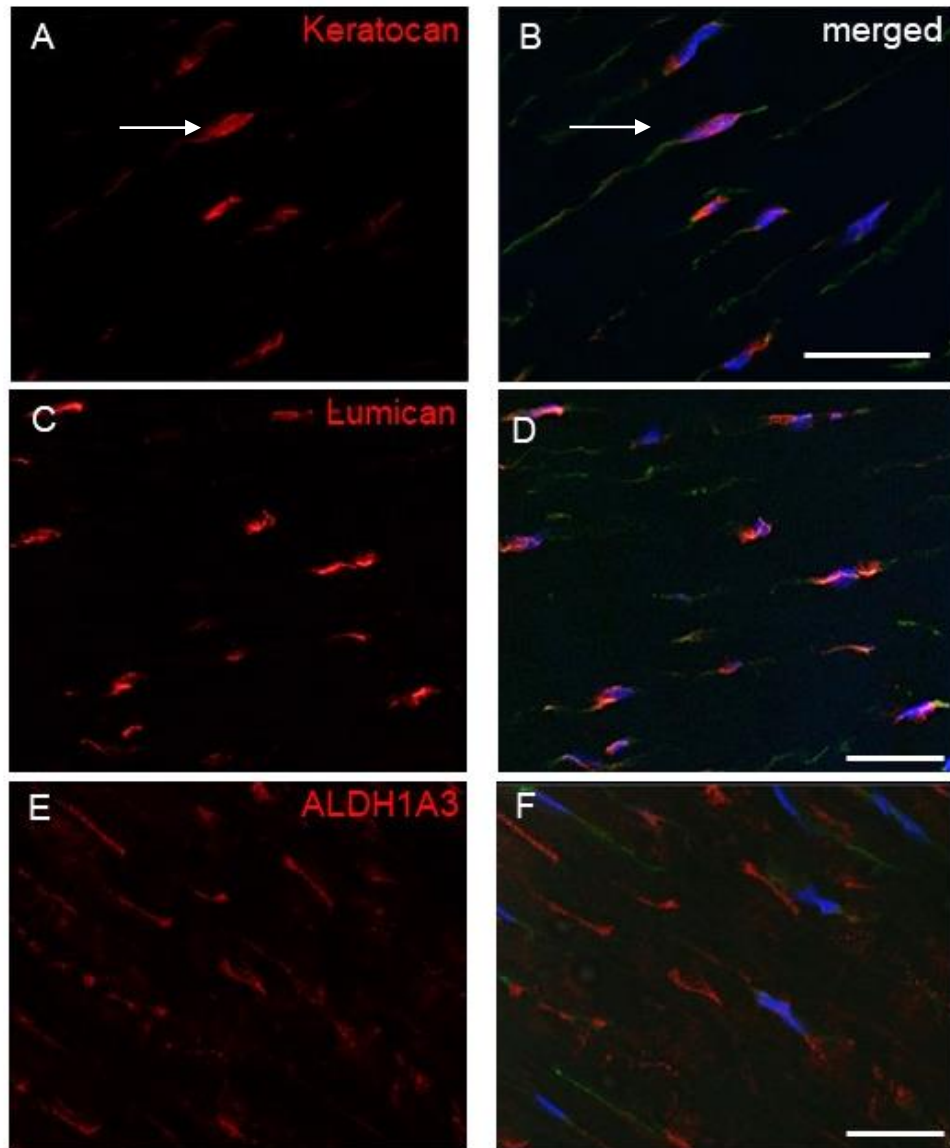


Figure 3.11 Immunohistology of the corneal stroma with keratocyte markers Lumican, Keratocan and ALDH1A3 (positive control)

Immunohistochemistry of the corneal stroma showed that the keratocyte cytoplasm (white arrow) stained positive for Keratocan (A), Lumican (C) and ALDH1A3 (E). B/D/F Merged images with DAPI counter staining (blue) and the cytoskeleton by Phalloidin (green). This was performed in a biological triplicate (donor # 11,12,13). Scale bar: 20 μ m

3.3.4 Short-term culturing of isolated corneal cells contains small population of mesenchymal stromal cells

Isolated limbal epithelial and underlying stromal cells were cultured in CSSC media for a maximum of 48h. The outgrowing and expanding CSC from these islands were monitored (Figure 3. 12. I). There was a small number of CD90 expressing polygonal to slightly elongated cells interpreted as CSC surrounding the corneal epithelial islands (Figure 3.12 II-E). A small population of Pax6 expressing cells were noted. Small stromal cells with a high nucleus:cytoplasm ratio showed Pax6 positive nucleus expression (Figure 3.12 II-A). At 48h before the first passage, most stromal cells were elongated spindle cells, surrounding the corneal epithelial cell islands, which expressed the keratocyte marker Lumican (Figure 3.12 II- I).

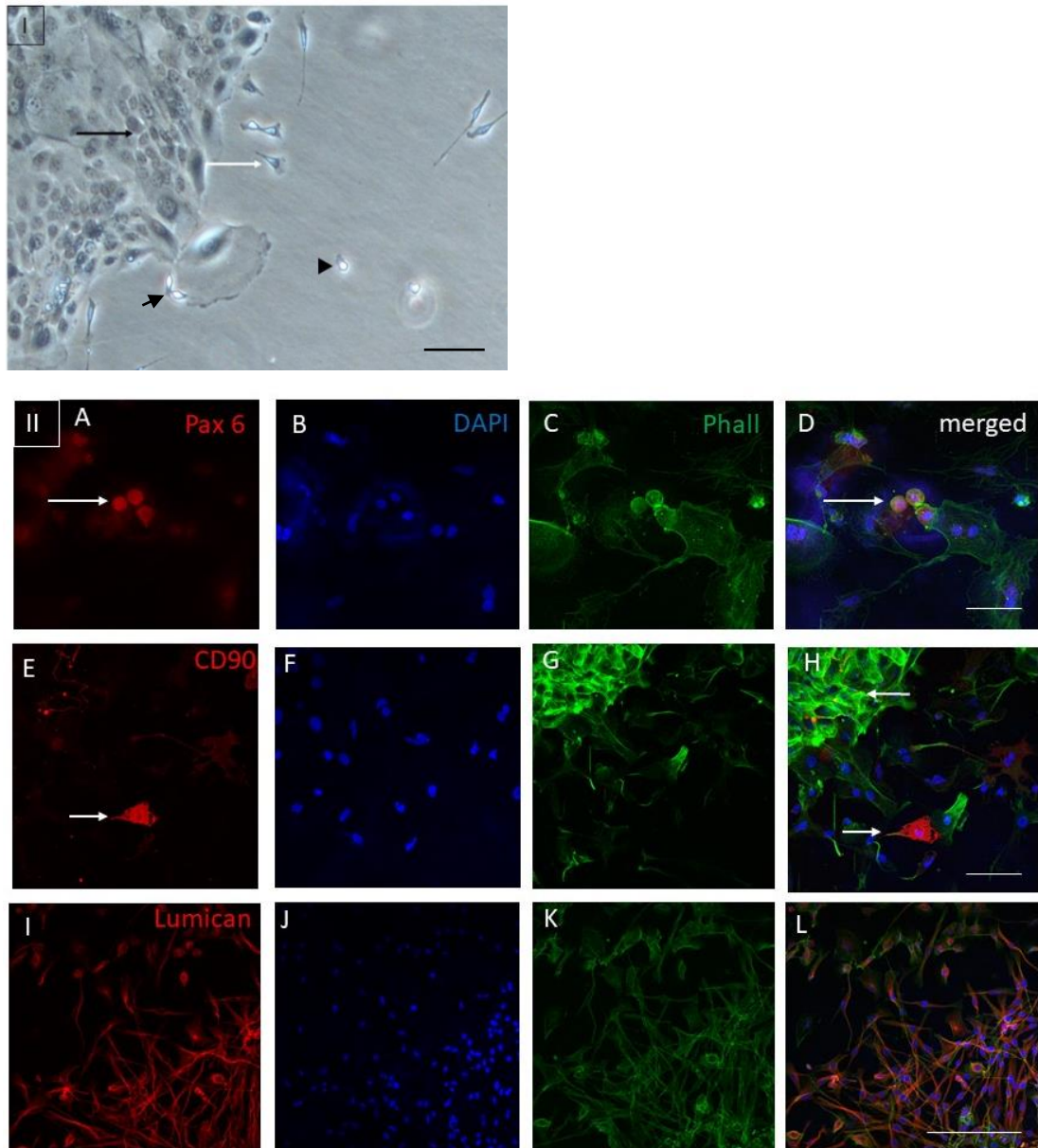


Figure 3.12 Phase contrast image of limbal epithelial cells and outgrowing corneal stromal cells (CSC) and immunocytological staining of short term cultured corneal stromal cells (P0)

I: Phase contrast image of limbal epithelial cells (black arrow) with outgrowing spindle (white arrow) and polygonal dividing stromal cells (black arrow heads) at P0 (12h post seeding). II: Isolated epithelial cell island and CSC cultured in CSSC media for 48h. A-D: Single stromal cells with a high nucleus:cytoplasm ratio showed Pax 6 expression (A, D, white arrow). E-H: Single CD90+ cells were present, which were in close contact with the island of the remaining epithelium (H, white arrow: cytoskeleton of epithelium (green)). I-L: The majority of stromal cells were long spindle cells expressing Lumican. The short-term CSC culture observation was performed in a biological triplicate (donor # 11,12,13). Nuclei are shown by DAPI counter staining and the cytoskeleton by Phalloidin (Phall); Scale bar: 20µm

3.3.5 The CSC cell morphology changes with cell density

Limbal and central-derived canine CSC were freshly isolated and cultured from a total of 10 out of 15 corneas. The five excluded corneas showed lack of cell expansion (3/5 corneas were kept in organ culture medium for more than 3 weeks; two started proliferating after ten days but reached senescence after the second passage).

All seeded limbal and central-derived CSCs showed stable attachment to the culture flask, which was fibronectin-collagen coated (Athena Enzyme System) at P0 but were not coated in higher passages. The CSCs showed small, oval-shaped cell profile. They were 8-10 μm in size with a prominent round nucleus, diffuse cytoplasmic extension to one side and fine spike-like extension at the opposite side which were interpreted as filopodia (Figure 3.13 A). The cells were dividing and became more elongated with a half-moon shaped cytoplasmic extension to one side (Figure 3.13 B). In the log-phase, fast dividing cells were kept in their oval-shaped, stem cell-like morphology by keeping them subconfluent (confluency of 60-70%). However, with increasing expansion and higher cell confluence to allow cell-to-cell contact, the nucleus to cytoplasm ratio decreased, cells enlarged and developed two or three elongated cytoplasmic extension and a smaller, flat nucleus (Figure 3.13 C). Upon approaching confluency, a syncytium of stellate shaped cells was formed, with interconnecting cell-to-cell dendrites (Figure 3.13 D).

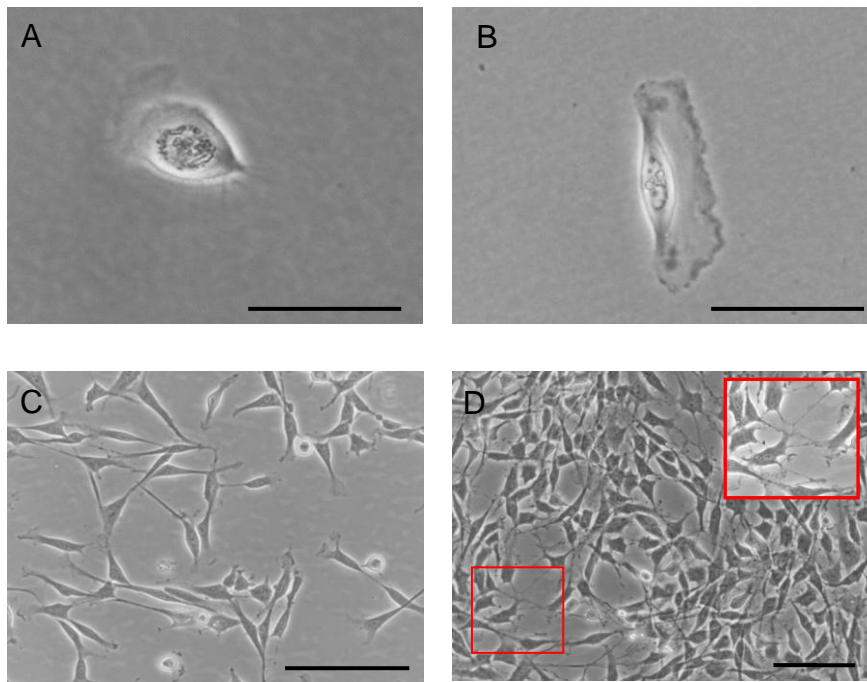


Figure 3.13 Morphological changes of corneal stromal cells (CSC) during cell culture expansion and confluency

Phase-contrast images demonstrating the small, oval-shaped cell morphology of CSC (A) which became more elongated with expansion (B) and morphologically more elongated, dendritic cells (C) forming an interconnecting cell syncytium (D) with increasing confluency. A magnified area is shown in the red square. The cell cultures were monitored in 11 replicates (donor #10-15) in limbal and central derived CSC. Scale bar: A, B: 10 μ m; C, D: 20 μ m

3.3.6 Cell culture kinetics of limbal and central derived CSC are similar, and both have limited self-renewal potential

A) The mean maximal culture time and passage frequency

The maximal passage time and days in cultured cells isolated from the limbal and central cornea of five adult donors with a mean age of 9.2 ± 4.1 years (range: 2-12 years) were evaluated. The culture results of four limbal donors were available; one sample (donor #10) was excluded. The culture results

revealed a mean of 23.5 ± 3.31 maximum culture days (range: 19-27 days) with a mean of 9 ± 2.94 passages (range: 6-13) (Figure 3.14). An increased passage frequency of up to 24h was observed between day 10 and 15 in CSCs isolated from the limbal cornea. The central CSC showed similar culture results. The results of five donors revealed a mean of 19.6 ± 4.33 culture days (range: 16-27) with a mean of 8 ± 1.64 passages (range: 6-10) (Figure 3.14). An increased passage frequency was also observed between day 10 and 14. No significant statistical difference between culture days and passage frequency between the limbal and the central cornea was determined (T-test, $P= 0.18$).

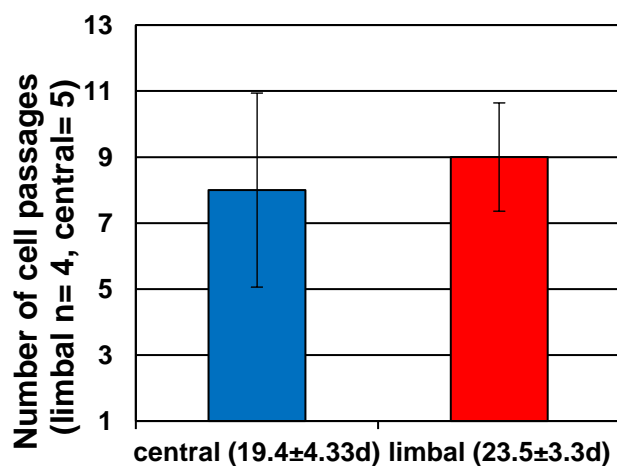


Figure 3.14 Comparison of the mean maximal culture time and passage frequency in four limbal and five central derived corneal stromal cells (CSC)

The graph demonstrates the maximal number of cell passages (mean \pm SD) in number of days (mean \pm SD) was without significant difference between limbal and central CSC.

Abbreviation: n, number of biological replicates (limbal CSC of donor # 11-15; central CSC of donor # 10-15)

B) The mean cell number over 6 passages

Cell number of the limbal cornea of three young donors aged 6.6 ± 1.1 weeks (age range: 6-8 weeks) over six passages in 21 days ranged between a mean of 3.06×10^5 cells (P1) and reached a maximum of 14×10^6 cells (P5). The mean cell number of the central cornea was lower with a range of 2×10^5 cells (P1) and a maximal mean cell count of 8×10^6 /cells at P5 (Figure 3.15). There was no statistically significant difference between the cell numbers of the central and the limbal CSCs at each passage (T-test, $P > 0.05$). There was a trend for the central CSC number to be lower at passage 4 (T-test, $P = 0.063$). However, there was a high degree of individual heterogeneity in cell numbers (i.e. high standard deviation) between different donors (Figure 3.15). The cell number of P0 was not included as CSC derived from cultured limbal and central cells had epithelial cell contamination.

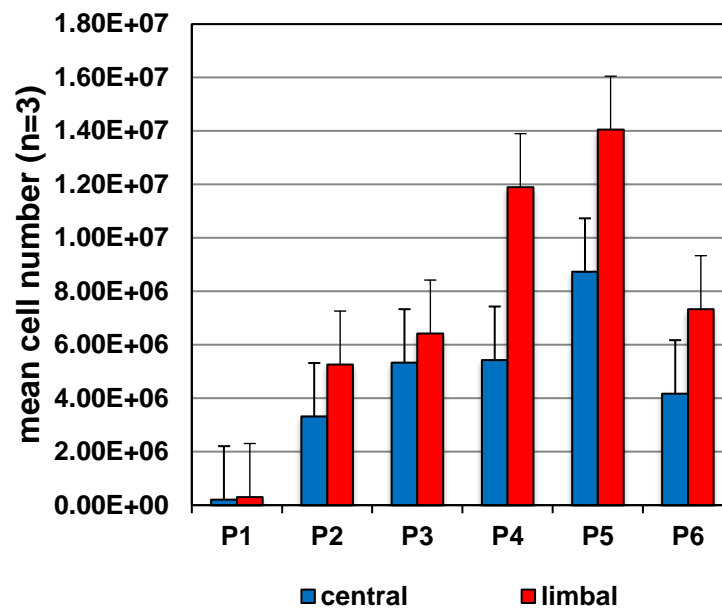


Figure 3.15 Comparison of the cell numbers of limbal and central corneal stromal cells (CSC) over six passages

The graph demonstrates the cell number of CSCs over six passages (mean \pm SD) counted over 21 days, which was without significant difference between limbal and central CSC. This was counted in a biological triplicate (donor #7-9). Abbreviations: n, number of biological replicates; P, passages

C) The population doubling time and population doublings

Comparing the mean population doubling times between limbal and central derived CSC, there was a trend noted that the central derived CSC reached the stationary phase at earlier passage (P3-4) than the limbal derived CSC, but the difference reached not a statistically significant level (T-test, $P=0.067$). Similar PDT to MSC was observed only in the early log-phase between P1-2 in limbal (25,02h) and central (21,67h) derived CSC (Corradetti, Meucci et al. 2013). The mean PDT increased exponentially at

P3-4 to 220h in central derived CSC and at P4-5 to 198h in limbal derived CSC before the stationary phase was reached after P5 (Figure 3.16 A). The accumulative number of cell doublings between P1-P5 was 12.84 and 11.15 in limbal and central derived CSC respectively (Figure 3.16 B).

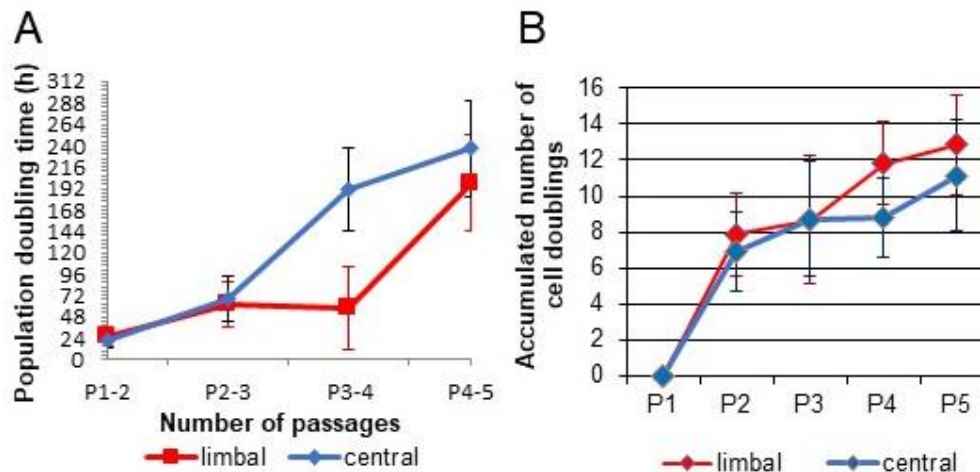


Figure 3.16 Comparison of the population doubling time (PDT) and cumulative cell doublings of limbal and central corneal stromal cells (CSC)

(A) The mean (\pm SD) population doubling time (h) and (B) mean (\pm SD) cumulative number of cell doublings of three biological replicates (donor # 10-12) showed exponential growth over five passages and then reached senescence. (A) There was a trend (P 3-4) of central CSCs having a higher PDT (T-test, $P=0.067$) than limbal CSCs. Abbreviations: h, hours; P, passages

D) The change of the cell composition based on cell morphology

The change in cell culture morphology of limbal and central derived CSC of three different donors (# 7, 8, 9) at each passage and passage days were described. Three images (10 high power fields (HPF)) per flask (limbal, central) using a phase-contrast microscope were taken. The observer (Christiane Kafarnik) was masked to the image origin (limbal, central), cells

were categorized according to their morphology (as epithelial, polygonal (presumed CSC), spindle-oval (presumed more differentiated CSC), dendritic (presumed keratocyte), fibroblastic (presumed fibro/myofibroblastic) cells (Figure 3.17). An average cell count of three images per time point was used for statistical calculation. Further immunocytological investigations were not performed at this stage in this study.

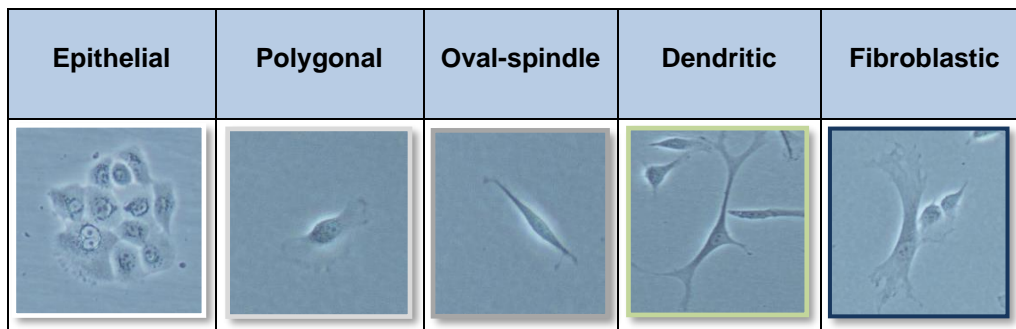


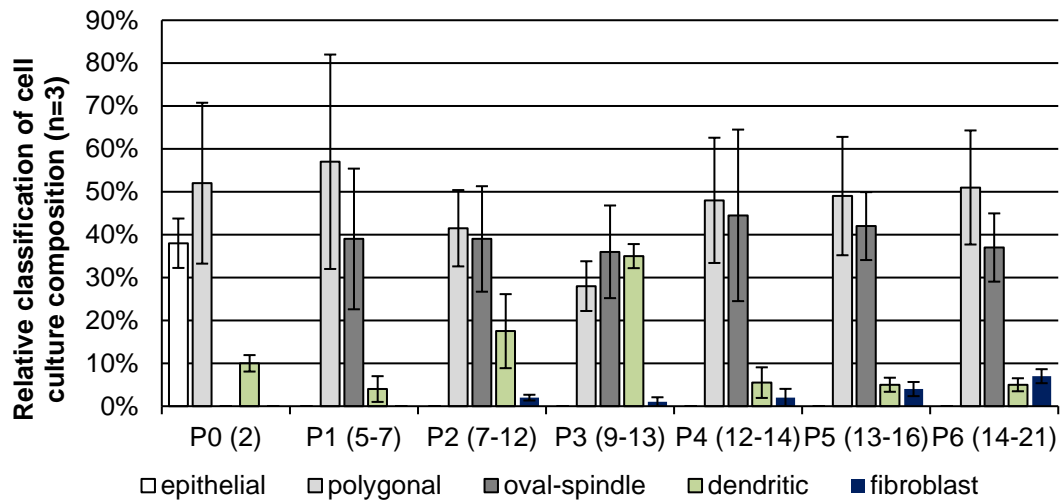
Figure 3.17 Morphological classification of corneal cells cultured isolated from fresh corneal tissue

Cell culture phase-contrast images (20x) categorized in epithelial, polygonal, oval-spindle, dendritic, fibroblastic cell morphology.

The cell composition of the cell morphology of freshly isolated cells from the limbal (Figure 3.18 A) and central cornea (Figure 3.18 B) in a biological triplicate of young dogs aged 6.6 ± 1.1 weeks (age range: 6-8 weeks) were described and quantified. At passage 0 (day 2), dendritic cells (interpreted as keratocytes) and polygonal cells (interpreted as CSC) dominated the relative cell classification (Figure 3.18 A, B). Furthermore, islands of epithelial cells were present. It could be confirmed that after the selective trypsinisation, after passage 0, epithelial cells were not evident at any later culture stage. With selective passaging and care of subconfluency (60-70%) the cell composition of polygonal and oval-spindle cells (interpreted as more

differentiated CSC) was the prominent cell type. Overall, there were more dendritic cells counted at P1-P6 of the cells cultured from the central cornea (Figure 3.18 B). Fibroblastic appearing cells were increasingly counted from P2-P6 from both locations (limbal and central), but there were more fibroblastic appearing cells at P6 in the cell culture from the central cornea (Figure 3.18 B). However, a significant difference between the central and the limbal cell culture composition at each passage and all different cell subgroups was not evident (ANOVA, $P > 0.05$). Overall, a high degree of individual heterogeneity between the donors is reflected in the high standard error.

A limbal



B central

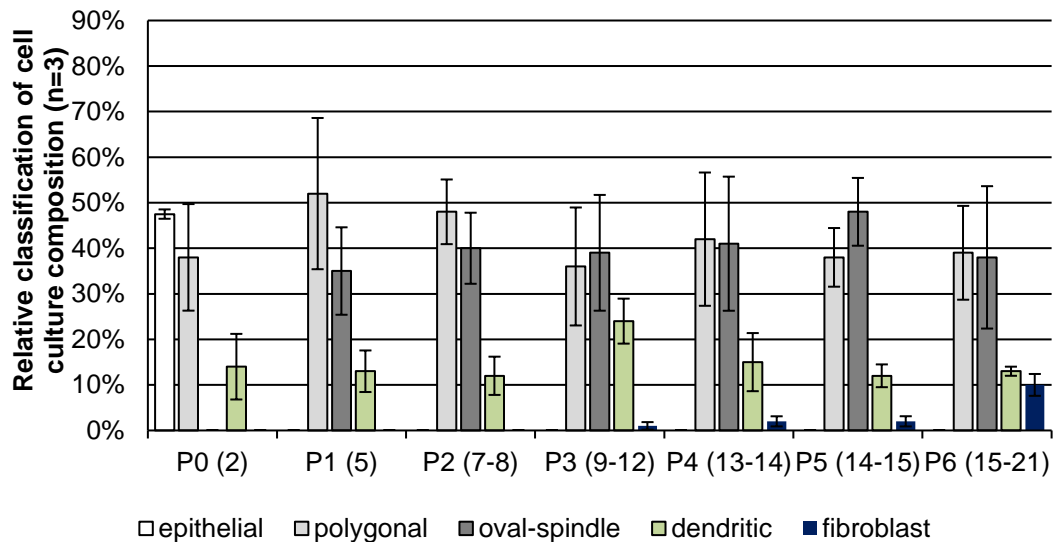


Figure 3.18 Comparison of the relative classification of the cell culture composition between limbal and central corneal stromal cells (CSC)

The graphs illustrate the relative classification of the cell culture composition (%) based on the cell morphology of the (A) limbal and (B) central derived corneal cells (mean \pm SE) over 6 passages (in days). There was no significant difference between both locations (limbal/central) in any subgroup at any time point. However, more cells classified as dendritic and fibroblastic appearing cells at P6 were noted in the central derived cell culture system (B). Abbreviations: P, passage; n= 3, biological triplicate (limbal and central CSC of donor # 7-9).

3.3.7 Limbal and central derived CSCs have mesenchymal stromal cell characteristics

Cultured limbal and central derived CSC expressed MSC markers. There was no difference noted between limbal (Figure 3.19.A.I/II) or central derived CSC (Figure 3.19.B.I/II). CSC showed expression of the MSC surface markers CD90, cytoplasmic positive marker expression of CD73 and CD105. In addition, the nuclear-paired box protein Pax6 and the intercellular membrane marker N-cadherin was expressed (Figure 3.19.A.I, Figure 3.19.B.I). CD34, a hematopoietic stem cell surface marker and alpha-smooth muscle actin (α -SMA), a myofibroblastic marker were absent (Figure 3.19.A.II, Figure 3.19.B.II).

The CSC staining results were compared to canine adMSC which served as positive control (Figure 3.19.C.I/II). AdMSC expressed a similar marker expression to limbal and central CSC; however, Pax6 was not expressed (Figure 3.19.C.I) but α -SMA (Figure 3.19 CII). Canine PBMC expressed CD34 and served as positive control (Figure 3.20). (Find positive control for keratocyte markers (Figure 3.10) and for α -SMA (Figure 3.11) in 3.3).

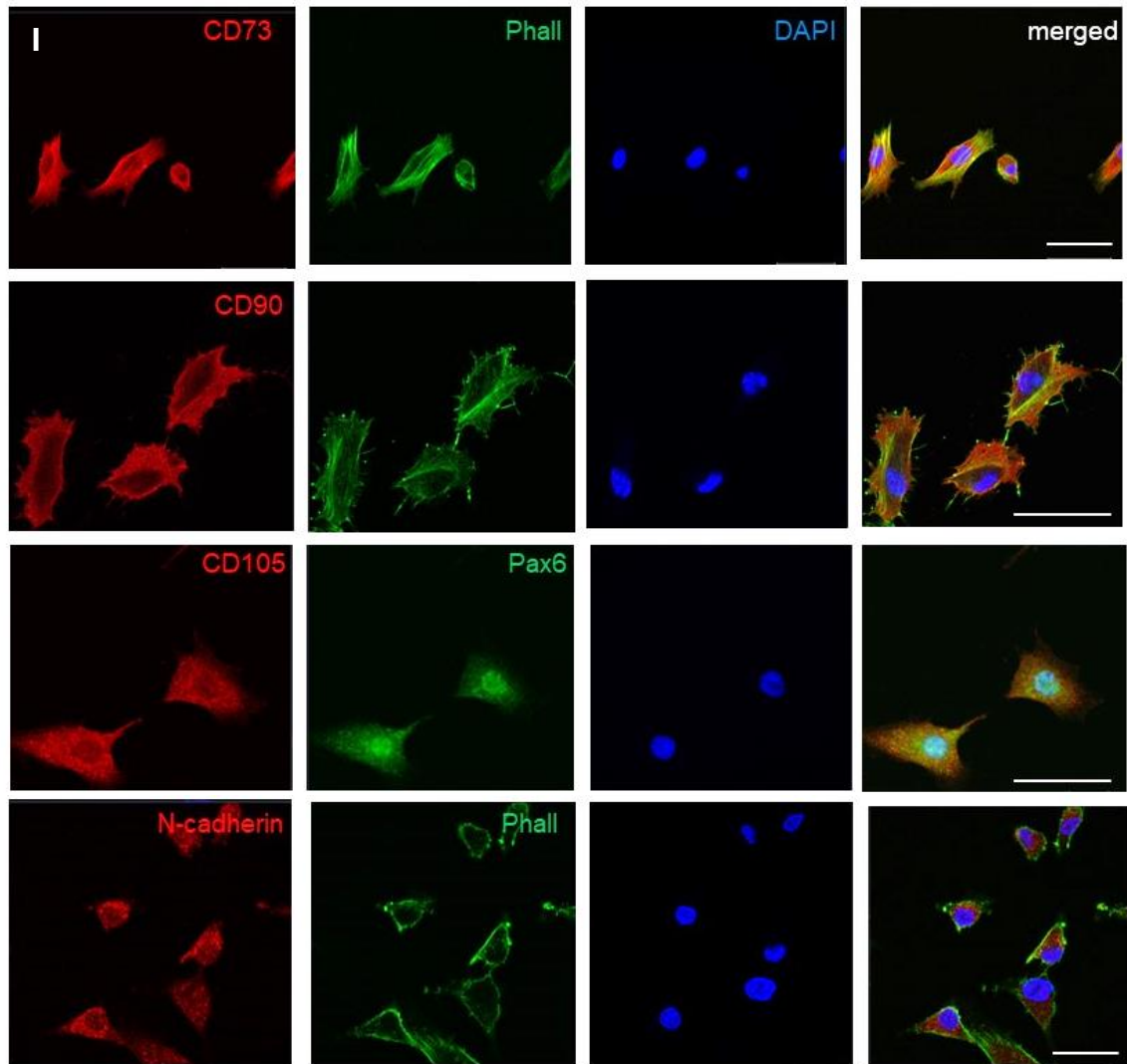


Figure 3.19.A (I) Immunocytochemical staining results of limbal corneal stromal cells (CSC)

(A I): Summarised the immunocytochemical staining results of freshly isolated and cultured limbal CSC (passage 3-5). CD90, CD73, CD105 and N-cadherin is expressed. CD105 (red cytoplasm) and Pax6 (green nuclear stain) was stained as double immunocytochemistry. This was performed in a biological triplicate (cells of donor # 1,2,4). Phalloidin (Phall) was used to stain the cytoskeleton (F-actin) and DAPI as nuclear marker. Scale bar: 20 μ m

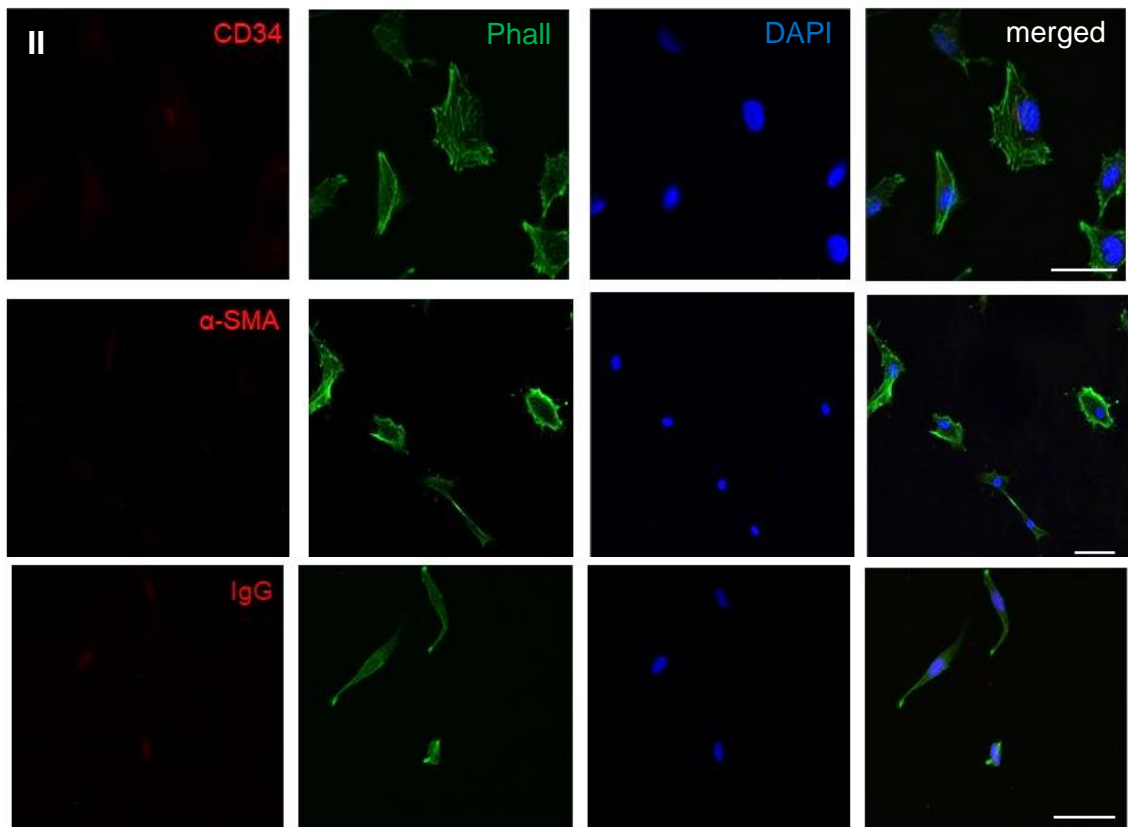


Figure 3.19.A (II) Immunocytological staining results of limbal corneal stromal cells (CSC)

(A II): CD34 and α -SMA is not expressed. This was performed in a biological triplicate (cells of donor # 1, 2, 4). Phalloidin (Phall) was used to stain the cytoskeleton (F-actin) and DAPI as nuclear marker. Abbreviations: IgG, immunoglobulin G (negative control). Scale bar: 20 μ m

B. Central corneal stromal cell

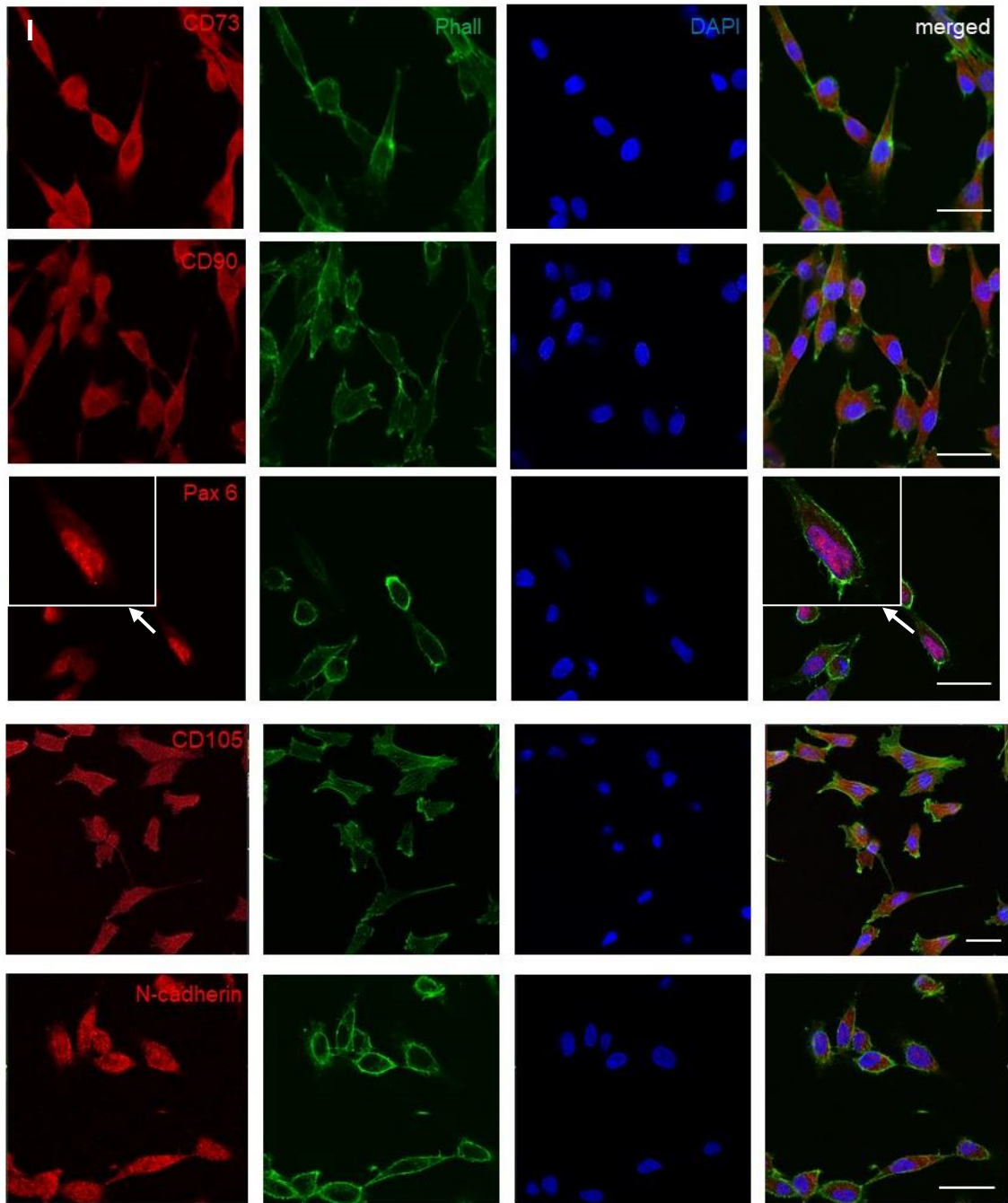


Figure 3.19.B (I) Immunocytological staining results of central corneal stromal cells (CSC)

(A I): Summarised the immunocytological staining results of fresh isolated and cultured central CSC (passage 3-5). CD90, CD73, CD105 and N-cadherin is expressed. Pax6 is expressed in the nucleus (white arrow, magnified in white box). This was performed in a biological triplicate (cells of donor # 1,4,6). Phalloidin (Phall) was used to stain the cytoskeleton (F-actin) and DAPI as nuclear marker. Scale bar: 20 μ m

B. Central corneal stromal cell

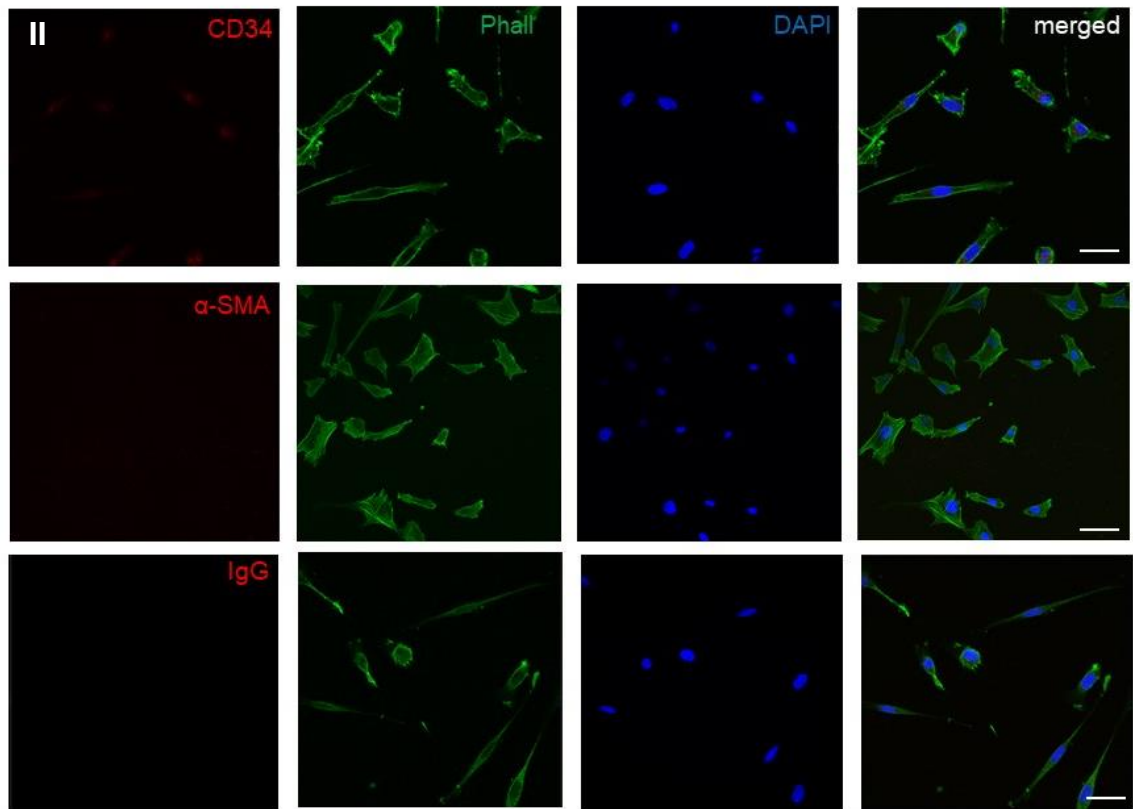


Figure 3.19.B (II) Immunocytochemical staining results of central corneal stromal cells (CSC)

(B II): CD34 and α -SMA is not expressed. This was performed in a biological triplicate (cells of donor # 1,4,6) Phalloidin (Phall) was used to stain the cytoskeleton (F-actin) and DAPI as nuclear marker. Abbreviations: IgG, immunoglobulin G (negative control). Scale bar: 20 μ m

C. Adipose derived MSC (positive control)

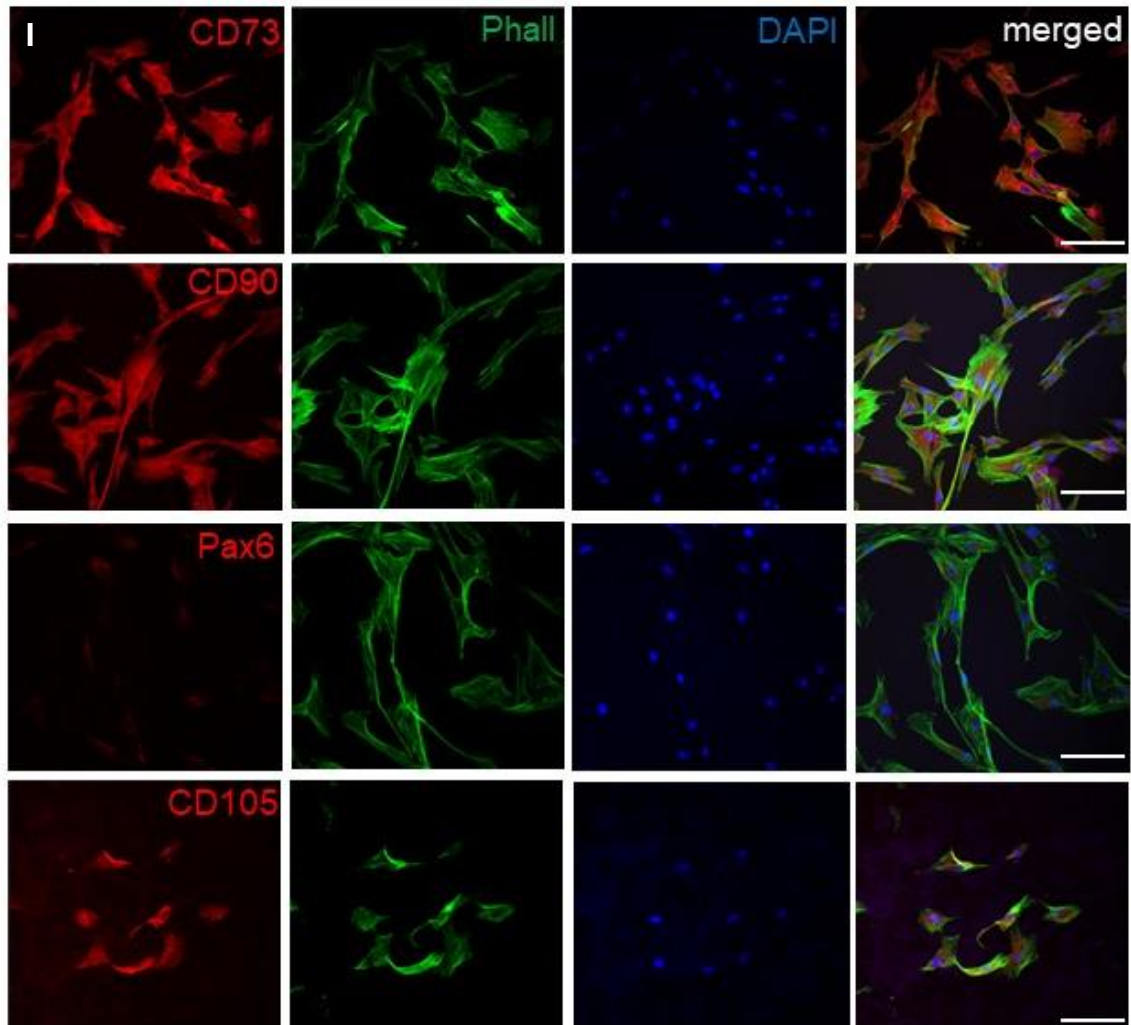


Figure 3.19.C (I) Immunocytochemical staining results of adipose derived MSCs

(C I): Summarised the immunocytochemical staining results of frozen, cultured adMSC (passage 4-6) which served as positive control and exhibited similar protein expression to CSC (CD73, CD90, CD105 positive) whereas Pax 6 was not expressed. This was performed in a biological triplicate (cells of donor #16-18) Phalloidin (Phall) was used to stain the cytoskeleton (F-actin) and DAPI as nuclear marker. Scale bar: 20 μ m

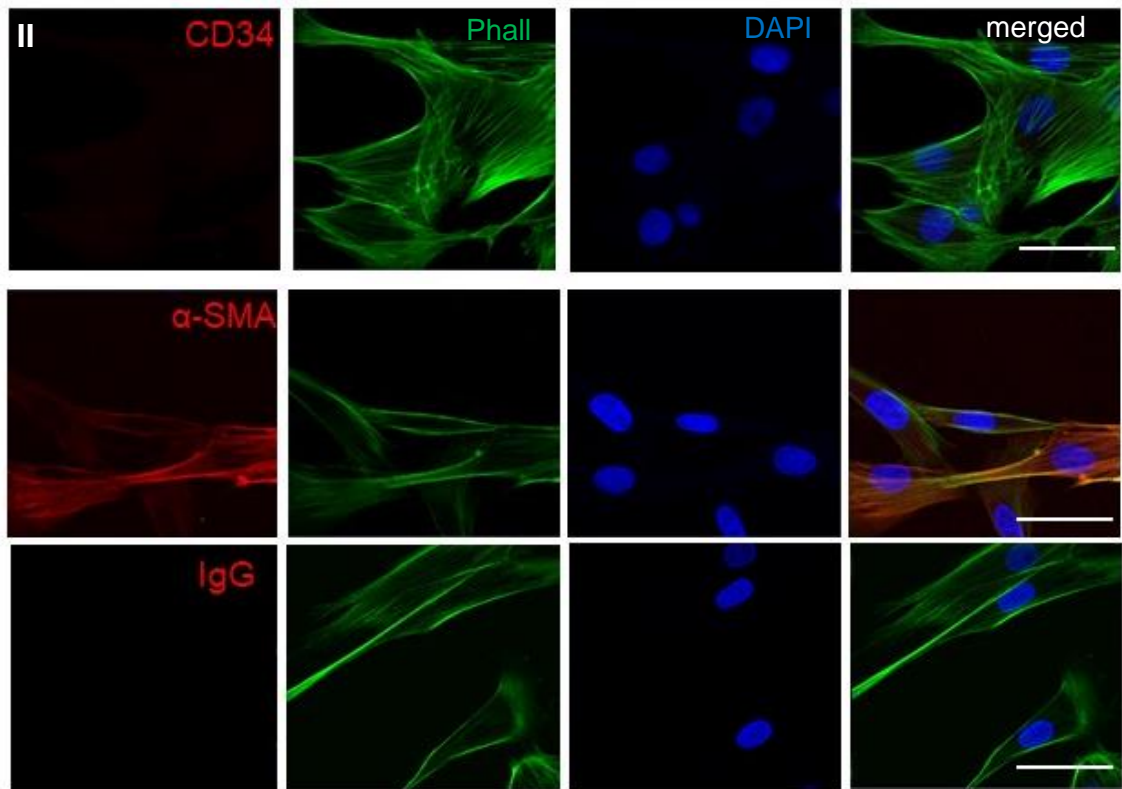


Figure 3.19.C (II) Immunocytological staining results of adipose derived MSCs

(C II): Summarised the immunocytological staining results of frozen cultured adMSC (passage 4-6) which served as positive control and exhibited similar protein expression to CSC (CD34 negative) but expressed α -SMA. This was performed in a biological triplicate (cells of donor # 16-18). Phalloidin (Phall) was used to stain the cytoskeleton (F-actin) and DAPI as nuclear marker. Abbreviations: IgG, immunoglobulin G (negative control). Scale bar: 20 μ m

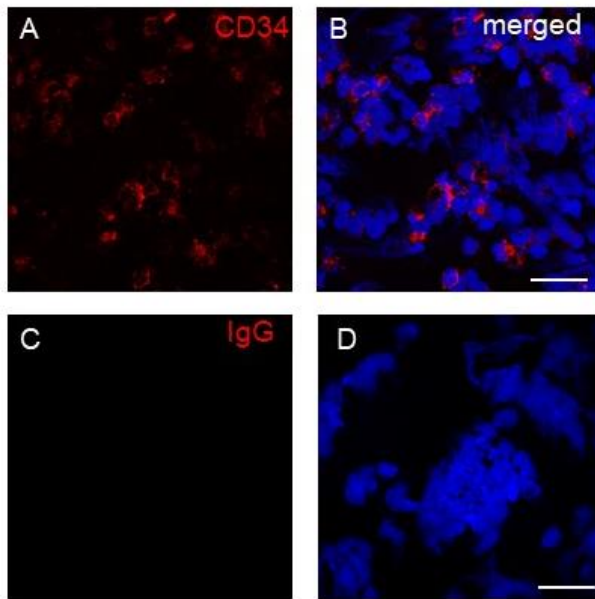


Figure 3.20 CD34 positive control on peripheral blood mononuclear cells

(A): Immunocytochemical image of CD34 positive stained PBMCs used as a positive control. This was performed as singlicate on cells of donor # 20. (C): IgG negative control. (B, D): merged images, nuclei are shown by DAPI. Abbreviation: Rb, Rabbit; Scale bar: 20µm

The mesenchymal marker (CD90, CD73, CD34) and Pax6 in limbal derived CSC were quantified by flow cytometry. These cells were of a primary cell culture composed of a mixed population of cells, cryopreserved and then expanded up to passage six. Flow cytometry demonstrated that the great majority of cells between passage P4-P6 express Pax6, CD73, CD90 (Table 3.3) and CD34 as hemotopoietic stem cell marker was quantified in very low value and considered as negative (Dominici, Le Blanc et al. 2006).

The results are illustrated in Figure 3.21 and summarised for each donor in Table 3.2.

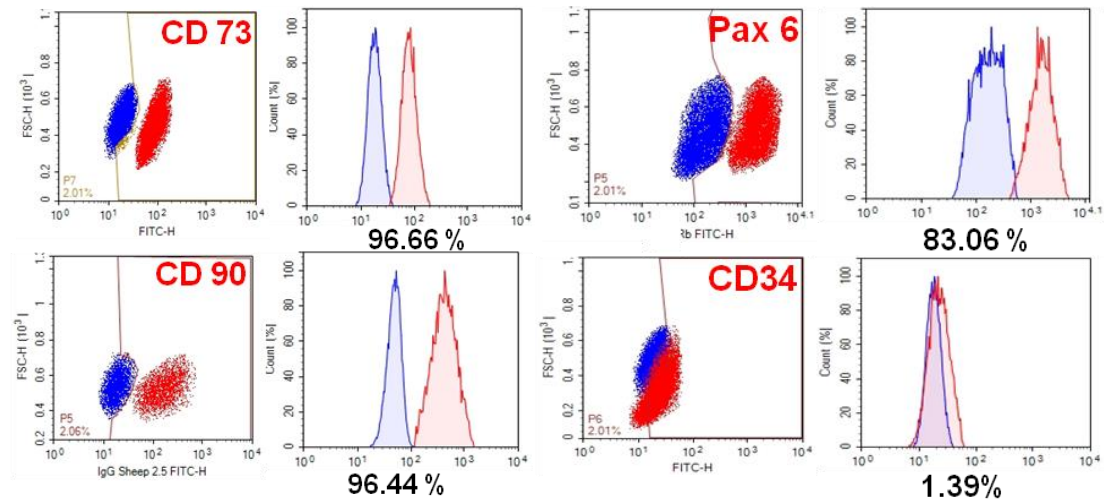


Figure 3.21 Flow cytometry results of MSC markers and Pax6 in limbal CSC

The graphs are showing the dot plots (FSC-H/FITC-H) with IgG isotype control (blue) and CD73, CD90, Pax6 and CD34 in limbal CSC (in red). To the right are the normalised histograms of each marker (red) and the IgG isotype (blue), which demonstrates the cell count in %/FITC-H. Summarised (%) are the mean positive gated cells of each marker under the histograms. This was performed as biological triplicate on cells of donor # 11, 12, 13. Abbreviations: FSC-H, forward scatter height, FITC-H, Fluorescein isothiocyanate – height.

Limbal CSC % positive gated cells	CD73	CD90	Pax6	CD34
#11	99.2	98.15	98.1	1.72
# 12	91.5	95.2	85.5	0.67
# 13	99.1	96.02	65.6	1.79
Mean (%) ± SD	96.6(±4.41)	96.44(±1.52)	83.06(±7.6)	1.39(±0.62)

Table 3.2 Overview of flow cytometry results of three donors

Flow cytometry was performed on limbal CSC in a biological triplicate. The results of gated limbal corneal stromal cells (= % positive events) in relation to concurrent IgG isotype (rabbit/sheep); This was performed as biological triplicate on cells of donor # 11, 12, 13. Fluorochrome: FITC; Emission filters: 530/30; Laser lines: 488 nm; Abbreviation: SD, standard deviation.

Similar to MSCs, limbal and central CSCs could be differentiated into bone, fat and cartilage producing cells demonstrating their multipotency (Figure 3.22). While there were no apparent differences in the efficiency of CSC and MSC differentiation into bone and fat cells, to drive CSC differentiation into cartilage in 2D and 3D a higher concentration of TGF- β 1 had to be used than for MSC differentiation (15 ng/ml versus 10 ng/ml).

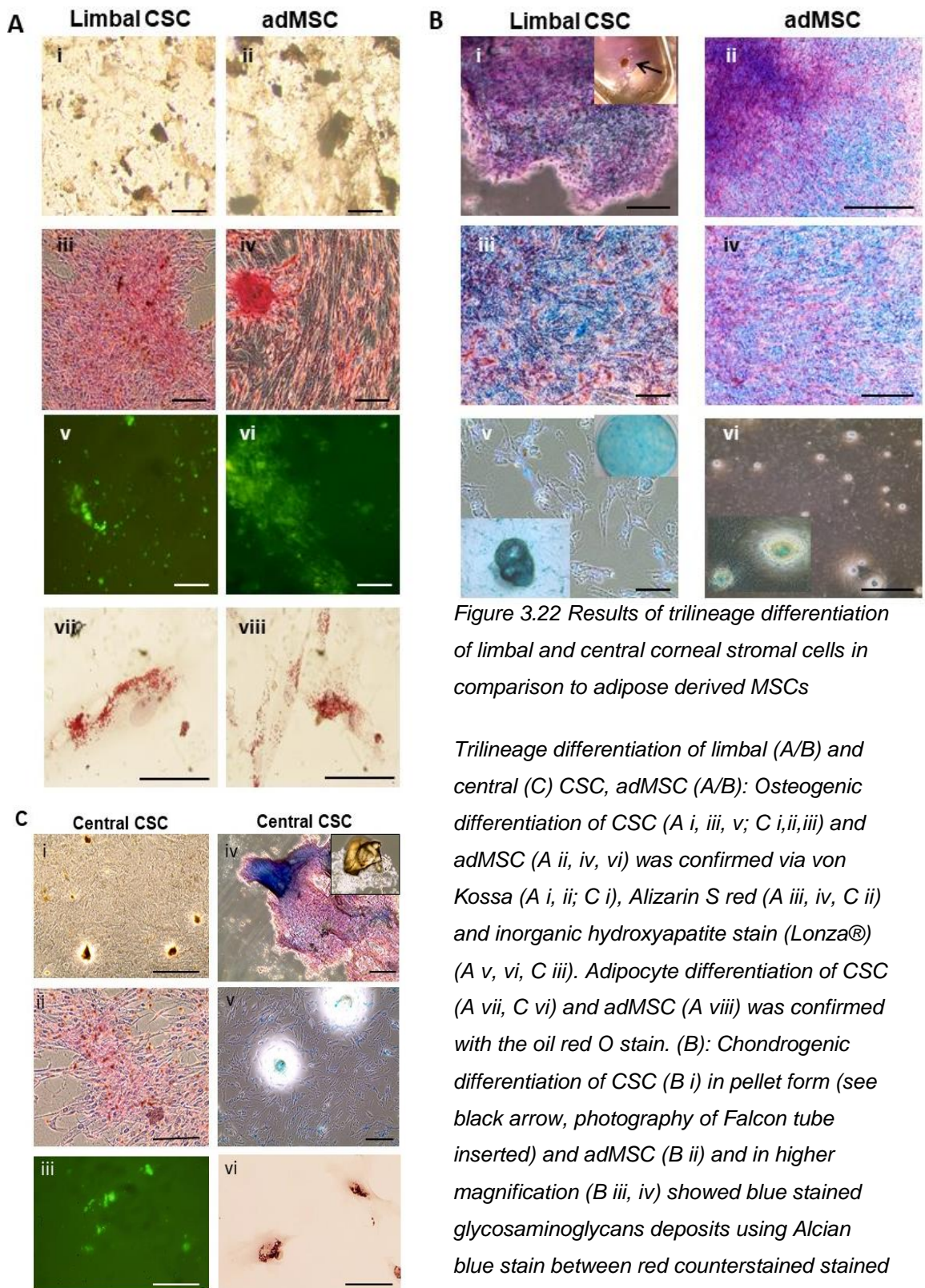


Figure 3.22 Results of trilineage differentiation of limbal and central corneal stromal cells in comparison to adipose derived MSCs

Trilineage differentiation of limbal (A/B) and central (C) CSC, adMSC (A/B): Osteogenic differentiation of CSC (A i, iii, v; C i,ii,iii) and adMSC (A ii, iv, vi) was confirmed via von Kossa (A i, ii; C i), Alizarin S red (A iii, iv, C ii) and inorganic hydroxyapatite stain (Lonza®) (A v, vi, C iii). Adipocyte differentiation of CSC (A vii, C vi) and adMSC (A viii) was confirmed with the oil red O stain. (B): Chondrogenic differentiation of CSC (B i) in pellet form (see black arrow, photography of Falcon tube inserted) and adMSC (B ii) and in higher magnification (B iii, iv) showed blue stained glycosaminoglycans deposits using Alcian blue stain between red counterstained stained cells.

CSCs (B vi) and adMSC (B vii) showed chondrogenic differentiation in 2D (cell culture dish photography inserted) forming Alcian blue stained nodular formation (highlighted in magnified image boxes). (C): chondrogenic differentiation of central CSC in the pellet (iv: see photograph inserted) stained in Alcian blue stain between red counterstained stained cells (iv) and 2D stained with Alcian blue (v). This was performed in a biological triplicate (find donor details in 3.2.8) . Scale bar: 20 μ m, B i,ii; C iv: 500 μ m

3.3.8 Evaluation of corneal stromal cells in PBMC co-culture assay

Limbal CSCs were investigated whether these cells are stimulating the proliferation of PBMCs, or a baseline proliferation was maintained. Hence, CSC need to be growth arrested to act as stimulator and not contributing to any cell proliferation, which consequently lead to false positive results. Given instable results in the first set-up of experiments a growth arrest assay was conducted. CSCs were counted, growth arrested using three different concentrations of Mytomycin C (MMC) (Sigma-Aldrich) for 2hours at 37°C, cultured in PBMC media for 4 days and a cell count was performed using the automated cell counter (Biorad). First, a concentration of 10µg, 25µg and 50 µg MMC/ml was tested on limbal CSCs donor #6. Hence, the two higher doses of 50µg and 25 µg was leading to 75% and 35% cell loss with 25% and 66% living cells respectively, the MMC concentration of 10µg, 15µg, and 25µg was further evaluated.

This was performed before each PBMC co-culture assay of limbal CSCs of donor # 2, 3 and 12 (Figure 3.23). MMC concentration of 15µg/ml MMC revealed the most stable cell numbers with a mean of $85.33 \pm 10.96\%$ live cells (not included in Figure 3.23). The reason for the decline of cell number after 10µg MMC treatment in CSC donor #3 remains unclear (Figure 3.23).

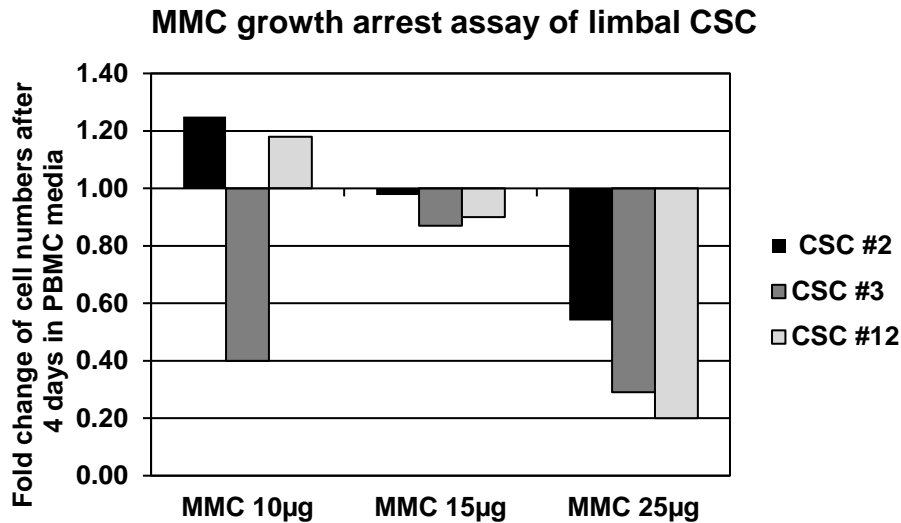


Figure 3.23 Mytomycin C (MMC) growth arrest assay of limbal corneal stromal cells (CSC)

The graphic demonstrates the fold change of cell numbers of limbal CSC in a biological triplicate of three different donors (# 2, 3, 12) which were growth arrested using 10µg, 15µg and 25µg of MMC respectively. The growth arrested cells were then cultured for 4 days in PBMC media. CSCs treated with 15µg MMC were most stable (= not expanding).

Secondly, the cell density of CSC/well of a 96well plate (= 0.32cm² surface area/well) was investigated. The aim was to expose the PBMCs to a monolayer of live, but not proliferative CSCs for 4 days. Following, 5x10⁴ cells (donor # 2), 1x10⁵ and 1.5x10⁵ cells were cultured per well in triplicate for 4 days in PBMC media. Phase contrast images were taken on day 4. The cells were detached, and an automated cell count was performed. As shown in Figure 3.24, 5x10⁴cells/well had a nearly confluent monolayer, 98% living cells and a cell count of 4.49x10⁴ cells/well. The higher cell density of 1x10⁵ per well was over confluent, 8.9x10⁴ with 89% live cells were counted and the cell density of 1.5x10⁵ cells dehisced after 2 days. Therefore, 5x10⁴ CSC /well were seeded for each PBMC co-culture experiment.

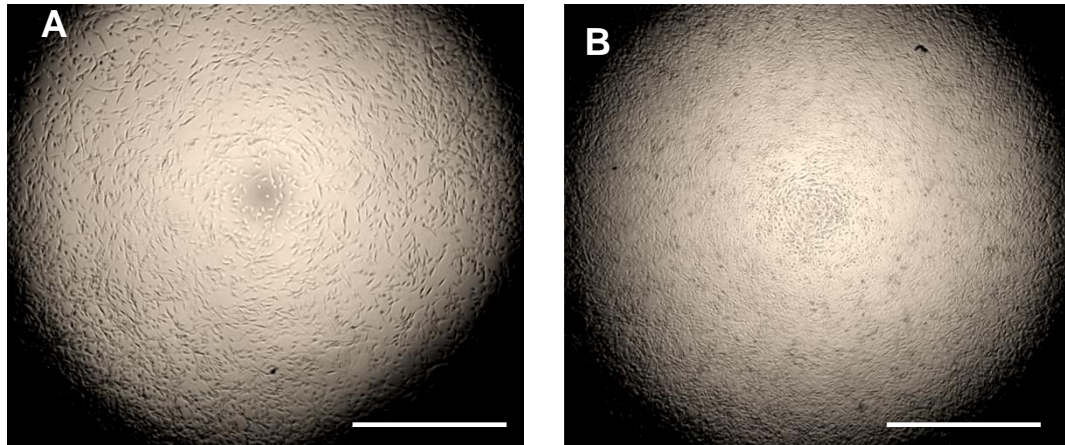


Figure 3.24 Evaluation of limbal corneal stromal cell density for peripheral blood mononuclear (PBMC) co-culture assay

Phase contrast images of (A) monolayer of 5×10^4 CSC/well of 96well plate (surface area = 0.32 cm^2) after 4 days culture in PBMC media. (B) 1×10^5 cells/well showed an over confluent layer with a reduced number of 89% live cells. This was performed in biological triplicate (donor # 2, 3, 12). White bar = $500 \mu\text{m}$

3.3.9 CSCs are immune privileged *in vitro*

Co-cultures with PBMCs were performed to determine whether limbal CSCs were immune privileged. Allogeneic limbal CSC co-cultured with effector PBMCs in a ratio of 1:5 (CSC: PBMC) did not modify the baseline level PBMC proliferation. In comparison, co-cultures of effector PBMCs with allogenic PBMCs showed a significant increase (T-test, $P = 0.00044$) in proliferation compared to non-activated PBMC (Figure 3.25).

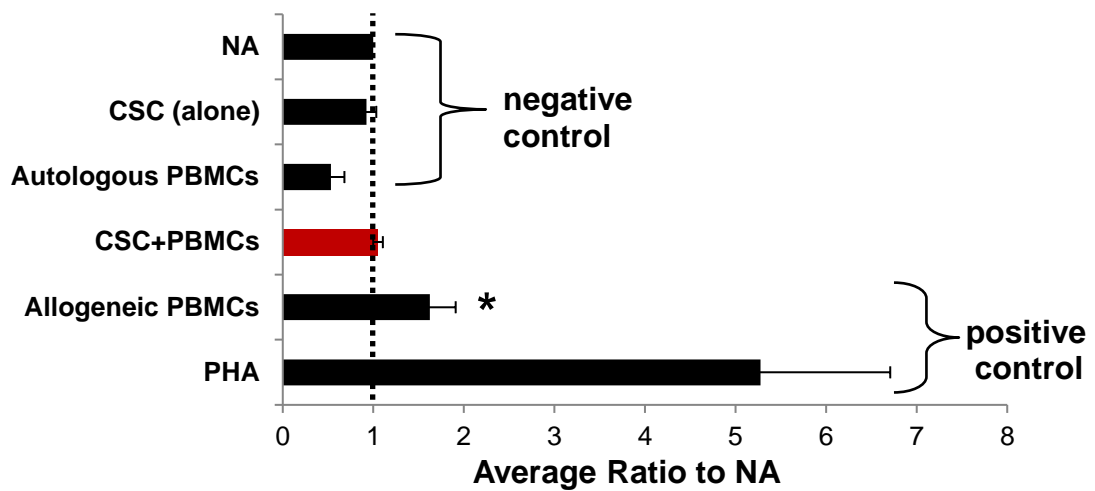


Figure 3.25 Co-culture results of allogeneic limbal CSC with peripheral blood mononuclear cells (PBMCs)

Allogeneic limbal CSC co-cultured with PBMCs (red bar) did not modify the baseline level PBMC proliferation. In comparison, co-cultures of effector PBMCs with allogeneic PBMCs showed a significant increase in proliferation compared to non-activated PBMC. The values represent the mean average proliferation ratio of three biological replicates (\pm SE) to non activated PBMC (value 1) highlighted with a dashed line; *, $p < .05$. This was performed in a biological triplicate (limbal cells of donor 2, 3, 12; PBMCs of # 20-23). Abbreviations: CSC, corneal stromal cells; NA, non-activated; PBMC, peripheral blood mononuclear cells; PHA, Phytohemagglutinin

3.3.10 CSC differentiate into keratocyte-like cells in vitro during which bFGF plays an essential role in downregulation of α -SMA

An initial seeding number of 1×10^4 cells/cm² cultured in a 4cm² chamber slide in KDM (supplemented with bFGF) revealed in rapid confluence, cell sheet formation and dehiscence after 11 to 16 days and a fourfold cell expansion. Therefore, the seeding number had to be established (Figure 3.26):

1. 1×10^2 , 1×10^3 , 5×10^3 cells/cm²

KDM containing basic FGF with a cell seeding number of 1×10^3 cells in a T25 flask revealed a density not greater of 80% confluency. However, 1-2x

additional passage steps (day 13-15) in T75 culture flasks were still necessary to avoid confluence, contracting cell sheet formation and dehiscence before the end of the experiment at 21 days. A twofold cell expansion factor was counted.

2. $1 \times 10^3/\text{cm}^2$ without substituted bFGF (-)

A seeding number of 1×10^3 cells/cm² cultured in KDM without substituted bFGF revealed stable cell numbers. However, a more fibroblastic cell appearance was noted after 10 to 12 days. The myofibroblastic marker α -SMA was exhibited in the third week of keratocyte differentiation in the media lacking bFGF. The keratocyte differentiation media containing bFGF showed morphologically increasing fibroblastic appearance after 16 days but did not express α -SMA immunocytochemically. In general, canine CSC in KDM were continuously expanding within the 21 days (Figure 3.26).

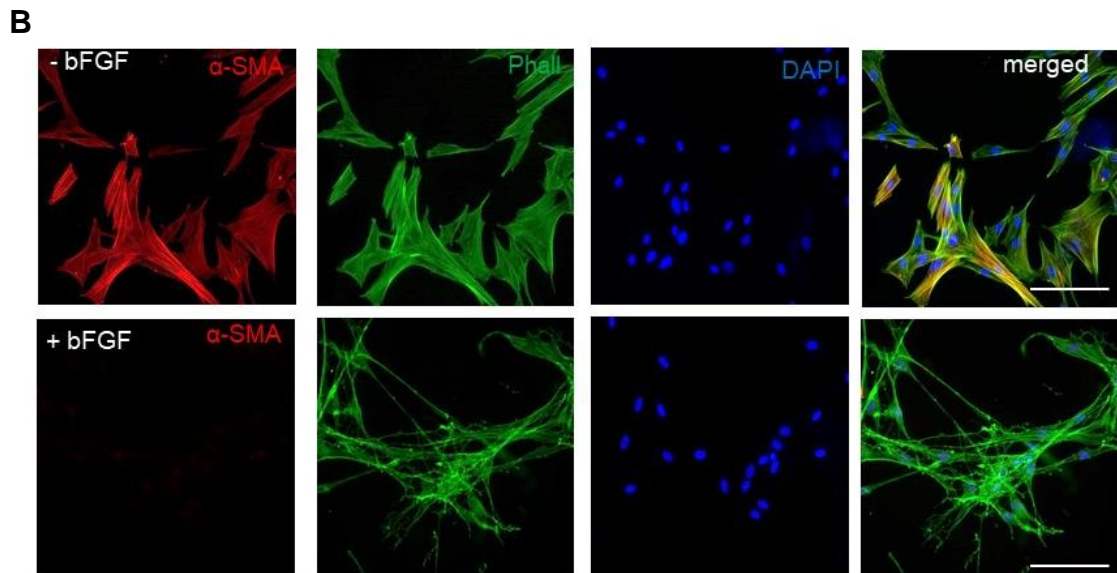
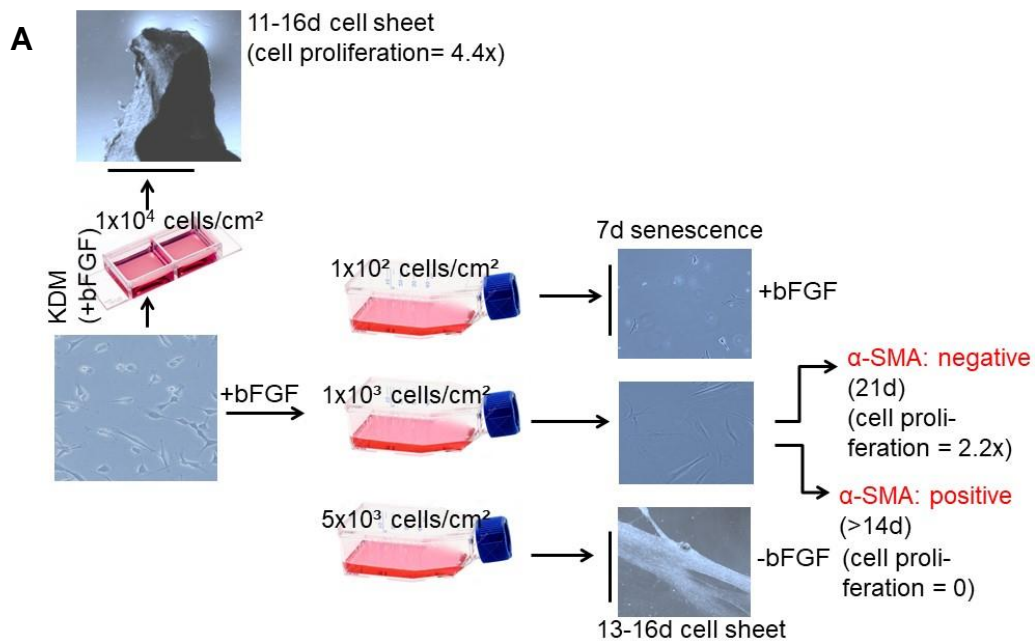


Figure 3.26 Results of the cell culture conditions of limbal corneal stromal cells (CSC) undergo keratocyte differentiation

(A) The schematic illustrates the results of the culture condition established to differentiate limbal CSC into keratocyte-like cells over 21 days. The seeding number of 1×10^3 cells/cm² and KDM with substituted bFGF is essential to prevent myfibroblast differentiation, but CSC-KDCs will further expand during the differentiation. (B) Without bFGF the CSC-KDC express α -SMA. This was performed in a biological triplicate (cells of donor # 16, 19, 21).

Abbreviations: α -SMA, alpha smooth muscle actin; bFGF, basic fibroblastic growth factor; d, days, KDC, keratocyte differentiated cells, KDM, keratocyte differentiation media; Phalloidin (Phall) was used to stain the cytoskeleton (F-actin) and DAPI as nuclear marker; Scale bar: 20 μ m

Limbal derived CSC were cultured under low glucose, serum-free conditions with substituted ascorbic acid (KDM) to induce their differentiation into keratocyte-like cells (CSC derived keratocyte differentiated cells (CSC-KDC)). The small, polygonal morphology characteristic of CSCs changed to a dendritic morphology typical of keratocytes within 7-10 days (Figure 3.27).

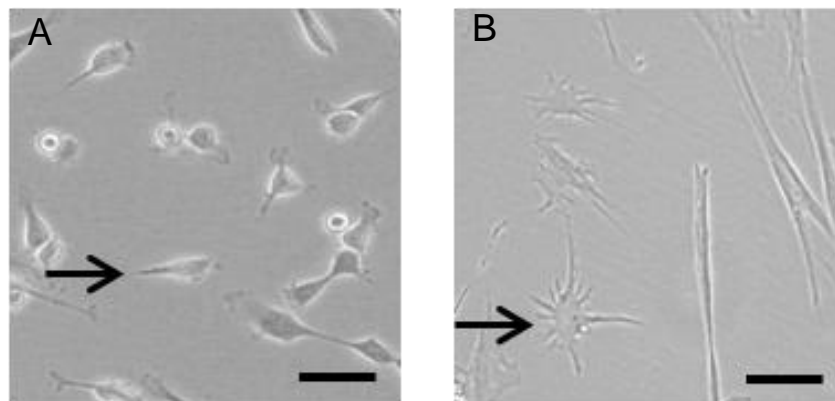


Figure 3.27 Morphological change of corneal stromal cells (CSC) in keratocyte differentiated cells (KDC) in keratocyte differentiation media

(A) Phase contrast images of CSCs; (B) CSC-KDCs increasing in cell size and develop a dendritic and elongated cell morphology highlighted by the black arrow. The keratocyte differentiation was performed in a biological triplicate (donor # 16, 19, 21) Scale bar: 20µm

CSC-KDCs showed protein expression of Lumican, Keratocan and ALDH1A3. Pax6 expression was subjectively weaker expressed without performing quantitative ICC image analysis (Chlipala, Bendzinski et al. 2020). N-cadherin protein expression became undetectable following differentiation (Figure 3.28). This was also reflected at the gene expression level where following differentiation *Keratocan* was significantly upregulated (T-test, $P=0.041$). In contrast, the stem cell associated genes *N-cadherin* (T-test, $P=0.025$) was significantly downregulated and a trend of *Pax6* downregulation

was present (T-test, P= 0.077) (Figure 3.29). The relative gene expressions are summarised in Supplementary Figure S1.

Alpha-SMA is a myofibroblastic marker, which is not expressed in undifferentiated CSCs (Figure 3.19.A.II, Figure 3.19.B.II) or following keratocyte differentiation in the presence of bFGF in KDM (Figure 3.26. B). However, in the absence of bFGF, α -SMA protein is detected in the differentiated cells (Figure 3.26.A). At the gene expression level, CSCs in the undifferentiated state express very low levels of α -SMA and this is maintained following keratocyte differentiation in the presence of bFGF (Figure 3.29, 3.30). When differentiated in the absence of bFGF, α -SMA gene expression is significantly upregulated (T-test, P= 0.00019) reaching a similar level to skin fibroblasts which were encouraged to undergo myofibroblast differentiation using TGF β -1 (Figure 3.30).

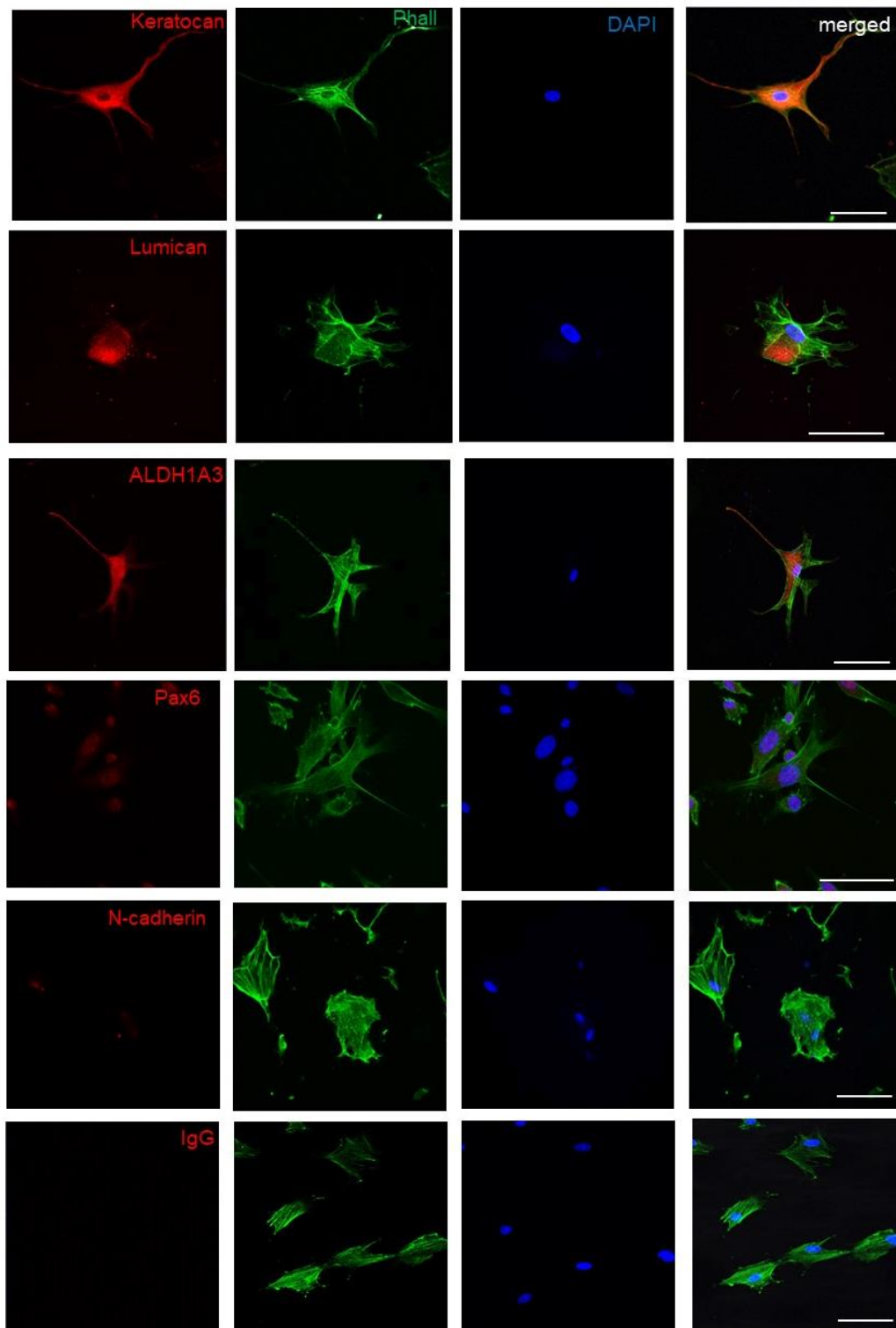


Figure 3.28 Immunocytochemical staining results of limbal corneal stroma cell derived keratocyte differentiated cells (CSC-KDC)

The keratocyte marker Lumican, Keratocan, ALDH1A3 are expressed in KDC, the nuclear stem cell marker Pax6 is weakly, and N-cadherin is not expressed. This was performed in a biological triplicate (donor # 16, 19, 21) Nuclei are shown by DAPI counter staining and the cytoskeleton by Phalloidin (Phall). Scale bar: 20 μ m

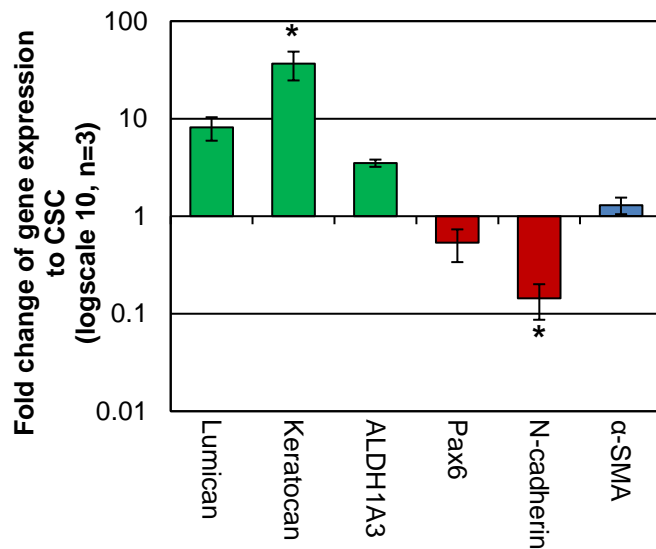


Figure 3.29 Fold change of gene expression (qPCR) of corneal stroma cell derived keratocyte differentiated cells (CSC-KDC)

Fold changes of qPCR data to undifferentiated CSC calculated relative to canine 18S is showing the significant upregulation of Keratocan (T-test, $P=0.041$) and downregulation of N-cadherin (T-test, $P=0.025$). Values represent mean \pm SE, $n=3$, biological triplicate (donor # 12-14); *, $p < .05$.

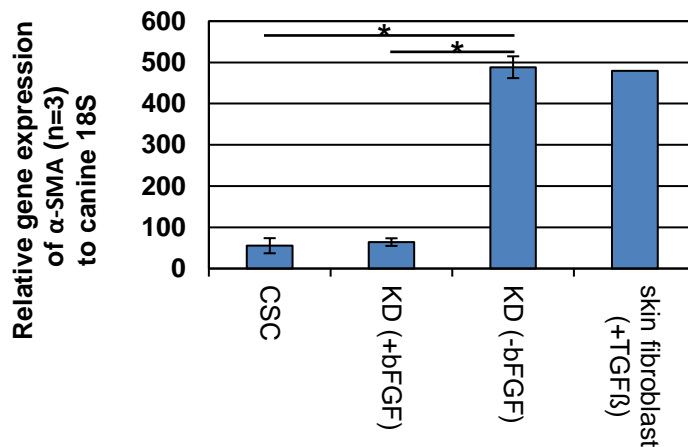


Figure 3.30 Relative gene expression data of α-SMA in corneal stromal cell derived keratocyte differentiated cells (CSC-KDC) cultured without and without basic fibroblastic growth factor (bFGF)

QPCR relative gene expression data of α-SMA in CSC-KDC cultured without (-bFGF) showed significant upregulation to CSC (T-test, $P=0.00019$) and KDC cultured with bFGF (+bFGF) (T-test, $P=0.0001$). Skin fibroblast cultured with substituted TGFβ to induce upregulation of α-SMA served as positive control (technical singlicate donor # 25). Values represent mean \pm SE, $n=3$, biological triplicate (donor 16, 19, 21), *, $p < .05$. Abbreviations: bFGF, basic human fibroblast growth factor; TGFβ, transforming growth factor beta.

3.4 Discussion

The chapter aimed to characterise corneal stromal cells in the anterior stroma from the limbus and central cornea and determine the multipotent mesenchymal stromal cell potential in healthy dogs. Additionally, essential baseline data of the limbal anatomy in dogs was described.

In the first part of this chapter, the corneal limbus and central cornea in healthy dogs were investigated histologically. A major anatomical difference to humans was the absence of limbal crypts and palisades of Vogt (Patruno, Perazzi et al. 2017). A slight invagination of the epithelium in the stroma was also confirmed as described by Patruno et al. 2017 (Patruno, Perazzi et al. 2017). Well-defined palisades of Vogt are present in the porcines but not in the rabbit and rodent limbus (Gipson 1989, Notara, Schrader et al. 2011). The appearance of an undulating basal membrane in dogs have similarities to rabbits, where epithelial rete ridges project into the subjacent stroma, exhibits discontinuities with the basal lamina which is interrupted with evidence of direct interaction between stromal and limbal epithelial cells (Goldberg and Bron 1982, Gipson 1989, Goes, Barbosa et al. 2008).

Dziasko and co-workers (2014) used three-dimensional electron microscopy and discovered focal direct interactions between the small basal epithelial cells of the human crypt-rich zones (i.e. presumed LESC) and cells in the subjacent stroma. These stromal cells were positive for CD90 and CD105 (Dziasko, Armer et al. 2014).

To date, there has only been speculation as to whether a higher degree of limbal pigmentation, while lacking any limbal crypts, acts as additional protection against UV-light in dogs. In contrast to human, the ratio of cornea to sclera is smaller and the globe is deeper set in the orbit. Hence, the canine limbus will be fully covered by the eyelids, with the eyelids acting as protection against UV light. Studies of breed-related differences in the future are of great interest for veterinary science as brachycephalic breeds have exposed eyes (lagophthalmus) and therefore, a relative higher degree of exposed limbal area, and are more prone to pigmentary keratopathy and corneal ulcerations (Sanchez and Daniels 2016).

However, further basic research including 3D-electron microscopy and in vivo confocal microscopy of the canine LESC niche is warranted.

Following on, this chapter provides the first description of limbal and central derived corneal stromal cells with multipotent mesenchymal stromal cell characteristics in dogs, similar to those described in human publications (Du, Funderburgh et al. 2005, Funderburgh, Du et al. 2005, Li, Dai et al. 2015, Tomasello, Musso et al. 2016, Vereb, Poliska et al. 2016).

In humans, limbal stromal cells were found to have mesenchymal stromal cell characteristics and were described as corneal stromal stem cells (CSSC) (Hertsenberg and Funderburgh 2015, Dziasko and Daniels 2016) or limbal mesenchymal stromal cells (L-MS)(Polisetty, Fatima et al. 2008, Branch, Hashmani et al. 2012). In humans, these stromal cells are hypothesized to assist in the maintenance of the LESC niche (Polisetti, Agarwal et al. 2010). This theory is supported by the fact that basal epithelial cells in the limbal

niche are in direct contact with stromal cells. Both cells produce N-cadherin, a cell-cell junction protein. Human LESC co-cultured with limbal CSSC have higher expansion and clonogenicity rates. This was less intense with central corneal stromal cells (Higa, Kato et al. 2013, Dziasko, Armer et al. 2014).

Immunohistologically, a small cell population of CD90+ expressing stromal cells in the limbal as well as in the central anterior corneal stroma was present, which seems a finding unique to the canine cornea. CD90 is a well-accepted mesenchymal stromal cell marker, however, it can also be expressed by fibroblasts (Dominici, Le Blanc et al. 2006). The question arose as to whether the CD90+ stromal cell population are potential residual fibroblasts that act as progenitor cells. However, the described stromal cell population did not express alpha-smooth muscle actin (ACTA2, α -SMA), which is mainly expressed by corneal myofibroblasts and to a lesser degree by fibroblasts (Jester, Petroll et al. 1995, Hinz, Phan et al. 2007). It was demonstrated that alpha smooth muscle actin was solely located in the surrounding scleral blood vessels towards the limbal junction (Figure 3.10). Double or even triple IHC using CD90, α -SMA and Vimentin would have clarified this question in more detail, but this was not performed at this stage in this study.

N-cadherin is an intercellular neural adhesion protein and is also described as a putative marker for LESC (Hayashi, Yamato et al. 2007, Higa, Kato et al. 2013) and was included in our study as an additional stem cell marker of interest. Interestingly, single stromal cells were expressing N-cadherin in the limbal anterior stroma, but the results were inconsistent between donors and

therefore not included in the results. This observation should be followed in more detail in future studies.

Funderburgh et al. 2005 described a small population of limbal stromal cells expressing the transcription factor Pax6 (oculorhombin) in bovine corneas (Funderburgh, Du et al. 2005). This could not be confirmed histologically in canine corneas. A recent study characterised CSSC derived from the central cornea in human, however the study was lacking any immunohistochemistry (Vereb, Poliska et al. 2016).

Stromal cells from the limbal and central cornea were successfully isolated and cultured from healthy dogs using the same protocol as described in the human literature. Differential trypsinisation of small polygonal cells, which reached a maximal confluency of 60-70%, allowed the selective culture of CSC. A small, stem cell-like appearance could also largely be maintained throughout several passages in canine CSCs (Figure 3.17). It is described that CSC when cultured subconfluent with limited cell-to-cell contact keep their small, stem-like morphology (Kureshi, Funderburgh et al. 2014). However, more detailed ICC and qPCR (stem cell and keratocyte marker) to compare the morphological classification to the protein and RNA expression level or even RNA sequencing, is warranted to provide more evidence base in future studies. Particularly with regards to further characterise limbal and central derived CSC.

QPCRs are limited to measuring single transcripts and relying on low-throughput methods as used in the study. RNA sequencing uses the capabilities of high-throughput sequencing methods to provide more

information on the transcriptome of a cell. This also includes, apart from polyadenylated messenger RNA (mRNA) transcripts, investigations of total RNA, pre-mRNA, and noncoding RNA (microRNA and long noncoding RNA) (Kukurba and Montgomery 2015). Zaoh et al. 2018 compared two main RNA-sequencing approaches and concluded to select polyA+ over rRNA depletion in context of gene quantification in clinical RNA sequencing (Zhao, Zhang et al. 2018).

A limitation of this study was that a colony formation assay of limbal and central CSCs was not performed but should be included in future studies (Kureshi, Funderburgh et al. 2014). Another limitation of this study is the general compromise of research in domestic species, that commercially validated primers are not available. Future work should include sequencing the product amplified to confirm the identity of the amplified product. This was not performed in the current study.

Comparing the cell composition based on cellular morphology, increasing numbers of fibroblastic cells were observed after the fifth passage. This is a relevant finding for future research working with canine CSCs as this indicates that there is a relatively narrow window of proliferating cells retaining stem cell properties. At least under the current culture conditions and absence of fibroblasts. Interestingly, Hashmani et al 2013 used only human CSSC not greater than P3 in their study but did not provide an explanation for the choice (Hashmani, Branch et al. 2013).

In contrast to Du et al 2005, selective cell sorting to expand ABCG2 labelled human CSSC “side population” was not available in the present study period

(Du, Funderburgh et al. 2005). The ABCG2 positive cell-sorted side population showed a replicative lifespan typical of stem cells with 18 passages and a cumulative population doubling of 80 until senescence was reached (Du, Funderburgh et al. 2005). Polisetty et al 2008 characterised human limbal derived MSC without cell sorting, similar to the present study in dogs, and revealed 22.9 cell doublings at passage 2-6, which is higher than in dogs. However, a PDT of 29.1h and 34.1h similar to BM-MSC was also observed only at P2-3, with fast increasing time until passage P6, similar to the present study (Polisetty, Fatima et al. 2008).

The culture kinetics of canine CSC selected by passaging had accumulative population doublings of 12 and 11 for the limbal and central derived CSC over five passages respectively until senescence was reached. A population doubling time of approximately 24-30h as described in canine (amniotic) mesenchymal stem cells was only reached in the early log phase (P1-P2) (Park, Seo et al. 2012). Guercio et al 2013 also reports a limited life-span and senescence after passage 6 in canine adMSC (cultured in DMEM low glucose, 20% FBS) and revealed similar accumulated PD (11-12) in a similar time (27-28 d) to the present study of CSC (Guercio, Di Bella et al. 2013). Bearden and colleagues 2017 showed that adipose and synovium canine MSCs proliferated first more rapidly with a rapid decline after passage 3, than bone-marrow cMSCs (Bearden, Huggins et al. 2017). This is similar to the observation in the CSC study.

Therefore, the limited self-renewal of the CSC population in dogs represents rather proliferating progenitor cells than stem cells or might resemble a mixed

population of cells (Seaberg and van der Kooy 2003). Future studies are needed to assess the potential to self-renewal, for example on cell-sorted population of CSC and in optimisation of the human CSSC media to canine CSC requirements.

The maximal passage frequency, culture time and cell number were evaluated. No difference was observed between limbal and central derived CSC, although the central CSC showed a trend towards lower frequency of passage, lower cell numbers and reaching the point of senescence sooner. This trend might have reached significance if additional cells from further donors would have been evaluated. There was a high degree of individual heterogeneity in cell expansion which might be explained by the wide age range of donor tissue (0.2-12 years) donated to this study as donor age can negatively impact human MSC cell expansion and differentiation (Choudhery, Badowski et al. 2014). Volk and colleagues 2012 studied the effects of age in skeletally immature and mature dogs on canine BM-MSCs. BM cells isolated from long bones, cultured in high glucose DMEM substituted with 10% FBS, showed a significant negative effect of age to differentiate along the osteogenic lineage (Volk, Wang et al. 2012). Guerico et al (2013) compared the harvest site (subcutaneous/visceral) and age (young dogs: 1–4 years; adult dogs: 8–14 years) of adMSCs cultured in low glucose DMEM and 20% FBS. Population doubling values were significantly higher for MSCs derived from subcutaneous fat and in younger dogs. CFU-f assay in low glucose DMEM and 5% FBS did not differ according to age and harvest location site but declined after passage > 2 (Guericio, Di Bella et al. 2013).

The variation of donor ages is a limitation of the study (donors aged 0.2-12 years). To fulfil the ethical approval the present study had to be based on donated tissue of animals euthanized unrelated to this study. However, despite the age differences, the breed selection was limited strictly to mesocephalic (medium length skull) dog breeds. This was set as an inclusion criterion to minimise the skull form with more exposed eyes of brachycephalic breeds as potential influencing factor. Another influencing factor on cell culture systems is the impact of cryopreservation. The creation of cryopreserved cell banks for allogeneic applications are essential for cell therapy treatment. This would necessitate the characterisation of cryopreserved in comparison to freshly cultured CSC, to assess for endotoxins and purity (Dutton, Church et al. 2018). This was not an objective of the present chapter, cells expanded from fresh isolates and cryopreserved CSC were used for different assays. However, there are currently no comparative data in the human-based CSC literature available.

Canine MSCs are characterised in the veterinary field, including adipose derived, bone marrow derived MSC's and other tissue sources as amniotic-derived, synovial –derived, periosteum (Kisiel, McDuffee et al. 2012, Park, Seo et al. 2012, Takemitsu, Zhao et al. 2012, Russell, Chow et al. 2016, Bearden, Huggins et al. 2017, Kriston-Pal, Czibula et al. 2017, Uder, Bruckner et al. 2018). Positive and negative MSC marker profiles differ in various studies, some studies also demonstrated cells were positive for the pluripotency-associated genes NANOG, OCT4, and SOX2 (Guercio, Di Bella et al. 2013, Bearden, Huggins et al. 2017).

The proliferation capacity of bone marrow (BM)-MSCs are lower than in adMSCs and synovial MSCs (Russell, Chow et al. 2016, Bearden, Huggins et al. 2017). Breed-related differences are described for BM-MSCS of Howavart's which had significantly fewer colony- forming units (CFU) than German Shepherd, Flat coated Retriever or Golden Retriever (Bertolo, Steffen et al. 2015).

This study described the canine MS-like cells of corneal origin, and the results were primarily compared to human corneal stromal MSC studies. The CSCs are isolated and cultured using different culture conditions to MSCs. However, it would be beneficial to compare CSCs to canine MSCs in terms of culture conditions, cell proliferation and marker expression.

Optimisation of canine CSC media to maximise self-renewal and differentiation potential are required in the future. CSSC media contains low serum levels of 2% FBS but most canine MSC culture conditions uses 10% or higher aFBS concentrations. Higher serum concentrations have been shown to induce a myofibroblastic cell fate in rabbit keratocytes (Jester, Barry-Lane et al. 1996). Serum supplementation (10% v/v) led to human keratocyte differentiation into fibroblasts with loss of keratocan expression in human CSSC (Du, Funderburgh et al. 2005, Foster, Gouveia et al. 2015, Kureshi, Dziasko et al. 2015). Whether this holds for canine keratocytes and canine CSC is unknown. The CSSC media also contains PDGF and EGF. Factors as FGF, TGF- β , PDGF, insulin-like growth factor 1 (IGF-1) and EGF regulate keratocyte differentiation, migration and expression and are known to be essential growth factors in corneal *in vitro* studies (Kim, Lakshman et al.

2010, Lakshman and Petroll 2012). A canine study of BM-MSCs reported that cells expanded best in α -MEM supplemented with bFGF (Bertolo, Steffen et al. 2015).

The basic characteristic of multipotent MSCs is their ability to give rise to a variety of different lineages. Both limbal, central derived CSC and adMSC were differentiated into chondrogenic, adipogenic, and osteogenic lineages *in vitro*. It is important to note that chondrogenesis in canine MSC has not been robustly shown as for adipogenesis and difficulties to establish a protocol are known (Kisiel, McDuffee et al. 2012, Russell, Chow et al. 2016). However, a differentiation protocol of CSCs towards chondrogenic lineage differentiation was established. In contrast to adMSCs, the concentration of TGF- β 1 had to be increased from 10 ng/ml to 15 ng/ml. Future work could also optimise the osteogenic differentiation protocol, for example through the addition of BMP-2 or IGF-1 (Volk, Diefenderfer et al. 2005, Levi, Nelson et al. 2011, Bearden, Huggins et al. 2017).

The immunophenotyping of limbal and central derived CSC were very similar to the surface antigen profile of adMSC. Like the adMSC, the central and limbal CSC showed similar expression patterns of CD90, CD73, CD105, N-cadherin and CD34. Canine adipose derived and bone marrow MSCs are well characterised in the literature (Takemitsu, Zhao et al. 2012).

This chapter reports that the limbal and central derived CSCs meet the minimal criteria of ISCT, including adherence to plastic and marker expression of CD90, CD73, CD105 and absence of marker expression of CD34 (Dominici, Le Blanc et al. 2006). This was also confirmed by flow

cytometry, but only for limbal derived CSC. In contrast to most human studies characterising limbal MSCs, it can be argued that the present study used only a limited number of protein markers; however, this reflects the challenge of establishing protocols for the use of markers on canine tissue and cells. Most of the markers and all of the primers are not established in this species and therefore, western blot analysis had to confirm the specific binding and canine specific primers needed to be designed.

The expression of CD34 in CSSC and keratocytes is controversial in corneal research. CD34 is a hematopoietic stem cell surface marker, which is defined to be absent (<2%) in MSC (Dominici, Le Blanc et al. 2006). This was also confirmed for human limbal and central CSSC (Polisetty, Fatima et al. 2008, Vereb, Poliska et al. 2016).

Joseph et al. 2003 described CD34 as a characteristic marker of quiescent keratocytes in the human cornea (Joseph, Hossain et al. 2003). Another study characterising limbal mesenchymal stromal cells showed a drop of CD34 marker expression with increasing cell proliferation and a shift to more progenitor cell type expressing CD34, Pax6, ABCG2, SSEA-4. This seems to be influenced significantly by the composition of culture media (Branch, Hashmani et al. 2012, Hashmani, Branch et al. 2013, Sidney, Branch et al. 2015). In this chapter, the CD34 protein expression in less than 2% of canine CSC were found and was therefore considered as negative. Also canine adMSC used in the present study did not express CD34, which is similar to other reports for canine MSCs (Takemitsu, Zhao et al. 2012, Russell, Chow et al. 2016, Kriston-Pal, Czibula et al. 2017).

AdMSC, unlike CSC, did not express Pax6 which was also expected given their origin. However, adMSC did express α -SMA which was not detected at the protein level in undifferentiated CSCs. α -SMA expression has been reported in human, rat and murine MSCs previously (Peled, Zipori et al. 1991, Liu, Deng et al. 2013, Talele, Fradette et al. 2015).

It was demonstrated that the CSC from both the limbal and central cornea had no significant differences in their culture kinetics or marker expression. Vereb et al. (2016), described a higher mRNA gene expression of *CD44*, *CD90*, *CD105*, *CD117*, *CD140* in human central corneal MSC-like cells whereas *CD49f*, *CD104*, *CD146* and *CXCR4* showed less expression compared to the LSCs. This indicates possibly the presence of different cell types within the limbal and central microenvironments (i.e. stem cell niche) in the human cornea (Vereb, Poliska et al. 2016). If that holds in the canine cornea would require more detailed immunophenotyping and RNA sequencing, and also larger scale-studies in central versus limbal CSC in the future.

Human CSSCs have been shown to not only fail to induce the proliferation of allogeneic PBMCs but also to suppress the proliferation of activated PBMCs *in vitro* (Vereb, Poliska et al. 2016). In this chapter it was demonstrated that canine CSCs also appear to be immune-privileged *in vitro* as they fail to induce the proliferation of allogeneic PBMCs. PBMC assays were performed on three different lines of CSCs each using PBMCs from two different donors (with PBMCs isolated from both lymph nodes and commercial suppliers). However, the cells were not typed for dog leukocyte antigens (DLA) and

therefore we cannot rule out the possibility that the cells were not true mismatches.

The baseline data for the future work (MMC growth arrest concentration, cell density) was established, but further work is required to determine if they are also immune suppressive. Immune suppression by human CSCs is increased following their stimulation with proinflammatory- cytokines. Inhibition of neutrophil infiltration of CSSC via TSG6 expression might help to reduce *in vivo* scarring (Vereb, Poliska et al. 2016, Hertsenbergh, Shojaati et al. 2017).

Canine CSCs (limbal and central derived) were differentiated into cells with stellate keratocyte typical morphology that expressed keratocyte markers Keratocan, Lumican and ALDH1A3 (Carlson, Liu et al. 2005, Lakshman, Kim et al. 2010, Kureshi, Funderburgh et al. 2014). ALDH1A1 is a common associated marker for human keratocytes, however there was no commercial antibody that showed cross-reactivity to the canine protein (see Supplementary table S1). *ALDH1A3* is expressed in the murine cornea and is also required for corneal maintenance (Stagos, Chen et al. 2010, Kumar, Dolle et al. 2017). Similar to human studies, the chapter demonstrated that the gene expression levels of stem cell markers were down-regulated and keratocyte markers were up-regulated after 21 days of differentiation (Du, Funderburgh et al. 2005, Park, Kim et al. 2012).

Canine CSCs continued to proliferate during the keratocyte differentiation process which might be driven by basic FGF (Hassell and Birk 2010). Dasei et al. 2014, demonstrated that bFGF containing media, in contrast to TGF β ,

resulted in a marked downregulation of α -SMA expression, collagen I, fibronectin, and loss of focal adhesions and stress fibers in adMSCs (Desai, Hsia et al. 2014). Therefore, a trial of KDM without substituted bFGF was initiated, leading to stable cell numbers during the differentiation period. Although the absence of bFGF during the differentiation did not influence on keratocyte marker expression, it did lead to a significant increase in α -SMA gene expression and the induction of detectable levels of protein. In the injured cornea, keratocytes differentiate into myofibroblasts in response to TGF β 1 and will further undergo apoptosis (Jester, Petroll et al. 1995). To date, the reverse process to turn myofibroblasts into keratocytes has not been described and the mechanisms and underlying genetic regulation are not fully understood (Maycock and Marshall 2014). From a clinical perspective using α -SMA expressing cells *in vivo* need to be investigated carefully in future studies.

The limitations of this chapter are discussed in detail after each section accordingly. However, a focus should be the completion of the characterisation of central derived CSC in comparison to adMSC (flow cytometry and PBMC co-culturing in both) in future studies. Given the time and financial limitation of this project, the focus was kept on limbal derived CSC as these are described in more detail in the human-based literature.

Chapter 4:

Differentiation of adipose derived mesenchymal stromal cells into keratocyte-like cells

4.1. Introduction

Adipose derived mesenchymal stromal cells (adMSC) seem an ideal source for cell-based therapies: they are an abundant cell population of adult stem cells in adipose tissue, which are minimally invasive to retrieve. The isolation and culturing method is well established, they can be differentiated into multiple lineages, have immunomodulatory, anti-angiogenesis and anti-inflammation capacities, which seem ideal for corneal reconstruction (Yi and Song 2012, Mansoor and Ong 2019)(see details in 1.5).

Canine MSCs seem therefore also an ideal source for cell-based therapies in dog corneas, considering that canine CSC, as characterised in the previous chapter, would still require the necessity of donor corneas and these cells showed relatively limited expansion capacities

Veterinary ophthalmology related studies are limited but include treatment of immune-mediated KCS and immune-mediated keratitis in horses (see 1.8.D).

In vitro studies of canine adMSC differentiated into keratocyte-like cells are not available in the literature. Hence, this chapter aimed to study canine adMSC and their response to keratocyte differentiation protocols *in vitro*.

4.2. Materials and methods

AdMSCs were differentiated in CSSC media for 7 days and KDM, or only in KDM, for 21 days. The differentiated cells, adipose derived mesenchymal stromal cell derived corneal stromal cells (adMSC-CSC), adipose derived mesenchymal stromal cell derived corneal stromal cells differentiated into

keratocyte-like cells (adMSC-CSC-KDC) and adipose derived mesenchymal stromal cell derived differentiated keratocyte-like cells (adMSC-KDC) were characterised by immunocytochemistry and qPCR. The qPCR data of undifferentiated adMSC were established, where as immunocytochemistry on the undifferentiated adMSCs has been already described (see 3.3.7 Limbal and central derived CSCs have mesenchymal stromal cell characteristics

The general methods of cell culture are described in chapter 2.2 Cell culture. The materials used were cryopreserved adMSCs from three donors (dog # 16, 17, 18). The donor details are included in Table 2.1.

4.2.1 Cell culture of adipose-derived mesenchymal stromal cells

The detailed cell culture conditions of adMSC are described in 3.2.7, the media details are in Supplementary table S5.

4.2.2 Corneal stromal stem cell media

AdMSC were either cultured in KDM or in CSSC media before the keratocyte differentiation in KDM to determine whether this additional step would have a positive impact on keratocyte-like cell expression. The results were then compared based on qPCR data. The media details are described in detail in the Supplementary table S4.

4.2.3 Keratocyte differentiation of adMSC: culture condition

The cell culture conditions were established similar for CSC undergoing keratocyte differentiation (see 3.3.10). First the seeding densities with and without substituted bFGF in a biological triplicate (donor # 16-18) were

evaluated. Secondly, to enhance the potential towards keratocyte-like cell expression, adMSC were pre-cultured in CSSC media for 7 days and then followed by KDM for 21 days.

The following cell culture differentiation experiments were performed using a seeding density of:

1. 1×10^4 cells/cm²
2. 1×10^2 , 1×10^3 , 5×10^3 cells/cm²
3. KDM supplemented with (+) and without (-) bFGF, seeding density: 1×10^3 , 2.5×10^3 , 5×10^3 cells/cm²
4. Pre-culture in CSSC media (7 days), KDM supplemented with +/- bFGF, seeding density: 2.5×10^3 cells/cm² (21 days)

4.3 Results

4.3.1 AdMSC-KDC show keratocyte-like morphology and form a cell syncytium. The cell expansion of adMSC-KDC is influenced by the seeding density and bFGF.

Canine adMSC started to elongate and orient to each other in a line or grid formation after 2-3 days in KDM, which progressed more extensively over the following 8-10 days. Cell expansion continued during the differentiation period and was influenced by the seeding number. When using a seeding density of 5×10^3 and 1×10^4 cells/cm², cells started to form cell aggregates, or cell sheets, which began to contract and dehisced after 10-14 days (Figure 4.1). To enhance the potential for keratocyte-like cell expression, adMSC were pre-cultured in CSSC media for 7 days. The MSC cell morphology changed to a smaller and polygonal morphology similar to CSC within 7 days (Figure 4.1).

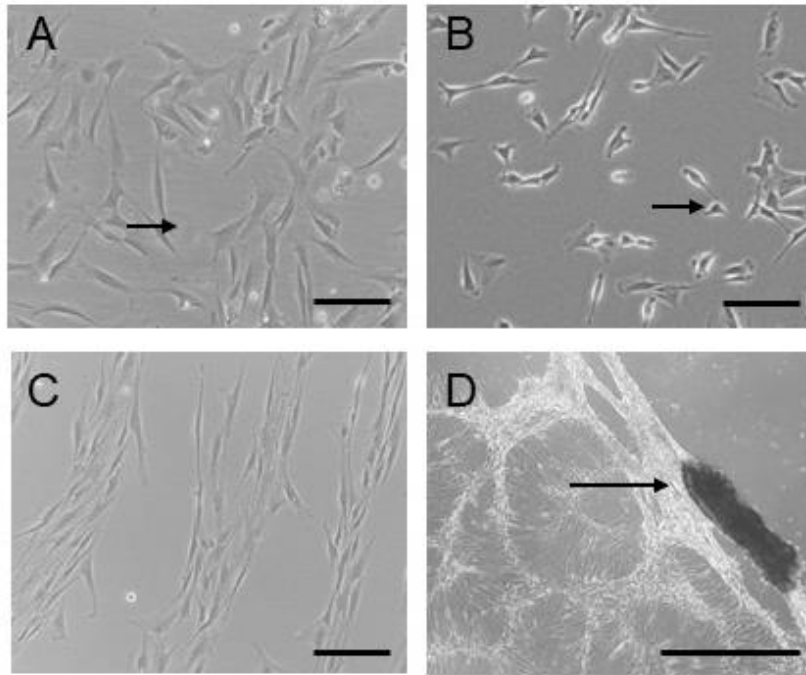


Figure 4.1 Change of cell morphology and cell orientation of adipose derived mesenchymal stromal cells (adMSC) cultured in corneal stem cell media (CSSC) followed by keratocyte differentiation media (KDM)

Phase-contrast images (A) adMSC with spindle cell morphology (black arrow). (B) Cells changed to a polygonal cell morphology after 7 days in CSSC media (black arrow). (C) A line formation of elongated cells was noted after 2 days in KDM (+bFGF), with expanding, elongated cells forming a grid pattern with intercellular connections. (D) If not passaged, the cells further expanded and formed a contracting cell sheet which dehisced after 21 days in KDM (note the detached, dark area of the cell sheet highlighted by the black arrow). This cell culture experiment was performed in a biological triplicate (donor # 16-18). Abbreviation: bFGF, basic fibroblast growth factor; Scale bar: 20 μm , D: scale bar: 500 μm

Following this preliminary testing, the effect of bFGF on cell expansion was evaluated. AdMSCs were seeded at different densities in KDM media with and without supplemented bFGF. It was noted that KDM supplemented with bFGF supported an increased cell proliferation rate. This was noted to be significantly higher with higher seeding numbers, 2.5×10^3 cells/cm² compared to 1×10^3 cell/cm² (T-test, $P = 0.0041$) (Figure 4.2).

Secondly, adMSC differentiated in CSSC and KDM (+bFGF) seeded at 2.5×10^3 cells/cm² resulted in stable cell attachment to reach the 21-day differentiation period. However, seeding densities of 5×10^3 cells/cm² or higher were lost due to cell sheet formation and dehiscence after 10 to 12 days (Figure 4.1). Comparing adMSC-KDCs to CSC-KDCs, adMSC-KDCs were less stellate and retained elongated, more fibroblastic morphology (Figure 4.3 A, C).

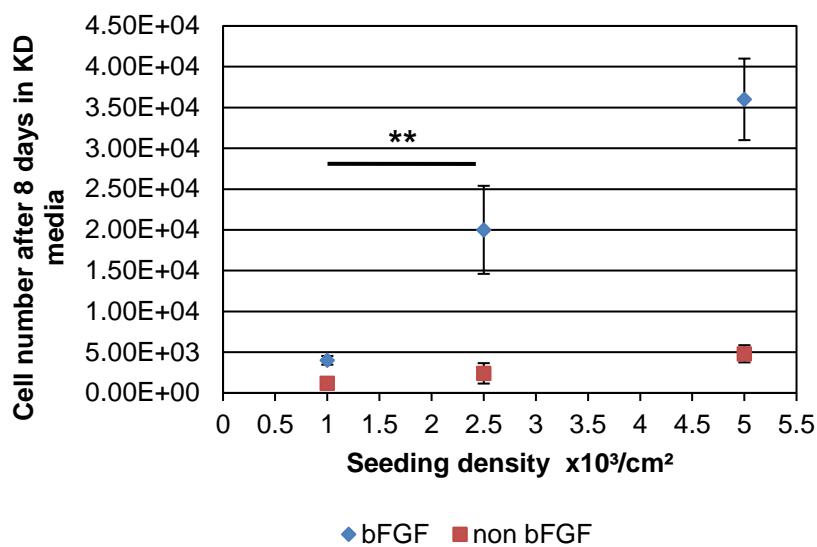


Figure 4.2 Influence of the seeding density and basic fibroblastic growth factor on cell expansion of adipose derived mesenchymal stromal cell differentiated keratocytes (adMSC-KDC)

The graphic illustrates the mean cell number (\pm SD) of canine adMSC pre-cultured in CSSC media (7 days) and differentiated in KDM (8 days) with and without supplemented bFGF seeded at three different densities. The cell expansion of cells seeded at 2.5×10^3 cells/cm² was significantly higher than in cells seeded in 1×10^3 cells/cm² in KDM +bFGF (T-test, $P=0.0041$). Cells differentiated in KDM (-bFGF) did not expand. This was performed in a biological triplicate (donor # 16-18). Abbreviation: KD, keratocyte differentiation; ** $p < 0.01$

Cell proliferation was nearly absent in non-bFGF containing media. The cells oriented into a line or grid formation which was evident after 10 days. In contrast to CSC-KDC, adMSC derived cells exhibited a fibroblastic

appearance during the entire differentiation period (21 days) (Figure 4.3). Likewise, cell loss and signs of degenerated cells in the third week in KDM without bFGF was noted (Figure 4.3 B).

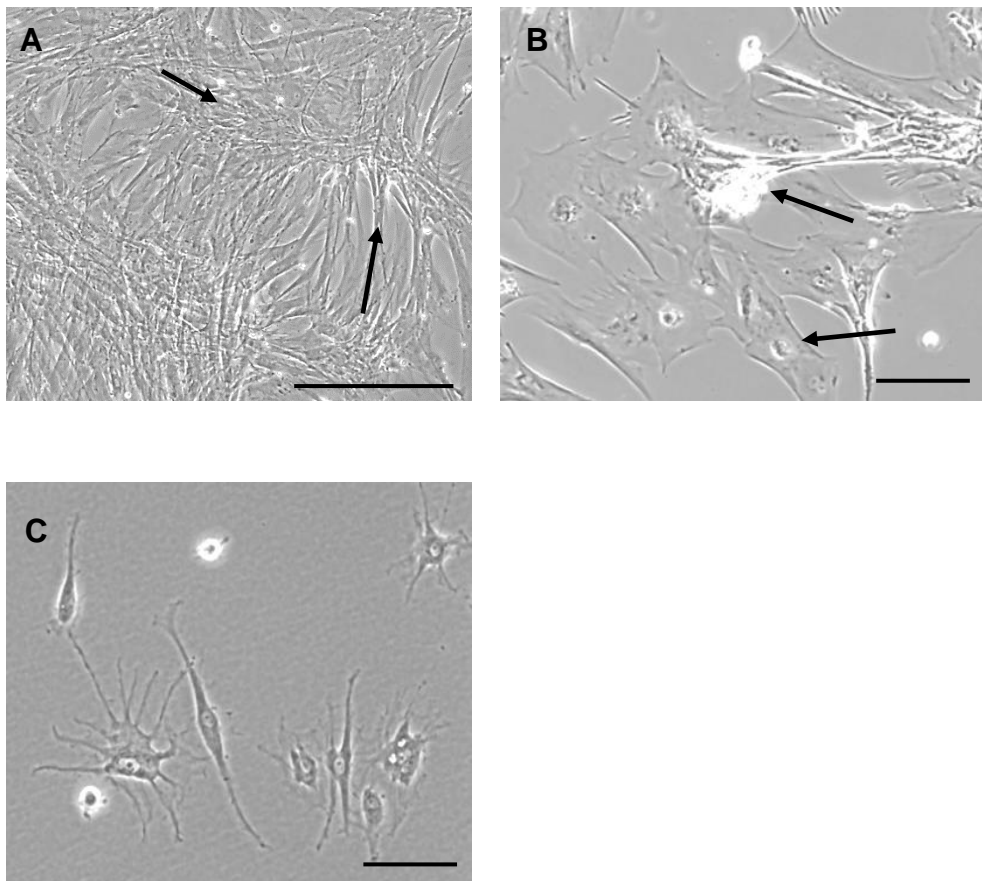


Figure 4.3 The cell morphology of adipose derived MSC differentiated keratocytes (adMSC-KDC) cultured in keratocyte differentiation media (KDM) in comparison to limbal CSC-KDC

Phase-contrast images of adMSC-KDC (day 21) differentiated in KDM +bFGF (A), showed an elongated, spindle cell morphology forming an interconnected syntyium of cells (black arrows) and high cell density. Cells differentiated in KDM without bFGF (B), stayed fibroblastic with increase of cell loss (black arrow with detached clumps of cells). (C) That was in contrast to CSC-KDC, which expressed a stellate cell morphology and stayed attached during the 21-day differentiation period. This was performed in a biological triplicate (#16-18). Scale barr:, (A) 20 μ m; (B), (C) 10 μ m

At this stage of the study, it was decided to characterise only cells differentiated in KDM with substituted bFGF via immunocytochemistry and qPCR.

4.3.2 Pre-culturing adMSC in CSSC media up regulates *Keratocan* and *Lumican* expression. AdMSC respond similar to the keratocyte differentiation than corneal stromal cells but retain myofibroblastic expression.

AdMSC were either pre-cultured in CSSC media and then differentiated in keratocyte differentiation media, or adMSC were directly differentiated in KDM.

Pax6 protein was not detected in undifferentiated adMSCs (Figure 3.19.C.II) but following culture in CSSC media for 7 days (Figure 4.4). MSC protein markers CD90, CD73 and N-cadherin along with α -SMA were expressed after one week in CSSC media (Figure 4.4).

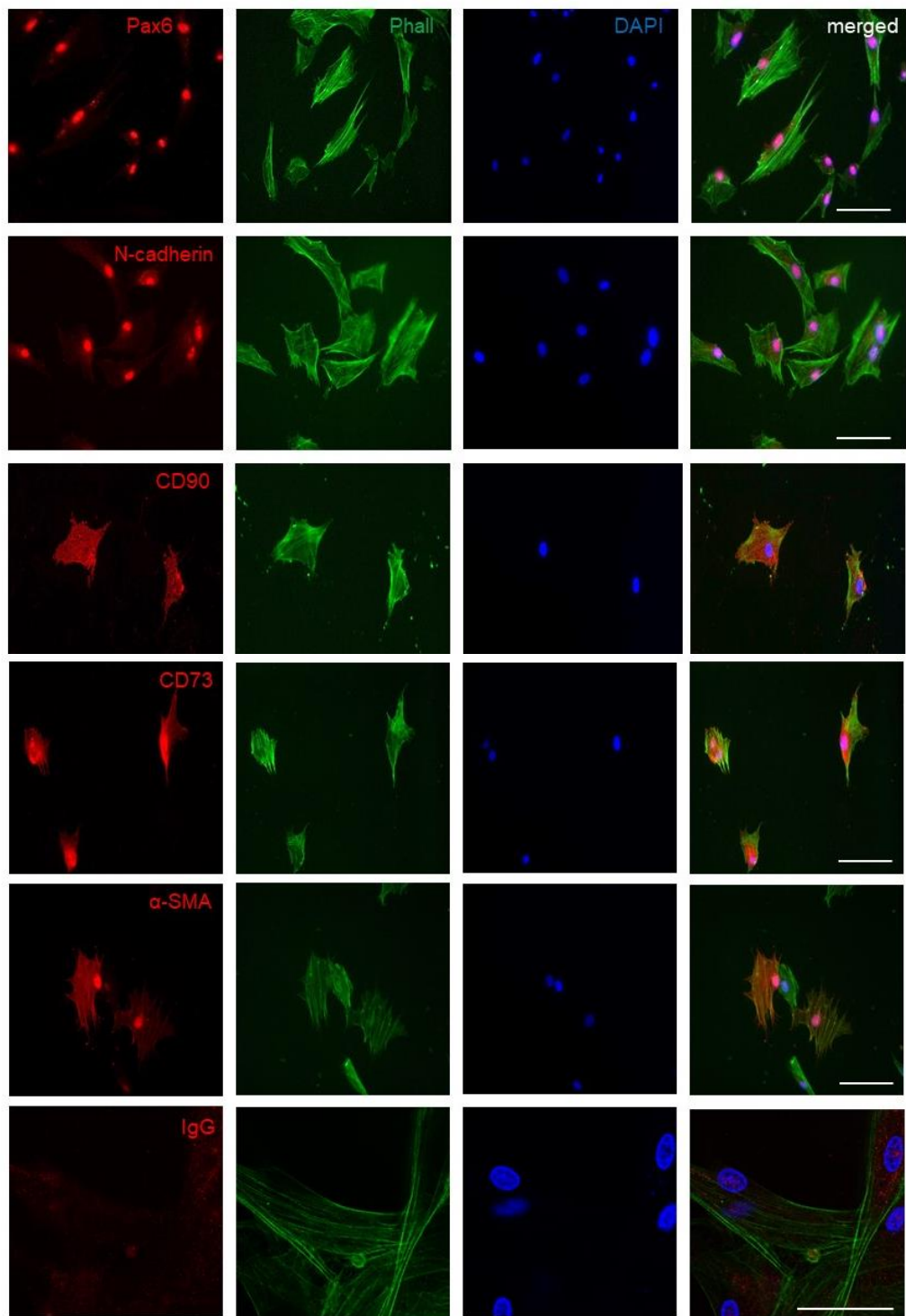


Figure 4.4. Adipose derived MSC cultured in corneal stromal stem cell media (CSSC). Immunocytochemistry demonstrates the positive nuclear marker expression of Pax6 in adMSC-CSC, which was not evident in adMSC (compare Figure 3.19.C.I). N-cadherin expressed a nuclear marker expression. CD90, CD73 and α -SMA was expressed similar to undifferentiated adMSC. This was performed in a biological triplicate (donor #16-18). Abbreviations: IgG, immunoglobulin G (negative contro), Phalloidin (Phall) was used to stain the cytoskeleton (F-actin) and DAPI as nuclear marker. Scale bar: 20 μ m

Keratocyte-like differentiated adMSCs, pre-cultured in CSSC media expressed the keratocyte associated protein marker Lumican, Keratocan and ALDH1A3 (Figure 4.5A), as well as CD90 and α -SMA. Following the keratocyte differentiation, the protein expression of Pax 6 was not evident anymore (Figure 4.5 B).

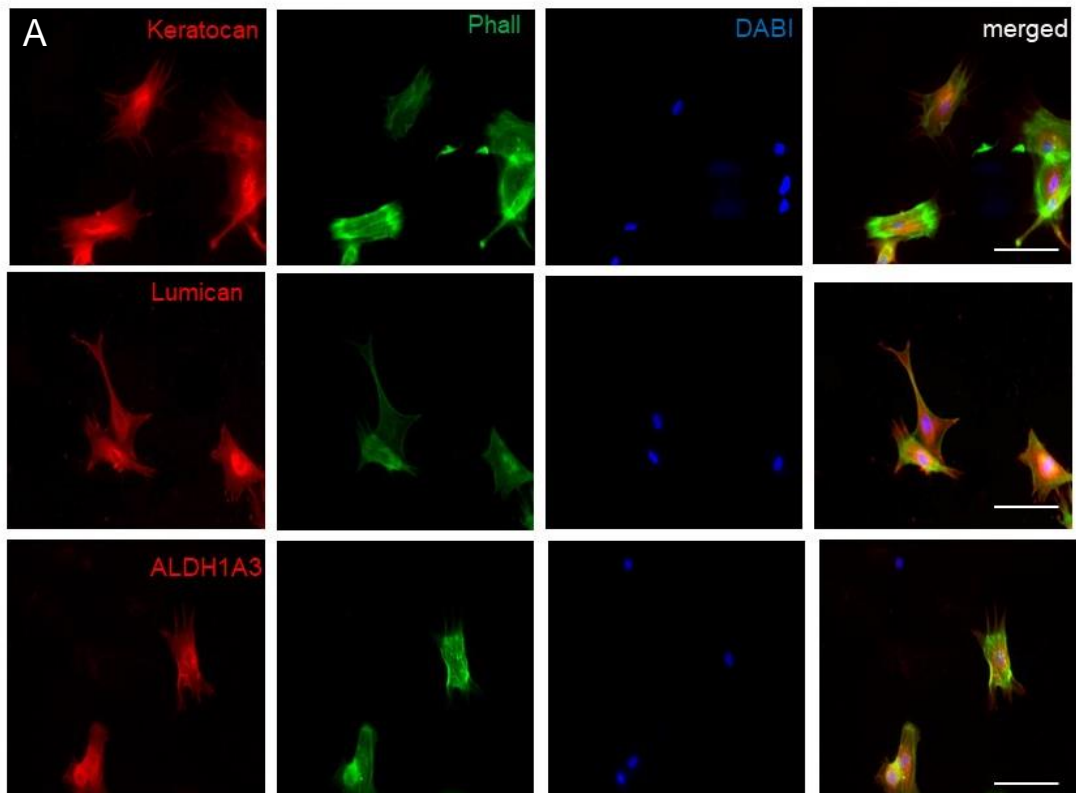


Figure 4.5.A Adipose derived MSC cultured in corneal stromal stem cell (CSSC) followed by keratocyte differentiation media

Immunocytochemistry of adMSC-CSC-KDC revealed positive protein expression of the keratocyte markers Lumican, Keratocan and ALDH1A3. This was performed in three independent biological replicates (donor # 16-18). Abbreviations: IgG, immunoglobulin G (negative contro), Phalloidin (Phall) was used to stain the cytoskeleton (F-actin) and DAPI as nuclear marker. Scale bar: 20 μ m

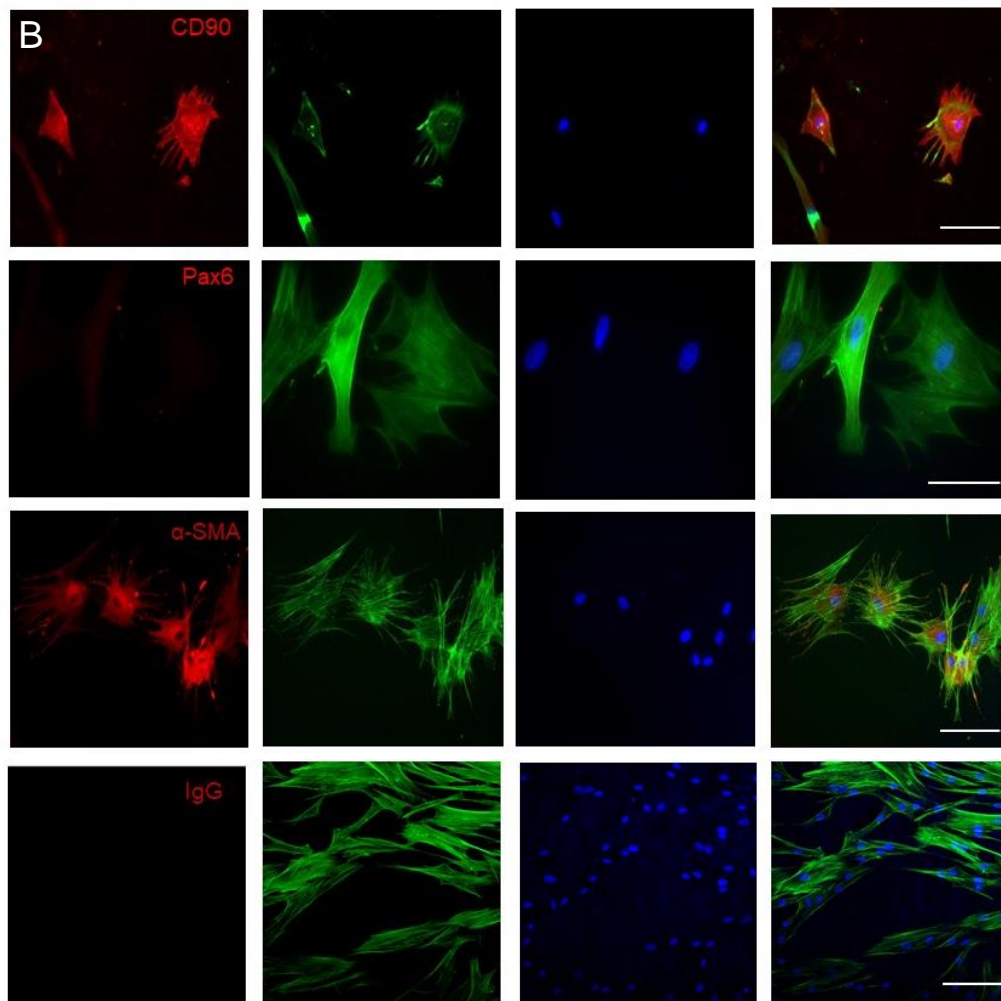


Figure 4.5.B Adipose derived MSC cultured in corneal stromal stem cell (CSSC) followed by keratocyte differentiation media (KDM)

Immunocytochemistry of adMSC-CSC-KDC revealed positive protein expression of CD90 and α -SMA whereas Pax was not expressed (compare Figure 4.4). This was performed in three independent biological replicates (donor #16-18). Abbreviations: IgG, immunoglobulin G (negative control), Phalloidin (Phall) was used to stain the cytoskeleton (F-actin) and DAPI as nuclear marker. Scale bar: 20 μ m

Pax6 gene expression demonstrated that adMSC cultured in CSSC media showed a trend of upregulation (Tukey's test, $P= 0.066$) and there was a trend of *Pax6* downregulation after the keratocyte differentiation (Tukey's test, $P= 0.091$). There was also a trend that *N-cadherin* (Tukey's test, $P= 0.068$) gene expression was downregulated after the keratocyte differentiation (without CSSC media) (Tukey's test, $P= 0.068$). The gene

expression of *Keratocan* in adMSC was significantly upregulated after the keratocyte differentiation (Tukey's test, $P= 0.045$) and in cells pre-cultured in CSSC media (Tukey's test, $P= 0.049$). *Lumican* was significantly upregulated (Tukey's test, $P= 0.031$) after the CSSC and KD differentiation (Figure 4.6). The keratocyte differentiation without CSSC media had no impact on the expression levels of ALDH1A3 and α -SMA (ANOVA, $P> 0.05$). Overall, adMSC-KDCs have keratocyte-like properties but retain myofibroblastic expression.

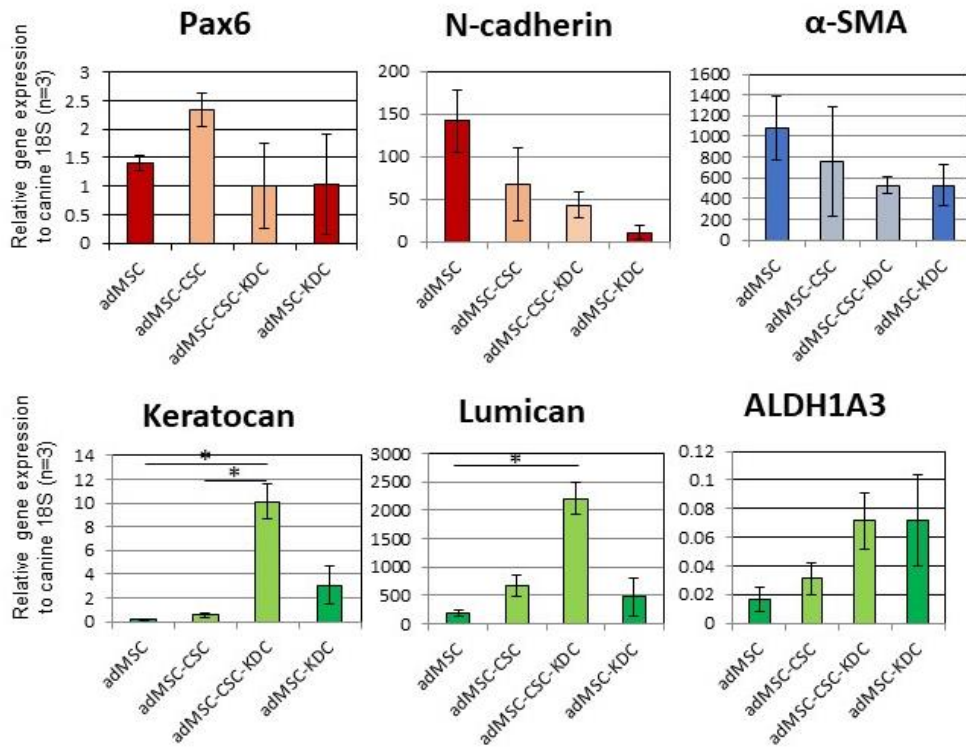


Figure 4.6 Relative gene expression level of adipose derived MSCs with and without pre-culturing in CSSC media followed by keratocyte differentiation

The graphs demonstrating the mean (\pm SE) relative gene expression levels of Pax6, N-cadherin, α -SMA, Keratocan, Lumican and ALDH1A3 to canine 18S in adMSCs +/-pre-cultured in CSSC and keratocytes differentiation media. Keratocan was significantly upregulated after the keratocyte differentiation (Tukey's test, $P= 0.045$) in cells pre-cultured in CSSC media (Tukey's test, $P= 0.049$). Lumican was significantly upregulated after the CSSC and KD differentiation (Tukey's test, $P= 0.0031$). Error bars represent the standard error of three biological replicates. Abbreviations: *, $P<.05$; n, number of biological replicates (donor # 16-18); CSC, corneal stromal cell; KDC, keratocyte differentiated cell

When comparing the level of relative gene expression of adMSC-KDCs or adMSC-CSC-KDCs to the tissue-specific corneal derived stromal cells (CSC) and their differentiated cells (CSC-KCDs), a similar response to the keratocyte differentiation could be observed. Overall, there was a trend that keratocyte associated genes were upregulated, and Pax6 and N-cadherin

were downregulated. The relative expression level of *ALDH1A3* in CSC-KDC was 100 times higher than in adMSC-KDCs, also the *Keratocan* expression level was 17 times higher in CSC-KDCs. Interestingly, this is in contrast to the level of relative gene expression of *Lumican* after the keratocyte differentiation, which reached similar levels in CSC-KDCs and adMSC-CSC-KDCs, but not in adMSC-KDCs (Figure 4.7). *Pax6* was 3.5 times higher expressed in CSC-KDCs compared to adMSC derived keratocyte-like cells. The opposite holds for α -*SMA*, which was about 19 times higher expressed in adMSC compared to CSC, and there was a trend of downregulation after keratocyte differentiation, but the expression was still 8 times higher in both, adMSC-CSC-KDCs and adMSC-KDCs, than in CSC-KDCs (Figure 4.7).

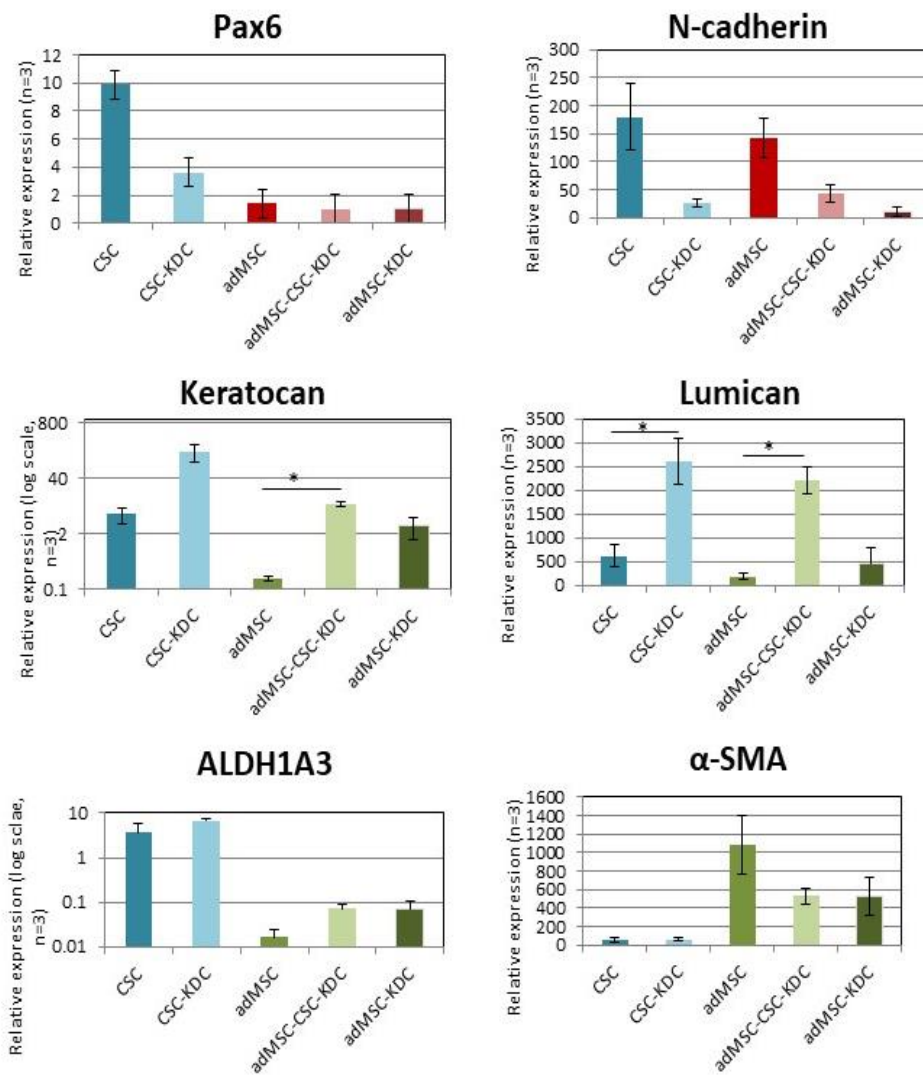


Figure 4.7 Comparison of the relative gene expression level of keratocyte, stem cell genes and α -SMA of corneal and adMSC derived cells and their keratocyte-differentiated cells

The graphs compare the mean relative gene expression normalised to the housekeeping gene 18S of Pax6, N-cadherin, Keratocan, Lumican, ALDH1A3 and α -SMA of corneal stromal cells (CSCs) and adipose derived MSCs (adMSCs) and their keratocyte differentiated cells (KDC). Error bars represent the standard error of the mean of three independent biological replicates (CSC donor# 11-13; adMSC donor # 16-18). Abbreviations: *, $P < .05$; n, number of biological replicates

In summary, cells with a seeding density of 2.5×10^3 cells/cm² reached the differentiation protocol of 7 days in CSSC media and 21 days in KDM without cell detachment or cell sheet formation. BFGF increased the cell expansion but was an essential factor to reduce a fibroblastic cell morphology. Culturing adMSC in CSSC media before exposure to keratocyte differentiation media has had a significant impact on the final level of *Keratocan* and *Lumican* expression. The same holds true for *Pax6* where a trend of up- and downregulation was observed in response to exposure to CSSC media. Overall, the relative keratocyte genes expression (apart from ALDH1A3) was upregulated but less compared to corneal derived CSC differentiated KDCs. Before and at all stages of the cell differentiation α -SMA was expressed at the protein and gene level. AdMSC derived keratocytes had eight times higher levels of α -SMA than corneal derived KDCs. Overall, there is a high heterogeneity of cell response to the differentiation process.

4.4 Discussion

This chapter aimed to study canine adMSC and their response to keratocyte differentiation *in vitro* and to initiate basic research on whether these cells could serve as a potential source for a cell-based therapy in the future.

This was based on human studies that demonstrated human MSCs had the potential to differentiate into keratocyte-like cells (Arnalich-Montiel, Pastor et al. 2008, Du, Roh et al. 2010, Park, Kim et al. 2012, Dos Santos, Balayan et al. 2019). In this chapter preliminary data were presented that canine adMSC have the potential to differentiate into keratocyte-like cells *in vitro* but further in-depth studies are warranted in the future (including flow cytometry and PMC co-culture assays). Overall, the keratocyte differentiation response revealed only significant upregulation for keratocyte markers such as *Keratocan* and *Lumican*, otherwise trends than significant changes of up/downregulation were present. The cell response of the differentiation process was heterogen leading to high standard error in qPCR results which limits the interpretation of the results and further optimised studies are required in the future.

There is scientific evidence that various types of MSCs (bone-marrow, adipose-derived, dental pulp, umbilli cord) in humans, rabbits, and rats, independent of their origin, have similar response to be differentiated into a keratocyte-like phenotype *in vivo* while also exhibit immunomodulatory properties. The strongest evidence exists regarding expression of keratocytes markers were tested on null mutant animal models with MSC of different origin (Harkin, Foyin et al. 2015).

MSCs have the ability to secrete paracrine factors, for example vascular endothelial growth factor (VEGF), PDGF, HGF, and TGF β 1 (Harkin, Foyn et al. 2015, Alio Del Barrio and Alio 2018). The precise actions of corneal wound healing and different growth factors requires is still currently not known, however there is evidence that these factors inhibit keratocyte apoptosis, promote cell migration, and up regulate ECM genes expression in keratocytes (Jiang, Liu et al. 2017). Human adMSCs differentiated in keratocyte differentiation conditions express collagens and corneal-specific ECM *in vitro*. This gene expression (keratocan, keratan sulphate, ALDH3A1) was quantitatively similar to CSSC when cultured 3D (pelett) (Du, Roh et al. 2010). This is in contrast to the result of the present study were only *Lumican* reached a similar gene expression level to CSC derived keratocytes (see Figure 4.7).

Also *in vivo* studies of human adMSC-KDCs transplanted intrastromally in rabbit corneas have shown to express collagen I and V (the main components of corneal extracellular matrix), keratocan and ALDH, without inducing an immune or inflammatory response (Arnalich-Montiel, Pastor et al. 2008). This was similar reported by Harkin and co-workers (2015) (Harkin, Foyn et al. 2015).

In this chapter the seeding number was first established and the differentiation protocol to derive keratocyte-like cells from canine adMSC. The same KDM containing ascorbic acid and bFGF was used for CSC derived keratocytes (see Supplementary table S2).

Rapid cell proliferation, cell sheet formation with contraction and dehiscence of adMSC in keratocyte differentiation media, led to the trial not to supplement bFGF to KDM. Even more than with CSCs, bFGF was found to have a crucial role as a proliferating factor on adMSC. KDM containing bFGF supported an increase in cell number of 7-10-fold within 8 days, whereas KDM without bFGF showed nearly stable cell numbers. This is following the description by Hassell and Birk 2010, describing bFGF as a proliferating factor on keratocytes but further information on human MSC research is lacking. Likewise, the presence or absence of bFGF in culture conditions of human CSSC-derived keratocytes did not affect the expression of keratocyte markers (Hassell and Birk 2010). This was not further evaluated in the present study, given the fibroblastic and degenerative morphological change of cells cultured in KDM lacking bFGF. This might be of interest for future studies, especially the potential difference in gene expression of α -SMA, which is a major component of myofibroblasts.

Pre-differentiated adMSC in CSSC media gave rise to the morphological change of adMSC into more polygonal-shaped cells, similar to CSCs. The protein and a trend of *Pax6* upregulation in CSSC media and then downregulation following subsequent keratocyte differentiation. This observation cannot be explained at this stage, but the transcription factor Pax6 is one the most influential factor for the ocular development and is retained to certain degree by mature corneal cells (Harkin, Foyn et al. 2015). This change did not have a longer-lasting influence, as with or without pre-culturing in CSSC media, a similarly low level of Pax6 expression was

observed in both, in adMSC-KDCs and adMSC-CSC-KDCs. There is no literature available to compare this observation.

The morphological changes found during the keratocyte differentiation, with a more stellate cell shape and the fact the interconnecting network of cells was formed, is a typical feature of keratocytes (Lakshman, Kim et al. 2010). This was potentially driven by several factors. KDM contains ascorbic acid, which is an essential factor for the stratification of cells, the collagen I synthesis and the hydroxylation of proline and lysine (Hassell and Birk 2010). The absence of the serum in KDM is essential in keratocyte maintaining culture systems, as serum is a driving factor to fibroblast and myofibroblast differentiation (Beales, Funderburgh et al. 1999). Overall, the canine adMSC-KDCs retained a more fibroblastic appearance in comparison to CSC-KDCs. Future studies are warranted on a molecular level, but also the mechanical phenotypes comparing both cell types in 3-D culture for example with dynamic imaging using differential interference contrast microscopy.

Lakshman and co-workers 2010 cultured rabbit corneal keratocytes and fibroblasts transplanted in a collagen matrix. Then cells were imaged using 3-D optical section via laser confocal microscopy dynamic imaging with differential interference contrast microscopy. They then modeled the ECM deformations. This technique provided a quantitative investigation of the morphological, cytoskeletal and contractile changes of rabbit corneal keratocytes (i.e. their mechanical phenotype) in a 3-D environment (Lakshman, Kim et al. 2010).

The influence of CSSC-media on the differentiation process had a significant impact on *Keratocan* and *Lumican*, two essential keratocyte markers. Both keratocyte-like differentiated cells, whether pre-cultured with/without CSSC media, expressed the keratocyte protein marker Lumican, Keratocan and ALDH1A3.

Lumican is expressed in many different tissues throughout the mammalian body and is essential in the maintenance of corneal transparency. Lumican is an extracellular matrix glycoprotein modified with keratan sulphate and is one of the major corneal proteoglycans (Carlson, Liu et al. 2005). That could also hold for the adMSC-CSC-KDCs, as *Lumican* gene expression was nearly as high as in corneal derived KDCs (CSC-KDCs) but the keratocan expression was 10 times lower compared to CSC-KDCs. Longer culture times might have a positive impact on the *Keratocan* expression and should be considered in future studies.

Keratocan and ALDH1A1 are important in the maintenance of corneal transparency (see 1.1.C). The present study has measured ALDH1A3, one of the ALDH1-family of corneal aldehydes because the ALDH1A1 antibody demonstrated non-specific binding in canine tissue and cells (Jester 2008). Upregulation of *Keratocan* and *Lumican* but not *ALDH1A3*-mRNA strengthens the argument that these cells may be differentiating into keratocytes-like cells (Du, Roh et al. 2010, Park, Kim et al. 2012). Although these are markers of keratocyte phenotype, the keratocyte function is based on highly organized, transparent extracellular matrix (ECM) in the corneal stroma (see 1.1.C). Thus, further 3D investigations are required in the future

which might also enhance the *ALDH1A3* expression. Human CSSCs when grown on an appropriate 3D matrix can produce a highly organised tissue with enhanced keratocyte gene expression (Wu, Du et al. 2012).

At this stage, it can be only speculated whether the combination of growth factors EGF, PDGF, as substituted in CSSC media, and bFGF in KDM, are essential to enhance the gene expression of *Keratocan*. It is described that factors as FGF, TGF- β , PDGF, IGF, EGF regulate keratocyte differentiation, migration and expression of *Lumican* and *Keratocan* (Kim, Lakshman et al. 2010, Lakshman and Petroll 2012).

The impact of CSSC media on stem cell markers needs to be further investigated. However, the present study has shown that CD90 and CD73 are still expressed on a protein level in adMSC-CSCs, but comparative gene expression and other stem cell markers (*ABCG2*) and pluripotent factors Sox2, OCT4 could be further investigated (Takemitsu, Zhao et al. 2012).

The role of N-cadherin and stemness in adMSCs and their differentiated keratocytes requires further investigation. In the present study nuclear protein marker binding were observed, which can not be fully explained. McCrea and colleagues (2015) describing in their review article, that “cadherin intracellular binding partners also localise to the nucleus”. It is hypothesized that “a cadherin-dependent, membrane-proximal event may “prime” β -catenin for nuclear signaling. N-cadherin expression in cortical neural progenitors favored stemness through maintaining β -catenin signaling. Reduction in N-cadherin levels led to premature differentiation of neurons and their migration away from the stem cell niche” (McCrea, Maher et al. 2015).

Contrary to Park et al. 2012 where α -SMA expression was lost in human bone marrow MSC-derived keratocytes, the canine cells of the present study maintained the expression of α -SMA through all stages of the differentiation process (Park, Kim et al. 2012). Although, the fold change of gene expression was not significantly reduced during the differentiation process and the expression level was 6 times higher than in CSC-KDCs, which seems a novel finding in dogs. The reduction of α -SMA could be influenced by bFGF in KDM, as FGF2 has been shown to reduce expression of α -SMA in keratocyte derived myofibroblasts, but this was not confirmed by the present data (Maltseva, Folger et al. 2001).

The high level of α -SMA is a concern in view of cell-based therapies given α -SMA is a major component of myofibroblasts producing non-organised ECM in corneal wound healing subsequently leading to scar formation (see Chapter 1.2.2 Corneal fibrosis). Further 3D studies to establish the relevance of α -SMA expression for *in vivo* clinical translation or *in vitro* disease modelling is required. Triple immunophenotyping to further characterise these cells as myofibroblasts should include Vimentin and Desmin stains. Likewise, optimising the culture conditions for canine adMSC differentiation and comparing with bone-marrow derived MSC is an essential future step (Harking, Foyn et al. 2015, Park et al 2012). Cen and co-workers 2021 seeded rabbit BM-MSC in a decellularised *in vivo* cornea model and showed promising results with less neovascularisation 3 month post-surgery (Cen, You et al. 2021).

The immunomodulatory effects of human and canine adMSCs are another important aspect of their potential use in cell-based therapy (see 1.6). Future studies are required to further assess whether the immune suppression holds also true for adMSC derived keratocytes in form of PBMC co-cultures and suppression assays.

In conclusion, our results provide preliminary results documenting the potential of canine adMSCs to differentiate into a keratocyte phenotype *in vitro*. However, more detailed molecular characterisation, comparison to BM-MDSCs and 3D studies of the tissue formed by MSC will be necessary, to determine their potential to generate corneal ECM *in vitro*.

**Chapter 5:
Establishing a differentiation
protocol for canine induced
pluripotent stem cells into
keratocyte-like cells**

5.1. Introduction

IPSCs opened a new research field not only in human but also in the veterinary field. Methodology to derive ciPSCs has been established (Lee, Xu et al. 2011, Luo, Suhr et al. 2011, Whitworth, Frith et al. 2014, Baird, Barsby et al. 2015, Koh and Piedrahita 2015, Luo and Cibelli 2016, Goncalves, Bressan et al. 2017, Nishimura, Hatoya et al. 2017, Tsukamoto, Nishimura et al. 2018). (Details see 1. 7.1)

The following chapter is based on the NCC differentiation protocol of Fukuta et al. (2014) and Naylor et al. (2016). Naylor and colleagues (2016) established a chemically defined culture method to differentiate human iPSc into neural crest cells (NCC) (Chambers, Mica et al. 2016), and further into keratocyte-like cells free of a feeder cell system (Naylor, McGhee et al. 2016). There are no reports in dogs.

The keratocyte differentiation methods established in chapter 3 (CSC) and 4 (adMSC) were used to initiate keratocyte cell fate.

5.2. Materials and methods

5.2.1 Primary mouse embryonic fibroblast (MEF) cell culture and inactivation (feeder cells)

Cryopreserved primary MEFs ($2-3 \times 10^6$ cells/ vial) (Stem Cell institute, tissue culture facility, University of Cambridge) at passage 1 were expanded until passage 5, growth-arrested and stored in liquid nitrogen until use.

Briefly, following standard thawing procedures (see 2.2.2 Cryopreservation and thawing) $8.5-10000$ cells/cm² were seeded on 10 cm plates. Cells were observed daily, the media was changed every second day and cells were passaged when 60-70% confluent (passage seeding density: 8-9000 cells/cm²). Details of the media can be found in the Supplementary table S5.

Confluent cells were inactivated using Mytomycin C (Sigma-Aldrich) at a concentration of 10 µg/ml media and incubated for 2 h under standard culture conditions (5% CO₂, 37°C). The cells were then washed in PBS, trypsinised, pelleted (1000 rpm, 5min) resuspended in 1 ml culture media, a cell count was performed, and cells were frozen in 1 ml aliquots of 1×10^6 cells/ ml cells in 10% DMSO freezing media at -70°C before transferred into liquid nitrogen. When used, the inactivated MEFS (= feeder cells) were fast thawed and seeded onto a 6-well plate/vial of cells. (For details see in General materials and methods, 2.2.2 Cryopreservation and thawing). Feeder cells were incubated for 24h before seeding iPSCs.

5.2.2 Canine iPSC

Baird et al. 2015 established canine iPSCs (ciPSC) from adMSCs of one donor, which were used in this chapter (details find in 2.1 Canine tissue and ethics statement), (Baird, Barsby et al. 2015). Briefly, adMSCs were derived from subdermal adipose tissue and expanded under routine conditions (details see 3.2.6 Cell culture of adipose-derived mesenchymal stromal cells). Transfection was performed with plasmid vectors containing the human sequences of the Yamanaka factors (3 µg): pMXs.hOCT 4 (Addgene 17217), pMXs.hSox2 (Addgene 17218), pMXs.hKlf4 (Addgene 17219) and pMXs.hc-MYC (Addgene 17220). Green fluorescent protein PMX. GFP (Cell Biolabs, San Diego, CA, USA) was used to monitor the efficiency of the initial transfection and subsequently viral transduction of the canine cells.

In each transfection reaction, viral vectors were pseudotyped with the VSVg envelope protein by including 3 µg of pVPack-VSV-G (Agilent Technologies, Stockport, Cheshire, UK). To increase the transfection efficiency, lipofectamine 2000 and optimum media (both Invitrogen) were carried out according to the manufacturer's instructions. In total were three rounds of retroviral infection performed. Transduction efficiency (i.e. GFP expression) were calculated by the percentage of GFP-positive cells in a minimum of 10 random fields. 5×10^3 canine cells were plated onto 10 cm plates on feeder cells (MEFS) on day 4 after the last infection. The then formed cell colonies were manually picked and expanded up to 20 passages.

Details of the iPSC media are in the Supplementary table S6. A) Cell culture of ciPSC on a feeder system

Cryopreserved ciPSCs of one donor (# 19, passage 5-7), which were manually harvested from one 6-well plate, were thawed (fast thawing procedure) approximately one minute at 37°C in a waterbath, transferred in 10 ml of iPSC media, pelleted (1000 rpm, 5min) and resuspended in 12 ml of iPS media. Rho-associated kinase (ROCK) inhibitor (1 mM) (StemMACS Thiazovivin, Miltenyi Biotec, Bisley, Surrey, UK) was only added to the iPSC media for 24 h after the thawing procedure until the first media change, or when passaging the ciPSCs. A seeding density of approximately 10-15 small colonies were plated per well of a 6-well plate with pre-seeded feeders (MEF). One day after plating iPSC colonies the medium was changed daily.

Canine iPSCs were observed daily. After 2 days of first seeding ciPSC, colonies with fibroblastic morphology or colonies which were not fully attached were manually picked using a pulled Pasteur pipette. If necessary, the picking procedure was repeated daily. Slightly dome-shaped iPSC colonies with a high nucleous-to-cytoplasm ratio typical of ciPSC were left in place. Colonies were expanded until a diameter of approximately 1.5-2 mm was reached. The feeder cells were not used for more than 10 days. The colonies were mechanically passaged (every 5 to 7 days) using scalpel blade (No 10) with the help of an inverted phase contrast microscope (EVOS® XL Core Imaging System). One ciPSC colony was cut into 6-10 pieces, depending on the size. Only the central quadrants were used for passaging

(Figure 5.1). The description of ciPSC pieces and small colonies are used interchangeably in the following text.

CiPSCs were cultured for more than 10 passages with repeated free-thaw cycles were performed. Freezing media was composed of iPSC media containing 15% FBS and 10% DMSO.



Figure 5.1 Manual passaging of canine induced pluripotent stem cells (ciPSC) on feeder cell

Phase-contrast images of (A): ciPSC colony on inactivated MEFs (feeder cells), which were (B) manually cut in a grid formation with the help of a microscope. (C) Higher magnification of one piece (square) of small cells, which were manually passaged to expand into a larger colony. Scale bars: A: 1mm, B: 500 μ m, C: 200 μ m

B) CiPSC colony dissociation and a feeder-free coating system

In preparation for the differentiation of ciPSC into NCCs, ciPSCs were manually removed from the feeder cells and passaged on coated 6 well plate with either Geltrex® (Thermo Fisher) or FNC Coating Mix® (Athena ES). This was repeated 5 times as technical replicates per coating system. The ciPSC colonies were then cultured in iPSC media containing ROCK inhibitor (see under A) above) for 24 h before being changed to NCC induction media.

Geltrex® (15mg/ml) is a lactose-free dehydrogenase elevating virus (LDEV-Free) reduced growth factor basement membrane matrix in soluble form and

was extracted from murine Engelbreth-Holm-Swarm (EHS) tumours. The major components are laminin, collagen IV, entactin, and heparin sulphate proteoglycans. Depending on the application for the Geltrex® matrix different concentrations (i.e. thicknesses) can be used. In general, a protein concentration < 9 mg/mL (5 mg/ml was used in this chapter) does not form a gel and will only support the propagation and maintenance of pluripotency of primary cells in 2D systems (not suitable for 3D systems), which need a protein layer and not a protein matrix, i.e., thin gel method (non-gelling).

One Geltrex® vial (5 ml) was thawed on ice and diluted in cold DMEM/F12 to a stock concentration of 5mg/ml, aliquoted and frozen at -20°C until use. The stock solution was diluted to cover a surface area of 20 µg/ cm². The working volume for eachwell of a 6-well plate was 1 ml; therefore 36 µl Geltrex® stock solution per ml DMEM/F12 (Gibco) was added. The coated 6 well plate was incubated at 37°C for a minimum of 60 minutes before use.

Alternatively, the FNC Coating Mix® was used, which is a serum-free tissue culture reagent containing bovine fibronectin, collagen, and albuminates. Immediately before use, the 6-well plate was coated with 0.2 ml/ cm² FNC Coating Mix for 30 seconds at RT and the residual mix was removed before seeding the ciPSC colonies.

Small pieces of ciPSC colonies were dissociated to single cells using Accutase® (STEMCELL technologies, Cambridge, UK) or TrypLE Select® (Gibco). The influence of both cell detachment solutions was compared for relative cell survival (% of living cells). After two washes in PBS, automated

cell counts (T20 automated cell counter, BioRad) were performed. This was performed in technical triplicates per dissociation media.

The pieces of ciPSC colonies of one 6 well plate, were briefly washed in PBS, centrifuged (1000 rpm/ 5min) and dissociated into single cell using 300 μ l of pure Accutase® for 10, 15 and 30 minutes in the incubator under standard culture conditions. During this process the cell suspension was mixed 3 times, the reaction was stopped by adding 10 ml iPSC media and then centrifuged (1000 rpm, 5min). The same procedure was followed using TrypLE Select® (300 μ l) at RT, 5 minutes at 37°C and for 10min at 37°C, with regular mixing by pipetting.

Both single-cell suspensions were seeded on Geltrex®/ FNC Coating Mix® incubated in iPSC media containing ROCK inhibitor (see 5.2.2 A) above) for 24 h before the neural crest cell (NCC) differentiation was started.

5.2.3 Neural crest induction and keratocyte differentiation: culture condition and protocol

A) Seeding density

To establish culture conditions for the NCC-KDC differentiation, the optimal seeding density was determined. Firstly, representative cell counts of dissociated ciPSC colonies were performed, which were cultured on feeder cells of one well per 6 -well plate. The cell counts of 5 technical replicates (passages 10-16) were averaged \pm SD.

1. Single ciPSCs were seeded as: 1×10^3 , 1×10^4 and 1×10^5 cells/ cm^2 .

2. Pieces of ciPSC colonies per well (of a 6 well plate) were seeded as: 5-10 colonies, 20-30 colonies, or >30 colonies/ well.

B) Neural crest and keratocyte differentiation

The NCC differentiation protocol used in this chapter was based on the findings in human iPSC studies of Fukuta et al. 2014 and then further modified based on the results of Chamber et al. (2016) and Mendendez et al. (2011). The insulin concentration was adjusted according to Rhee et al. (2013) (Menendez, Yatskievych et al. 2011, Rhee, Choi et al. 2013, Fukuta, Nakai et al. 2014, Chambers, Mica et al. 2016). After the NCC induction, the cells were differentiated in CSSC and further differentiated in keratocyte differentiation media (see details of media components in the Supplementary table S4 and S2). The neural crest induction contained first 10 μ M SB431542 and 1 μ M CHIR99021 (referred to Media 1) for 8 days, this was increased to 20 μ M SB431542 and 2 μ M CHIR99021 (referred to Media 2) for 12 days in three technical replicates. The number of live cells and cell expansion (%) was compared. The total differentiation protocol was 41 days (Figure 5.2).

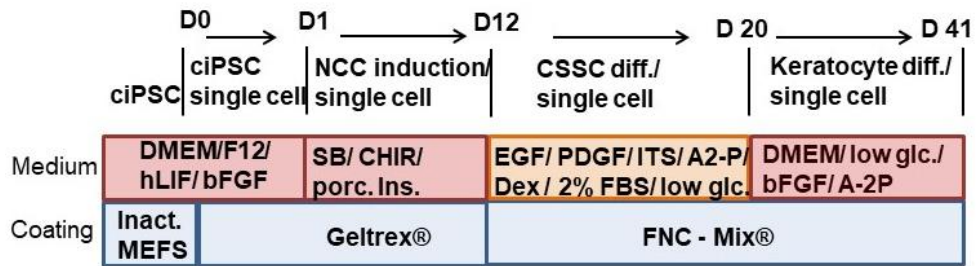


Figure 5.2 Differentiation protocol of canine induced pluripotent stem cells (ciPSC), neural crest induction (Media2), CSSC media culture and keratocyte differentiation

The schematic of the differentiation protocol: time in days (D), the basic contents of the media and the coating system used. Abbreviations: ciPSC, canine induced pluripotent stem cell; diff, differentiation; Inact. MEFS, inactivated mouse embryonic fibroblasts; hLIF, human leukemia inhibitory factor; bFGF, basic fibroblastic growth factor; SB, inhibitor of Activin/Nodal/TGF β signalling; CHIR, GSK3 β inhibitor; porc. Ins., porcine insulin; EGF, epidermal growth factor; bFGF, basic fibroblastic growth factor; ITS, insulin-transferrin-selenium; Dex, dexamethasone; low glc., low glucose; A-2P, L-Ascorbic Acid 2-phosphate

Single cells of ciPSC were passaged on a 6 well plate coated with Geltrex®, maintained on iPSC media with ROCK inhibitor for 24h (as described in 5.2.2.). Then cells were cultured in the NCC induction media for 12 days with a media change every second day (Supplementary table S7, Figure 5.2). When the cells became confluent, they were passaged into an FNC® coated T25 flask. After the NCC induction, the cells were cultured in CSSC media for 8 days before the keratocyte differentiation was started using KDM for 21 days. Depending on the cell expansion, the cells were passaged into T25 or T75 if necessary.

5.2.4 RNA extraction, qPCR and primers

The RNA was extracted from cells originating from iPSC single cells after the NCC induction step and at the end of the keratocyte differentiation.

In general, one 6-well plate of ciPSCs were required to get enough RNA to assess the change of gene expression via qPCR of the different differentiation steps.

The RNA was extracted after the CSSC media step and after completion of the keratocyte differentiation protocol (iPSC-NCC-CSSC and iPSC-NCC-CSSC-KDC).

RNA yields were in the range of 155–680 ng per sample. The 260/280 nm ratios ranged between 1.7 and 1.99 (Nanodrop, Thermofisher Scientific). The RNA was stored at -70°C until use.

Find details of RNA extraction (2.4.1) and qPCR (2.4.2) in the general materials and methods.

The primers P75 and Sox 10 were designed to determine the NCC gene expression and were tested on canine cerebellum RNA (Table 2.7).

To evaluate the external pluripotent gene expression, a repeated attempt was made to design or use canine NANOG and Rex1 primer from the literature (Luo, Suhr et al. 2011, Whitworth, Frith et al. 2014). The primers failed the efficiency tests on canine iPSCs and were without reliable results. Positive test tissue or cells from canine embryos were not available in the present study.

Therefore, a human OCT4 primer was used which showed partial overlap with the canine genome (Table 2.6).

5.2.5 Immunofluorescence staining

Immunocytochemistry (ICC) in a technical triplicate was performed on ciPSC cells off feeders (MEF) as single cells. after the NCC induction supplemented with 10 μ M SB431542/ 1 μ M CHIR99021 (media 1) and a concentration of 20 μ M SB431542/ 2 μ M CHIR99021 (media 2). ICC was performed on cells after the neural crest induction and CSSC media step (NCC/CSCs) and after completion of the different keratocyte differentiation protocols (KDC). The cells were not stained with Phalloidin (F-actin) because of the similar fluorescence excitation/emission (495/588nm) to green fluorescein protein (GFP: 489/530nm). The ciPSC used in this study were of passage 5-7 (see 5.2.2.A). The cells still exhibited GFP which was not downregulated at this passage frequency (see 5.2.2, see Supplementary Figure S4).

Four chamber slides (2.4 cm²/ well, Nunc™ Lab-Tek™ Chamber Slide System, soda glass, Fisher Scientific) were coated with FNC® Coating Mix. Differentiated NCC/CSSC and its KDCs were seeded in a density of 1x10⁴ cells/ chamber.

The chamber slides were then cultured under standard conditions for 2-3 days, before fixation with 3% PFA as described in 2.2.3 Cell observation and fixation. The details of the staining protocol are described in 2.3.1.

5.3 Results

5.3.1 Establishing a ciPSC-NCC differentiation protocol

A) Culture conditions

First, representative cell counts of ciPSC colonies cultured on inactivated MEFS (P10-16) of one 6-well plates, when considered ready to be passaged, had an average cell number of $1.73 \times 10^6 \pm 0.13$ cells (range: $1.62 - 1.9 \times 10^6$ cells).

The seeding density of $1 \times 10^3/\text{cm}^2$ or $1 \times 10^5 \text{ cells}/\text{cm}^2$ resulted in cell degeneration and cell detachment. The seeding density of $1-2 \times 10^4 /\text{cm}^2$ single cells or 20-30 small pieces of colonies per one well of a 6-well plate (= $4.4 - 6.6 \times 10^3$ cells) stayed cells attached and reached the end of the differentiation protocol (Figure 5.3).

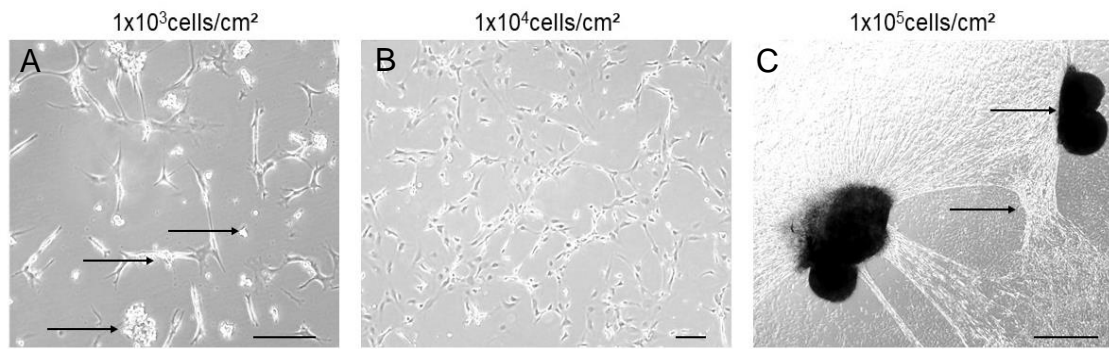


Figure 5.3 Comparison of different seeding densities for the neural crest induction

(A): The seeding density of $1 \times 10^3/\text{cm}^2$ induced pluripotent stem cells (iPSC) in neural crest cell (NCC) induction media at day 7 led to cell detachment and clumps of detached cells (black arrows). (C): The high seeding density of $1 \times 10^5/\text{cm}^2$ resulted in cell sheet formation and detachment (black arrow). (B): The seeding density of 1×10^4 cell/ cm^2 resulted in attached cells during the NCC differentiation protocol (12 days). This was performed in a technical triplicate. Scale bar: A,B: 20 μm ; C: 500 μm

Morphologically, the colonies were attached within 6h on both coating matrixes, Geltrex® and Fibronectin® coating. The cell dissociation trial compared the immediate effect of Accutase® (StemCell Technologies) and TrypLe Select® (Gibco). Incubating small pieces of colonies of one 6 well plate in Accutase® (StemCell Technology) for 30min at 37°C (pipetted every 10min) produced a single-cell suspension with scattered small cell colonies (10-20 cells). The automated cell count revealed 100% live cells in all three replicates. A shorter dissociation times led to clumping of cell colonies. Triple Select® (Gibco) had to be used for 10min at 37°C to reach colony dissociation and 77.3 ± 2.05 % live cells were counted. Shorter dissociation time of 5min at RT or 37°C was not efficient to achieve cell dissociation.

B) Higher concentration of Activin/Nodal/TGF β inhibitor (SB) and Wnt/ β -catenin activator (CHIR) changed the ciPSC-NCC cell morphology and marker expression of Sox10

In NCC induction media 1 (10 μ M SB431542 and 1 μ M CHIR99021), the cell morphology changed within few days to a neuronal/dendritic cell morphology. Furthermore, $11.3 \pm 1.24\%$ of cells were lost of which $71 \pm 1.4\%$ were live cells. SB431542 is a inhibitor of the transforming growth factor-beta superfamily type I, specifically the activin receptor-like kinase (ALK) receptors ALK4, ALK5, and ALK7. CHIR (CHIR 99021) induces the activation of Wnt/ β -catenin signaling (find more details in the general introduction 1.7.A). When SB431542 and CHIR99021 were increased in media 2 to 20 μ M SB431542 and 2 μ M CHIR99021, and longer culture days (8 to 12 days), the relative cell survival ($90.66 \pm 2.85\%$ live cells) and the cell expansion ($11.33 \pm 1.77\%$) was increased. The cell morphology changed to a stellate-polygonal cell morphology typically described for NCC (Figure 5.4) (Gericota, Anderson et al. 2014, Sakaue and Sieber-Blum 2015).

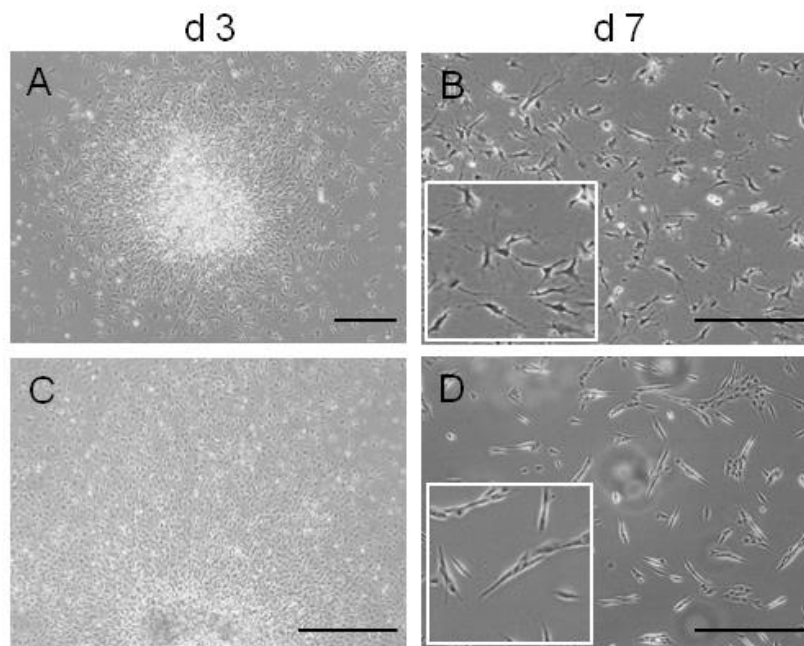


Figure 5.4 Change of cell morphology with increased concentration of SB431542 and CHIR99021

Phase-contrast images of (A) expanding cells from ciPS colonies on Geltrex® coating 3 days in neural crest induction containing 10 μ M SB431542, 1 μ M CHIR99021 and (B) CiPSC-NCCs at day 7 (passage 1). CiPS cells in colonies after 3 days (C) in neural crest induction Media containing 20 μ M SB431542, 2 μ M CHIR99021 and after 7 days and one passage (D). This was performed in a technical triplicate. Scale bar: A), C) = 500 μ m; B), D) = 50 μ m

Putative NCCs expressed a similar protein marker expression. The neural crest markers P75 was expressed in both media (Media 1 (lower) and Media 2 (higher SB431542 and CHIR99021), but Sox 10 was only expressed in NCCs cultured in Media 2 (compare Figure 5.5. A and Figure 5.6. A). P75 revealed nuclear and cytoplasmic marker expression in Media 1 and cytoplasmatic expression in Media 2. Pax6 was expressed in the nucleus and cytoplasm in both media (Figure 5.5 A, Figure 5.6.A). NCCs of both media expressed β Tubulin III, which is a microtubule element of the tubulin family found in neurons (Liu, Jin et al. 2015). Alpha- SMA was not expressed in either of the NCCs (Figure 5.5.B., Figure 5.6.B.).

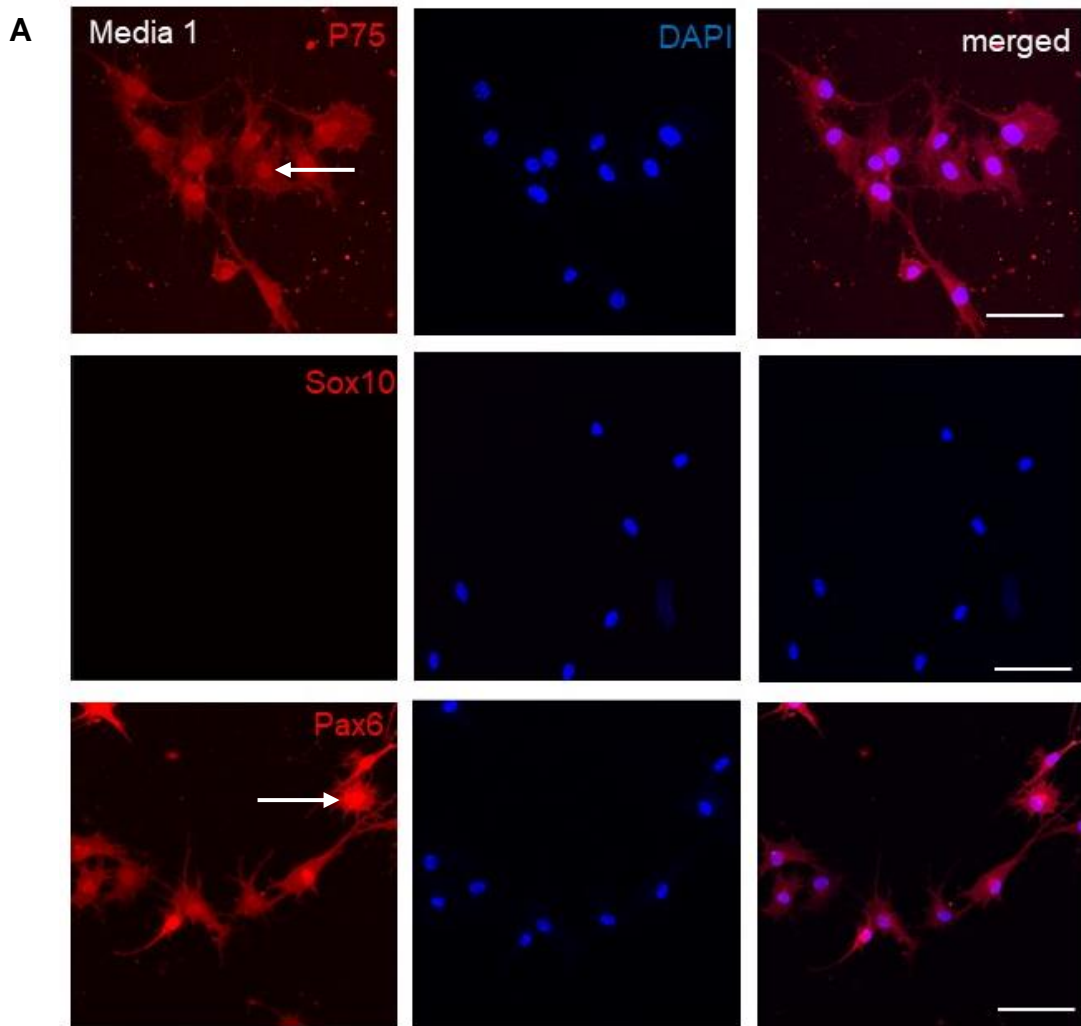


Figure 5.5.A Immunocytochemical staining results of ciPSCs induced neural crest cells (ciPSC-NCC) cultured in Media 1 (10 μ M SB431542, 1 μ M CHIR99021)

A: The neural crest marker P75 showed cytoplasmatic but also nuclear expression (white arrow) after 7 days in Media 1. The neural crest marker Sox 10 was not expressed. Pax 6 showed expression (cytoplasmatic and nuclear, white arrow) This was performed in a technical triplicate. Nuclei are shown by DAPI counter staining. Scale bar: 20 μ m

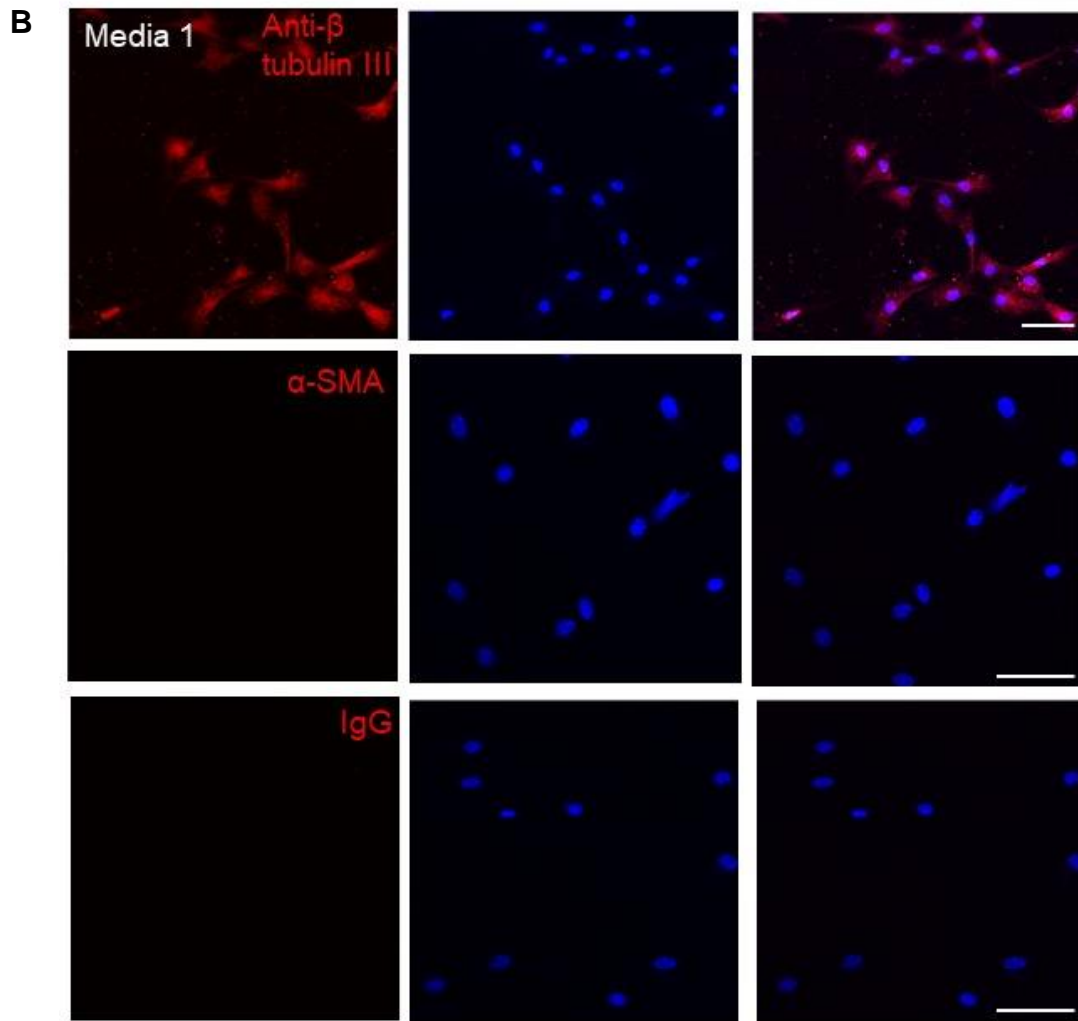


Figure 5.5.B Immunocytochemical staining results of ciPSCs induced neural crest cells (ciPSC-NCC) cultured in Media 1 (10 μ M SB431542, 1 μ M CHIR99021)

B: Anti β tubulin III was expressed but not α -SMA. This was performed in a technical triplicate. Nuclei are shown by DAPI counter staining. Abbreviation: IgG, immunoglobulin G (negative control). Scale bar: 20 μ m

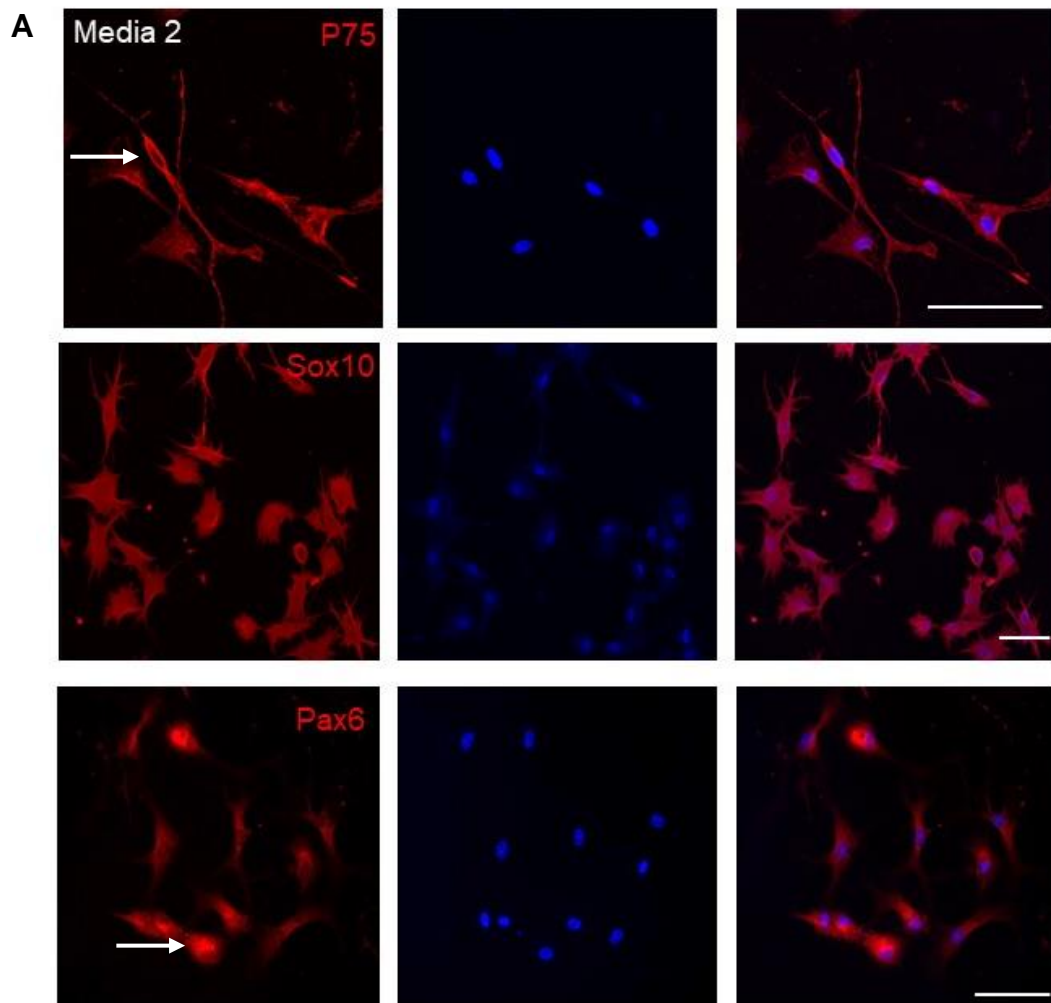


Figure 5.6.A Immunocytochemical staining results of ciPSCs induced neural crest cells (ciPSC-NCC) cultured in Media 2 (20 μ M SB431542, 2 μ M CHIR99021)

(A): The neural crest marker P75 showed cytoplasmatic expression after 7 days in Media 2. The neural crest marker Sox 10 was not expressed in Media 1 but in Media 2 (compare Figure 5.5.A). Pax 6 showed expression (cytoplasmatic and nuclear, white arrow) in NCCs of Media 1 and in Media 2 (compare Figure 5.5.A). This was performed in a technical triplicate. Nuclei are shown by DAPI counter staining. Scale bar: 20 μ m

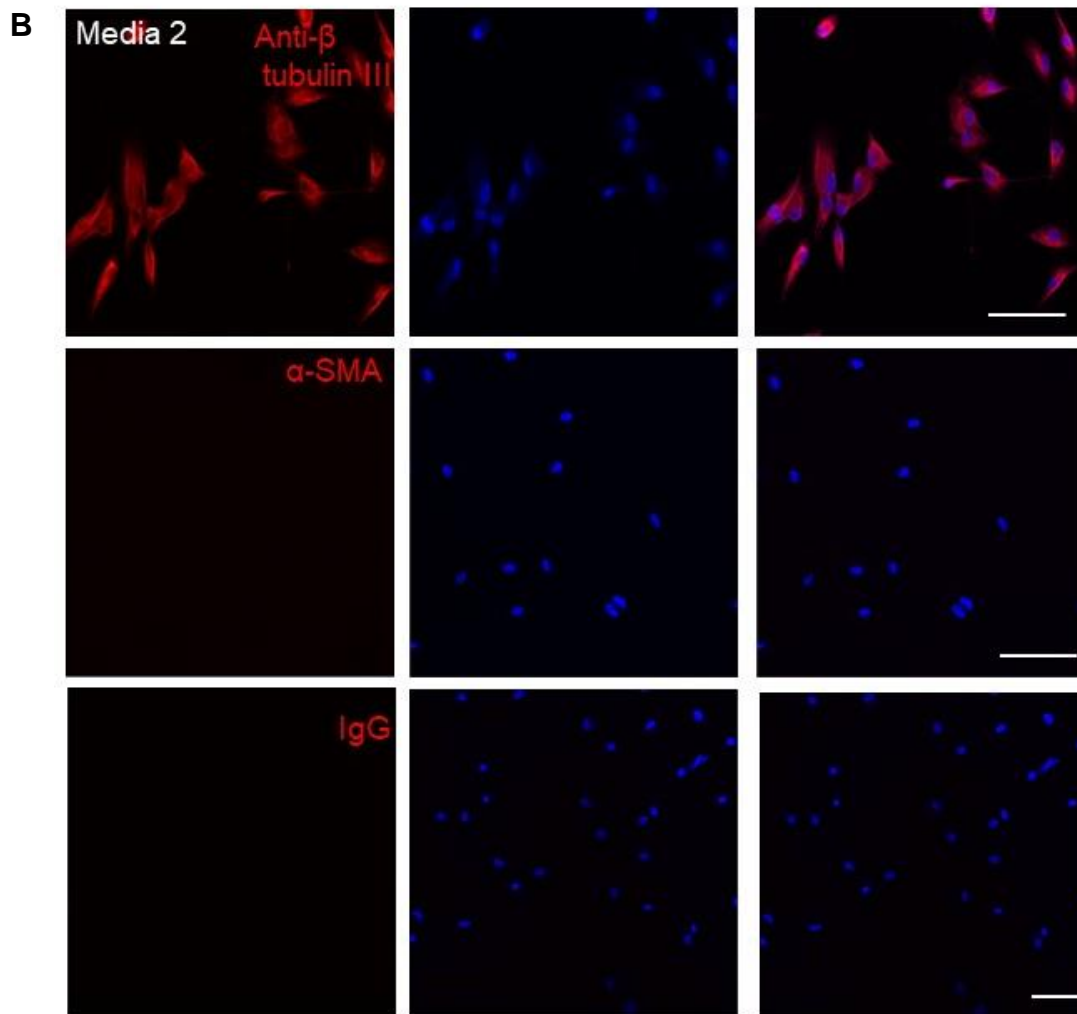


Figure 5.6.B Immunocytochemical staining results of canine iPSCs induced neural crest cells (ciPSC-NCC) cultured in Media 2 (20 μ M SB431542, 2 μ M CHIR99021)

(B): NCCs cultured in Media 2 did not express α -SMA but Anti β -Tubulin III. This was performed in a technical triplicate. Nuclei are shown by DAPI counter staining. Abbreviation: IgG, immunoglobulin G (negative control). Scale bar: 20 μ m

5.3.2 CiPSC-NCC-KDCs exposed to corneal stromal stem cell media expressed keratocyte markers but not Keratocan

Morphologically, the cells aligned and formed an interconnecting cell syncytium after 3-5 days in CSSC media. The cell morphology changed to elongated spindle and stellate cells. After three weeks in KDM, cells continued to align further and stellate as well as spindle formed cells were observed (Figure 5.7). However, in the third week of the keratocyte differentiation, cell degeneration, detachment and cell loss was noted.

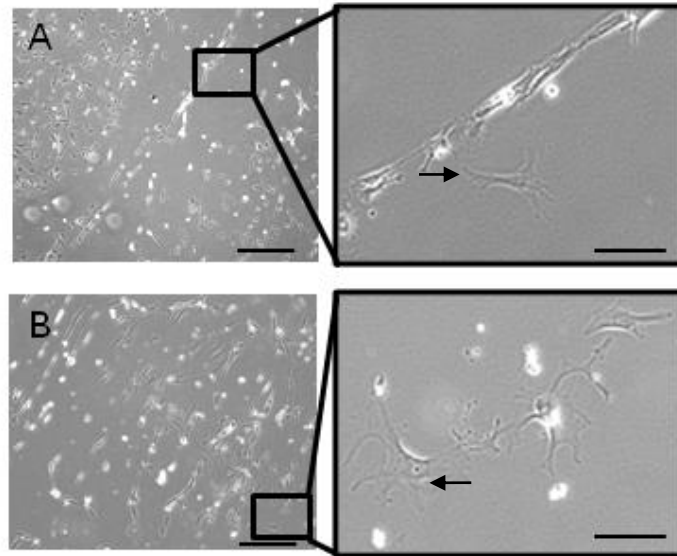


Figure 5.7 Change of cell morphology of ciPSC-NCCs in corneal stromal stem cell (CSSC) and keratocyte differentiation media (KDM)

Phase-contrast images of A) ciPSC-NCCs aligned in CSSC media and changed to stellate cell morphology after 4 days (black arrow). B) After 18 days in KDM, cells were aligned, interconnected, and exhibited stellate cell morphology (black arrow). This was observed in all three technical replicates. Find magnified images in the black box to the right. Scale bar: A, B) 100 μm ; magnified images: 20 μm

Similar positive protein expression of Lumican, ALDH1A3 and P75 after the CSSC media step and after the KD was noted. Keratocan and Sox10 were not expressed at either stage of the differentiation (Figure 5.8.A./B., Figure 5.9.A./B.). Pax6 revealed cytoplasmic marker expression after the CSSC media step but shifted to nuclear and cytoplasmic marker expression after the keratocyte differentiation (Figure 5.8.B, Figure 5.9.B).

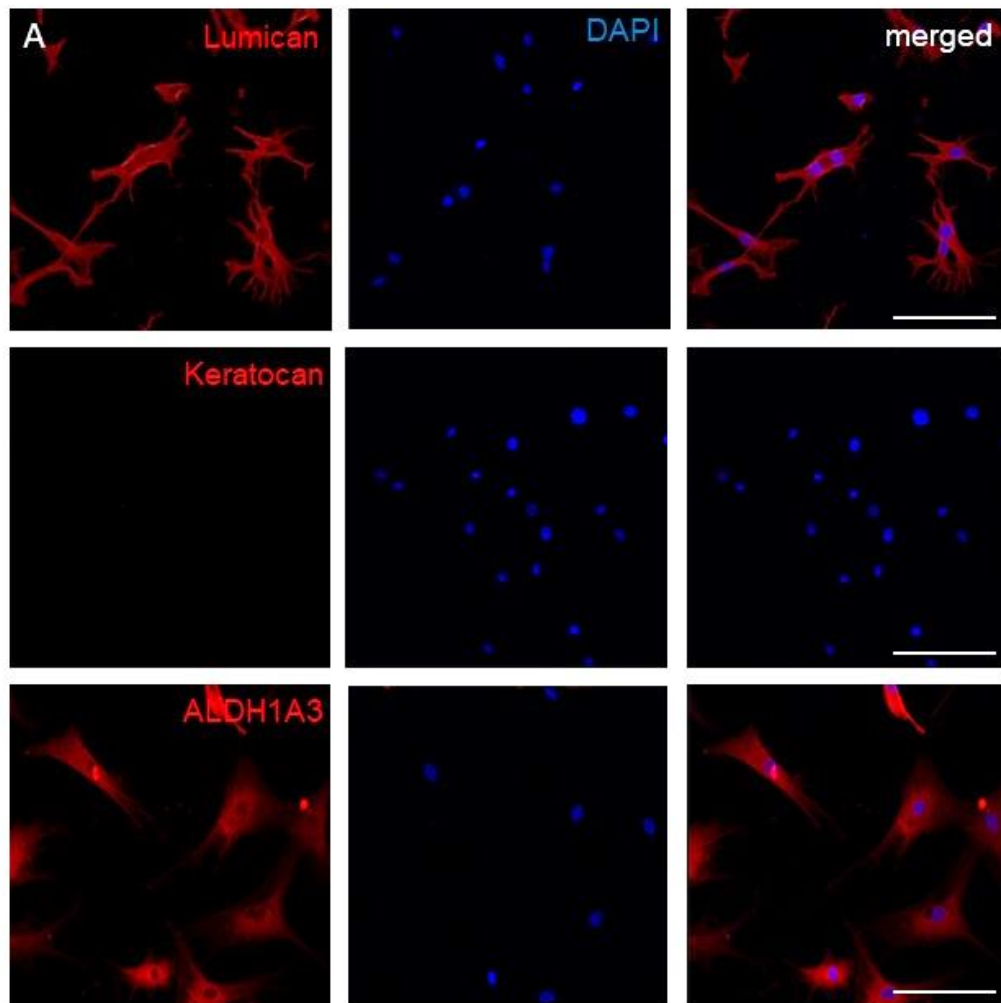


Figure 5.8.A Immunocytochemical staining results of canine iPSC neural crest differentiated cells (ciPSCs-NCC) cultured in CSSC media

(A): Keratocyte marker Lumican and ALDH1A3 were expressed whereas Keratocan was not expressed. This was performed in a technical triplicate. Nuclei are shown by DAPI counter staining. Scale bar: 20 μ m

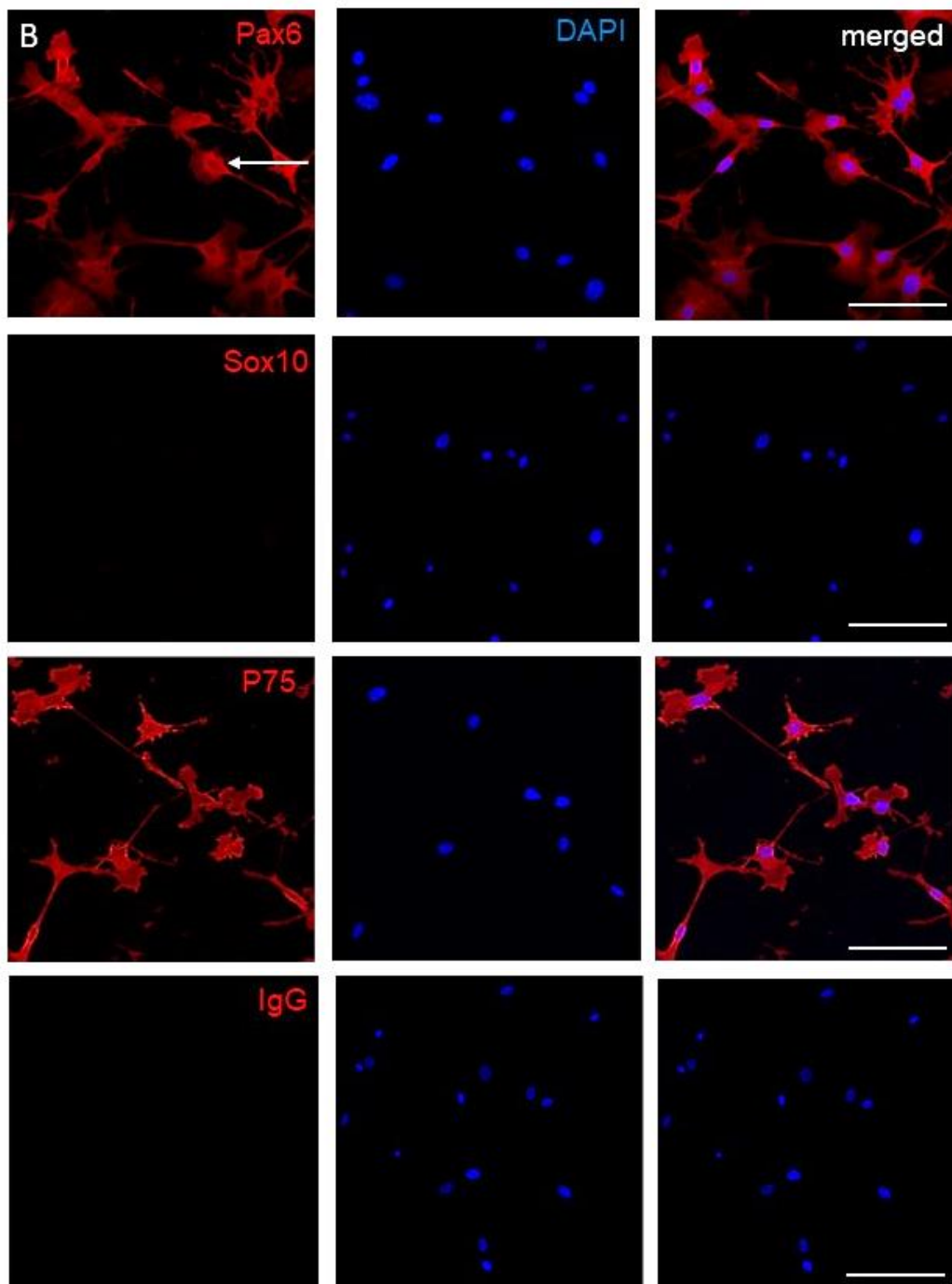


Figure 5.8.B Immunocytochemical staining results of canine iPSC neural crest differentiated cells (ciPSCs-NCC) cultured in CSSC media

(B): Pax6 was expressed in the cytoplasm and but not nuclear (white arrow). P75 as neural crest marker was expressed whereas Sox 10 was not expressed (compare to Figure 5.6. A.) This was performed in a technical triplicate. Nuclei are shown by DAPI counter staining. Abbreviation: IgG, immunoglobulin G (negative control). Scale bar: 20 μ m

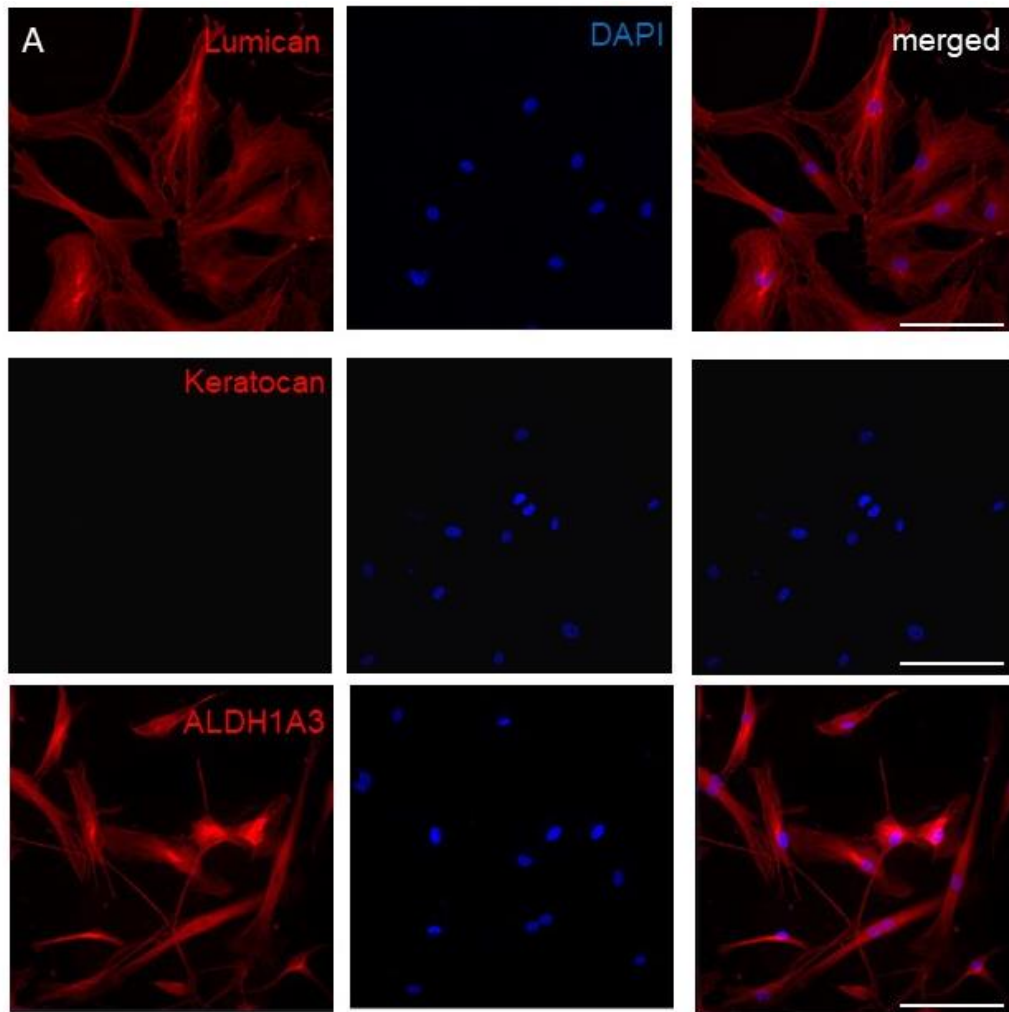


Figure 5.9.A Immunocytochemical staining results of ciPSCs-NCCs cultured in corneal stromal stem cell (CSSC) and keratocyte differentiation media (KDM)

(A): Lumican and ALDH1A3 was expressed whereas Keratocan was not expressed. This was performed in a technical triplicate. Nuclei are shown by DAPI counter staining. Scale bar: 20 μ m

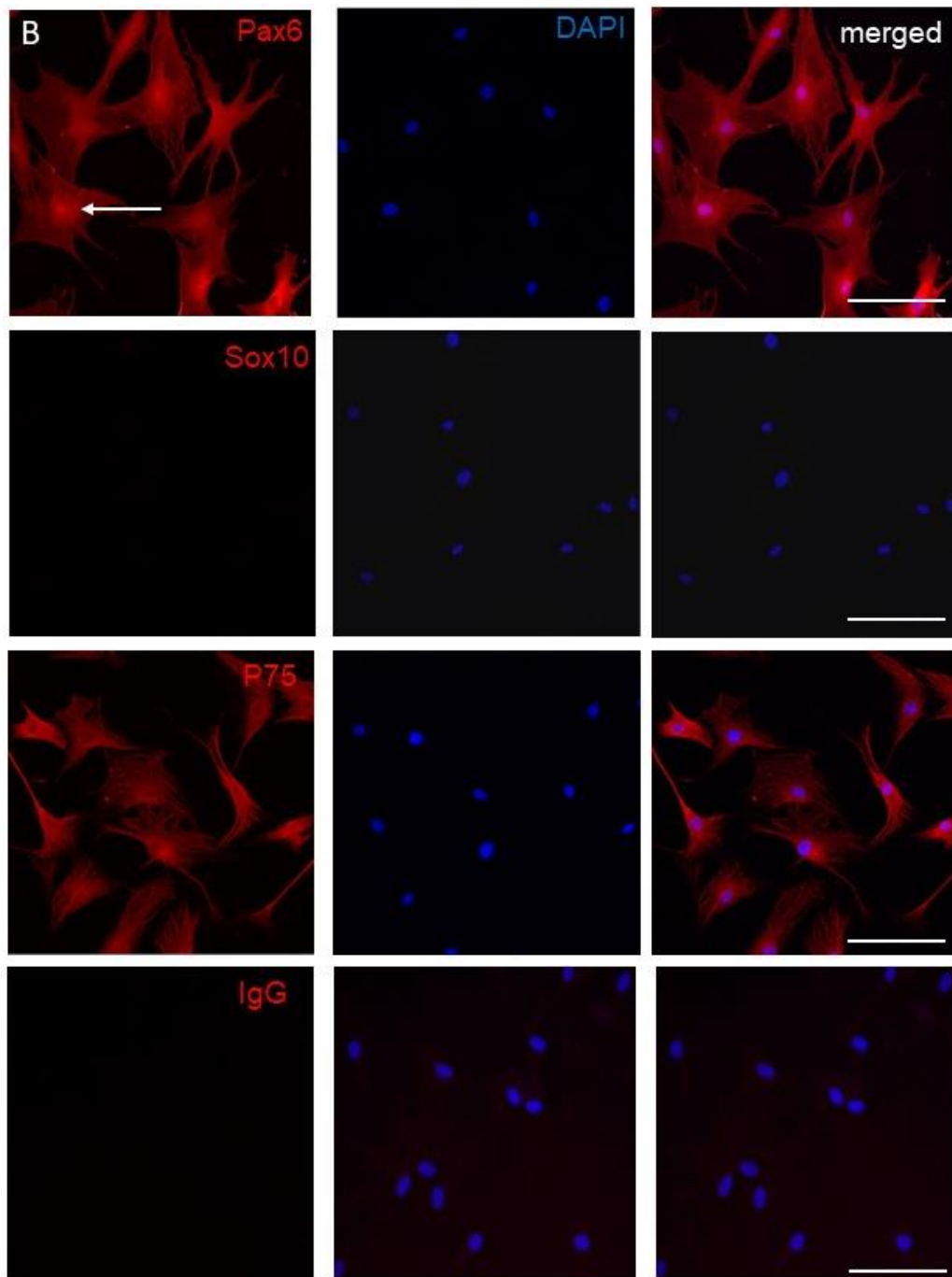


Figure 5.9.B Immunocytochemical staining results of ciPSCs-NCCs cultured in corneal stromal stem cell (CSSC) media and keratocyte differentiation media (KDM)

(B): Pax 6 showed nuclear (white arrow) and cytoplasmatic expression. The neural crest marker P75 is expressed but not Sox 10. This was performed in a technical triplicate. Nuclei are shown by DAPI counter staining. Abbreviation: IgG, immunoglobulin G (negative control); Scale bar: 20 μ m

Comparison of the gene expression after the NCC-CSSC media step (Tukey's test, $P= 0.046$) and at the end of the KD demonstrated significant

upregulation of *Lumican* (Tukey's test, $P= 0.017$) and *ALDH1A3* (Tukey's test, both $P<0.001$). *Sox10* after culture NCC-CSSC media was significantly upregulated (Tukey's test, $P= 0.002$) and significantly downregulated (Tukey's test, $P= 0.001$) after the KD (Figure 5.10. A). *Keratocan* was not expressed in any of the three technical replicates, but in the positive control (Figure 5.10 B).

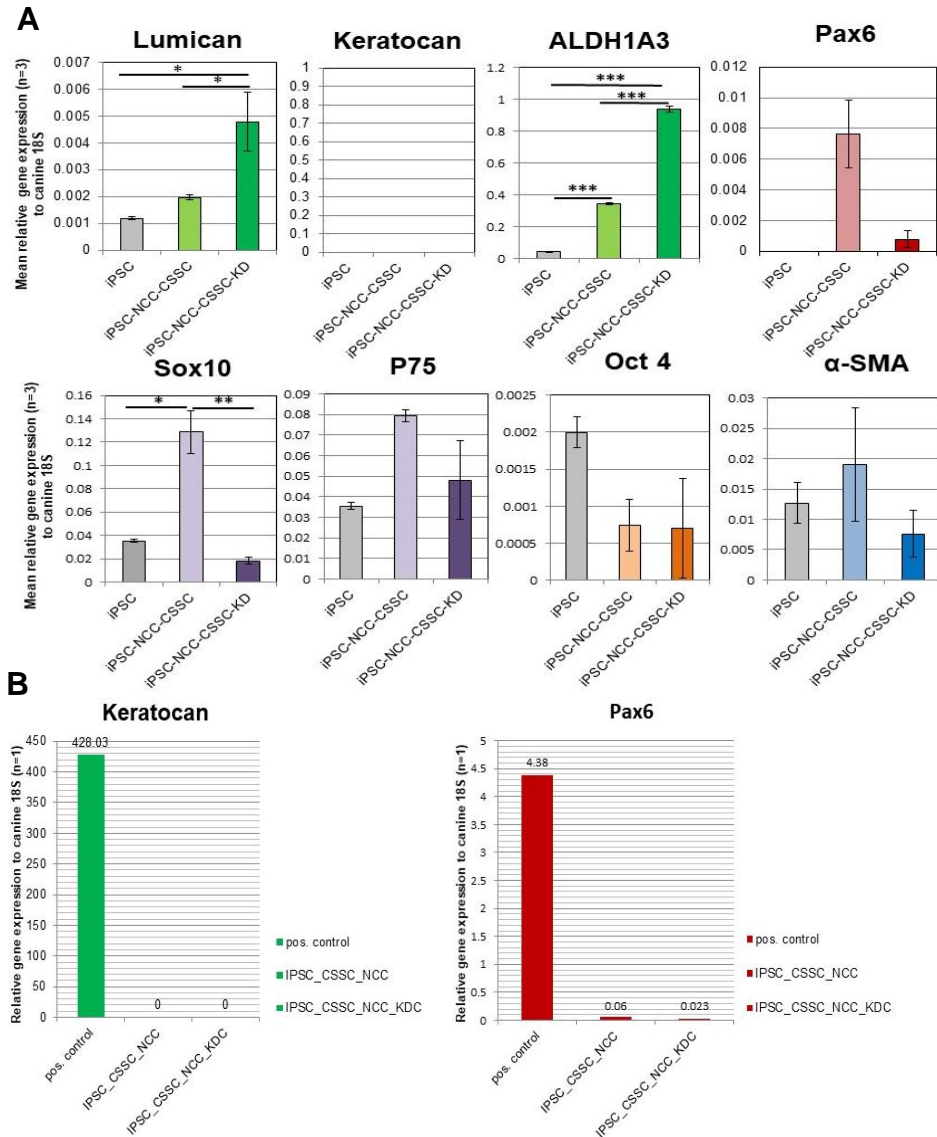


Figure 5.10 The relative gene expression level of keratocyte-, neural crest-, stem cell genes and α -SMA of ciPSCs, iPSC-NCCs derived cells cultured in CSSC media and their keratocyte differentiated cells

(A): The graphs demonstrate the mean (\pm SE) relative gene expression ($n=3$) to canine 18S of Keratocan, Lumican, ALDH1A3, Sox 10, P75, OCT4 and α -SMA of iPSC-NCC-CSCs and their keratocyte differentiated cells. Lumican (Tukey's test, $P=0.046$; Tukey's test, $P=0.017$) and ALDH1A3 (Tukey's test, both $P<0.001$) were significantly upregulated after the NCC-CSSC induction and keratocyte differentiation. Sox10 was significantly upregulated (Tukey's test, $P=0.002$) after NCC-CSSC and significantly downregulated (Tukey's test, $P=0.001$) after the KD. Keratocan was not expressed in any of the three technical replicates, (B) but in the positive control (cornea #15 (see 2.4.1) in one technical experiment). Pax 6 positive control was performed on CSC-KDCs (#13) as one technical singlicate. Abbreviations: *, $P<.05$; **, $P<.01$, ***, $P<.001$; n, number of technical replicates; NCC-CSSC, neural crest – corneal stromal stem cell; KD, keratocyte differentiation; KDC, keratocyte differentiated cells

When comparing the overall fold change in relative gene expression in response to keratocyte differentiation in corneal stroma cells (see 3.3.9), adMSC induced in CSSC media followed by KD (see 4.3.2) and ciPSCs revealed that some keratocyte markers reached a level of significant upregulation and N-cadherin downregulation and overall exhibited a similar change of gene expression pattern or trend (Figure 5.11).

However, the overall relative gene expression levels when compared to CSC and their differentiated KDCs revealed very low amplification levels in response to the entire keratocyte differentiation protocol (Figure 5.10, compare to Supplementary Figure S1).

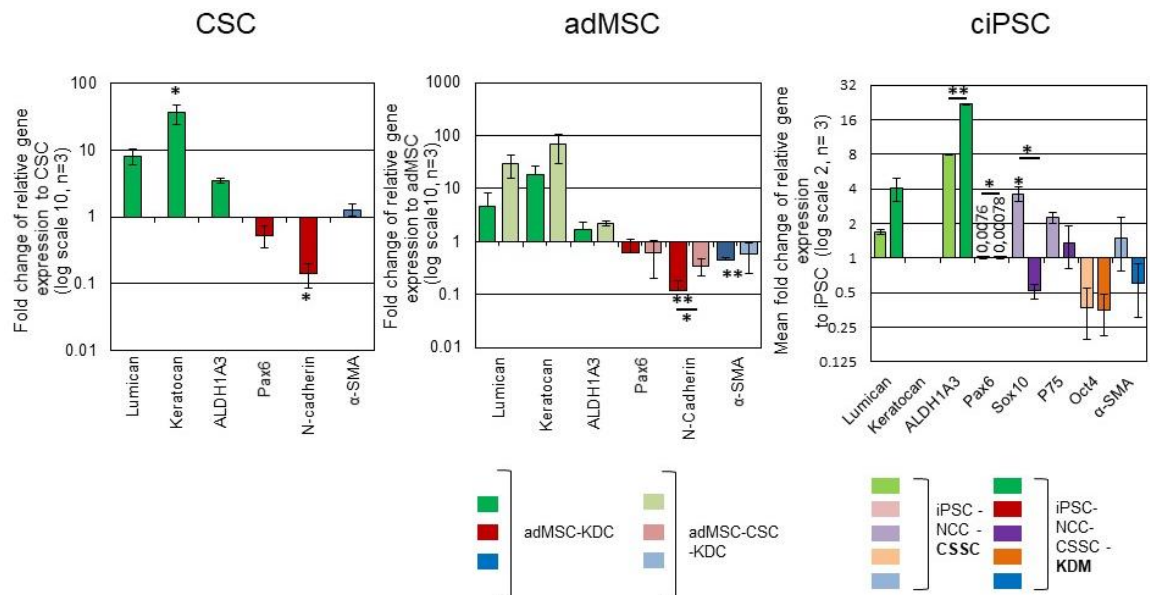


Figure 5.11 Comparison of the fold change of gene expression level to the keratocyte differentiation (KD) in corneal stromal cells, adipose derived MSC and canine iPSCs

The fold change expression of CSC after the KD revealed significant upregulation of Keratocan (T-test, $P=0.041$) and downregulation of N-cadherin (T-test, $P=0.025$). N-cadherin was significantly downregulated in adMSC-KDC (T-test, $P=0.0003$) and adMSC-CSC-KDC (T-test, $P=0.012$) to undifferentiated adMSCs, which was significantly lower in adMSC-KDC (T-test, $P=0.0023$) compared to adMSC-CSC-KDCs. Likewise, α -SMA was downregulated reaching the level of significance in adMSC-KDC (T-test, $P=0.0017$). The fold change of ciPSC-NCCs when cultured in CSSC showed significant upregulation of ALDH1A3 (T-test, $P=0.00074$) and Sox10 (T-test, $P=0.002$). After the keratocyte differentiation, ALDH1A3 (T-test, $P<0.001$) were further upregulated whereas Sox10 (T-test, $P=0.0041$) and Pax6 were downregulated (T-test, $P=0.039$). Results are based on a biological triplicate ($n=3$) in CSC and adMSC, and technical triplicates in ciPSCs differentiated cells and were normalised to the canine housekeeping gene 18S. Abbreviations: *, $P<0.05$; **, $P<0.01$, error bar = \pm SE.

5.4. Discussion

This chapter aimed to start establishing methods to generate keratocytes from healthy ciPSCs. In the future, the derivation of keratocytes from ciPSCs may provide a laboratory tool to study inherited corneal stromal dystrophies in dogs and provide a potential source of cells for transplantation.

This chapter provides preliminary data that ciPSCs derived NCC-like cells adopt keratocyte-like characteristics (i.e. cell morphology with stellate and interconnecting cells) when cultured 2D. Lumican and ALDH1A3 were expressed and the gene expression was significantly upregulated however, a corneal specific proteoglycan, Keratocan, was not expressed at the protein or gene level. Nevertheless, the overall changes (up- and /downregulation) of relative gene expression in response to the NCC-KDC differentiation steps were low when compared to corneal stromal stem cells and their keratocyte differentiated cells. A general limitation of this chapter is the fact that all results are based on ciPSC of one donor and therefore only technical triplicates were performed which question how valid the statistical results are and what conclusions can be made. At this stage of the projects, the results are seen as preliminary and not 'representative'. Future projects should be performed as biological replicates followed by technical replicates per biological sample (Vaux, Fidler et al. 2012). The reprogrammed ciPSC were not fully characterised (see Baird, Barsby et al. 2015) and could not be further analysed in this study. This limitation was based on time and funding constraints.

The aim was to start the NCC induction protocol with dissociated cells instead of cells expanding out of colonies, as it can be assumed that a more homogeneous differentiation of cells can be achieved. Further flow cytometry would show evidence for that but could not be performed in this chapter. This is in accordance with human publications, where single hiPSC and small colonies (20-30 cells) were seeded (Fukuta, Nakai et al. 2014, Chambers, Mica et al. 2016).

The optimal seeding density of $1-2 \times 10^4$ /cm² ciPSC single cells or 20-30 small pieces of colonies per one well of a 6-well plate were similar to that described in hiPSC-NCC-KDC study (Naylor, McGhee et al. 2016).

Subjectively, the preferred coating system was Geltrex®, as colonies seemed to attach more evenly than on the FNC® Coating Mix, but this was further investigated in the present study. Matrigel® is used in most human-based literature, and is similar to Geltrex® but is a more cost intensive product (Fukuta, Nakai et al. 2014, Chambers, Mica et al. 2016, Naylor, McGhee et al. 2016).

The use of Matrigel® or Geltrex®, was no influencing factor in a study comparing feeder-free systems and culture media in hESCs (Akopian, Andrews et al. 2010), whether there is an influence of the coating system on differentiation experiments remains unknown.

Accutase® was the preferred dissociation solution given the excellent cell survival (100% live cell). Accutase® is also used in hiPSC neural crest lineage differentiation studies (Menendez, Yatskievych et al. 2011, Fukuta, Nakai et al. 2014, Chambers, Mica et al. 2016, Naylor, McGhee et al. 2016).

Other studies also used trypsin successfully in experiments establishing feeder-free and serum-free culture conditions in ciPSCs (Nishimura, Hatoya et al. 2017).

The increase of SB431542 and CHIR99021 concentration and extended culture days had a positive impact on the NC cell morphology when compared to human and canine epidermal NCC phase-contrast images (Gericota, Anderson et al. 2014, Sakaue and Sieber-Blum 2015). Likewise, Sox10 and P75 protein expression was evident. The fact that protein expression of β Tubulin III +/ Pax6 +/P75 +/ α -SMA - was indicative of a neurogenic precursor cells differentiation. For example, Schwann cells would express S100, α -SMA, glial fibrillary acidic protein (GFAP), however double or triple stained immunocytochemistry would be indicated to characterise the NNCs in more detail (Menendez, Yatskievych et al. 2011, Gericota, Anderson et al. 2014, Liu, Jin et al. 2015).

The fact that Pax6 protein was expressed in both, the cytoplasm and nucleus, could be explained by exposure to oxidative stress. Human corneal epithelial cells demonstrated nuclear-cytoplasmic shuttling of Pax6 under oxidative stress condition *in vitro*. The authors concluded this might be a result of a cellular protective mechanism against cellular stress (Shukla and Mishra 2018). However, after the submission of the thesis (January 2020) an updated company information (Biolegend) about Anti-Pax6 ((Cat No 901301) Clone: Poly 19013 used in the study), described "it has also shown reactivity with GFP and is therefore not recommended for use in GFP-expressing systems (as determined by in-house testing)". This could likely explain the

unspecific staining given the ciPSC in the current study still expressed GFP (Supplementary Figure S4).

Therefore, before investigating in modifying the culture protocol (i.e. KDM does not contain serum that could contribute to cellular stress), the Pax6 protein marker needs to be re-evaluated. A limitation of this study was that Pax6 positive control tissue, not of corneal origin, such as retina (i.e., amacrine cells) was not included in the study (see introduction 1.1. A) (Macdonald and Wilson 1997). However, Macdonald and Wilson (1997) also described the existence of Pax6 in corneal epithelia in differentiated ocular tissue. *Pax6* was expressed in corneal control tissue (see Figure 5.10 and 2.4.1). There was also specific nuclear staining of CSC (see Figure 3.2), confirmed by Western blot (see 3.3.2).

The translocation of nuclear expression of P75 cannot be explained but nerve growth factors can induce the release of neurotrophin receptor (p75^{ICD}) and facilitate its translocation to the nucleus. This effect was seen in schwannoma and Schwann cells cultured under serum-free conditions and mimicked by brain-derived neurotrophic factor or neurotrophin-3. CSSC media contains only 2% serum and keratocyte differentiation media is lacking serum which might be an influencing factor (Frade 2005). The immunocytological results should be compared to gene expression level (PCR) in a biological triplicate in future studies. Further marker evaluation using positive control tissue (cerebellum) for P75 and Sox10 should be performed. The markers used in the present study were established in other studies and therefore not evaluated in the present study (see 3.3.2).

The insulin concentration is reported to be critical in culturing human neural stem cells and neurons. It is described that prolonged exposure at the concentrations optimised for rodent neural stem cells (NSCs) (high insulin concentration) is toxic to human NSCs, whereas withdrawal of insulin led to reduced cell survival and cell death in human NSCs. The underlying cell death mechanism at high insulin concentrations is explained in the reduction of activation of the PI3K/Akt pathway (phosphatidylinositol 3-kinase and Akt stands for Protein Kinase B) which is critical to cell survival signalling. This is also seen in insulin resistance (Rhee, Choi et al. 2013). CiPSC in the chapter were cultured in high porcine insulin concentration (4.3 μ M) but future studies should further assess whether canine NCCs require culture conditions of rodent (high insulin) or human NCCs (low insulin). This study only used relative cell survival measures (i.e. % living cells) but more detailed research should include cell viability and cytotoxicity assays, apoptotic markers Caspase 3, and protein marker and gene expression of pAkt (Twentyman and Luscombe 1987).

To optimise the NCC induction media, a concentration series of CHIR (including far higher concentrations than in the present study) should be performed in future studies, also the substitution of Noggin as BMP blocking (Gong, Duan et al. 2021) and the role of bFGF on canine cells should be further assessed (Leung, Murdoch et al. 2016).

Interestingly, NCC-like cells upregulated *Sox10*, which might enter a neurogenic cell fate after (and before) the NCC induction step, downregulated *Sox10* when differentiated in KDM into cells and displayed

cell keratocyte morphology and expressed *Lumican* and *ALDH1A3*, both on a gene and protein expression level. These were upregulated after the CSSC media step. In addition, the cell profile changed to more stellate cells with an additional CSSC media step. CSSC media contains PDGF and EGF and low serum concentrations. It is described that factors such as FGF, TGF- β , PDGF, IGF, EGF regulate the keratocyte differentiation, migration and expression of *Lumican* and *Keratocan* (Kim, Lakshman et al. 2010, Lakshman and Petroll 2012). CSSC media contains a low serum concentration (2%) because higher serum concentration has an impact on keratocytes to differentiate into fibroblast and myofibroblasts (Beales, Funderburgh et al. 1999).

P75 was still expressed after the KD and was also expressed in keratocytes generated from CSC of corneal origin (see Supplementary figure S5), suggesting they retain expression of this neural crest associated marker even in adulthood. This was also described for AP2a (neural crest marker) which is still expressed in corneal -scleral rims and keratocytes generated from hiPSCs (Naylor, McGhee et al. 2016). Naylor et al. (2016) also report the response of upregulation of keratocyte genes and downregulation of NCC genes; however, the results are based on a 3D study (cell pellet). The human-generated cells showed a higher degree of upregulation of keratocyte genes and downregulation of NCC genes than in the present chapter, this was based on fold change calculation, but relative expression levels were not provided. Interestingly, the study of Naylor et al. (2016) compares the results to the gene expression (fold change) of keratocyte of corneal origin; these were higher than in keratocyte-like cells generated from hiPSCs. This is

similar to the findings of the present chapter, even no comparison to canine keratocytes were performed, which is a limitation of this study, the gene expression level of keratocytes-like generated from ciPSC were far lower than in keratocyte-like cells differentiated from corneal stromal cells. Naylor and co-workers (2016) could also demonstrate that the gene expression (keratocyte, NCC) was similar to keratocytes of corneal origin when hiPSC-NCCs are seeded on decellularised corneal tissue. It was concluded that also during embryogenesis NCC migration and differentiation is closely associated to the ECM structure. The diameter of matrix fibres is an essential factor to define neuronal and neural crest differentiation *in vitro* (Lim, Liu et al. 2010, Endo, Ishiwata-Endo et al. 2012, Ren, Zhang et al. 2013). The corneo-scleral rim offered a matrix (such as orientation and diameter of the collagen fibrils) to hiPSC-NCCs and possibly enables the acquisition of a corneal keratocyte-like fate. 3D studies using a corneal scaffold are warranted to further optimise the differentiation process to generate keratocyte from ciPSC in the future.

Three main factors should be considered for future studies: a) the quality of cells, i.e. status of true pluripotency of ciPSC, b) the method to assess the state of pluripotency and c) the culture media to maintain pluripotency under feeder-independent conditions and as single cells.

a) The general question is how truly these ciPSC were reprogrammed, which is a general burden in contrast to hiPSC when introducing human reprogramming factors (c-MYC, Klf 4, Sox2, OCT4) in another species (dog), i.e. species-specific differences underpinning pluripotency in iPSC of

domestic animals remains still uncertain. In the future, basic research is required into the factors for maintaining pluripotency and the application of next generation sequencing technologies to characterise the cells (Paterson, Kafarnik et al. 2017).

In the future, it would be preferable to establish and fully characterise ciPSCs of different donors using a Sendai virus system, which was successfully integrated by two independent groups (Chow, Johnson et al. 2017, Tsukamoto, Nishimura et al. 2018). Sendai virus is a genome integration-free and completely exogenous gene-silenced (footprint-free) RNA virus, which are believed to be safer to use in vivo (find more details in the general introduction, 1.7). To increase the induction additional introduction of NANOG and/or Lin28 reprogramming factors could be considered for future studies.

In this chapter, ciPSCs of passage 10 to 16 were used, but with several freeze-thaw cycles, which might have had a negative effect on maintaining the state of pluripotency. However, the ciPSC in this study would have been not feasible for translational purposes, because an integrating retroviral gene transduction methodology was used, iPSC not silenced GFP at this passage stage and karyotype analysis displayed aneuploidy and chromosomes with a metacentric appearance (Baird, Barsby et al. 2015). Even the safety of MSC generated from ciPSC with an integrated retrovirus system has been demonstrated in vivo, but the general cancerogenic risk and alteration of host genome has to be taken into account (Herberts, Kwa et al. 2011, Chow, Johnson et al. 2017).

b) A limitation of the chapter was that the gene expression of endogenous and exogenous pluripotent genes in ciPSC on/off feeder cells and single cells were not assessed but would be of importance for future studies. In this chapter we used only *OCT4*, and it remains unclear whether the *OCT4* expressed is endogenous, from the canine cells, or exogenous, from the introduced human gene. A repeated attempt was made to self-design or use canine NANOG and Rex1 primer from the literature (Luo, Suhr et al. 2011, Whitworth, Frith et al. 2014), but the efficiency tests on canine iPSCs did not determine reliable results. A positive control tissue or cells of a canine embryo was not available in the present study. Spermatogonial stem cells were not considered but are described in canines and would be valuable positive control for future studies (Zheng, Zhang et al. 2014).

c) The composition of different components in the iPSC media is another factor to maintain the pluripotency and growth of ciPSC off feeder cells. It is well established that both FGF and Activin/nodal/TGF-beta signaling are critical for hESC/hiPSC maintenance. MTeSR1 and STEM PRO™ were described to support the stem cell growth in contrast to non-commercial media. However, these are cost-intensive commercial media, but comparative studies would be of interest in future studies. The same study used Matrigel® or Geltrex®, which was found not be an influencing factor (Akopian, Andrews et al. 2010). Another consideration to improve the culture media for canine iPSC is the substitution of doxycycline. Nishimura et al. (2017) showed that exogenous transgenes were expressed in ciPSC over 50 passages cultured with doxycycline but declined after withdrawal. Doxycycline increased also the embryoid body formation. The same group

showed that when taking ciPSs off the feeder system as colonies or single cells, high concentration of bFGF (10 times higher than in the present chapter), upregulated OCT3/4 and Sox2. Furthermore, the growth rate of ciPSC was higher on the feeder + serum system but the pluripotency marker transcripts were significantly higher in cells cultured in N2B27 + Matrigel® (Nishimura, Hatoya et al. 2017).

Chapter 6:

General discussion and future work

6.1 General discussion

This thesis provides methodologies and creates a basic platform to initiate further research in the field of canine corneal stem cell therapies and to develop a laboratory model to study inherited diseases such as crystalline corneal dystrophy.

The thesis provides novel findings, which are discussed alongside the limitations within each chapter discussion. Overall, this thesis confirmed the first hypothesis that a subpopulation of limbal and central corneal stromal cells have mesenchymal stromal cell properties similar to corneal stromal stem cells described in humans and was published in *Stem Cells and Development* (Kafarnik, McClellan et al. 2020). There are differences compared to human CSSCs and therefore the term CSC for dogs was preferred at this stage. The small subpopulation of CD90+ cells in the human limbal crypts/limbal areas in dogs are described, but the presence of CD90+ cells in the central corneal stroma seems unique to the canine cornea and was not confirmed in IHC on human corneas in our lab (Dziasko, Armer et al. 2014).

Secondly, the present thesis confirmed the hypothesis that canine adMSCs can be differentiated into cells with keratocyte characteristics *in vitro*. This has also been shown in human adMSCs (Dos Santos, Balayan et al. 2019). The upregulation of α -SMA has not been reported in the human literature (i.e. BM-MSc derived keratocytes) (Park, Kim et al. 2012). Although, α -SMA was significantly reduced during the keratocyte differentiation process, the expression level was still 6 times higher than in CSC-KDCs, which seems a

novel finding, and it remains unknown whether or not that is unique in dogs. Thirdly, it was hypothesised that ciPSC can be differentiated into keratocyte-like cells. The hypothesis was partially confirmed by the fact that two out of three keratocyte markers were upregulated but *Keratocan* as the most cornea specific marker was not expressed. Hence, further research is needed to establish a laboratory tool to study inherited corneal stromal dystrophies (see future work). Furthermore, research into NCC expansion essential is an essential future step. The low cell yield is a restricting factor for potential cell-based therapies. (Fukuta, Nakai et al. 2014) The results of Chapter 5 is seen as preliminary given the limitations discussed in 5.4.

When comparing the keratocyte-like cells of three different cell origins (CSC, adMSC, ciPSC), a change of cell morphology to more dendritic and elongated cells with cell interconnections forming a cell syncytium was similar observed in all three KDCs. The change of protein and gene expression level showed a similar pattern (see Figure 5.11). with some m-RNA fold change in gene expression showing a statistical trend or significance but more scientific conclusions cannot be drawn. The keratocyte gene expression of *Lumican* and *ALDH1A3* keratocyte-like cells was upregulated after 3 weeks in differentiation media (except for *Keratocan* in ciPSC derived KDCs) and trend that stem cell markers were downregulated (*Pax6*, *N-cadherin*). Neural crest gene expression (*Sox10*) was upregulated after initial neural crest induction of ciPSCs and then downregulated after the KD, this was not assessed in CSC or adMSC derived cells. Given all limitations discussed in 5.4 (results are in technical triplicate, the ciPSC were not fully characterised, the neural

crest induction protocol needs further optimisation) these are promising first results for future studies.

However, when focusing on the relative m-RNA expression, the KDCs of corneal origin showed the highest expression levels of keratocyte relevant genes, followed by KDCs of adMSCs origin (Figure 4.9). Overall, the relative m-RNA expression of KDCs derived from ciPSCs was very low and in just detectable amplification levels (Figure 5.16). Hence, further work is required to establish a more robust differentiation protocol. Interestingly, adMSCs and ciPSCs showed a similar response to CSSC media before the keratocyte differentiation, which seemed to induce a keratocyte primed cell fate and should be considered in future protocols. However, if this holds for adMSC needs further be evaluated in more biological replicates and in optimised CSSC media for MSCs given the lack of statistically significant upregulation for *ALDH1A3*. CSSC media contains PDGF and EGF and low serum concentrations. It is described that factors such as FGF, TGF- β , PDGF, IGF, and EGF regulate keratocyte differentiation, migration and expression of *Lumican* and *Keratocan* (Kim, Lakshman et al. 2010, Lakshman and Petroll 2012).

In general, more evidence-based clinical data are required to study corneal stromal (crystalline) dystrophy and canine corneal fibrosis (see 6.2. future work) to deepen the understanding of the disease process. This should go in line with future research to develop the use of corneal stromal (stem) cells, their KDCs (from different cell sources) in clinical applications or establishing a corneal disease model.

This project was based on establishing corneal stromal cells of three different origins and firstly baseline data on KDCs from corneal tissue had to be established (i.e. methodology, protein and gene expression levels) considering these cells were not described in the literature. Keeping in mind to find a cell source for potential cell-based therapies, tissue-derived CSCs showed promising features such as immune privilege. Whether or not they are also immunomodulatory needs to be further assessed followed by the question if this holds for the differentiated KDCs. Secondly, whether CSC and/or their differentiated KDCs can be seeded into scaffold tissue should be established in future studies. A downside of CSCs is the requirement for donor tissue, the limited expansion rate and lifespan of these cells, and the high heterogeneity observed between donors in response to the differentiation process. Human CSSCs have been shown to reduce corneal scarring in an in vivo mouse model (Basu, Hertsberg et al. 2014) and the same author presented the first clinical trial in humans (NCT02948023) (Gordon Research Meeting, Ventura, USA, 2018), but peer-reviewed publications are not yet available. In their study CSSCs are suspended in a fibrinogen solution and immediately applied to the cornea which limits therapeutic use to laboratories with GMP facilities. This is an important aspect given that most human corneal scarring is described for people in areas with potentially limited access to hospitals with associated GMP facilities. Therefore, recent research was conducted to disconnect the stabilisation, storing, and transportation of CSSC and clinical applications from the facility where the cells were produced. CSSC in a compressed collagen gel (RAFT) were more effective at blocking scarring than CSSC

delivered directly in a fibrin. These are mechanically more stable in contrast to fibrinogen gels (Shojaati, Khandaker et al. 2018). GMP facilities in veterinary research are rare and unique to a few academic institutions worldwide. Therefore, careful selection of carrier media and production costs are inevitable for future research planning.

Taking the disadvantages of CSSCs into account, canine adMSCs seemed to present an alternative cell source. A great advantage seems the immunomodulatory aspects of MSCs (Dias, Pinto et al. 2019) and the fact that adMSCs are considered relatively safe as shown also in veterinary clinical studies (Uder, Bruckner et al. 2018). However, the levels of α -SMA in KDCs derived from adMSCs are a concern regarding cell-based therapies and further research is needed whether these cells show more features similar to myofibroblasts. Three-dimensional models are warranted to further assess these cells (see future work). It should be also considered to use BM-MSC instead of adMCS in future experiments (see 4.4).

In regard to safety, as discussed later in this chapter, the application site needs to be carefully considered. For example, intravitreal autologous adMSCs injections were performed in three patients with age-related macular degeneration led to permanent blindness (Kuriyan, Albin et al. 2017). Although the development of teratomas with MSCs is seen as unlikely, a case report demonstrated that a patient developed a large tumour-like mass inside the spinal cord after the transplantation of olfactory mucosa cells. These cells were not MSCs but neoplastic transformation could potentially also occur following MSC transplantation (Dlouhy, Awe et al. 2014).

It is important to keep in mind that over the last years some researchers have questioned the regenerative capacities of MSC treatments.

The primary function of MSCs to form new tissues *in vivo* is considered as limited, questioning the therapeutic properties of such cells when transplanted in a naive state (Dias, Pinto et al. 2019). For example naive MSCs only showed <5% survival after 10 days post-injection into damaged superficial flexor tendon in horses (Guest, Smith et al. 2010). Likewise, another group reported that a single intralesional injection of adMSCs in surgically created superficial flexor tendon lesions did not result in improvement in comparison to the control group (Geburek, Roggel et al. 2017). However, significant clinical improvement of lameness in dogs with moderate to severe osteoarthritis after one or repeated intra-articular injections of allogeneic neonatal MSCs in a 24month follow-up study are reported but cells were not followed by *in vivo* imaging and the positive clinical outcome was discussed as immune-modulatory effects of MSCs (Cabon, Febre et al. 2019).

The overall question is whether there is a need for a paradigm shift in (mesenchymal) stem cell research.

A research group working on cardiac progenitor cells reported that injecting either cardiac progenitor cells, or bone marrow cells into the injured mouse hearts were unspecific and triggered by the immune system (CCR2+ and CX3CR1+ macrophages) reaction to the degenerated cells (Vagnozzi, Maillet et al. 2019).

Even so, MSCs have shown some therapeutic potential in the first clinical studies of immune-mediated disease in the veterinary field (Dias, Pinto et al. 2019) and corneal host-versus-graft disease in humans (Lohan, Murphy et al. 2018). However, whether or not adMSC differentiated KDCs are capable of directly contributing to corneal regeneration by producing an organised extracellular matrix when transplanted in a cornea needs to be carefully assessed in future studies.

To bring the ciPSC differentiation results into context is somewhat limited given the preliminary nature of the results of this project. Likewise, the information in the human field of iPSC based cell therapies is limited to one *in vitro* study of human KDCs derived from hiPSCs (Naylor, McGhee et al. 2016). In view of corneal stromal disease and the use of iPSC for disease modelling, Joseph et al. 2016 developed a model for keratoconus and showed that inhibition of the FGFR2-Pi3-Kinase pathway affected the AKT phosphorylation and keratocytes survival (Joseph, Srivastava et al. 2016). There is currently no further information available on corneal stromal dystrophies in humans or canines.

The canine iPSCs research is generally in a “juvenile” stage in comparison to the human research field. A recent review article was tellingly titled: “The road less travelled: The efficacy of canine pluripotent stem cells” (Menon, Patel et al. 2019). However, in the sense of “one health” (Stroud, Dmitriev et al. 2016) there is a lot of scope to develop the field of ciPSC further, not only for the veterinary sector. Menon et al. (2019) and Gong et al. (2019) both

pointed out the important role of dogs as research models in their review articles (Cong, Zhang et al. 2019, Menon, Patel et al. 2019).

When comparing genetic disease of dogs and humans, 360/450 types of genetic diseases related to humans in dogs are found, which is higher than in other domestic animals. The canine genome project sequenced the whole genome of a female Boxer. This was a 30-million-dollar mission by the National Human Genome Research Institute (NHGRI) was completed in 2004 at the National Institute of Health (NIH). The canine genome map offers a prospect to comprehend the genetic complexities underlying common genetic diseases in dogs as well as genetic disorders in human populations such as various congenital malformations, cardiovascular diseases, diabetes mellitus, muscular dystrophy, epilepsy, retinal atrophy, Alzheimer's disease(AD), and several forms of cancers (Menon, Patel et al. 2019) and canine Duchenne muscular dystrophy (DMD) (McGreevy, Hakim et al. 2015). The application of stem cells to treat pathological conditions in the dog would benefit the dogs as companion animals, but also will tremendously promote the progress of human regenerative medicine. The generation and application of ciPSCs may allow the evaluation of the safety and efficacy of hiPSC-based therapy (Cong, Zhang et al. 2019).

Any stem cell-based therapy considered as medical product need to be assessed for potential risk factors and risk evaluation. Stem cells have similar features to cancer cells, such as a long life span, relative resistance to apoptosis and the ability to replicate for extended periods (Li, Stoicov et al. 2006, Werbowetski-Ogilvie, Bosse et al. 2009). Also similar cell growth and

control mechanisms influence the maintenance of cancer and stem cells (Li, Stoicov et al. 2006). These aspects of potential tumor formation need to be carefully considered in translational medicine also in the veterinary field. Briefly, the tumorigenic potential of stem cells also depends on risk factors such as the local environment for the stem cell in the injection/transplantation area of the recipient and the need for *in vitro* culturing of the cells. *In vitro* expansion of stem cells can lead to introduction of cell mutations. Physiological mechanisms to correct these alterations could potentially not function (e.g. immune recognition, cell cycle arrest, DNA repair) (Shih, Forman et al. 2007).

The use of retroviruses and lentiviruses to reprogram iPSCs raises safety issues due to the integration of therapeutic vectors activating oncogenes (Bushman 2007). This was observed in 50% of chimeric mice, where reactivation of c-MYC resulted in tumour formation (Okita, Ichisaka et al. 2007). Therefore has recent research focused on the use of Sendai virus system (RNA virus) that was found to be an effective method for generating integration-free and exogenous gene-silenced “footprint-free” ciPSCs (Tsukamoto, Nishimura et al. 2018).

The use of animal products such as FBS or xenogenic feeder cells in tissue culture is a risk of potential disease transmission of disease such as prion diseases. Additionally, could the host immune system be activated by biomolecules such as nonhuman sialic acid Neu5G (Martin, Muotri et al. 2005).

To identify the pluripotency and overcome the risk to use reprogramming factors in ciPSC, it would be of great interest to study canine microRNA systems in the future. These are noncoding RNA molecules that predominately regulate mRNA. A single microRNA regulates the expression of hundreds of mRNAs, a feature of a short sequence also described as seed. The seed is essential for the binding of the microRNA to the mRNA (Bartel 2009, Moro, Amin et al. 2018). MicroRNAs (miR-302 family) are closely connected with OCT4, SOX-2 and NANOG mRNAs in a relative expression level to maintain pluripotency. Without OCT4/SOX-2/KLF4/c-MYC reprogramming factors, have human and murine iPSCs been generated by inducing the expression of the miR-302/367 cluster (Anokye-Danso, Trivedi et al. 2011). MicroRNA has been evaluated in equine iPSCs to identify pluripotent cells, and it was confirmed that the expression of the miR-302 family (miR-302a, miR-302b, miR-302c and miR-302d), miR-9 and miR-96 in eiPSCs was strongly induced after cell reprogramming (Moro, Amin et al. 2018).

Taking the risk factors into account, the potential low survival rate and low treatment efficacy of stem cell-based therapies (i.e. any surgical corneal procedure will lead to the release of TGF- β which can have a negative impact on the survival rate of implanted stem cells), recent research is focused on the use of extracellular vesicles (EV) (e.g. ecto- and exosomes) as cell-free therapy alternative instead (see details in 1.8.C))

A recent report has shown that human CSSC-Exos reduced corneal fibrosis CSSC via decreased expression of Col3a1 and α -SMA and blocked

neutrophil infiltration in a mouse cornea model (Shojaati, Khandaker et al. 2019) (see details in 1.4.4.B)).

In conclusion, future regenerative therapies might shift away from using stem cells and focus on research into microRNAs and the use of exosome-based delivery systems.

6.2 Future work

1. Canine corneal stromal (stem) cells

a) Essential baseline data on the limbal anatomy and ultra structure in dogs is sparse. Hence, basic research of the interaction between limbal epithelial stem cells and underlying stromal cells should include immunohistochemistry, 3D-electron microscopy, and in vivo confocal microscopy of the canine LESC niche.

b) To investigate the CD90+ population of stromal cells via immunohistochemistry (double or triple IHC using CD90, α -SMA and Vimentin) and alternative stem cell markers (i.e. ABCG2, Bmi1, HLA-ABC)

c) To investigate the MSC properties of limbal and central canine CSC and their keratocytes in more detail. Hence, to compare more detailed immunophenotyping and RNA sequencing data. Furthermore, a colony formation assay of limbal and central CSCs should be included in future studies. Thirdly, to assess the potential to self-renewal via expanding a cell sorted population of CSC and optimisation of the human CSSC media to canine CSC requirements.

d) To determine whether CSC (limbal and central) are also immune suppressive by immune suppression assays

2. Keratocyte-like cells derived from adMSC

a) To quantify MSC and keratocyte marker via flow cytometry

b) To determine the relevance of α -SMA expression of KD-MSCs in a 3D model (decellularised porcine cornea) in vitro or ex vivo cornea model. Triple immunophenotyping to further characterise these cells as myofibroblasts should include vimentin and desmin.

c) To study the immune-suppressive capacities via PBMC immune suppression assays and the immunomodulatory capacity of KD derived from adMSCs in 2D and 3D

d) Keratocyte function is based on highly organised, transparent extracellular matrix (ECM) in the corneal stroma, thus 3D investigations are required in the future.

3. Keratocyte-like cells derived from ciPSCs

a) To establish and fully characterise ciPSCs of three different donors using a Sendai virus system (Chow, Johnson et al. 2017, Tsukamoto, Nishimura et al. 2018).

b) To optimise the NCC induction media for canine cells by including a concentration series of CHIR (including far higher concentrations than in the present study). Secondly, to then assess the NCCs in more depth via

immunocytochemistry (i.e. S100, α -SMA, GFAP), flow cytometry and cell sorting.

c) The corneoscleral rim offers a matrix (such as orientation and diameter of the collagen fibrils) to hiPSC-NCCs and possibly enables the acquisition of a corneal keratocyte- like fate.

d) To collect subcutaneous samples of dogs with stromal crystalline corneal dystrophy, expand their adMSCs and store them at low passage. Once the ciPSC –NCC induction and keratocyte differentiation is further developed, the keratocytes from healthy and diseased dogs can be compared (i.e. RNA sequencing).

4. Complementary clinical/genetic investigations

a) To increase the clinical knowledge of crystalline stromal dystrophy in dogs of various breeds, a larger scale retrospective and study (multicentre study) is required along with a prospective study to include DNA sampling.

b) To increase the clinical information on canine corneal fibrosis, a clinical retrospective study is required –post injury, post infection, post surgery (deep lamellar techniques versus penetrating keratoplasties) possibly as a multicentre study.

- To investigate the role of canine TGF- β 1, TGF- β 2, TGF- β 3 and PDGF in the stroma and their role in corneal fibrosis. Basic research of TGF β 1 in the dog cornea in response to an injury is available (Gronkiewicz, Giuliano et al. 2016), but information on TGF β 2, 3 and PDGF is lacking.

Supplementary material

Supplementary tables

Primary AB IHC/ICC	Company (cat. number), Clone	Raised in	Clonality	Reactivity	Dilution	Comment
Not suitable stem cell marker						
CD90	Abcam (ab1235119)	mouse	monoclonal	human, porcine, canine, nonhuman primates	1:100	negative IF
CD73	Abcam (ab133582)	rabbit	monoclonal	mouse, rat, human	1:100	negative IF
N-cadherin	Santa Cruz (H-63: sc-7939)	rabbit	polyclonal	mouse, rat, human	1:100	very weak IF
Not suitable keratocyte marker						
ALDH1A1	Abcam (ab131068)	rabbit	polyclonal	mouse, rat, human	1:100	negative IF
Keratocan	Abcam (ab113115)	rabbit	polyclonal	human	1:100	negative IF
Keratocan	Bioss (bs-11054R)	rabbit	polyclonal	human, mouse, rat	1:100	weak IF, negative WB
Decorin	Abcam (ab137508)	rabbit	polyclonal	mouse, human	1:100	negative WB
Not suitable control						
Rabbit IgG	BioVision (1268-100)	rabbit	polyclonal/IgG	rabbit	1:500	unspecific binding

Table S1 Overview of primary antibodies tested to be negative in immunofluorescence or Western blot assay. These markers were not suitable to use in canine species.

Keratocyte differentiation media	Unit	Company
Advanced DMEM	NA	Sigma-Aldrich
human basic fibroblast growth factor	10 ng/mL	Sigma-Aldrich
L-ascorbic acid-2-phosphate (0.1 mM	Sigma-Aldrich
Penicillin-Streptomycin solution	1%	Gibco
Gluta-MAX® (100x)	1%	Gibco

Table S2 Composition of the keratocyte differentiation media (Kureshi, Funderburgh et al. 2014). Abbreviation: Na, not applicable, DMEM, Dulbecco's Modified Eagle's Medium.

Corneal stromal cell <u>isolation</u> media (DFO)	Unit	Company
DMEM high glucose	50%	Gibco
DMEM/F12	50%	Gibco
Gentamicin	50µg/ml	Gibco
Penicillin/Strepomycin	1%	Gibco

Table S3 Composition of the corneal stromal cell isolation media (Kureshi, Funderburgh et al. 2014). Abbreviation: DMEM, Dulbecco's Modified Eagle's Medium.

Corneal stromal stem cell media	Unit	Company
DMEM low glucose	60%	Gibco
MCDB-201	40%	Sigma -Aldrich
Epidermal growth factor	10 ng/mL	Sigma-Aldrich
Platelet-derived growth factor (PDGF-BB)	10 ng/mL	R&D Systems, Abingdon, Oxford, UK
Insulin-Transferrin-Selenium solution	1%	Gibco
Ascorbic acid-2-phosphate	0.1 mM	Sigma-Aldrich
Dexamethasone	10 ⁻⁸ M	Sigma-Aldrich
Gentamicin	50µg/ml	Gibco
Cholera toxin	100 ng/mL	Sigma-Aldrich
Fetal bovine serum	2%	Invitrogen, Life Technologies, Paisley, UK

Table S4 Composition of the corneal stromal stem cell media (Kureshi, Funderburgh et al. 2014). Abbreviation: DMEM, Dulbecco's Modified Eagle's Medium

Mesenchymal stromal cell media/ Mouse embryonic fibroblast media	Unit	Company
DMEM (1x)	NA	Gibco
Fetal bovine serum	10%	Gibco
L-glutamine	2mM	Gibco
Penicillin/Strepomycin	1%	Gibco

Table S5 Composition of the mesenchymal stromal cell media. Abbreviation: DMEM, Dulbecco's Modified Eagle's Medium

Induced pluripotent stem cell media	Unit	Company
DMEM/F12	50%/50%	Gibco
Leukaemia inhibitory factor	1000U/ml	Sigma
Human basic fibroblast growth factor	10ng/ml	Preprotech, London, UK
Fetal bovine serum	15%	Gibco
L-glutamine	2mM	Invitrogen
1% non-essential amino acids	1%	Invitrogen
Sodium pyruvate	1mM	Invitrogen
Mercaptoethanol	0.1mM	Invitrogen

Table S6 Composition of the induced pluripotent stem cell media. Abbreviation: DMEM, Dulbecco's Modified Eagle's Medium

Neural crest induction media	Unit	Company
Iscove's Modified Dulbecco's and Ham's F-12	1:1	Gibco
SB431542 (1614, selective inhibitor of TGF- β RI, ALK4 and ALK),	20 μ M	Tocris Bioscience Abingdon, UK
CHIR99021 (4423, GSK3 inhibitor)	2 μ M	Tocris Bioscience
Chemically defined lipid concentrate	1x	Gibco
Apo-transferrin	15 μ g/ml	Sigma
Monothioglycerol	450 μ M	Sigma
Purified bovine serum albumin (BSA)	5 mg/ml	Sigma
Porcine insulin	4.3 μ M	Sigma -Aldrich
Penicillin-Streptomycin solution	1%	Gibco

Table S7 Overview of the compositions of the neural crest induction media. Abbreviation: DMEM, Dulbecco's Modified Eagle's Medium.

Fat induction media	Unit	Company
DMEM (1x)	NA	Gibco
Fetal bovine serum	10%	Gibco
Rabbit serum	15%	Invitrogen
Bovine insulin	10µg/ml	Sigma
Dexamethasone	1 µM	Sigma-Aldrich
Indomethacin	.02 mM	Sigma-Aldrich
3-isobutyl-1-methylxanthine	0.5 mM	Sigma-Aldrich
Fat maintenance media		
DMEM 1x	NA	Gibco
Bovine insulin	10µg/ml	Sigma

Table S8 Overview of the compositions of the fat induction and maintenance media. Abbreviation: DMEM, Dulbecco's Modified Eagle's Medium.

Bone differentiation media	Unit	Company
DMEM (1x)	NA	Gibco
Fetal bovine serum	10%	Gibco
L-glutamine	2mM	Sigma
Penicillin/Streptomycin	100 U/ml/100 µg/ml	Sigma
β-glycerophosphate	10 mM	Sigma
Dexamethasone	10 nM	Sigma
Ascorbic acid	0.1 mM	Sigma

Table S9 Overview of the compositions of the fat induction and maintenance media. Abbreviation: DMEM, Dulbecco's Modified Eagle's Medium.

Cartilage differentiation media	Unit	Company
DMEM (1x)	NA	Gibco
Fetal bovine serum	10%	Gibco
L-glutamine	2mM	Sigma
Penicillin/Streptomycin	100 U/ml/100 µg/ml	Sigma
Dexamethasone	10 nM	Sigma
TGF-β1	10ng/ml	PeptoTech, London, UK

Table S10 Overview of the compositions of the cartilage differentiation media. Abbreviation: DMEM, Dulbecco's Modified Eagle's Medium; TGF, transforming growth factor.

PBMC media	Unit	Company
RPMI 1630 media	NA	Sigma Aldrich
Fetal bovine serum	10%	Gibco
L-glutamine	2mM	Sigma
Penicillin/Streptomycin	100 U/ml/100 µg/ml	Sigma
2-β mercaptoethanol	55 µM	Sigma Aldrich

Table S11 Overview of the compositions of PBMC media. Abbreviation: RPMI, Moore and Roswell Park Memorial Institute; PBMC, peripheral blood mononuclear cell

Supplementary figures

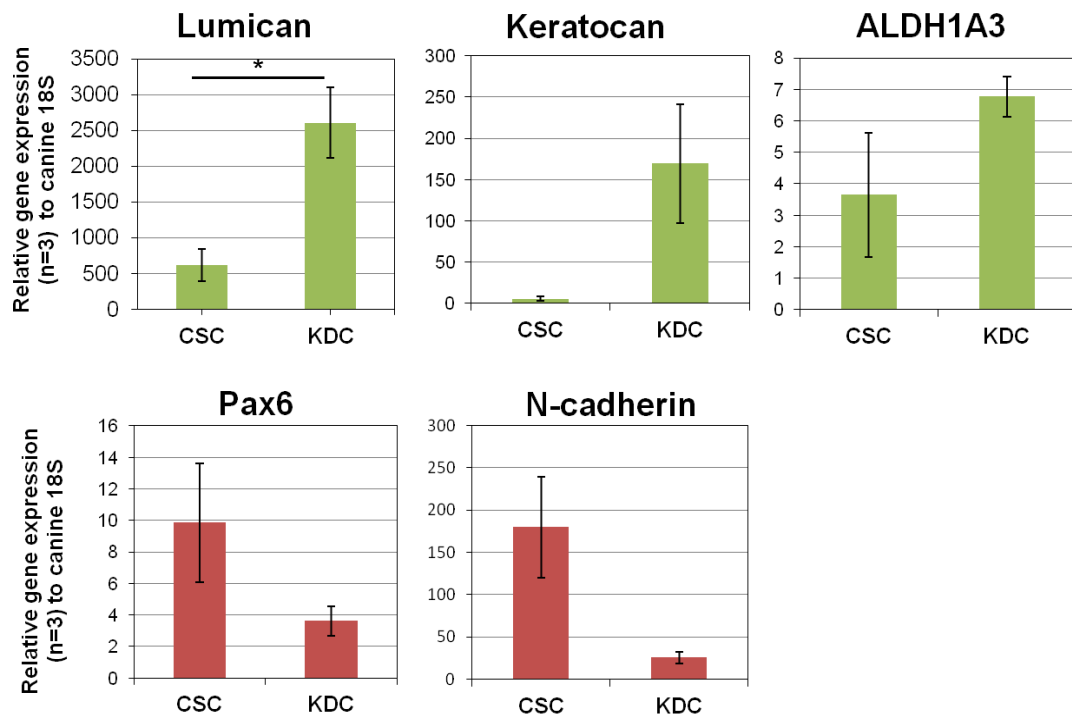


Figure S1 The graphs are demonstrating the mean relative gene expression levels to canine 18S of limbal CSC differentiated into keratocyte differentiated cells (KDC), Lumican was significantly upregulated ($P= 0.021$). Mean values of three independent biological replicates ($n=3$) \pm SE.

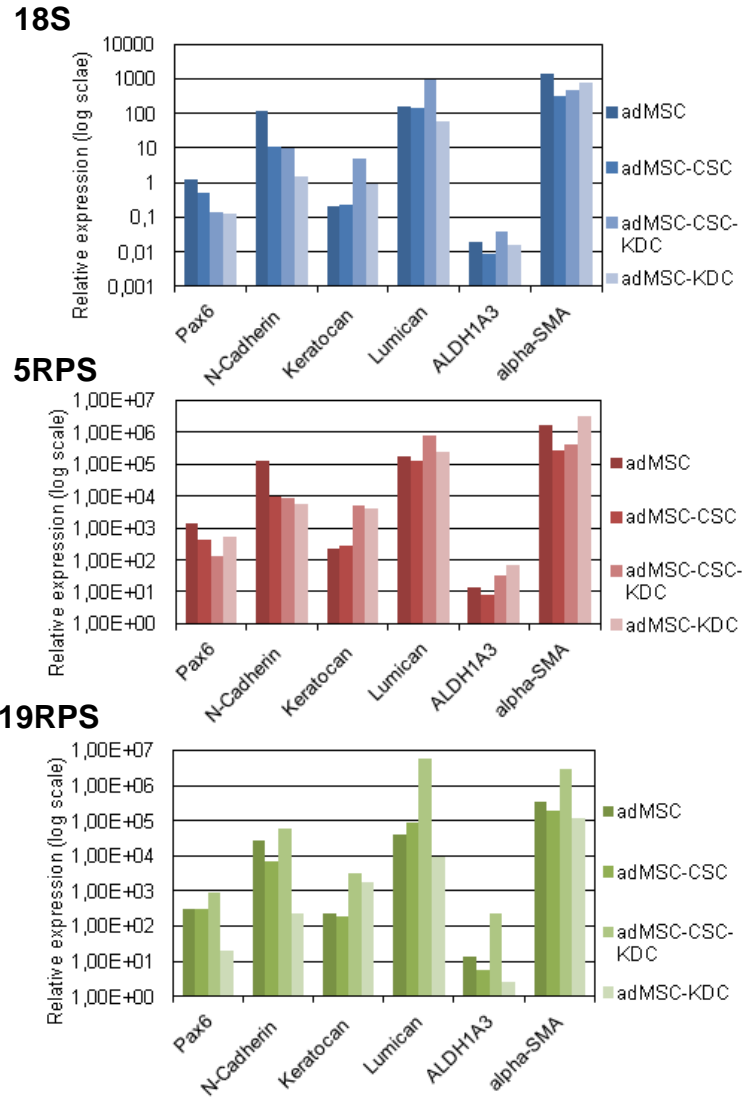


Figure S 2 The graphs demonstrating the relative gene expression levels of Pax6, N-cadherin, Keratocan, ALDH1A3, Lumican and α -SMA normalised to canine 18S, 5 ribosomal protein S (RPS) and 19RPS in adMSCs, adMSC-CSC, adMSC-CSC-KDC and adMSC-KDC of one donor (#17).

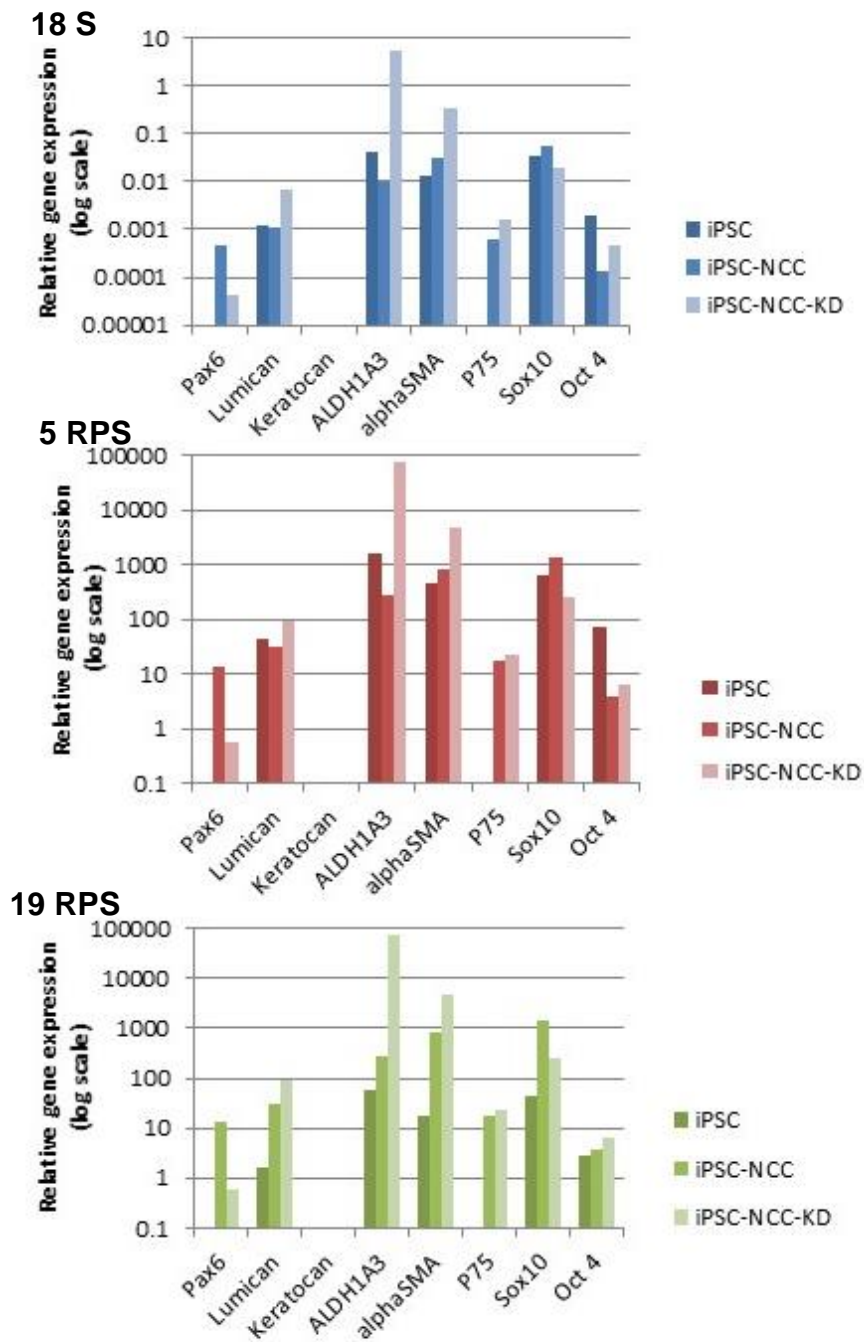


Figure S 3 The graphs demonstrating the relative gene expression levels of Pax6, N-cadherin, Keratocan, ALDH1A3, Lumican and α -SMA normalised to canine 18S, 5ribosomal protein S (RPS) and 19 RPS in iPSC, iPSC – NCC and iPSC-NCC-KD of one donor (#19).

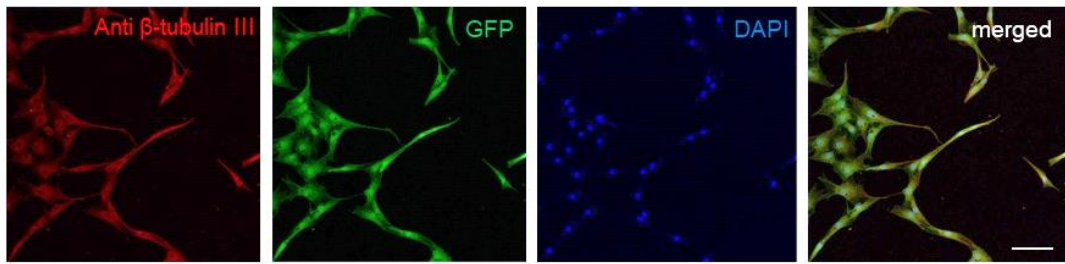


Figure S 4 CiPSC neural crest differentiated cells showed positive emission green fluorescent protein (GFP). Immunocytochemical staining of CiPSCs-NCCs (Media2) expressed Anti β -tubulin III. Nuclei are shown by DAPI counter staining. Scale bar: 20 μ m

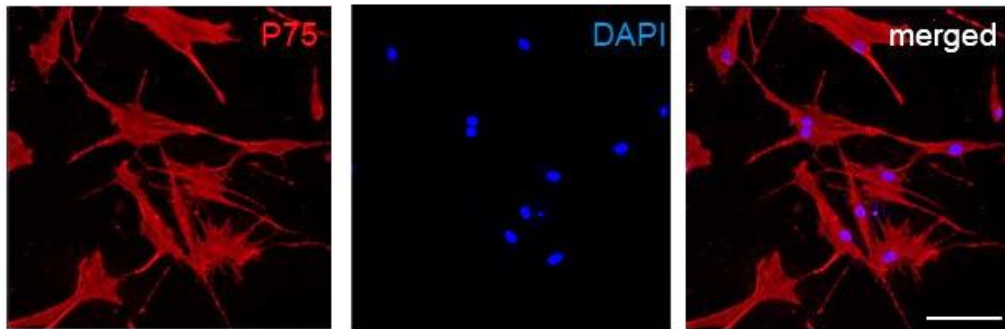


Figure S 5 Immunocytochemical staining of P75 on corneal stromal cells differentiated in keratocyte differentiation media. Nuclei are shown by DAPI counter staining. Scale bar: 20 μ m

References

Aboshiha, J., M. N. A. Jones, C. L. Hopkinson and D. F. P. Larkin (2018). "Differential Survival of Penetrating and Lamellar Transplants in Management of Failed Corneal Grafts." JAMA Ophthalmol **136**(8): 859-865.

Aharony, I., S. Michowiz and N. Goldenberg-Cohen (2017). "The promise of stem cell-based therapeutics in ophthalmology." Neural Regen Res **12**(2): 173-180.

Ahmad, S., R. Stewart, S. Yung, S. Kolli, L. Armstrong, M. Stojkovic, F. Figueiredo and M. Lako (2007). "Differentiation of human embryonic stem cells into corneal epithelial-like cells by in vitro replication of the corneal epithelial stem cell niche." Stem Cells **25**(5): 1145-1155.

Akhtar, S., B. C. Kerr, A. J. Hayes, C. E. Hughes, K. M. Meek and B. Caterson (2008). "Immunochemical localization of keratan sulfate proteoglycans in cornea, sclera, and limbus using a keratanase-generated neopeptide monoclonal antibody." Invest Ophthalmol Vis Sci **49**(6): 2424-2431.

Akopian, V., P. W. Andrews, S. Beil, N. Benvenisty, J. Brehm, M. Christie, A. Ford, V. Fox, P. J. Gokhale, L. Healy, F. Holm, O. Hovatta, B. B. Knowles, T. E. Ludwig, R. D. McKay, T. Miyazaki, N. Nakatsuji, S. K. Oh, M. F. Pera, J. Rossant, G. N. Stacey and H. Suemori (2010). "Comparison of defined culture systems for feeder cell free propagation of human embryonic stem cells." In Vitro Cell Dev Biol Anim **46**(3-4): 247-258.

Alexander, J. S., O. W. Blaschuk and F. R. Haselton (1993). "An N-cadherin-like protein contributes to solute barrier maintenance in cultured endothelium." J Cell Physiol **156**(3): 610-618.

Alio Del Barrio, J. L. and J. L. Alio (2018). "Cellular therapy of the corneal stroma: a new type of corneal surgery for keratoconus and corneal dystrophies." Eye Vis (Lond) **5**: 28.

Alió, J. L., J. L. Alió Del Barrio, M. El Zarif, A. Azaar, N. Makdissy, C. Khalil, W. Harb, I. El Achkar, Z. A. Jawad and M. P. De Miguel (2019). "Regenerative Surgery of the Corneal Stroma for Advanced Keratoconus: 1-Year Outcomes." Am J Ophthalmol **203**: 53-68.

Anokye-Danso, F., C. M. Trivedi, D. Jühr, M. Gupta, Z. Cui, Y. Tian, Y. Zhang, W. Yang, P. J. Gruber, J. A. Epstein and E. E. Morrisey (2011). "Highly efficient miRNA-mediated reprogramming of mouse and human somatic cells to pluripotency." Cell Stem Cell **8**(4): 376-388.

Armitage, W. J., C. Goodchild, M. D. Griffin, D. J. Gunn, J. Hjortdal, P. Lohan, C. C. Murphy, U. Pleyer, T. Ritter, D. M. Tole and B. Vabres (2019). "High-risk Corneal Transplantation: Recent Developments and Future Possibilities." Transplantation **103**(12): 2468-2478.

Arnalich-Montiel, F., S. Pastor, A. Blazquez-Martinez, J. Fernandez-Delgado, M. Nistal, J. L. Alio and M. P. De Miguel (2008). "Adipose-derived stem cells are a source for cell therapy of the corneal stroma." Stem Cells **26**(2): 570-579.

Arpitha, P., N. V. Prajna, M. Srinivasan and V. Muthukkaruppan (2005). "High expression of p63 combined with a large N/C ratio defines a subset of human limbal epithelial cells: implications on epithelial stem cells." Invest Ophthalmol Vis Sci **46**(10): 3631-3636.

Ashworth, S., J. Harrington, G. M. Hammond, K. K. Bains, E. Koudouna, A. J. Hayes, J. R. Ralphs, J. W. Regini, R. D. Young, R. Hayashi, K. Nishida, C. E. Hughes and A. J. Quantock (2020). "Chondroitin Sulfate as a Potential Modulator of the Stem Cell Niche in Cornea." Front Cell Dev Biol **8**: 567358.

Baird, A., T. Barsby and D. J. Guest (2015). "Derivation of Canine Induced Pluripotent Stem Cells." Reprod Domest Anim **50**(4): 669-676.

Baird, A. E. G., T. Barsby and D. J. Guest (2015). "Derivation of canine induced pluripotent stem cells." Reprod Dom Anim **50**: 669-676.

Bang, J. S., N. Y. Choi, M. Lee, K. Ko, H. J. Lee, Y. S. Park, D. Jeong, H. M. Chung and K. Ko (2018). "Optimization of episomal reprogramming for generation of human induced pluripotent stem cells from fibroblasts." Anim Cells Syst (Seoul) **22**(2): 132-139.

Barry, F., R. Boynton, M. Murphy and J. Zaia (2001). "The SH-3 and SH-4 Antibodies Recognize Distinct Epitopes on CD73 from Human Mesenchymal Stem Cells." Biochemical and Biophysical Research Communications **289**(2): 519-524.

Barry, F. P., R. E. Boynton, S. Haynesworth, J. M. Murphy and J. Zaia (1999). "The monoclonal antibody SH-2, raised against human mesenchymal stem cells, recognizes an epitope on endoglin (CD105)." Biochem Biophys Res Commun **265**(1): 134-139.

Barry, F. P. and J. M. Murphy (2004). "Mesenchymal stem cells: clinical applications and biological characterization." Int J Biochem Cell Biol **36**(4): 568-584.

Bartel, D. P. (2009). "MicroRNAs: target recognition and regulatory functions." Cell **136**(2): 215-233.

Bartholomew, A., C. Sturgeon, M. Siatskas, K. Ferrer, K. McIntosh, S. Patil, W. Hardy, S. Devine, D. Ucker, R. Deans, A. Moseley and R. Hoffman (2002). "Mesenchymal stem cells suppress lymphocyte proliferation in vitro and prolong skin graft survival in vivo." Exp Hematol **30**(1): 42-48.

Basu, S., A. J. Hertsberg, M. L. Funderburgh, M. K. Burrow, M. M. Mann, Y. Du, K. L. Lathrop, F. N. Syed-Picard, S. M. Adams, D. E. Birk and J. L. Funderburgh (2014). "Human limbal biopsy-derived stromal stem cells prevent corneal scarring." Sci Transl Med **6**(266): 266ra172.

Baum, J. L. (1970). "Melanocyte and Langerhans cell population of the cornea and limbus in the albino animal." Am J Ophthalmol **69**(4): 669-676.

Beales, M. P., J. L. Funderburgh, J. V. Jester and J. R. Hassell (1999). "Proteoglycan synthesis by bovine keratocytes and corneal fibroblasts: maintenance of the keratocyte phenotype in culture." Invest Ophthalmol Vis Sci **40**(8): 1658-1663.

Bearden, R. N., S. S. Huggins, K. J. Cummings, R. Smith, C. A. Gregory and W. B. Saunders (2017). "In-vitro characterization of canine multipotent stromal cells isolated from synovium, bone marrow, and adipose tissue: a donor-matched comparative study." Stem Cell Res Ther **8**(1): 218.

Benati, D., C. Patrizi and A. Recchia (2020). "Gene editing prospects for treating inherited retinal diseases." J Med Genet **57**(7): 437-444.

Berg, J. M., J. L. Tymoczko and L. Stryer (2011). Biochemistry. New York, W. H. Freeman and Company.

Berkowski, W. M., D. J. Gibson, S. Seo, L. R. Proietto, R. D. Whitley, G. S. Schultz and C. E. Plummer (2018). "Assessment of Topical Therapies for Improving the Optical Clarity Following Stromal Wounding in a Novel Ex Vivo Canine Cornea Model." Invest Ophthalmol Vis Sci **59**(13): 5509-5521.

Bertolo, A., F. Steffen, C. Malonzo-Marty and J. Stoyanov (2015). "Canine Mesenchymal Stem Cell Potential and the Importance of Dog Breed: Implication for Cell-Based Therapies." Cell Transplant **24**(10): 1969-1980.

Bittencourt, M. K., M. A. Barros, J. F. Martins, J. P. Vasconcellos, B. P. Morais, C. Pompeia, M. D. Bittencourt, K. D. Evangelho, I. Kerkis and C. V. Wenceslau (2016). "Allogeneic Mesenchymal Stem Cell Transplantation in Dogs With Keratoconjunctivitis Sicca." Cell Med **8**(3): 63-77.

Blazquez, R., F. M. Sanchez-Margallo, O. de la Rosa, W. Dalemans, V. Alvarez, R. Tarazona and J. G. Casado (2014). "Immunomodulatory Potential of Human Adipose Mesenchymal Stem Cells Derived Exosomes on in vitro Stimulated T Cells." Front Immunol **5**: 556.

Booth, C. and C. S. Potten (2000). "Gut instincts: thoughts on intestinal epithelial stem cells." J Clin Invest **105**(11): 1493-1499.

Branch, M. J., K. Hashmani, P. Dhillon, D. R. Jones, H. S. Dua and A. Hopkinson (2012). "Mesenchymal stem cells in the human corneal limbal stroma." Invest Ophthalmol Vis Sci **53**(9): 5109-5116.

Brinkhof, B., B. Spee, J. Rothuizen and L. C. Penning (2006). "Development and evaluation of canine reference genes for accurate quantification of gene expression." Anal Biochem **356**(1): 36-43.

Bunel, M., G. Chaudieu, C. Hamel, L. Lagoutte, G. Manes, N. Botherel, P. Brabet, P. Pilorge, C. André and P. Quignon (2019). "Natural models for retinitis pigmentosa: progressive retinal atrophy in dog breeds." Hum Genet **138**(5): 441-453.

Burgess, R. (2016). Fundamentals of stem cells. Stem Cells. B. R. Hoboken, New Jersey, John Wiley&Sons. **1**: 43-297.

Bushman, F. D. (2007). "Retroviral integration and human gene therapy." J Clin Invest **117**(8): 2083-2086.

Cadiou, E. and E. A. Ostrander (2007). "Canine genetics offers new mechanisms for the study of human cancer." Cancer Epidemiol Biomarkers Prev **16**(11): 2181-2183.

Carlson, E. C., C. Y. Liu, T. Chikama, Y. Hayashi, C. W. Kao, D. E. Birk, J. L. Funderburgh, J. V. Jester and W. W. Kao (2005). "Keratocan, a cornea-specific keratan sulfate proteoglycan, is regulated by lumican." J Biol Chem **280**(27): 25541-25547.

Català, P., N. Groen, J. A. Dehnen, E. Soares, A. J. H. van Velthoven, R. Nuijts, M. M. Dickman and V. L. S. LaPointe (2021). "Single cell transcriptomics reveals the heterogeneity of the human cornea to identify novel markers of the limbus and stroma." Sci Rep **11**(1): 21727.

Cen, Y. J., D. B. You, W. Wang and Y. Feng (2021). "Preliminary studies of constructing a tissue-engineered lamellar corneal graft by culturing mesenchymal stem cells onto decellularized corneal matrix." Int J Ophthalmol **14**(1): 10-18.

Chakravarti, S., W. M. Petroll, J. R. Hassell, J. V. Jester, J. H. Lass, J. Paul and D. E. Birk (2000). "Corneal opacity in lumican-null mice: defects in collagen fibril structure and packing in the posterior stroma." Invest Ophthalmol Vis Sci **41**(11): 3365-3373.

Chambers, I., D. Colby, M. Robertson, J. Nichols, S. Lee, S. Tweedie and A. Smith (2003). "Functional expression cloning of Nanog, a pluripotency sustaining factor in embryonic stem cells." Cell **113**(5): 643-655.

Chambers, S. M., Y. Mica, G. Lee, L. Studer and M. J. Tomishima (2016). "Dual-SMAD Inhibition/WNT Activation-Based Methods to Induce Neural Crest and Derivatives from Human Pluripotent Stem Cells." Methods Mol Biol **1307**: 329-343.

Chan, A. A., A. J. Hertsberg, M. L. Funderburgh, M. M. Mann, Y. Du, K. A. Davoli, J. D. Mich-Basso, L. Yang and J. L. Funderburgh (2013). "Differentiation of human embryonic stem cells into cells with corneal keratocyte phenotype." PLoS One **8**(2): e56831.

Chaurasia, S. S., H. Kaur, F. W. de Medeiros, S. D. Smith and S. E. Wilson (2009). "Dynamics of the expression of intermediate filaments vimentin and desmin during myofibroblast differentiation after corneal injury." Exp Eye Res **89**(2): 133-139.

Chen, S. Y., Y. Hayashida, M. Y. Chen, H. T. Xie and S. C. Tseng (2011). "A new isolation method of human limbal progenitor cells by maintaining close association with their niche cells." Tissue Eng Part C Methods **17**(5): 537-548.

Chen, Z., C. S. de Paiva, L. Luo, F. L. Kretzer, S. C. Pflugfelder and D. Q. Li (2004). "Characterization of putative stem cell phenotype in human limbal epithelia." Stem Cells **22**(3): 355-366.

Chlipala, E. A., C. M. Bendzinski, C. Dorner, R. Sartan, K. Copeland, R. Pearce, F. Doherty and B. Bolon (2020). "An Image Analysis Solution For Quantification and Determination of Immunohistochemistry Staining Reproducibility." Applied Immunohistochemistry & Molecular Morphology **28**(6): 428-436.

Choudhery, M. S., M. Badowski, A. Muise, J. Pierce and D. T. Harris (2014). "Donor age negatively impacts adipose tissue-derived mesenchymal stem cell expansion and differentiation." J Transl Med **12**: 8.

Chow, L., V. Johnson, J. Coy, D. Regan and S. Dow (2017). "Mechanisms of Immune Suppression Utilized by Canine Adipose and Bone Marrow-Derived Mesenchymal Stem Cells." Stem Cells Dev **26**(5): 374-389.

Chow, L., V. Johnson, D. Regan, W. Wheat, S. Webb, P. Koch and S. Dow (2017). "Safety and immune regulatory properties of canine induced pluripotent stem cell-derived mesenchymal stem cells." Stem Cell Res **25**: 221-232.

Chow, R. L. and R. A. Lang (2001) "Early eye development in vertebrates." Ann Rev Cell Develop Biol **17**, 255-296

Clevers, H., K. M. Loh and R. Nusse (2014). "Stem cell signaling. An integral program for tissue renewal and regeneration: Wnt signaling and stem cell control." Science **346**(6205): 1248012.

Cong, X., S. M. Zhang, M. W. Ellis and J. Luo (2019). "Large Animal Models for the Clinical Application of Human Induced Pluripotent Stem Cells." Stem Cells Dev **28**(19): 1288-1298.

Cook, C. S. (2013). Ocular malformation and congenital malformations. Veterinary Ophthalmology. K. N. Gelatt, Gilger B.C., Kern T.J., Wiley-Blackwell. **1**: 3-38.

Cooley, P. L. and P. F. Dice, 2nd (1990). "Corneal dystrophy in the dog and cat." Vet Clin North Am Small Anim Pract **20**(3): 681-692.

Corradetti, B., A. Meucci, D. Bizzaro, F. Cremonesi and A. Lange Consiglio (2013). "Mesenchymal stem cells from amnion and amniotic fluid in the bovine." Reproduction **145**(4): 391-400.

Cotsarelis, G., S. Z. Cheng, G. Dong, T. T. Sun and R. M. Lavker (1989). "Existence of slow-cycling limbal epithelial basal cells that can be preferentially stimulated to proliferate: implications on epithelial stem cells." Cell **57**(2): 201-209.

Cotsarelis, G., T. T. Sun and R. M. Lavker (1990). "Label-retaining cells reside in the bulge area of pilosebaceous unit: implications for follicular stem cells, hair cycle, and skin carcinogenesis." Cell **61**(7): 1329-1337.

Crispin, S. (1987). Crystalline stromal dystrophy in the Cavalier King Charles Spaniel. Proceedings of the 17th Annual Meeting of the American College of Veterinary Ophthalmologists

Crispin, S. (2002). "Ocular lipid deposition and hyperlipoproteinaemia." Prog Retin Eye Res **21**(2): 169-224.

Crispin, S. M. (1988). "Crystalline corneal dystrophy in the dog. Histochemical and ultrastructural study." Cornea **7**(2): 149-161.

Crispin, S. M. (2016). "Lipids and the eye." Vet J **212**: 90-98.

Cvekl, A. and E. R. Tamm (2004). "Anterior eye development and ocular mesenchyme: new insights from mouse models and human diseases." Bioessays **26**(4): 374-386.

Davis, A. B., L. V. Schnabel and B. C. Gilger (2019). "Subconjunctival bone marrow-derived mesenchymal stem cell therapy as a novel treatment alternative for equine immune-mediated keratitis: A case series." Vet Ophthalmol **22**(5): 674-682.

Dawson, G., J. L. Ubels and H. F. Edelhauser (2011). Cornea and sclera. In Adler's physiology of the eye. L. A. Levin, S. F. E. Nilsson, J. Ver Hoeve et al., Elsevier Saunders: 71-130.

De Castro, R. V. G., M. R. Tavares, F. F. Bressan, N. C. G. Pieri, A. Baracho Trindade Hill, A. F. Souza, R. N. C. N. da, D. S. Martins, C. E. Ambrosio, F. V. Meirelles and J. M. Garcia (2018). "In vitro identification of a stem cell population from canine hair follicle bulge region." Tissue Cell **50**: 43-50.

Desai, V. D., H. C. Hsia and J. E. Schwarzbauer (2014). "Reversible modulation of myofibroblast differentiation in adipose-derived mesenchymal stem cells." PLoS One **9**(1): e86865.

Di Iorio, E., V. Barbaro, A. Ruzza, D. Ponzin, G. Pellegrini and M. De Luca (2005). "Isoforms of DeltaNp63 and the migration of ocular limbal cells in human corneal regeneration." Proc Natl Acad Sci U S A **102**(27): 9523-9528.

Dias, I. E., D. F. Cardoso, C. S. Soares, L. C. Barros, C. A. Viegas, P. P. Carvalho and I. R. Dias (2021). "Clinical application of mesenchymal stem cells therapy in musculoskeletal injuries in dogs-a review of the scientific literature." Open Vet J **11**(2): 188-202.

Dias, I. E., P. O. Pinto, L. C. Barros, C. A. Viegas, I. R. Dias and P. P. Carvalho (2019). "Mesenchymal stem cells therapy in companion animals: useful for immune-mediated diseases?" BMC Vet Res **15**(1): 358.

Dice, P. (1974). Corneal dystrophy in the Airedale 5th Annual meeting of the American College of Veterinary Ophthalmologists.

Dlouhy, B. J., O. Awe, R. C. Rao, P. A. Kirby and P. W. Hitchon (2014). "Autograft-derived spinal cord mass following olfactory mucosal cell transplantation in a spinal cord injury patient: Case report." J Neurosurg Spine **21**(4): 618-622.

Dominici, M., K. Le Blanc, I. Mueller, I. Slaper-Cortenbach, F. Marini, D. Krause, R. Deans, A. Keating, D. Prockop and E. Horwitz (2006). "Minimal criteria for defining multipotent mesenchymal stromal cells. The International Society for Cellular Therapy position statement." Cytotherapy **8**(4): 315-317.

Dos Santos, A., A. Balayan, M. L. Funderburgh, J. Ngo, J. L. Funderburgh and S. X. Deng (2019). "Differentiation Capacity of Human Mesenchymal Stem Cells into Keratocyte Lineage." Invest Ophthalmol Vis Sci **60**(8): 3013-3023.

Doss, M. X. and A. Sachinidis (2019). "Current Challenges of iPSC-Based Disease Modeling and Therapeutic Implications." Cells **8**(5).

Du, J., Y. Wu, Z. Ai, X. Shi, L. Chen and Z. Guo (2014). "Mechanism of SB431542 in inhibiting mouse embryonic stem cell differentiation." Cell Signal **26**(10): 2107-2116.

Du, Y., E. C. Carlson, M. L. Funderburgh, D. E. Birk, E. Pearlman, N. Guo, W. W. Kao and J. L. Funderburgh (2009). "Stem cell therapy restores transparency to defective murine corneas." Stem Cells **27**(7): 1635-1642.

Du, Y., M. L. Funderburgh, M. M. Mann, N. SundarRaj and J. L. Funderburgh (2005). "Multipotent stem cells in human corneal stroma." Stem Cells **23**(9): 1266-1275.

Du, Y., D. S. Roh, M. L. Funderburgh, M. M. Mann, K. G. Marra, J. P. Rubin, X. Li and J. L. Funderburgh (2010). "Adipose-derived stem cells differentiate to keratocytes in vitro." Mol Vis **16**: 2680-2689.

Dubielzig, R. R., K. Ketring, G. McLellan and D. Albert (2010). Veterinary Ocular Pathology Saunders Elsevier: 800.

Dutton, L. C., S. A. V. Church, H. Hodgkiss-Geere, B. Catchpole, A. Huggins, J. Dudhia and D. J. Connolly (2018). "Cryopreservation of canine

cardiosphere-derived cells: Implications for clinical application." Cytometry A **93**(1): 115-124.

Dutton, L. C., J. Dudhia, B. Catchpole, H. Hodgkiss-Geere and D. Werling (2018). "Cardiosphere-derived cells suppress allogeneic lymphocytes by production of PGE2 acting via the EP4 receptor." Scien Rep **8**: 3351.

Dziasko, M. A., H. E. Armer, H. J. Levis, A. J. Shortt, S. Tuft and J. T. Daniels (2014). "Localisation of epithelial cells capable of holoclone formation in vitro and direct interaction with stromal cells in the native human limbal crypt." PLoS One **9**(4): e94283.

Dziasko, M. A. and J. T. Daniels (2016). "Anatomical features and cell-cell interactions in the human limbal epithelial stem cell niche." Ocul Surf **14**(3): 322-330.

Ekins, M., G. Waring and R. Harris (1980). "Oval lipid corneal opacities in Beagles. PartII: Natural history over four years and study of tear function." Journal- American Animal Hospital Association: 101-106.

Endo, Y., H. Ishiwata-Endo and K. M. Yamada (2012). "Extracellular matrix protein anosmin promotes neural crest formation and regulates FGF, BMP, and WNT activities." Dev Cell **23**(2): 305-316.

Engerman, R. L. and P. J. Colquhoun (1982). "Epithelial and mesothelial basement membranes in diabetic patients and dogs." Diabetologia **23**(6): 521-524.

Eslani, M., I. Putra, X. Shen, J. Hamouie, A. Tadepalli, K. N. Anwar, J. A. Kink, S. Ghassemi, G. Agnihotri, S. Reshetylo, A. Mashaghi, R. Dana, P. Hematti and A. R. Djalilian (2018). "Cornea-Derived Mesenchymal Stromal Cells Therapeutically Modulate Macrophage Immunophenotype and Angiogenic Function." Stem Cells **36**(5): 775-784.

Ezashi, T., Y. Yuan and R. M. Roberts (2016). "Pluripotent Stem Cells from Domesticated Mammals." Annu Rev Anim Biosci **4**: 223-253.

Fagerholm, P. (2003). "Phototherapeutic keratectomy: 12 years of experience." Acta Ophthalmol Scand **81**(1): 19-32.

Fernandez-Perez, J., M. Binner, C. Werner and L. J. Bray (2017). "Limbal stromal cells derived from porcine tissue demonstrate mesenchymal characteristics in vitro." Sci Rep **7**(1): 6377.

Figueiredo Pessôa, L. V. F. B., F.; Freude, K.K. (2019). "Induced pluripotent stem cells throughout the animal kingdom: Availability and applications." World Journal of Stem Cells **11**(8): 491-505.

Fini, M. E. and B. M. Stramer (2005). "How the cornea heals: cornea-specific repair mechanisms affecting surgical outcomes." Cornea **24**(8 Suppl): S2-s11.

Fonsatti, E., L. Sigalotti, P. Arslan, M. Altomonte and M. Maio (2003). "Emerging role of endoglin (CD105) as a marker of angiogenesis with clinical potential in human malignancies." Curr Cancer Drug Targets **3**(6): 427-432.

Forrester, J. V., A. D. Dick, P. G. McMenamin, F. Roberts and E. Pearlman (2016). Anatomy of the eye and orbit. The Eye, 4th edition, Basic Sciences in Practice, Saunders Ltd

Basic Sciences in Practice. A. D. D. Forrester J.V., Paul G. McMenamin, Fiona Roberts, Eric Pearlman, Elsevier: Pages 1-102. e 102.

Foster, J. W., R. M. Gouveia and C. J. Connon (2015). "Low-glucose enhances keratocyte-characteristic phenotype from corneal stromal cells in serum-free conditions." Sci Rep **5**: 10839.

Foster, J. W., K. Wahlin, S. M. Adams, D. E. Birk, D. J. Zack and S. Chakravarti (2017). "Cornea organoids from human induced pluripotent stem cells." Sci Rep **7**: 41286.

Frade, J. M. (2005). "Nuclear Translocation of the p75 Neurotrophin Receptor Cytoplasmic Domain in Response to Neurotrophin Binding." The Journal of Neuroscience **25**(6): 1407.

Fukuta, M., Y. Nakai, K. Kirino, M. Nakagawa, K. Sekiguchi, S. Nagata, Y. Matsumoto, T. Yamamoto, K. Umeda, T. Heike, N. Okumura, N. Koizumi, T. Sato, T. Nakahata, M. Saito, T. Otsuka, S. Kinoshita, M. Ueno, M. Ikeya and J. Toguchida (2014). "Derivation of mesenchymal stromal cells from pluripotent stem cells through a neural crest lineage using small molecule compounds with defined media." PLoS One **9**(12): e112291.

Funderburgh, M. L., Y. Du, M. M. Mann, N. SundarRaj and J. L. Funderburgh (2005). "PAX6 expression identifies progenitor cells for corneal keratocytes." Faseb j **19**(10): 1371-1373.

Gao, F., S. M. Chiu, D. A. Motan, Z. Zhang, L. Chen, H. L. Ji, H. F. Tse, Q. L. Fu and Q. Lian (2016). "Mesenchymal stem cells and immunomodulation: current status and future prospects." Cell Death Dis **7**: e2062.

Garcia, B., O. Garcia-Suarez, J. Merayo-Lloves, I. Alcalde, J. F. Alfonso, L. Fernandez-Vega Cueto, A. Meana, F. Vazquez and L. M. Quiros (2016). "Differential Expression of Proteoglycans by Corneal Stromal Cells in Keratoconus." Invest Ophthalmol Vis Sci **57**(6): 2618-2628.

Geburek, F., F. Roggel, H. T. M. van Schie, A. Beineke, R. Estrada, K. Weber, M. Hellige, K. Rohn, M. Jagodzinski, B. Welke, C. Hirschler, S. Conrad, T. Skutella, C. van de Lest, R. van Weeren and P. M. Stadler (2017). "Effect of single intralesional treatment of surgically induced equine superficial digital flexor tendon core lesions with adipose-derived mesenchymal stromal cells: a controlled experimental trial." Stem Cell Res Ther **8**(1): 129.

Gelatt, K., Brooks, DE (2011). Penetrating corneal grafts. Chapter 8: Surgery of the cornea and sclera. Veterinary Ophthalmic Surgery. K. Gelatt, Gelatt JP Philadelphia, USA, Saunders Elsevier: 223.

Gericota, B., J. S. Anderson, G. Mitchell, D. L. Borjesson, B. K. Sturges, J. A. Nolta and M. Sieber-Blum (2014). "Canine epidermal neural crest stem cells: characterization and potential as therapy candidate for a large animal model of spinal cord injury." Stem Cells Transl Med **3**(3): 334-345.

Giangreco, A., S. D. Reynolds and B. R. Stripp (2002). "Terminal bronchioles harbor a unique airway stem cell population that localizes to the bronchoalveolar duct junction." Am J Pathol **161**(1): 173-182.

Gilger, B. C., R. D. Whitley, S. A. McLaughlin, J. C. Wright and J. W. Drane (1991). "Canine corneal thickness measured by ultrasonic pachymetry." Am J Vet Res **52**(10): 1570-1572.

Gipson, I. K. (1989). "The epithelial basement membrane zone of the limbus." Eye (Lond) **3 (Pt 2)**: 132-140.

Glickman, L. T., M. Raghavan, D. W. Knapp, P. L. Bonney and M. H. Dawson (2004). "Herbicide exposure and the risk of transitional cell carcinoma of the urinary bladder in Scottish Terriers." J Am Vet Med Assoc **224**(8): 1290-1297.

Goes, R. M., F. L. Barbosa, E. S. S. J. De Faria and A. Haddad (2008). "Morphological and autoradiographic studies on the corneal and limbal epithelium of rabbits." Anat Rec (Hoboken) **291**(2): 191-203.

Goldberg, M. F. and A. J. Bron (1982). "Limbal palisades of Vogt." Trans Am Ophthalmol Soc **80**: 155-171.

Goncalves, N. J., F. F. Bressan, K. C. Roballo, F. V. Meirelles, P. L. Xavier, H. Fukumasu, C. Williams, M. Breen, S. Koh, R. Sper, J. Piedrahita and C. E. Ambrosio (2017). "Generation of LIF-independent induced pluripotent stem cells from canine fetal fibroblasts." Theriogenology **92**: 75-82.

Gong, Y., H. Duan, X. Wang, C. Zhao, W. Li, C. Dong, Z. Li and Q. Zhou (2021). "Transplantation of human induced pluripotent stem cell-derived neural crest cells for corneal endothelial regeneration." Stem Cell Res Ther **12**(1): 214.

Gonzalez, F., S. Boue and J. C. I. Belmonte (2011). "Methods for making induced pluripotent stem cells: reprogramming a la carte." Nature Reviews Genetics **12**: 231-242.

Gray, M. E. and C. E. West (2014). "Corneal injuries from liquid detergent pods." J aapos **18**(5): 494-495.

Gronkiewicz, K. M., E. A. Giuliano, A. Sharma and R. R. Mohan (2016). "Molecular mechanisms of suberoylanilide hydroxamic acid in the inhibition of

- TGF-beta1-mediated canine corneal fibrosis." Vet Ophthalmol **19**(6): 480-487.
- Guell, J. L., P. Verdaguer, D. Elies, O. Gris and F. Manero (2015). "Persistent stromal scar after PRK and CXL: different preoperative findings, similar complication." J Refract Surg **31**(3): 211-212.
- Guercio, A., S. Di Bella, S. Casella, P. Di Marco, C. Russo and G. Piccione (2013). "Canine mesenchymal stem cells (MSCs): characterization in relation to donor age and adipose tissue-harvesting site." Cell Biol Int **37**(8): 789-798.
- Guerrero-Esteo, M., T. Sanchez-Elsner, A. Letamendia and C. Bernabeu (2002). "Extracellular and cytoplasmic domains of endoglin interact with the transforming growth factor-beta receptors I and II." J Biol Chem **277**(32): 29197-29209.
- Guest, D. J., J. C. Ousey and M. R. Smith (2008). "Defining the expression of marker genes in equine mesenchymal stromal cells." Stem Cells Cloning **1**: 1-9.
- Guest, D. J., M. R. Smith and W. R. Allen (2010). "Equine embryonic stem-like cells and mesenchymal stromal cells have different survival rates and migration patterns following their injection into damaged superficial digital flexor tendon." Equine Vet J **42**(7): 636-642.
- Guo, G., J. Yang, J. Nichols, J. S. Hall, I. Eyres, W. Mansfield and A. Smith (2009). "Klf4 reverts developmentally programmed restriction of ground state pluripotency." Development **136**(7): 1063-1069.
- Guresh, A. M., S. J. Horvath, A. Gemensky-Metzler, E. Miller, V. Yildiz, J. V. Myers and G. M. Newbold (2021). "The effect of central corneal thickness on intraocular pressure values using various tonometers in the dog." Vet Ophthalmol **24 Suppl 1**: 154-161.
- Gwin, R. M., I. Lerner, J. K. Warren and G. Gum (1982). "Decrease in canine corneal endothelial cell density and increase in corneal thickness as functions of age." Invest Ophthalmol Vis Sci **22**(2): 267-271.
- Gwin, R. M., J. K. Warren, D. A. Samuelson and G. G. Gum (1983). "Effects of phacoemulsification and extracapsular lens removal on corneal thickness and endothelial cell density in the dog." Invest Ophthalmol Vis Sci **24**(2): 227-236.
- Hahnel, C., S. Somodi, D. G. Weiss and R. F. Guthoff (2000). "The keratocyte network of human cornea: a three-dimensional study using confocal laser scanning fluorescence microscopy." Cornea **19**(2): 185-193.
- Hall, M. N., W. S. Rosenkrantz, J. H. Hong, C. E. Griffin and C. M. Mendelsohn (2010). "Evaluation of the potential use of adipose-derived mesenchymal stromal cells in the treatment of canine atopic dermatitis: a pilot study." Vet Ther **11**(2): E1-14.

Harkin, D. G., L. Foyn, L. J. Bray, A. J. Sutherland, F. J. Li and B. G. Cronin (2015). "Concise reviews: can mesenchymal stromal cells differentiate into corneal cells? A systematic review of published data." Stem Cells **33**(3): 785-791.

Hashmani, K., M. J. Branch, L. E. Sidney, P. S. Dhillon, M. Verma, O. D. McIntosh, A. Hopkinson and H. S. Dua (2013). "Characterization of corneal stromal stem cells with the potential for epithelial transdifferentiation." Stem Cell Res Ther **4**(3): 75.

Hassell, J. R. and D. E. Birk (2010). "The molecular basis of corneal transparency." Exp Eye Res **91**(3): 326-335.

Hatoya, S., R. Torii, Y. Kondo, T. Okuno, K. Kobayashi, V. Wijewardana, N. Kawate, H. Tamada, T. Sawada, D. Kumagai, K. Sugiura and T. Inaba (2006). "Isolation and characterization of embryonic stem-like cells from canine blastocysts." Mol Reprod Dev **73**(3): 298-305.

Hayashi, R., Y. Ishikawa, Y. Sasamoto, R. Katori, N. Nomura, T. Ichikawa, S. Araki, T. Soma, S. Kawasaki, K. Sekiguchi, A. J. Quantock, M. Tsujikawa and K. Nishida (2016). "Co-ordinated ocular development from human iPS cells and recovery of corneal function." Nature **531**(7594): 376-380.

Hayashi, R., M. Yamato, H. Sugiyama, T. Sumide, J. Yang, T. Okano, Y. Tano and K. Nishida (2007). "N-Cadherin is expressed by putative stem/progenitor cells and melanocytes in the human limbal epithelial stem cell niche." Stem Cells **25**(2): 289-296.

Hayes, B., S. R. Fagerlie, A. Ramakrishnan, S. Baran, M. Harkey, L. Graf, M. Bar, A. Bendoraite, M. Tewari and B. Torok-Storb (2008). "Derivation, characterization, and in vitro differentiation of canine embryonic stem cells." Stem Cells **26**(2): 465-473.

Hensley, M. T., J. Tang, K. Woodruff, T. Defrancesco, S. Tou, C. M. Williams, M. Breen, K. Meurs, B. Keene and K. Cheng (2017). "Intracoronary allogeneic cardiosphere-derived stem cells are safe for use in dogs with dilated cardiomyopathy." J Cell Mol Med **21**(8): 1503-1512.

Hertsenberg, A. J. and J. L. Funderburgh (2015). "Stem Cells in the Cornea." Prog Mol Biol Transl Sci **134**: 25-41.

Hertsenberg, A. J. and J. L. Funderburgh (2016). "Generation of Corneal Keratocytes from Human Embryonic Stem Cells." Methods Mol Biol **1341**: 285-294.

Hertsenberg, A. J., G. Shojaati, M. L. Funderburgh, M. M. Mann, Y. Du and J. L. Funderburgh (2017). "Corneal stromal stem cells reduce corneal scarring by mediating neutrophil infiltration after wounding." PLoS One **12**(3): e0171712.

Higa, K., N. Kato, S. Yoshida, Y. Ogawa, J. Shimazaki, K. Tsubota and S. Shimmura (2013). "Aquaporin 1-positive stromal niche-like cells directly

interact with N-cadherin-positive clusters in the basal limbal epithelium." Stem Cell Res **10**(2): 147-155.

Hinrichs, K. (2018). "Assisted reproductive techniques in mares." Reprod Domest Anim **53 Suppl 2**: 4-13.

Hinz, B., G. Celetta, J. J. Tomasek, G. Gabbiani and C. Chaponnier (2001). "Alpha-smooth muscle actin expression upregulates fibroblast contractile activity." Mol Biol Cell **12**(9): 2730-2741.

Hinz, B., S. H. Phan, V. J. Thannickal, A. Galli, M. L. Bochaton-Piallat and G. Gabbiani (2007). "The myofibroblast: one function, multiple origins." Am J Pathol **170**(6): 1807-1816.

Hinz, B., S. H. Phan, V. J. Thannickal, M. Prunotto, A. Desmouliere, J. Varga, O. De Wever, M. Mareel and G. Gabbiani (2012). "Recent developments in myofibroblast biology: paradigms for connective tissue remodeling." Am J Pathol **180**(4): 1340-1355.

Hoehn, A. L., S. M. Thomasy, P. H. Kass, T. Horikawa, M. Samuel, O. R. Shull, K. A. Stewart and C. J. Murphy (2018). "Comparison of ultrasonic pachymetry and Fourier-domain optical coherence tomography for measurement of corneal thickness in dogs with and without corneal disease." Vet J **242**: 59-66.

Horwitz, E. M., K. Le Blanc, M. Dominici, I. Mueller, I. Slaper-Cortenbach, F. C. Marini, R. J. Deans, D. S. Krause and A. Keating (2005). "Clarification of the nomenclature for MSC: The International Society for Cellular Therapy position statement." Cytotherapy **7**(5): 393-395.

Hunter, L. S., D. J. Sidjanin, M. V. Hajar, J. L. Johnson, E. Kirkness, G. M. Acland and G. D. Aguirre (2007). "Cloning and characterization of canine PAX6 and evaluation as a candidate gene in a canine model of aniridia." Mol Vis **13**: 431-442.

Igwe, J. C., Q. Gao, T. Kizivat, W. W. Kao and I. Kalajzic (2011). "Keratocan is expressed by osteoblasts and can modulate osteogenic differentiation." Connect Tissue Res **52**(5): 401-407.

Isla-Magrané, H., A. Veiga, J. García-Arumí and A. Duarri (2021). "Multicellular organoids from human induced pluripotent stem cells displayed retinal, corneal, and retinal pigment epithelium lineages." Stem Cell Res Ther **Nov 22**(12).

Jaksz, M., M. C. Fischer, E. Fenollosa-Romero and C. Busse (2021). "Autologous corneal graft for the treatment of deep corneal defects in dogs: 15 cases (2014-2017)." J Small Anim Pract **62**(2): 123-130.

James, D., A. J. Levine, D. Besser and A. Hemmati-Brivanlou (2005). "TGFbeta/activin/nodal signaling is necessary for the maintenance of pluripotency in human embryonic stem cells." Development **132**(6): 1273-1282.

- Jester, J. V. (2008). "Corneal Crystallins and the Development of Cellular Transparency." Semin Cell Dev Biol **19**(2): 82-93.
- Jester, J. V., P. A. Barry-Lane, H. D. Cavanagh and W. M. Petroll (1996). "Induction of alpha-smooth muscle actin expression and myofibroblast transformation in cultured corneal keratocytes." Cornea **15**(5): 505-516.
- Jester, J. V., W. M. Petroll, P. A. Barry and H. D. Cavanagh (1995). "Expression of alpha-smooth muscle (alpha-SM) actin during corneal stromal wound healing." Invest Ophthalmol Vis Sci **36**(5): 809-819.
- Jiang, Z., G. Liu, F. Meng, W. Wang, P. Hao, Y. Xiang, Y. Wang, R. Han, F. Li, L. Wang and X. Li (2017). "Paracrine effects of mesenchymal stem cells on the activation of keratocytes." Br J Ophthalmol **101**(11): 1583-1590.
- Joseph, A., P. Hossain, S. Jham, R. E. Jones, P. Tighe, R. S. McIntosh and H. S. Dua (2003). "Expression of CD34 and L-selectin on human corneal keratocytes." Invest Ophthalmol Vis Sci **44**(11): 4689-4692.
- Joseph, R., O. P. Srivastava and R. R. Pfister (2016). "Modeling Keratoconus Using Induced Pluripotent Stem Cells." Invest Ophthalmol Vis Sci **57**(8): 3685-3697.
- Kafarnik, C., J. Fritsche and S. Reese (2007). "In vivo confocal microscopy in the normal corneas of cats, dogs and birds." Vet Ophthalmol **10**(4): 222-230.
- Kafarnik, C., J. Fritsche and S. Reese (2008). "Corneal innervation in mesocephalic and brachycephalic dogs and cats: assessment using in vivo confocal microscopy." Vet Ophthalmol **11**(6): 363-367.
- Kafarnik, C., A. McClellan, M. Dziasko, J. T. Daniels and D. J. Guest (2020). "Canine Corneal Stromal Cells Have Multipotent Mesenchymal Stromal Cell Properties In Vitro." Stem Cells Dev **29**(7): 425-438.
- Kalkan, T. and A. Smith (2014). "Mapping the route from naive pluripotency to lineage specification." Philos Trans R Soc Lond B Biol Sci **369**(1657).
- Karwacki-Neisius, V., J. Goke, R. Osorno, F. Halbritter, J. H. Ng, A. Y. Weisse, F. C. Wong, A. Gagliardi, N. P. Mullin, N. Festuccia, D. Colby, S. R. Tomlinson, H. H. Ng and I. Chambers (2013). "Reduced Oct4 expression directs a robust pluripotent state with distinct signaling activity and increased enhancer occupancy by Oct4 and Nanog." Cell Stem Cell **12**(5): 531-545.
- Kawakita, T., S. Shimmura, K. Higa, E. M. Espana, H. He, J. Shimazaki, K. Tsubota and S. C. Tseng (2009). "Greater growth potential of p63-positive epithelial cell clusters maintained in human limbal epithelial sheets." Invest Ophthalmol Vis Sci **50**(10): 4611-4617.
- Kern, T. J. (1990). "Ulcerative keratitis." Vet Clin North Am Small Anim Pract **20**(3): 643-666.

Kim, A., N. Lakshman, D. Karamichos and W. M. Petroll (2010). "Growth factor regulation of corneal keratocyte differentiation and migration in compressed collagen matrices." Invest Ophthalmol Vis Sci **51**(2): 864-875.

Kim, W. J., R. R. Mohan, R. R. Mohan and S. E. Wilson (1999). "Effect of PDGF, IL-1alpha, and BMP2/4 on corneal fibroblast chemotaxis: expression of the platelet-derived growth factor system in the cornea." Invest Ophthalmol Vis Sci **40**(7): 1364-1372.

Kishimoto, T. E. and K. Uchida (2018). "Expression of Oligodendrocyte Precursor Cell Markers in Canine Oligodendrogliomas." Vet Pathol **55**(5): 634-644.

Kisiel, A. H., L. A. McDuffee, E. Masaoud, T. R. Bailey, B. P. Esparza Gonzalez and R. Nino-Fong (2012). "Isolation, characterization, and in vitro proliferation of canine mesenchymal stem cells derived from bone marrow, adipose tissue, muscle, and periosteum." Am J Vet Res **73**(8): 1305-1317.

Klyushnenkova, E., J. D. Mosca, V. Zernetkina, M. K. Majumdar, K. J. Beggs, D. W. Simonetti, R. J. Deans and K. R. McIntosh (2005). "T cell responses to allogeneic human mesenchymal stem cells: immunogenicity, tolerance, and suppression." J Biomed Sci **12**(1): 47-57.

Koh, S., R. Thomas, S. Tsai, S. Bischoff, J. H. Lim, M. Breen, N. J. Olby and J. A. Piedrahita (2013). "Growth requirements and chromosomal instability of induced pluripotent stem cells generated from adult canine fibroblasts." Stem Cells Dev **22**(6): 951-963.

Köksal, M., S. Kargi, G. Gürelik and F. Akata (2004). "Phototherapeutic keratectomy in Schnyder crystalline corneal dystrophy." Cornea **23**(3): 311-313.

Kriston-Pal, E., A. Czibula, Z. Gyuris, G. Balka, A. Seregi, F. Sukosd, M. Suth, E. Kiss-Toth, L. Haracska, F. Uher and E. Monostori (2017). "Characterization and therapeutic application of canine adipose mesenchymal stem cells to treat elbow osteoarthritis." Can J Vet Res **81**(1): 73-78.

Ksander, B. R., P. E. Kolovou, B. J. Wilson, K. R. Saab, Q. Guo, J. Ma, S. P. McGuire, M. S. Gregory, W. J. Vincent, V. L. Perez, F. Cruz-Guilloty, W. W. Kao, M. K. Call, B. A. Tucker, Q. Zhan, G. F. Murphy, K. L. Lathrop, C. Alt, L. J. Mortensen, C. P. Lin, J. D. Zieske, M. H. Frank and N. Y. Frank (2014). "ABCB5 is a limbal stem cell gene required for corneal development and repair." Nature **511**(7509): 353-357.

Kukurba, K. R. and S. B. Montgomery (2015). "RNA Sequencing and Analysis." Cold Spring Harb Protoc **2015**(11): 951-969.

Kumar, A., H. Yun, M. L. Funderburgh and Y. Du (2021). "Regenerative therapy for the Cornea." Prog Retin Eye Res: 101011.

Kumar, S., P. Dolle, N. B. Ghyselinck and G. Duester (2017). "Endogenous retinoic acid signaling is required for maintenance and regeneration of cornea." Exp Eye Res **154**: 190-195.

Kureshi, A. K., M. Dziasko, J. L. Funderburgh and J. T. Daniels (2015). "Human corneal stromal stem cells support limbal epithelial cells cultured on RAFT tissue equivalents." Sci Rep **5**: 16186.

Kureshi, A. K., J. L. Funderburgh and J. T. Daniels (2014). "Human corneal stromal stem cells exhibit survival capacity following isolation from stored organ-culture corneas." Invest Ophthalmol Vis Sci **55**(11): 7583-7588.

Kuriyan, A. E., T. A. Albini, J. H. Townsend, M. Rodriguez, H. K. Pandya, R. E. Leonard, 2nd, M. B. Parrott, P. J. Rosenfeld, H. W. Flynn, Jr. and J. L. Goldberg (2017). "Vision Loss after Intravitreal Injection of Autologous "Stem Cells" for AMD." N Engl J Med **376**(11): 1047-1053.

Kuroda, T., M. Tada, H. Kubota, H. Kimura, S. Y. Hatano, H. Suemori, N. Nakatsuji and T. Tada (2005). "Octamer and Sox elements are required for transcriptional cis regulation of Nanog gene expression." Mol Cell Biol **25**(6): 2475-2485.

Labelle, A. L., K. Psutka, S. P. Collins and R. E. Hamor (2014). "Use of hydropulsion for the treatment of superficial corneal foreign bodies: 15 cases (1999-2013)." J Am Vet Med Assoc **244**(4): 476-479.

Lacerda, R. P., M. T. Pena Gimenez, F. Laguna, D. Costa, J. Rios and M. Leiva (2016). "Corneal grafting for the treatment of full-thickness corneal defects in dogs: a review of 50 cases." Vet Ophthalmol **20**(3): 222-231.

Lakshman, N., A. Kim and W. M. Petroll (2010). "Characterization of corneal keratocyte morphology and mechanical activity within 3-D collagen matrices." Exp Eye Res **90**(2): 350-359.

Lakshman, N. and W. M. Petroll (2012). "Growth factor regulation of corneal keratocyte mechanical phenotypes in 3-D collagen matrices." Invest Ophthalmol Vis Sci **53**(3): 1077-1086.

Le Blanc, K. and O. Ringdén (2007). "Immunomodulation by mesenchymal stem cells and clinical experience." J Intern Med **262**(5): 509-525.

Ledbetter, E., Gilger BC (2013). Disease and surgery of the canine cornea and sclera. Veterinary Ophthalmology. K. N. Gelatt, Gilger B.C., Kern T.J. Ames, Iowa, USA, Wiley-Blackwell. Vol 2: 976-1050.

Lee, A. S., D. Xu, J. R. Plews, P. K. Nguyen, D. Nag, J. K. Lyons, L. Han, S. Hu, F. Lan, J. Liu, M. Huang, K. H. Narsinh, C. T. Long, P. E. de Almeida, B. Levi, N. Kooreman, C. Bangs, C. Pacharinsak, F. Ikeno, A. C. Yeung, S. S. Gambhir, R. C. Robbins, M. T. Longaker and J. C. Wu (2011). "Preclinical derivation and imaging of autologously transplanted canine induced pluripotent stem cells." J Biol Chem **286**(37): 32697-32704.

- Lengner, C. J., G. G. Welstead and R. Jaenisch (2008). "The pluripotency regulator Oct4: a role in somatic stem cells?" Cell Cycle **7**(6): 725-728.
- Leonard, B. C., K. Cosert, M. Winkler, A. Marangakis, S. M. Thomasy, C. J. Murphy, J. V. Jester and V. K. Raghunathan (2020). "Stromal Collagen Arrangement Correlates with Stiffness of the Canine Cornea." Bioengineering **7**(1): 4.
- Leung, A. W., B. Murdoch, A. F. Salem, M. S. Prasad, G. A. Gomez and M. I. Garcia-Castro (2016). "WNT/beta-catenin signaling mediates human neural crest induction via a pre-neural border intermediate." Development **143**(3): 398-410.
- Levi, B., E. R. Nelson, K. Brown, A. W. James, D. Xu, R. Dunlevie, J. C. Wu, M. Lee, B. Wu, G. W. Commons, D. Vistnes and M. T. Longaker (2011). "Differences in osteogenic differentiation of adipose-derived stromal cells from murine, canine, and human sources in vitro and in vivo." Plast Reconstr Surg **128**(2): 373-386.
- Levis, H. J., A. K. Kureshi, I. Massie, L. Morgan, A. J. Vernon and J. T. Daniels (2015). "Tissue Engineering the Cornea: The Evolution of RAFT." J Funct Biomater **6**(1): 50-65.
- Levy, S. G., A. C. McCartney and J. Moss (1995). "The distribution of fibronectin and P component in Descemet's membrane: an immunoelectron microscopic study." Curr Eye Res **14**(9): 865-870.
- Li, H., Y. Dai, J. Shu, R. Yu, Y. Guo and J. Chen (2015). "Spheroid cultures promote the stemness of corneal stromal cells." Tissue Cell **47**(1): 39-48.
- Li, H. C., C. Stoicov, A. B. Rogers and J. Houghton (2006). "Stem cells and cancer: evidence for bone marrow stem cells in epithelial cancers." World J Gastroenterol **12**(3): 363-371.
- Lim, S. H., X. Y. Liu, H. Song, K. J. Yarema and H. Q. Mao (2010). "The effect of nanofiber-guided cell alignment on the preferential differentiation of neural stem cells." Biomaterials **31**(34): 9031-9039.
- Liu, C. Y., D. E. Birk, J. R. Hassell, B. Kane and W. W. Kao (2003). "Keratocan-deficient mice display alterations in corneal structure." J Biol Chem **278**(24): 21672-21677.
- Liu, H., O. Mohamed, D. Dufort and V. A. Wallace (2003). "Characterization of Wnt signaling components and activation of the Wnt canonical pathway in the murine retina." Dev Dyn **227**(3): 323-334.
- Liu, H., J. Zhang, C. Y. Liu, Y. Hayashi and W. W. Kao (2012). "Bone marrow mesenchymal stem cells can differentiate and assume corneal keratocyte phenotype." J Cell Mol Med **16**(5): 1114-1124.
- Liu, J. and Z. Li (2021). "Resident Innate Immune Cells in the Cornea." Front Immunol **12**: 620284.

Liu, Y., B. Deng, Y. Zhao, S. Xie and R. Nie (2013). "Differentiated markers in undifferentiated cells: expression of smooth muscle contractile proteins in multipotent bone marrow mesenchymal stem cells." Dev Growth Differ **55**(5): 591-605.

Liu, Z., Y. Q. Jin, L. Chen, Y. Wang, X. Yang, J. Cheng, W. Wu, Z. Qi and Z. Shen (2015). "Specific marker expression and cell state of Schwann cells during culture in vitro." PLoS One **10**(4): e0123278.

Livak, K. J. a. S., T.D. (2001). "Analysis of Relative Gene Expression Data Using Real-Time Quantitative PCR and the 2- $\Delta\Delta$ CT Method." Methods **25**(4): 402-408.

Ljubimov, A. V., R. E. Burgeson, R. J. Butkowski, A. F. Michael, T. T. Sun and M. C. Kenney (1995). "Human corneal basement membrane heterogeneity: topographical differences in the expression of type IV collagen and laminin isoforms." Lab Invest **72**(4): 461-473.

Lohan, P., N. Murphy, O. Treacy, K. Lynch, M. Morcos, B. Chen, A. E. Ryan, M. D. Griffin and T. Ritter (2018). "Third-Party Allogeneic Mesenchymal Stromal Cells Prevent Rejection in a Pre-sensitized High-Risk Model of Corneal Transplantation." Front Immunol **9**: 2666.

Luo, J. and J. B. Cibelli (2016). "Conserved Role of bFGF and a Divergent Role of LIF for Pluripotency Maintenance and Survival in Canine Pluripotent Stem Cells." Stem Cells Dev **25**(21):1670-1680.

Luo, J., S. T. Suhr, E. A. Chang, K. Wang, P. J. Ross, L. L. Nelson, P. J. Venta, J. G. Knott and J. B. Cibelli (2011). "Generation of leukemia inhibitory factor and basic fibroblast growth factor-dependent induced pluripotent stem cells from canine adult somatic cells." Stem Cells Dev **20**(10): 1669-1678.

Lwigale, P. Y. (2015). "Corneal Development: Different Cells from a Common Progenitor." Prog Mol Biol Transl Sci **134**: 43-59.

Ma, J. and P. Lwigale (2019). "Transformation of the transcriptomic profile of mouse periocular mesenchyme during formation of the embryonic cornea." Invest Ophthalmol Vis Sci **60**(2): 661-676.

Macdonald, R. and S. Wilson (1997). "Distribution of Pax6 protein during eye development suggests discrete roles in proliferative and differentiated visual cells." Dev Genes Evol **206**(6): 363-369.

Mahabadi, N., C. N. Czyz, M. Tariq and S. J. Havens (2021). Corneal Graft Rejection. StatPearls. Treasure Island (FL), StatPearls Publishing LLC. Bookshelf ID: NBK519043

Mai, J., Q. Hu, Y. Xie, S. Su, Q. Qiu, W. Yuan, Y. Yang, E. Song, Y. Chen and J. Wang (2015). "Dyssynchronous pacing triggers endothelial-mesenchymal transition through heterogeneity of mechanical stretch in a canine model." Circ J **79**(1): 201-209.

Maini, S., S. L. Ricketts, L. Pettitt, J. A. C. Oliver and C. S. Mellersh (2018). "Corneal dystrophy in the cavalier king charles spaniel—A candidate gene study." Abstract: Annual Scientific Meeting of the European College of Veterinary Ophthalmologists, Florence, Italy May 10 - 13, 2018. Vet Ophthalmol **21**: Pages E1-E35.

Majo, F., A. Rochat, M. Nicolas, G. A. Jaoudé and Y. Barrandon (2008). "Oligopotent stem cells are distributed throughout the mammalian ocular surface." Nature **456**(7219): 250-254.

Maltseva, O., P. Folger, D. Zekaria, S. Petridou and S. K. Masur (2001). "Fibroblast growth factor reversal of the corneal myofibroblast phenotype." Invest Ophthalmol Vis Sci **42**(11): 2490-2495.

Mansoor, H. and H. S. Ong (2019). "Current Trends and Future Perspective of Mesenchymal Stem Cells and Exosomes in Corneal Diseases." Int J Mol Sci **20** (12): 2853.

Marfurt, C. F., C. J. Murphy and J. L. Florczak (2001). "Morphology and neurochemistry of canine corneal innervation." Invest Ophthalmol Vis Sci **42**(10): 2242-2251.

Martin, M. J., A. Muotri, F. Gage and A. Varki (2005). "Human embryonic stem cells express an immunogenic nonhuman sialic acid." Nat Med **11**(2): 228-232.

Martinez-Carrasco, R., L. I. Sanchez-Abarca, C. Nieto-Gomez, E. Martin Garcia, F. Sanchez-Guijo, P. Argueso, J. Aijon, E. Hernandez-Galilea and A. Velasco (2019). "Subconjunctival injection of mesenchymal stromal cells protects the cornea in an experimental model of GVHD." Ocul Surf **17**(2): 285-294.

Mason, C. and P. Dunnill (2008). "A brief definition of regenerative medicine." Regen Med **3**(1): 1-5.

Maycock, N. J. and J. Marshall (2014). "Genomics of corneal wound healing: a review of the literature." Acta Ophthalmol **92**(3): e170-184.

McCabe, K. L. and R. Lanza (2014). Corneal Replacement Tissue. In Principles of Tissue Engineering. R. Lanza, R. Langer and V. J., Academic Press: 1413-1425.

McCrea, P. D., M. T. Maher and C. J. Gottardi (2015). "Nuclear signaling from cadherin adhesion complexes." Curr Top Dev Biol **112**: 129-196.

McGreevy, J. W., C. H. Hakim, M. A. McIntosh and D. Duan (2015). "Animal models of Duchenne muscular dystrophy: from basic mechanisms to gene therapy." Dis Model Mech **8**(3): 195-213.

McIntosh, K., S. Zvonic, S. Garrett, J. B. Mitchell, Z. E. Floyd, L. Hammill, A. Kloster, Y. Di Halvorsen, J. P. Ting, R. W. Storms, B. Goh, G. Kilroy, X. Wu

and J. M. Gimble (2006). "The immunogenicity of human adipose-derived cells: temporal changes in vitro." Stem Cells **24**(5): 1246-1253.

Medeiros, C. S., G. K. Marino, M. R. Santhiago and S. E. Wilson (2018). "The Corneal Basement Membranes and Stromal Fibrosis." Invest Ophthalmol Vis Sci **59**(10): 4044-4053.

Meekins, J., A. Rankin and D. A. Samuelson (2021). Ophthalmic anatomy. In Veterinary Ophthalmology. K. N. Gelatt. Hoboken, N.J., Wiley Blackwell. Vol 1: 41-124.

Mei, H., M. N. Nakatsu, E. R. Baclagon and S. X. Deng (2014). "Frizzled 7 maintains the undifferentiated state of human limbal stem/progenitor cells." Stem Cells **32**(4): 938-945.

Mellersh, C. (2012). "DNA testing and domestic dogs." Mamm Genome **23**(1-2): 109-123.

Menendez, L., T. A. Yatskievych, P. B. Antin and S. Dalton (2011). "Wnt signaling and a Smad pathway blockade direct the differentiation of human pluripotent stem cells to multipotent neural crest cells." Proc Natl Acad Sci U S A **108**(48): 19240-19245.

Menon, D. V., D. Patel, C. G. Joshi and A. Kumar (2019). "The road less travelled: The efficacy of canine pluripotent stem cells." Exp Cell Res **377**(1-2): 94-102.

Mercati, F., L. Pascucci, P. Ceccarelli, C. Dall'Aglio, V. Pedini and A. M. Gargiulo (2009). "Expression of mesenchymal stem cell marker CD90 on dermal sheath cells of the anagen hair follicle in canine species." Eur J Histochem **53**(3): 159-166.

Meyer-Lindenberg, A. and T. Kilchling (2018). "[Use of mesenchymal stemcells in dogs]." Tierarztl Prax Ausg K Kleintiere Heimtiere **46**(6): 416-425.

Meza-León, B., D. Gratzinger, A. G. Aguilar-Navarro, F. G. Juárez-Aguilar, V. I. Rebel, E. Torlakovic, L. E. Purton, E. M. Dorantes-Acosta, A. Escobar-Sánchez, J. E. Dick and E. Flores-Figueroa (2021). "Human, mouse, and dog bone marrow show similar mesenchymal stromal cells within a distinctive microenvironment." Exp Hematol **100**: 41-51.

Mienaltowski, M. J. and D. E. Birk (2014). "Mouse models in tendon and ligament research." Adv Exp Med Biol **802**: 201-230.

Mikhailova, A., T. Ilmarinen, A. Ratnayake, G. Petrovski, H. Uusitalo, H. Skottman and M. Rafat (2016). "Human pluripotent stem cell-derived limbal epithelial stem cells on bioengineered matrices for corneal reconstruction." Exp Eye Res **146**: 26-34.

Mikhailova, A., T. Ilmarinen, H. Uusitalo and H. Skottman (2014). "Small-molecule induction promotes corneal epithelial cell differentiation from human induced pluripotent stem cells." Stem Cell Reports **2**(2): 219-231.

Mitsui, K., Y. Tokuzawa, H. Itoh, K. Segawa, M. Murakami, K. Takahashi, M. Maruyama, M. Maeda and S. Yamanaka (2003). "The homeoprotein Nanog is required for maintenance of pluripotency in mouse epiblast and ES cells." Cell **113**(5): 631-642.

Mittal, S. K., M. Omoto, A. Amouzegar, A. Sahu, A. Rezazadeh, K. R. Katikireddy, D. I. Shah, S. K. Sahu and S. K. Chauhan (2016). "Restoration of Corneal Transparency by Mesenchymal Stem Cells." Stem Cell Reports **7**(4): 583-590.

Mochel, J. P., A. E. Jergens, D. Kingsbury, H. J. Kim, M. G. Martin and K. Allenspach (2017). "Intestinal Stem Cells to Advance Drug Development, Precision, and Regenerative Medicine: A Paradigm Shift in Translational Research." AAPS J **20**(1): 17.

Moller-Pedersen, T., T. Ledet and N. Ehlers (1994). "The keratocyte density of human donor corneas." Curr Eye Res **13**(2): 163-169.

Monteiro, I., S. Vigano, M. Faouzi, I. Treilleux, O. Michielin, C. Ménétrier-Caux, C. Caux, P. Romero and L. de Leval (2018). "CD73 expression and clinical significance in human metastatic melanoma." Oncotarget **9**(42): 26659-26669.

Morgan, S. R., E. P. Dooley, C. Kamma-Lorger, J. L. Funderburgh, M. L. Funderburgh and K. M. Meek (2016). "Early wound healing of laser in situ keratomileusis-like flaps after treatment with human corneal stromal stem cells." J Cataract Refract Surg **42**(2): 302-309.

Morita, M., N. Fujita, A. Takahashi, E. R. Nam, S. Yui, C. S. Chung, N. Kawahara, H. Y. Lin, K. Tsuzuki, T. Nakagawa and R. Nishimura (2015). "Evaluation of ABCG2 and p63 expression in canine cornea and cultivated corneal epithelial cells." Vet Ophthalmol **18**(1): 59-68.

Moro, L. N., G. Amin, V. Furmento, A. Waisman, X. Garate, G. Neiman, A. La Greca, N. L. Santín Velazque, C. Luzzani, G. E. Sevlever, G. Vichera and S. G. Miriuka (2018). "MicroRNA characterization in equine induced pluripotent stem cells." PLoS One **13**(12): e0207074.

Morrin, L. A., G. O. Waring, 3rd and W. Spangler (1982). "Oval lipid corneal opacities in beagles: ultrastructure of normal beagle cornea." Am J Vet Res **43**(3): 443-453.

Moshirfar, M., P. Bennett and Y. Ronquillo (2021). Corneal Dystrophy. StatPearls. Treasure Island (FL), StatPearls Publishing LLC. Bookshelf ID: NBK557865

Mukhey, D., J. B. Phillips, J. T. Daniels and A. K. Kureshi (2018). "Controlling human corneal stromal stem cell contraction to mediate rapid cell and matrix

organization of real architecture for 3-dimensional tissue equivalents." Acta Biomater **67**: 229-237.

Muller, L. J., L. Pels and G. F. Vrensen (1995). "Novel aspects of the ultrastructural organization of human corneal keratocytes." Invest Ophthalmol Vis Sci **36**(13): 2557-2567.

Murphy, C. a. P., RV (1993). The eye. In Miller's Anatomy of the dog. E. HE. Philadelphia, PA, W.B. Saunders: 1009-1055.

Nagayasu, A., T. Hirayanagi, Y. Tanaka, P. Tangkawattana, H. Ueda and K. Takehana (2009). "Site-dependent differences in collagen lamellae in the corneal substantia propria of beagle dogs." J Vet Med Sci **71**(9): 1229-1231.

Nagy, K., H.-K. Sung, P. Zhang, S. Laflamme, P. Vincent, S. Agha-Mohammadi, K. Woltjen, C. Monetti, I. P. Michael, L. C. Smith and A. Nagy (2011). "Induced pluripotent stem cell lines derived from equine fibroblasts." Stem Cell Rev and Rep **7**(3): 693-702.

Nakamura, M., T. Nishida, K. Ofuji, T. W. Reid, M. J. Mannis and C. J. Murphy (1997). "Synergistic effect of substance P with epidermal growth factor on epithelial migration in rabbit cornea." Exp Eye Res **65**(3): 321-329.

Nakatsu, M. N., Z. Ding, M. Y. Ng, T. T. Truong, F. Yu and S. X. Deng (2011). "Wnt/beta-catenin signaling regulates proliferation of human cornea epithelial stem/progenitor cells." Invest Ophthalmol Vis Sci **52**(7): 4734-4741.

Naylor, R. W., C. N. McGhee, C. A. Cowan, A. J. Davidson, T. M. Holm and T. Sherwin (2016). "Derivation of Corneal Keratocyte-Like Cells from Human Induced Pluripotent Stem Cells." PLoS One **11**(10): e0165464.

Nichols, J., B. Zevnik, K. Anastasiadis, H. Niwa, D. Klewe-Nebenius, I. Chambers, H. R. Scholer and A. G. Smith (1998). "Formation of pluripotent stem cells in the mammalian embryo depends in the POU transcription factor Oct4." Cell **95**: 379-391.

Nickerson, M. L., B. N. Kostihina, W. Brandt, W. Fredericks, K. P. Xu, F. S. Yu, B. Gold, J. Chodosh, M. Goldberg, D. W. Lu, M. Yamada, T. M. Tervo, R. Grutzmacher, C. Croasdale, M. Hoeltzenbein, J. Sutphin, S. B. Malkowicz, L. Wessjohann, H. S. Kruth, M. Dean and J. S. Weiss (2010). "UBIAD1 mutation alters a mitochondrial prenyltransferase to cause Schnyder corneal dystrophy." PLoS One **5**(5): e10760.

Nishimura, T., S. Hatoya, R. Kanegi, K. Sugiura, V. Wijewardana, M. Kuwamura, M. Tanaka, J. Yamate, T. Izawa, M. Takahashi, N. Kawate, H. Tamada, H. Imai and T. Inaba (2013). "Generation of functional platelets from canine induced pluripotent stem cells." Stem Cells Dev **22**(14): 2026-2035.

Nishimura, T., S. Hatoya, R. Kanegi, D. P. Wijesekera, K. Sanno, E. Tanaka, K. Sugiura, N. Kawate, H. Tamada, H. Imai and T. Inaba (2017). "Feeder-

independent canine induced pluripotent stem cells maintained under serum-free conditions." Mol Reprod Dev 84(4): 329-339.

Notara, M., S. Schrader and J. T. Daniels (2011). "The porcine limbal epithelial stem cell niche as a new model for the study of transplanted tissue-engineered human limbal epithelial cells." Tissue Eng Part A 17(5-6): 741-750.

Notara, M., A. J. Shortt, G. Galatowicz, V. Calder and J. T. Daniels (2010). "IL6 and the human limbal stem cell niche: a mediator of epithelial-stromal interaction." Stem Cell Res 5(3): 188-200.

O'Callaghan, A. R. and J. T. Daniels (2011). "Concise review: limbal epithelial stem cell therapy: controversies and challenges." Stem Cells 29(12): 1923-1932.

Okita, K., T. Ichisaka and S. Yamanaka (2007). "Generation of germline-competent induced pluripotent stem cells." Nature 448(7151): 313-317.

Orr, A., M. P. Dube, J. Marcadier, H. Jiang, A. Federico, S. George, C. Seamone, D. Andrews, P. Dubord, S. Holland, S. Provost, V. Mongrain, S. Evans, B. Higgins, S. Bowman, D. Guernsey and M. Samuels (2007). "Mutations in the UBIAD1 gene, encoding a potential prenyltransferase, are causal for Schnyder crystalline corneal dystrophy." PLoS One 2(8): e685.

Overton, W. R. (1988). "Modified Histogram Subtraction Technique for Analysis of Flow Cytometry Data." Cytometry 9(6):619-626.

Pajooresh-Ganji, A., S. Pal-Ghosh, S. J. Simmens and M. A. Stepp (2006). "Integrins in slow-cycling corneal epithelial cells at the limbus in the mouse." Stem Cells 24(4): 1075-1086.

Park, S. A., C. M. Reilly, J. A. Wood, D. J. Chung, D. D. Carrade, S. L. Deremer, R. L. Seraphin, K. C. Clark, A. L. Zwingenberger, D. L. Borjesson, K. Hayashi, P. Russell and C. J. Murphy (2013). "Safety and immunomodulatory effects of allogeneic canine adipose-derived mesenchymal stromal cells transplanted into the region of the lacrimal gland, the gland of the third eyelid and the knee joint." Cytherapy 15(12): 1498-1510.

Park, S. B., M. S. Seo, H. S. Kim and K. S. Kang (2012). "Isolation and characterization of canine amniotic membrane-derived multipotent stem cells." PLoS One 7(9): e44693.

Park, S. H., K. W. Kim, Y. S. Chun and J. C. Kim (2012). "Human mesenchymal stem cells differentiate into keratocyte-like cells in keratocyte-conditioned medium." Exp Eye Res 101: 16-26.

Pascolini, D. and S. P. Mariotti (2012). "Global estimates of visual impairment: 2010." Br J Ophthalmol 96(5): 614-618.

- Paterson, Y. Z., C. Kafarnik and D. J. Guest (2017). "Characterization of companion animal pluripotent stem cells." Cytometry A **93**(1):137-148.
- Patruno, M., A. Perazzi, T. Martinello, A. Blaseotto, E. Di Iorio and I. Iacopetti (2017). "Morphological description of limbal epithelium: searching for stem cells crypts in the dog, cat, pig, cow, sheep and horse." Vet Res Commun **41**(2): 169-173.
- Peled, A., D. Zipori, O. Abramsky, H. Ovadia and E. Shezen (1991). "Expression of alpha-smooth muscle actin in murine bone marrow stromal cells." Blood **78**(2): 304-309.
- Pellegrini, G., O. Golisano, P. Paterna, A. Lambiase, S. Bonini, P. Rama and M. De Luca (1999). "Location and clonal analysis of stem cells and their differentiated progeny in the human ocular surface." J Cell Biol **145**(4): 769-782.
- Perez-Merino, E. M., J. M. Uson-Casaus, J. Duque-Carrasco, C. Zaragoza-Bayle, L. Marinas-Pardo, M. Hermida-Prieto, M. Vilafranca-Compte, R. Barrera-Chacon and M. Gualtieri (2015). "Safety and efficacy of allogeneic adipose tissue-derived mesenchymal stem cells for treatment of dogs with inflammatory bowel disease: Endoscopic and histological outcomes." Vet J **206**(3): 391-397.
- Peters, I. R., D. Peeters, C. R. Helps and M. J. Day (2007). "Development and application of multiple internal reference (housekeeper) gene assays for accurate normalisation of canine gene expression studies." Vet Immunol Immunopathol **117**(1-2): 55-66.
- Pfaffl, M. W., A. Tichopad, C. Prgomet and T. P. Neuvians (2004). "Determination of stable housekeeping genes, differentially regulated target genes and sample integrity: BestKeeper--Excel-based tool using pair-wise correlations." Biotechnol Lett **26**(6): 509-515.
- Polisetti, N., P. Agarwal, I. Khan, P. Kondaiah, V. S. Sangwan and G. K. Vemuganti (2010). "Gene expression profile of epithelial cells and mesenchymal cells derived from limbal explant culture." Mol Vis **16**: 1227-1240.
- Polisetty, N., A. Fatima, S. L. Madhira, V. S. Sangwan and G. K. Vemuganti (2008). "Mesenchymal cells from limbal stroma of human eye." Mol Vis **14**: 431-442.
- Proietto, L. R., R. D. Whitley, D. E. Brooks, G. E. Schultz, D. J. Gibson, W. M. Berkowski, Jr., M. E. Salute and C. E. Plummer (2017). "Development and Assessment of a Novel Canine Ex Vivo Corneal Model." Curr Eye Res **42**(6): 813-821.
- Pumphrey, S. A., S. Pizzirani and C. G. Pirie (2011). "360-degree conjunctival grafting for management of diffuse keratomalacia in a dog." Vet Ophthalmol **14**(3): 209-213.

Ren, Y. J., S. Zhang, R. Mi, Q. Liu, X. Zeng, M. Rao, A. Hoke and H. Q. Mao (2013). "Enhanced differentiation of human neural crest stem cells towards the Schwann cell lineage by aligned electrospun fiber matrix." Acta Biomater **9**(8): 7727-7736.

Rhee, Y. H., M. Choi, H. S. Lee, C. H. Park, S. M. Kim, S. H. Yi, S. M. Oh, H. J. Cha, M. Y. Chang and S. H. Lee (2013). "Insulin concentration is critical in culturing human neural stem cells and neurons." Cell Death Dis **4**: e766.

Rider, C. C. (2006). "Heparin/heparan sulphate binding in the TGF-beta cytokine superfamily." Biochem Soc Trans **34**(Pt 3): 458-460.

Rio, D. C., M. Ares, Jr., G. J. Hannon and T. W. Nilsen (2010). "Purification of RNA using TRIzol (TRI reagent)." Cold Spring Harb Protoc **2010**(6): pdb.prot5439.

Robaei, D. and S. Watson (2014). "Corneal blindness: a global problem." Clin Exp Ophthalmol **42**(3): 213-214.

Romano, A. C., E. M. Espana, S. H. Yoo, M. T. Budak, J. M. Wolosin and S. C. Tseng (2003). "Different cell sizes in human limbal and central corneal basal epithelia measured by confocal microscopy and flow cytometry." Invest Ophthalmol Vis Sci **44**(12): 5125-5129.

Roth, A. M., M. B. Ekins, G. O. Waring, 3rd, L. M. Gupta and L. S. Rosenblatt (1981). "Oval corneal opacities in beagles. III. Histochemical demonstration of stromal lipids without hyperlipidemia." Invest Ophthalmol Vis Sci **21**(1 Pt 1): 95-106.

Russell, K. A., N. H. Chow, D. Dukoff, T. W. Gibson, J. LaMarre, D. H. Betts and T. G. Koch (2016). "Characterization and Immunomodulatory Effects of Canine Adipose Tissue- and Bone Marrow-Derived Mesenchymal Stromal Cells." PLoS One **11**(12): e0167442.

Sakaue, M. and M. Sieber-Blum (2015). "Human epidermal neural crest stem cells as a source of Schwann cells." Development **142**(18): 3188-3197.

Samaeekia, R., B. Rabiee, I. Putra, X. Shen, Y. J. Park, P. Hematti, M. Eslani and A. R. Djalilian (2018). "Effect of Human Corneal Mesenchymal Stromal Cell-derived Exosomes on Corneal Epithelial Wound Healing." Invest Ophthalmol Vis Sci **59**(12): 5194-5200.

Samuelson, D. (2013). Ophthalmic Anatomy. In Veterinary Ophthalmology. K. N. Gelatt, Gilger B.C., Kern T.J. Ames, Iowa, USA, Wiley-Blackwell. Vol 1: 39-171.

Sanchez-Abarca, L. I., E. Hernandez-Galilea, R. Lorenzo, C. Herrero, A. Velasco, S. Carrancio, T. Caballero-Velazquez, J. I. Rodriguez-Barbosa, M. Parrilla, C. Del Canizo, J. San Miguel, J. Aijon and J. A. Perez-Simon (2015). "Human Bone Marrow Stromal Cells Differentiate Into Corneal Tissue and Prevent Ocular Graft-Versus-Host Disease in Mice." Cell Transplant **24**(12): 2423-2433.

Sanchez, R. F. and J. T. Daniels (2016). "Mini-Review: Limbal Stem Cells Deficiency in Companion Animals: Time to Give Something Back?" Curr Eye Res **41**(4): 425-432.

Sareen, D., M. Saghizadeh, L. Ornelas, M. A. Winkler, K. Narwani, A. Sahabian, V. A. Funari, J. Tang, L. Spurka, V. Punj, E. Maguen, Y. S. Rabinowitz, C. N. Svendsen and A. V. Ljubimov (2014). "Differentiation of human limbal-derived induced pluripotent stem cells into limbal-like epithelium." Stem Cells Transl Med **3**(9): 1002-1012.

Scarfone, R. A., S. M. Pena, K. A. Russell, D. H. Betts and T. G. Koch (2020). "The use of induced pluripotent stem cells in domestic animals: a narrative review." BMC Vet Res **16**(1): 477.

Schlotzer-Schrehardt, U., T. Dietrich, K. Saito, L. Sorokin, T. Sasaki, M. Paulsson and F. E. Kruse (2007). "Characterization of extracellular matrix components in the limbal epithelial stem cell compartment." Exp Eye Res **85**(6): 845-860.

Schneider, M. R., H. Adler, J. Braun, B. Kienzle, E. Wolf and H. J. Kolb (2007). "Canine embryo-derived stem cells--toward clinically relevant animal models for evaluating efficacy and safety of cell therapies." Stem Cells **25**(7): 1850-1851.

Scott, J. E. (1995). "Extracellular matrix, supramolecular organisation and shape." J Anat **187** (Pt 2): 259-269.

Scott, J. E. and T. R. Bosworth (1990). "The comparative chemical morphology of the mammalian cornea." Basic Appl Histochem **34**(1): 35-42.

Seaberg, R. M. and D. van der Kooy (2003). "Stem and progenitor cells: the premature desertion of rigorous definitions." Trends Neurosci **26**(3): 125-131.

Secker, G. A. and J. T. Daniels (2008). Limbal epithelial stem cells of the cornea. StemBook. Cambridge (MA): DOI 10.3824/stembook.3821.3848.3821.

Seitz, B. and W. Lisch (2011). "Stage-related therapy of corneal dystrophies." Dev Ophthalmol **48**: 116-153.

Sgrignoli, M. R., D. A. Silva, F. F. Nascimento, D. A. M. Sgrignoli, G. A. Nai, M. G. da Silva, M. A. de Barros, M. K. W. Bittencourt, B. P. de Moraes, H. R. Dinallo, B. T. D. Foglia, W. B. Cabrera, E. C. Fares and S. F. Andrade (2019). "Reduction in the inflammatory markers CD4, IL-1, IL-6 and TNF α in dogs with keratoconjunctivitis sicca treated topically with mesenchymal stem cells." Stem Cell Res **39**: 101525.

Shaham, O., Y. Menuchin, C. Farhy and R. Ashery-Padan (2012). "Pax6: a multi-level regulator of ocular development." Progress in retinal and eye research **31**(5): 351-376.

Shalom-Feuerstein, R., L. Serró, D. De La Forest and I. Petit (2012). "Pluripotent Stem Cell Model Reveals Essential Roles for miR-450b-5p and miR-184 in Embryonic Corneal Lineage Specification." Stem Cells **30**: 898-909.

Sharma, A. and W. H. Coles (1989). "Kinetics of corneal epithelial maintenance and graft loss. A population balance model." Invest Ophthalmol Vis Sci **30**(9): 1962-1971.

Sharma, A., S. Sances, M. J. Workman and C. N. Svendsen (2020). "Multi-lineage Human iPSC-Derived Platforms for Disease Modeling and Drug Discovery." Cell Stem Cell **26**(3): 309-329.

Sharma, A., N. R. Sinha, S. Siddiqui and R. R. Mohan (2015). "Role of 5'TG3'-interacting factors (TGIFs) in Vorinostat (HDAC inhibitor)-mediated Corneal Fibrosis Inhibition." Mol Vis **21**: 974-984.

Sharma, R., D. Bose, A. Maminishkis and K. Bharti (2020). "Retinal Pigment Epithelium Replacement Therapy for Age-Related Macular Degeneration: Are We There Yet?" Annu Rev Pharmacol Toxicol **60**: 553-572.

Shi, Y., H. Inoue, J. C. Wu and S. Yamanaka (2017). "Induced pluripotent stem cell technology: a decade of progress." Nat Rev Drug Discov **16**(2): 115-130.

Shih, C. C., S. J. Forman, P. Chu and M. Slovak (2007). "Human embryonic stem cells are prone to generate primitive, undifferentiated tumors in engrafted human fetal tissues in severe combined immunodeficient mice." Stem Cells Dev **16**(6): 893-902.

Shimada, H., A. Nakada, Y. Hashimoto, K. Shigeno, Y. Shionoya and T. Nakamura (2010). "Generation of canine induced pluripotent stem cells by retroviral transduction and chemical inhibitors." Mol Reprod Dev **77**(1): 2.

Shively, J. N. and G. P. Epling (1970). "Fine structure of the canine eye: cornea." Am J Vet Res **31**(4): 713-722.

Shojaati, G., I. Khandaker, M. L. Funderburgh, M. M. Mann, R. Basu, D. B. Stolz, M. L. Geary, A. Dos Santos, S. X. Deng and J. L. Funderburgh (2019). "Mesenchymal Stem Cells Reduce Corneal Fibrosis and Inflammation Via Extracellular Vesicle-Mediated Delivery of miRNA." Stem Cells Transl Med **8**(11):1192-1201

Shojaati, G., I. Khandaker, K. Sylakowski, M. L. Funderburgh, Y. Du and J. L. Funderburgh (2018). "Compressed Collagen Enhances Stem Cell Therapy for Corneal Scarring." Stem Cells Transl Med **7**(6): 487-494.

Shukla, S. and R. Mishra (2018). "Level of hydrogen peroxide affects expression and sub-cellular localization of Pax6." Mol Biol Rep **45**(4): 533-540.

Sidney, L. E., M. J. Branch, H. S. Dua and A. Hopkinson (2015). "Effect of culture medium on propagation and phenotype of corneal stroma-derived stem cells." Cytotherapy **17**(12): 1706-1722.

Silva, J., J. Nichols, T. W. Theunissen, G. Guo, A. L. van Oosten, O. Barrandon, J. Wray, S. Yamanaka, I. Chambers and A. Smith (2009). "Nanog is the gateway to the pluripotent ground state." Cell **138**(4): 722-737.

Sloniecka, M., S. Le Roux, P. Boman, B. Bystrom, Q. Zhou and P. Danielson (2015). "Expression Profiles of Neuropeptides, Neurotransmitters, and Their Receptors in Human Keratocytes In Vitro and In Situ." PLoS One **10**(7): e0134157.

Soldner, F., Y. Stelzer, C. S. Shivalila, B. J. Abraham, J. C. Latourelle, M. I. Barrasa, J. Goldmann, R. H. Myers, R. A. Young and R. Jaenisch (2016). "Parkinson-associated risk variant in distal enhancer of alpha-synuclein modulates target gene expression." Nature **533**(7601): 95-99.

Stagos, D., Y. Chen, M. Cantore, J. V. Jester and V. Vasiliou (2010). "Corneal aldehyde dehydrogenases: multiple functions and novel nuclear localization." Brain Res Bull **81**(2-3): 211-218.

Steger, B., V. Romano, S. Biddolph, C. E. Willoughby, M. Batterbury and S. B. Kaye (2016). "Femtosecond Laser-Assisted Lamellar Keratectomy for Corneal Opacities Secondary to Anterior Corneal Dystrophies: An Interventional Case Series." Cornea **35**(1): 6-13.

Strom, A. R., D. E. Cortés, S. M. Thomasy, P. H. Kass, M. J. Mannis and C. J. Murphy (2016). "In vivo ocular imaging of the cornea of the normal female laboratory beagle using confocal microscopy." Vet Ophthalmol **19**(1): 63-67.

Stroud, C., I. Dmitriev, E. Kashentseva, J. N. Bryan, D. T. Curiel, H. Rindt, C. Reiner, C. J. Henry, P. J. Bergman, N. J. Mason, J. S. Gnanandarajah, J. B. Engiles, F. Gray, D. Laughlin, A. Gaurnier-Hausser, A. Wallecha, M. Huebner, Y. Paterson, D. O'Connor, L. S. Treml, J. P. Stannard, J. L. Cook, M. Jacobs, G. J. Wyckoff, L. Likins, U. Sabbagh, A. Skaff, A. S. Guloy, H. D. Hays, A. K. LeBlanc, J. R. Coates, M. L. Katz, L. A. Lyons, G. C. Johnson, G. S. Johnson, D. P. O'Brien, D. Duan, J. P. Calvet, B. Gandolfi, D. A. Baron, M. L. Weiss, D. A. Webster, F. N. Karanu, E. J. Robb and R. J. Harman (2016). "A One Health overview, facilitating advances in comparative medicine and translational research." Clin Transl Med **5**(Suppl 1): 26.

Syed-Picard, F. N., Y. Du, A. J. Hertsberg, R. Palchesko, M. L. Funderburgh and A. W. Feinberg (2016). "Scaffold-free tissue engineering of functional corneal stromal tissue." Stem Cell Res Ther **8**: 260

Takahashi, K. (2012). "Cellular reprogramming--lowering gravity on Waddington's epigenetic landscape." J Cell Sci **125**(Pt 11): 2553-2560.

Takahashi, K. and S. Yamanaka (2006). "Induction of pluripotent stem cells from mouse embryonic and adult fibroblast cultures by defined factors." Cell **126**(4): 663-676.

Takemitsu, H., D. Zhao, I. Yamamoto, Y. Harada, M. Michishita and T. Arai (2012). "Comparison of bone marrow and adipose tissue-derived canine mesenchymal stem cells." BMC Vet Res **8**: 150.

Talele, N. P., J. Fradette, J. E. Davies, A. Kapus and B. Hinz (2015). "Expression of alpha-Smooth Muscle Actin Determines the Fate of Mesenchymal Stromal Cells." Stem Cell Reports **4**(6): 1016-1030.

Tan, S. C. and B. C. Yiap (2009). "DNA, RNA, and protein extraction: the past and the present." J Biomed Biotechnol **2009**: 574398.

Tandon, A., J. C. Tovey, A. Sharma, R. Gupta and R. R. Mohan (2010). "Role of transforming growth factor Beta in corneal function, biology and pathology." Curr Mol Med **10**(6): 565-578.

Tasheva, E. S., A. Koester, A. Q. Paulsen, A. S. Garrett, D. L. Boyle, H. J. Davidson, M. Song, N. Fox and G. W. Conrad (2002). "Mimecan/osteoglycin-deficient mice have collagen fibril abnormalities." Mol Vis **8**: 407-415.

Thoft, R. A. and J. Friend (1983). "The X, Y, Z hypothesis of corneal epithelial maintenance." Invest Ophthalmol Vis Sci **24**(10): 1442-1443.

Thomas, P. B., Y. H. Liu, F. F. Zhuang, S. Selvam, S. W. Song, R. E. Smith, M. D. Trousdale and S. C. Yiu (2007). "Identification of Notch-1 expression in the limbal basal epithelium." Mol Vis **13**: 337-344.

Tidu, A., M. C. Schanne-Klein and V. M. Borderie (2020). "Development, structure, and bioengineering of the human corneal stroma: A review of collagen-based implants." Exp Eye Res **200**: 108256.

Tobias, I. C., C. R. Brooks, J. H. Teichroeb, D. A. Villagomez, D. A. Hess, C. A. Seguin and D. H. Betts (2016). "Small-Molecule Induction of Canine Embryonic Stem Cells Toward Naive Pluripotency." Stem Cells Dev **25**(16): 1208-1222.

Tomasello, L., R. Musso, G. Cillino, M. Pitrone, G. Pizzolanti, A. Coppola, W. Arancio, G. Di Cara, I. Pucci-Minafra, S. Cillino and C. Giordano (2016). "Donor age and long-term culture do not negatively influence the stem potential of limbal fibroblast-like stem cells." Stem Cell Res Ther **7**(1): 83.

Tse, W. T., J. D. Pendleton, W. M. Beyer, M. C. Egalka and E. C. Guinan (2003). "Suppression of allogeneic T-cell proliferation by human marrow stromal cells: implications in transplantation." Transplantation **75**(3): 389-397.

Tsukamoto, M., T. Nishimura, K. Yodoe, R. Kanegi, Y. Tsujimoto, M. E. Alam, M. Kuramochi, M. Kuwamura, M. Ohtaka, K. Nishimura, M. Nakanishi, T. Inaba, K. Sugiura and S. Hatoya (2018). "Generation of Footprint-Free

Canine Induced Pluripotent Stem Cells Using Auto-Erasable Sendai Virus Vector." Stem Cells Dev **27**(22): 1577-1586.

Twentyman, P. R. and M. Luscombe (1987). "A study of some variables in a tetrazolium dye (MTT) based assay for cell growth and chemosensitivity." Br J Cancer **56**(3): 279-285.

Uder, C., S. Bruckner, S. Winkler, H. M. Tautenhahn and B. Christ (2018). "Mammalian MSC from selected species: Features and applications." Cytometry A **93**(1): 32-49.

Vaags, A. K., S. Rosic-Kablar, C. J. Gartley, Y. Z. Zheng, A. Chesney, D. A. Villagomez, S. A. Kruth and M. R. Hough (2009). "Derivation and characterization of canine embryonic stem cell lines with in vitro and in vivo differentiation potential." Stem Cells **27**(2): 329-340.

Vagnozzi, R. J., M. Maillet, M. A. Sargent, H. Khalil, A. K. Johansen, J. A. Schwanekamp, A. J. York, V. Huang, M. Nahrendorf, S. Sadayappan and J. D. Molkentin (2019). "An acute immune response underlies the benefit of cardiac stem-cell therapy." Nature **577**: 405–409.

Vantrappen, L., K. Geboes, L. Missotten, P. C. Maudgal and V. Desmet (1985). "Lymphocytes and Langerhans cells in the normal human cornea." Invest Ophthalmol Vis Sci **26**(2): 220-225.

Vaux, D. L., F. Fidler and G. Cumming (2012). "Replicates and repeats--what is the difference and is it significant? A brief discussion of statistics and experimental design." EMBO Rep **13**(4): 291-296.

Vereb, Z., S. Poliska, R. Albert, O. K. Olstad, A. Boratko, C. Csontos, M. C. Moe, A. Facsko and G. Petrovski (2016). "Role of Human Corneal Stroma-Derived Mesenchymal-Like Stem Cells in Corneal Immunity and Wound Healing." Sci Rep **6**: 26227.

Villatoro, A. J., V. Fernandez, S. Claros, G. A. Rico-Llanos, J. Becerra and J. A. Andrades (2015). "Use of adipose-derived mesenchymal stem cells in keratoconjunctivitis sicca in a canine model." Biomed Res Int **2015**: 527926.

Volk, S. W., D. L. Diefenderfer, S. A. Christopher, M. E. Haskins and P. S. Leboy (2005). "Effects of osteogenic inducers on cultures of canine mesenchymal stem cells." Am J Vet Res **66**(10): 1729-1737.

Volk, S. W., Y. Wang and K. D. Hankenson (2012). "Effects of donor characteristics and ex vivo expansion on canine mesenchymal stem cell properties: implications for MSC-based therapies." Cell Transplant **21**(10): 2189-2200.

Wang, F., S. Thirumangalathu and M. R. Loeken (2006). "Establishment of new mouse embryonic stem cell lines is improved by physiological glucose and oxygen." Cloning Stem Cells **8**(2): 108-116.

Wang, L., R. Ma, G. Du, H. Guo and Y. Huang (2015). "Biocompatibility of helicoidal multilamellar arginine-glycine-aspartic acid-functionalized silk biomaterials in a rabbit corneal model." J Biomed Mater Res B Appl Biomater **103**(1): 204-211.

Waring, G. O., M. Ekins and W. Spangler (1979). "Oval lipid corneal opacities in Beagles and crystalline lipid corneal opacities in Siberian Huskies." Metabolic Pediatric Ophthalmology **3**: 203-213.

Waring, G. O., MacMillan, AD, Reveles, P (1986). "Inheritance of crystalline corneal dystrophy in Siberian huskies." J Am Anim Hosp Assoc **22**: 655-658.

Waring, G. O., F. M. Muggli and A. MacMillan (1977). "Oval corneal opacities in Beagles [involved in radionuclide toxicity studies, dogs] " J Am Anim Hosp Assoc **13**(2): 204-208.

Watanabe, K., K. Nishida, M. Yamato, T. Umemoto, T. Sumide, K. Yamamoto, N. Maeda, H. Watanabe, T. Okano and Y. Tano (2004). "Human limbal epithelium contains side population cells expressing the ATP-binding cassette transporter ABCG2." FEBS Lett **565**(1-3): 6-10.

Watanabe, K., M. Ueno, D. Kamiya, A. Nishiyama, M. Matsumura, T. Wataya, J. B. Takahashi, S. Nishikawa, S. Nishikawa, K. Muguruma and Y. Sasai (2007). "A ROCK inhibitor permits survival of dissociated human embryonic stem cells." Nat Biotech **25**(6): 681-686.

Watsky, M. A. (1995). "Keratocyte gap junctional communication in normal and wounded rabbit corneas and human corneas." Invest Ophthalmol Vis Sci **36**(13): 2568-2576.

Weng, L., J. L. Funderburgh, I. Khandaker, M. L. Geary, T. Yang, R. Basu, M. L. Funderburgh, Y. Du and G. H. Yam (2020). "The anti-scarring effect of corneal stromal stem cell therapy is mediated by transforming growth factor β 3." Eye Vis (Lond) **7**(1): 52.

Werbowski-Ogilvie, T. E., M. Bosse, M. Stewart, A. Schnerch, V. Ramos-Mejia, A. Rouleau, T. Wynder, M. J. Smith, S. Dingwall, T. Carter, C. Williams, C. Harris, J. Dolling, C. Wynder, D. Boreham and M. Bhatia (2009). "Characterization of human embryonic stem cells with features of neoplastic progression." Nat Biotechnol **27**(1): 91-97.

Werner, S. and R. Grose (2003). "Regulation of wound healing by growth factors and cytokines." Physiol Rev **83**(3): 835-870.

Whitley, R. and R. Hamor (2021). Disease and Surgery of the Canine Cornea and Sclera. In Veterinary Ophthalmology. K. N. Gelatt. Hoboken, N.J., Wiley Blackwell. Vol 2: 1082-1172.

Whitley, R. D. and B. C. Gilger (1999). Disease of the canine cornea and sclera. In Veterinary Ophthalmology. K. N. Gelatt, Lippincott Williams and Wilkins Vol 2: 635-671.

Whitworth, D. J., J. E. Frith, T. J. Frith, D. A. Ovchinnikov, J. J. Cooper-White and E. J. Wolvetang (2014). "Derivation of mesenchymal stromal cells from canine induced pluripotent stem cells by inhibition of the TGFbeta/activin signaling pathway." Stem Cells Dev **23**(24): 3021-3033.

Whitworth, D. J., D. A. Ovchinnikov and E. J. Wolvetang (2012). "Generation and characterization of LIF-dependent canine induced pluripotent stem cells from adult dermal fibroblasts." Stem Cells Dev **21**(12): 2288-2297.

Wiley, L. A., E. R. Burnight, A. E. Songstad, A. V. Drack, R. F. Mullins, E. M. Stone and B. A. Tucker (2015). "Patient-specific induced pluripotent stem cells (iPSCs) for the study and treatment of retinal degenerative diseases." Prog Retin Eye Res **44**: 15-35.

Williams, D. L. (2005). "Major histocompatibility class II expression in the normal canine cornea and in canine chronic superficial keratitis." Vet Ophthalmol **8**(6): 395-400.

Wilson, S. E. (2020). "Bowman's layer in the cornea- structure and function and regeneration." Exp Eye Res **195**: 108033.

Wilson, S. E. (2021). "TGF beta -1, -2 and -3 in the modulation of fibrosis in the cornea and other organs." Exp Eye Res **207**: 108594.

Wolfel, A. E., S. L. Pederson, A. M. Cleymaet, A. M. Hess and K. S. Freeman (2018). "Canine central corneal thickness measurements via Pentacam-HR((R)) , optical coherence tomography (Optovue iVue((R))), and high-resolution ultrasound biomicroscopy." Vet Ophthalmol **21**(4): 362-370.

Wu, J., Y. Du, M. M. Mann, J. L. Funderburgh and W. R. Wagner (2014). "Corneal stromal stem cells versus corneal fibroblasts in generating structurally appropriate corneal stromal tissue." Exp Eye Res **120**: 71-81.

Wu, J., Y. Du, S. C. Watkins, J. L. Funderburgh and W. R. Wagner (2012). "The engineering of organized human corneal tissue through the spatial guidance of corneal stromal stem cells." Biomaterials **33**(5): 1343-1352.

Xu, L., L. Tang and L. Zhang (2019). "Proteoglycans as miscommunication biomarkers for cancer diagnosis." Prog Mol Biol TransSci **162**: 59-92.

Yamamoto, M., H. K. Nakata, S.Hao, J., J. Chou and S. Kuroda (2014). "Osteogenic Potential of Mouse Adipose-Derived Stem Cells Sorted for CD90 and CD105 In Vitro." Stem Cells Int **2014**: 576358.

Yang, C. H., G. J. Culshaw, M. M. Liu, C. C. Lu, A. T. French, D. N. Clements and B. M. Corcoran (2012). "Canine tissue-specific expression of multiple small leucine rich proteoglycans." Vet J **193**(2): 374-380.

Yazdanpanah, G., Z. Haq, K. Kang, S. Jabbehdari, M. L. Rosenblatt and A. R. Djalilian (2019). "Strategies for reconstructing the limbal stem cell niche." Ocul Surf **17**(2): 230-240.

Yi, T. and S. U. Song (2012). "Immunomodulatory properties of mesenchymal stem cells and their therapeutic applications." Arch Pharm Res **35**(2): 213-221.

Yoshida, S., S. Shimmura, T. Kawakita, H. Miyashita, S. Den, J. Shimazaki and K. Tsubota (2006). "Cytokeratin 15 can be used to identify the limbal phenotype in normal and diseased ocular surfaces." Invest Ophthalmol Vis Sci **47**(11): 4780-4786.

Zhao, J. J. and N. A. Afshari (2016). "Generation of Human Corneal Endothelial Cells via In Vitro Ocular Lineage Restriction of Pluripotent Stem Cells." Invest Ophthalmol Vis Sci **57**(15): 6878-6884.

Zhao, S., Y. Zhang, R. Gamini, B. Zhang and D. von Schack (2018). "Evaluation of two main RNA-seq approaches for gene quantification in clinical RNA sequencing: polyA+ selection versus rRNA depletion." Scientific Reports **8**(1): 4781.

Zheng, Y., Y. Zhang, R. Qu, Y. He, X. Tian and W. Zeng (2014). "Spermatogonial stem cells from domestic animals: progress and prospects." Reproduction **147**(3): R65-R74.

Zieske, J. D., A. E. K. Hutcheon and X. Guo (2019). "Extracellular Vesicles and Cell-Cell Communication in the Cornea." Anat Rec. **303**(6):1727-1734.

Publications

Paterson, Y. Z., C. Kafarnik and D. J. Guest (2017). "Characterization of companion animal pluripotent stem cells." Cytometry A **93**(1):137-148.

Kafarnik, C., A. McClellan, M. Dziasko, J. T. Daniels and D. J. Guest (2020). "Canine Corneal Stromal Cells Have Multipotent Mesenchymal Stromal Cell Properties In Vitro." Stem Cells Dev. **29** (7): 425-439.